

**RESEARCH ON ELASTOHYDRODYNAMIC
LUBRICATION OF HIGH SPEED
ROLLING - SLIDING CONTACTS**

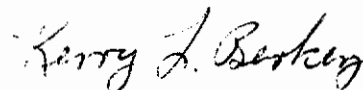
Richard Smith
Jed Walowit
Pradeep Gupta
John McGrew

FOREWORD

This report was prepared by Mechanical Technology Incorporated, 968 Albany-Shaker Road, Latham, New York under USAF Contract No. F33615-69-C-1305. The contract was initiated under Project No. 3048 Task No. 304806. The work was administered under the direction of the Air Force Aero Propulsion Laboratory, with Mr. M. R. Chasman (SFL) acting as project engineer.

This report covers work conducted from 1 February 1970 - 1 February 1971.

Publication of this report does not constitute Air Force approval of the report's findings or conclusions. It is published only for the exchange and stimulation of ideas.



KERRY L. BERKEY, ACTING CHIEF
Lubrication Branch
Fuels and Lubrication Division

ABSTRACT

A rolling disc apparatus has been designed and built. Traction between two crown discs lubricated with 5P4E polyphenyl ether have been measured as function of slip rate over a range of Hertz pressure (80,000 - 140,000 psi), rolling speeds (900 - 1820 ips), and temperatures (175 F - 215 F). Comparisons are made between measured tractions, Battelle data, and various analytical predictions. The MTI data agree qualitatively with Battelle measurements except that MTI data are found to be relatively insensitive to temperature whereas Battelle reports considerable temperature sensitivity. A semi-empirical mathematical model has been put forth to represent traction measurements.

A computer program for analyzing asperity interactions under partial elasto-hydrodynamic conditions has been written and a listing is contained in this report.

Contrails

Contrails

TABLE OF CONTENTS

	<u>Page</u>
I. INTRODUCTION -----	1
II. ELASTOHYDRODYNAMIC TEST APPARATUS -----	3
1. TEST RIG DESIGN -----	3
2. THE TEST FACILITY -----	4
3. ROLLING DISC MACHINE DETAILS -----	8
a. Base Plate and Pedestal -----	8
b. Temperature Detection -----	12
c. Speeds Monitored and Controlled -----	12
d. Lubricant Supply -----	23
e. Torque Detection -----	23
f. Loading Mechanism -----	27
g. Motor Drive System -----	30
4. TRACTION MEASUREMENT -----	34
5. ASPERITY CONTACT AND CAPACITANCE FILM THICKNESS TECHNIQUES -----	38
6. OPTICAL FILM THICKNESS TECHNIQUES -----	45
7. X-RAY FILM THICKNESS TECHNIQUES -----	51
III. TRACTION DATA AND ANALYSIS -----	57
1. TRACTION DATA -----	57
2. COMPARISON WITH BATTELLE DATA -----	62
3. COMPARISON OF TRACTION DATA WITH PERFORMANCE CODE PREDICTIONS -----	65
4. COMPARISON BETWEEN MEASURED TRACTION AND PREDICTIONS BASED UPON EXISTING VISCOSITY DATA -----	68
5. APPARENT VISCOSITY RELATIONSHIPS BASED UPON TRACTION DATA -----	72
IV. ASPERITY INTERACTIONS AND PARTIAL ELASTOHYDRODYNAMIC LUBRICATION IN ROLLING ELEMENT BEARINGS -----	83
1. STATISTICAL ANALYSIS OF ROUGH SURFACES IN SLIDING INTERACTION -----	83

TABLE OF CONTENTS (Continued)

	<u>Page</u>
2. RESULTS OF ASPERITY INTERACTION ANALYSIS AS APPLIED TO A LUBRICATED ROLLING-SLIDING CONTACT -----	88
V. CONCLUSIONS -----	93
APPENDIX I - MTI ROLLING DISC DESIGN DRAWINGS -----	95
APPENDIX II - EQUIPMENT LIST -----	97
APPENDIX III - COMPUTER PROGRAM FOR EVALUATION OF ASPERITY INTERACTIONS IN PARTIAL ELASTOHYDRODYNAMIC LUBRICATION -----	99
Usage -----	99
Output -----	100
Summary of all External Subroutines -----	102
APPENDIX IV - EQUATIONS FOR DETERMINATION OF THE SEPARATION PROFILE FOR ELLIPTICAL HERTZ CONTACT -----	157
REFERENCES -----	161

LIST OF FIGURES

	<u>Page</u>
1. The Disc Machine: Conceptual Layout	5
2. Elastohydrodynamic Test Facility	6
3. Rolling Disc Machine During Construction	9
4. Rolling Disc Machine: Front View Cross-Section	10
5. Front View of Rolling Disc Machine Base Pedestal Assembly	11
6. Top View of Rolling Disc Machine Base and Motor Drive Layout	13
7. Thermocouple Detection Points in Rolling Disc Machine	14
8. Full Scale Side View of Mounted Rolling Disc Specimens Showing Thermocouple Placement Near Contact Zone	15
9. Temperature Sensing Details of Contact Zone Supply Lubricant	16
10. Motor Speed Sensing, Shaft Rotational Frequency Monitoring and Control Schematic	18
11. Details of Speed Monitoring Electrical Hook-up with Oscilloscope for Precise Pure Rolling Speed Check	19
12. Electronic Tachometer with Direct Current Analog Voltage Output	20
13. Rolling Disk Assembly Lubricant Dispensing System with Heat Exchanger	24
14. Contact Zone Lubricant Flow From Needle Valve Control for Three Operating Temperatures	25
15. Torque Detection, Signal Conditioning, and Readout Display Set-Up	26
16. Traction Versus Slip Curve Plotted by X-Y Plotter	28
17. Hydraulic Loading and Contact Load Indication Read-Out Assembly Schematic of the Rolling Disc Machine	29
18. Hertz Contact Pressure vs. Load for Identical 3 in. Diameter Crowned Steel Discs; Crown Radius = 36 in.	31
19. Nomogram Relating Disc Surface Velocity Rotational Frequency, and Disc Diameter Capability of the Present Test Facility	32
20. Torque Output Range of Twenty HP Rolling Disc Motors	33
21. Front View of Completed Rolling Disc Test Facility Showing Concrete Base, Motor Drives, and Upper Sliding Carriage with Load Cylinder Attached	35
22. Full Scale Plot of Total Traction vs. Slip Curve as Received on X-Y Plotter for Two Separate Loads Showing Relative Torque Levels and Support Bearing Losses	37
23. Traction for a Constant Slip Setting and a Variable Rate of Fluid Supplied to the Contact Zone	39

LIST OF FIGURES (Continued)

	<u>Page</u>
24. Test Specimen Mounting Assembly for Contact Zone Asperity and/or Capacitive Detection	40
25. Typical Contact Resistance Variations as a Function of Time. Ten Percent Contact Over One Second of Observation with Contact Resistance Dropping Below 1000 ohms 1500 Times Per Second	43
26. Functional Diagram of Input-Output Operations Available on Asperitac	44
27. Rolling Disc Specimens	47
28. Optical Interference Pattern Between Cylindrical Quartz Disc and Polished Steel Crowned Disc of the Same Diameter	48
29. Lower Disc Specimen Shaft Showing Mounting Arrangement and Optical Access	49
30. Optical Assembly Positioned for Viewing Contact Zone Interference Fringes. Test Specimens Shown Unmounted	50
31. Measured and Predicted Separations in Axial Direction	52
32. Theoretical Fringe Pattern	53
33. X-Ray Film Thickness Measurement Assembly Showing the Path of the Radiation Through the Contact Zone of Rolling Discs	55
34. Traction Data at 200° F at a Rolling Speed of 900 in./sec	58
35. Traction Data at 200° F at a Rolling Speed of 1360 in./sec	59
36. Traction Data at 200° F at a Rolling Speed of 1820 in./sec	60
37. Traction Coefficient at 200° F and 900 in./sec	61
38. High Slip-Rate Data at 200° F and a Rolling Speed of 900 in./sec ..	63
39. Comparison Between MTI and Battelle Traction Data at Different Temperatures	64
40. Comparison Between MTI and Battelle Traction Data at Different Rolling Speeds	66
41. Comparison Between MTI and Battelle Data at a Hertz Pressure of 140,000 psi	67
42. Comparison Between Measured Traction Coefficients and Performance Code Predictions	69
43. Performance Code Prediction of the Effect of Lubricant Temperature on Traction Coefficients	70
44. Viscosity Data for Polyphenyl Ether (5P4E)	71
45. Comparison Between Measured Traction and Theoretical Prediction ..	73

Contrails

LIST OF FIGURES (Continued)

	<u>Page</u>
46. Hypothetical High Pressure-Viscosity Relationship_____	75
47. Function $\Phi(\psi)$ Used in Predicting Traction_____	77
48. Comparison Between Predicted Traction Using Hypothetical Viscosity Model and Data at a Rolling Speed of 1820 in./sec_____	79
49. Comparison Between Predicted and Measured Traction at 1360 in./sec_____	80
50. Comparison Between Predicted and Measured Traction at 900 in./sec_____	81
51. Contact of a Pair of Rough Surfaces, Sliding Against Each Other___	85
52. The Standardized Normal Distribution Function for Z_____	86
53. Typical Solutions as a Function of the Mean Separation Between the Interacting Surfaces_____	89
54. Effect of Relative Sliding Speed_____	91
55. Variation of Friction Coefficient with Sliding Speed_____	92
III-1. Specification of Film Profile_____	101

Contrails

ABBREVIATIONS

a	Semi-major axis of contact ellipse, in.
A	Real contact area, in ²
b	Semi-minor axis of contact ellipse, in.
C	Electrical capacitance, Farads
d	Nondimensional mean separation between mating surfaces
d'	Mean separation between mating surfaces, in.
E ₁ , E ₂	Modulus of elasticity of body number 1 and number 2, lb-in ⁻²
f	Friction coefficient, based on asperity interactions
F	Tractive force, lb.
FET	Field effect transistor
F _x	Tractive force in x direction, lb.
G ₁ , G ₂ , G ₃	Dimensionless traction parameters
h	Film thickness, in.
h _A	Separation of surfaces at differential area dA, in.
H	Friction load supported by the asperities, lb.
K	Dielectric coefficient
K _f	Thermal conductivity of lubricant, lb-sec ⁻¹ -°F ⁻¹
M, M ₁ , M ₂	Mean peak height distributions, in.
p	Pressure, lb-in ⁻²
P _{HZ}	Maximum Hertz contact pressure, lb-in ⁻²
P	Load, lb.
T	Temperature, °F
T _o	Inlet oil temperature, °F
T _r	Reference temperature, °F
U ₁ , U ₂	Rolling speed at contact of body number 1 and body number 2, in/sec

ABBREVIATIONS (Continued)

u_s	$ U_2 - U_1 $, in/sec
V	Normal load supported by the asperities, lb.
x	Coordinate in rolling direction, in.
z	Coordinate in axial direction, in.
Z	Nondimensional peak height
Z'	$Z_1 + Z_2$, in.
Z_1, Z_2	Peak heights of asperities on body number 1 and number 2, in.
α, α^*	Viscosity pressure coefficients, $\text{in}^2\text{-lb}^{-1}$
$\bar{\beta}$	b/a
β, β_1, β_2	Viscosity temperature coefficients, $^{\circ}\text{F}^{-1}$
ϵ_0	Permittivity of free space = 8.85×10^{-12} farad/meter
γ	Viscosity-pressure-temperatures coefficient $\text{in}^2\text{-}^{\circ}\text{F}\text{-lb}^{-1}$
μ	Viscosity, lb-sec-in^{-2}
μ_0, μ_r, μ_0^*	Base viscosity coefficients, lb-sec-in^{-2}
ν_1, ν_2	Poisson's ratio of body numbers 1 and number 2
Φ	Dimensionless function used in predicting traction
$\bar{\Phi}$	Dimensionless elastic separation parameter
Ψ	Dimensionless traction parameter
$\sigma, \sigma_1, \sigma_2$	Standard deviation of peak height distributions, in.
τ_x	Shear stress in x direction, lb-in^{-2}

Contrails

SECTION I INTRODUCTION

At the conclusion of Phase I of this research program, a compendium of the state-of-the-art of elastohydrodynamic technology was compiled and a computer program was prepared to predict elastohydrodynamic performance characteristics on the basis of the best available theory and experimental data. It was found that considerable data were lacking in areas such as, elastohydrodynamic tractions, measurements of elastohydrodynamic film thickness and general behavior of partial elastohydrodynamic performance. These data are badly needed to provide improved design criteria for concentrated contact elements, to predict regimes in which enhanced life of various concentrated contact elements will result due to thick film hydrodynamic lubrication.

As a result of these findings, it was decided to design and build an experimental apparatus for measuring tractions and film thickness under elastohydrodynamic lubrication conditions. This apparatus was to be in the form of a disc machine having the flexibility to run at high speeds over a wide range of loads and slip rates and to have provision for varying disc geometry.

It was decided to start by measuring traction data for polyphenyl ether under conditions similar to those used by Battelle (1)*. Polyphenyl ether was selected both from the basis of it being of interest to the Air Force and the availability of independently determined traction data.

During the past reporting period, the rolling disc apparatus was designed, fabricated and run. Traction data were obtained for polyphenyl ether over a range of Hertz contact stresses extending from 80,000 to 140,000 psi, rolling speeds varying from 900 in./sec to 1820 in./sec, inlet oil temperatures ranging from 100°F to 240°F and slip rates up to 100 in./sec. Special emphasis was placed on low slip behavior to make comparisons between MTI data and Battelle data which were all obtained in the low slip region.

Two twenty horsepower motors were used in driving the rolling disc test machine, while both the rolling speed and the slip rate were controlled. A chart recorder was synchronized with the slip rate, which facilitated obtaining data in the form of traction versus slip rate curves.

In general, trends in traction data showing the variation of tractions with load and with rolling speed were at least in qualitative agreement with Battelle's data. The effects of temperature on traction were not in qualitative agreement in that the Battelle data indicated strong effects of temperature whereas the MTI data indicated very weak effects of temperature.

The data were analyzed in various ways. Comparisons were made between MTI data and elastohydrodynamic performance computer code predictions (2), theoretical predictions based on Midwest Research Institute viscosity data, and predictions based upon an empirical viscosity relationship which was evolved to correlate and predict measured tractions.

* Numbers in parenthesis refer to references listed at the end of this report.

Contrails

In addition to traction measurements, some preliminary optical data were obtained statically under elastic contact conditions. Elasticity calculations were performed to predict the shape and spacing of fringe patterns which compare reasonably well with experimental data.

Work was begun in order to prepare for investigations into the partial elasto-hydrodynamic regime. An asperity contact counter was built and checked out which works on an electrical continuity principle. This device measures the number of times electrical resistivity falls below selected discrimination levels which are proportional to the extent of solid-to-solid and film thickness of the lubricant present. Analyses were performed to predict the frictional behavior resulting from asperity interaction. These analyses considered elastic and plastic asperity interactions from which predictions of frictional force, real area of contact, and fraction of load supported by asperity contact were obtained.

The following sections of this report consist of a detailed discussion of the experimental apparatus and procedures, a presentation of the traction data, and a comparison of traction data with other data and with theory. A description of the asperity interaction analysis is presented and a documented computer program for performing the computations involved in the analysis is included in an appendix to this report.

SECTION II

ELASTOHYDRODYNAMIC TEST APPARATUS

This section presents a review of the test facility designed and completed during the second year of a three-year program in elasto-hydrodynamic research. The major piece of apparatus designed and constructed over a six month period was a high-speed, high-load rolling disc assembly. Included are discussions of the traction measurement techniques as well as descriptions of the concepts to be employed for measuring lubricant film thicknesses and asperity contact.

Key details of the machine design and construction are included as a reference for future use. Through the years many elasto-hydrodynamic tests have been performed with a variety of contrasting results. If the future work in lubrication theory and experimentation begins to reveal the reasons for such discrepancies, it is hoped that the information documented here would be used to clarify or separate any test dependent features contained within a machine of this design.

Included are many comments on the operational performance which are intended as "experience factors" for those who may be involved in the "next generation" design of rolling disc equipment.

1. TEST RIG DESIGN

Since 1935 a wide variety of test equipment has been built for studying elasto-hydrodynamic phenomenon. In the majority of the experimental tests the primary quantities measured were film thickness and frictional traction. Machines combining balls, flats, and cylinders with positive and negative curvatures in a multitude of ways have resulted in many man years of pertinent investigations.

Machines designed with one, two, three and four rotating discs, with chain, gear and belt drives, have been by far the most common method of investigating various lubricating mechanisms. The simplest arrangement suitable for the determination of film thickness and friction, used over the years in most studies, is the two disc machine. In such a design (3) the support bearing losses must normally be added to the measured traction which in some cases obscured the desired measurement. This difficulty was overcome by Crook (4) with a four disc arrangement and by Gupta, Hamilton, and Hirst (5) with a three disc set-up which incorporates a central disc supported on gas bearings.

The elasto-hydrodynamic test rig discussed in the following pages is of the two-disc, flat-belt-driven variety. Problems associated with support bearing losses do not inhibit data acquisition in the present case for three reasons. First, the total traction versus slip curve is a real time output of the test rig and is normally plotted within a one minute period for most observations. This technique allows one to quickly determine the support bearing losses and to verify the consistency of that level for any long period of testing. Second, since the torques in the support bearings do not change rapidly with time, the

total traction versus slip curve presents a simple way, through symmetry, of determining the effects of the support bearing system. Third, the present study was initiated for investigation of traction levels well above the basic torque level which exists in the support system used.

2. THE TEST FACILITY

Critical investigations of rolling contact phenomena and elastohydrodynamic lubrication require the use of a machine having a variable slide/rolling ratio as well as precise measurable tractions. In addition, precise control and readout of disc speeds and temperatures are required.

The present machine design began with the concept of incorporating as many variations of test parameters as could be allowed by the original test objectives. These objectives were to obtain state-of-the-art traction measurements and film thickness measurements using (1) capacitive (2) optical, and (3) x-ray techniques of measurement on one test rig. In addition, several ranges of required surface velocities, Hertzian contact loads, and lubricant temperatures were to be met with any proposed concept.

After evaluating several rolling-disc-rig concepts which would incorporate the three techniques of measurement, the simple two-disc arrangement was chosen as the most promising geometric arrangement. Figure 1 shows the conceptual features of the machine constructed. The selected test rig had to meet the following criteria:

1. Access must be available for detecting dynamic film thicknesses using capacitive, optical and x-ray techniques.
2. Total traction versus slip curves must be obtainable from the torque detection technique employed for determining the friction which exists between the rolling discs.
3. Disc surface speeds as well as speed differentials to be outputs of the test facility. Surface speeds up to 2400 in./sec must be achievable.
4. Hertz pressures approaching 500,000 psi should be attainable in the final scheme.
5. Test lubricant temperatures to be kept constant within $\pm 1^{\circ}$ F from ambient room temperature to 200° F, $\pm 2^{\circ}$ F between 200° F and 300° F, and $\pm 5^{\circ}$ F above 300° F.
6. Dynamic measurements of asperity contact between the rolling discs to be monitored during some tests.

The test facility, as completed, is shown diagrammatically in Figure 2. The constructed facility:

1. Allows the determination of lubricant film thicknesses by measuring the variations in capacitance of one electrically isolated disc relative to the other.

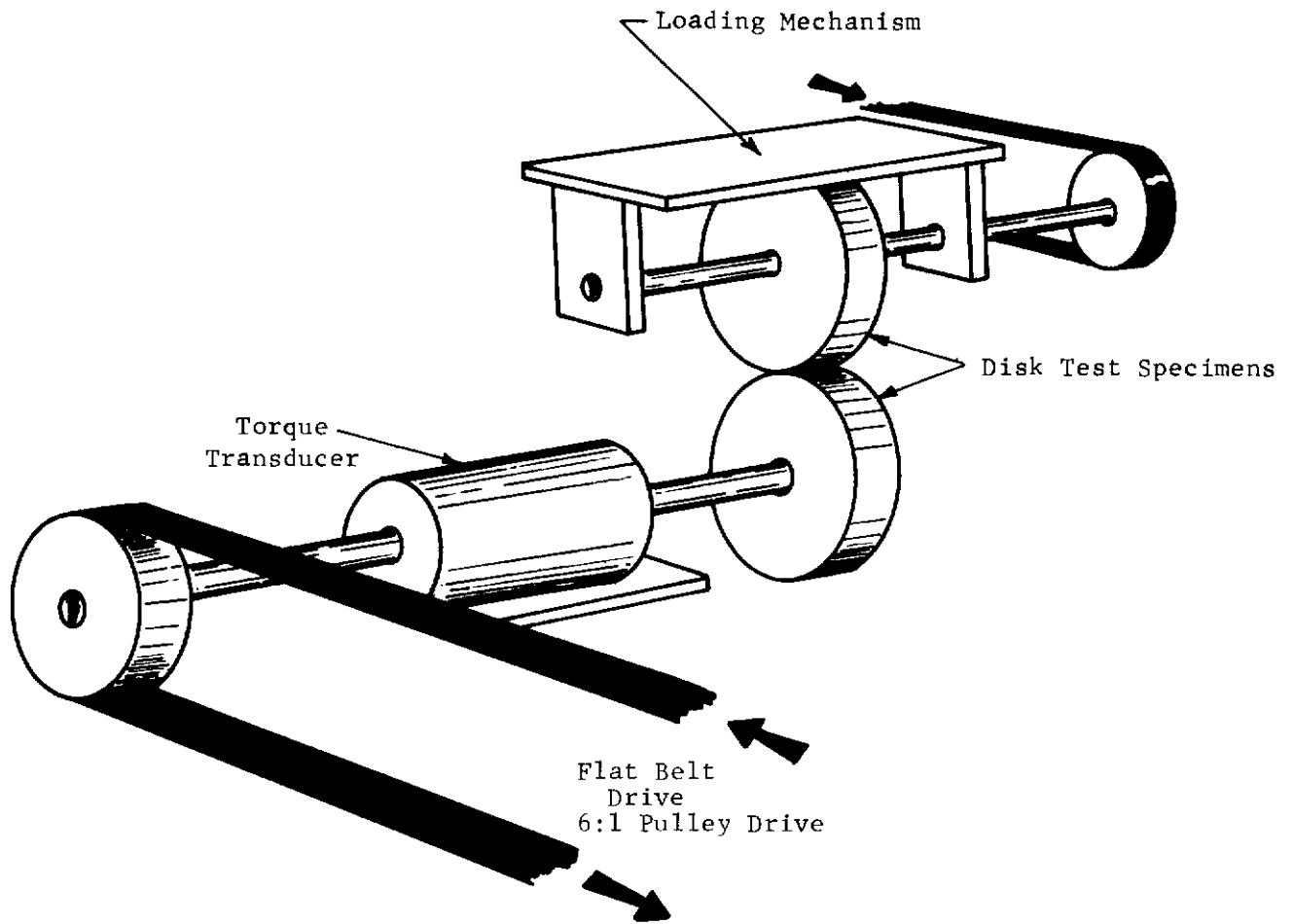


Fig. 1 The Disc Machine: Conceptual Layout

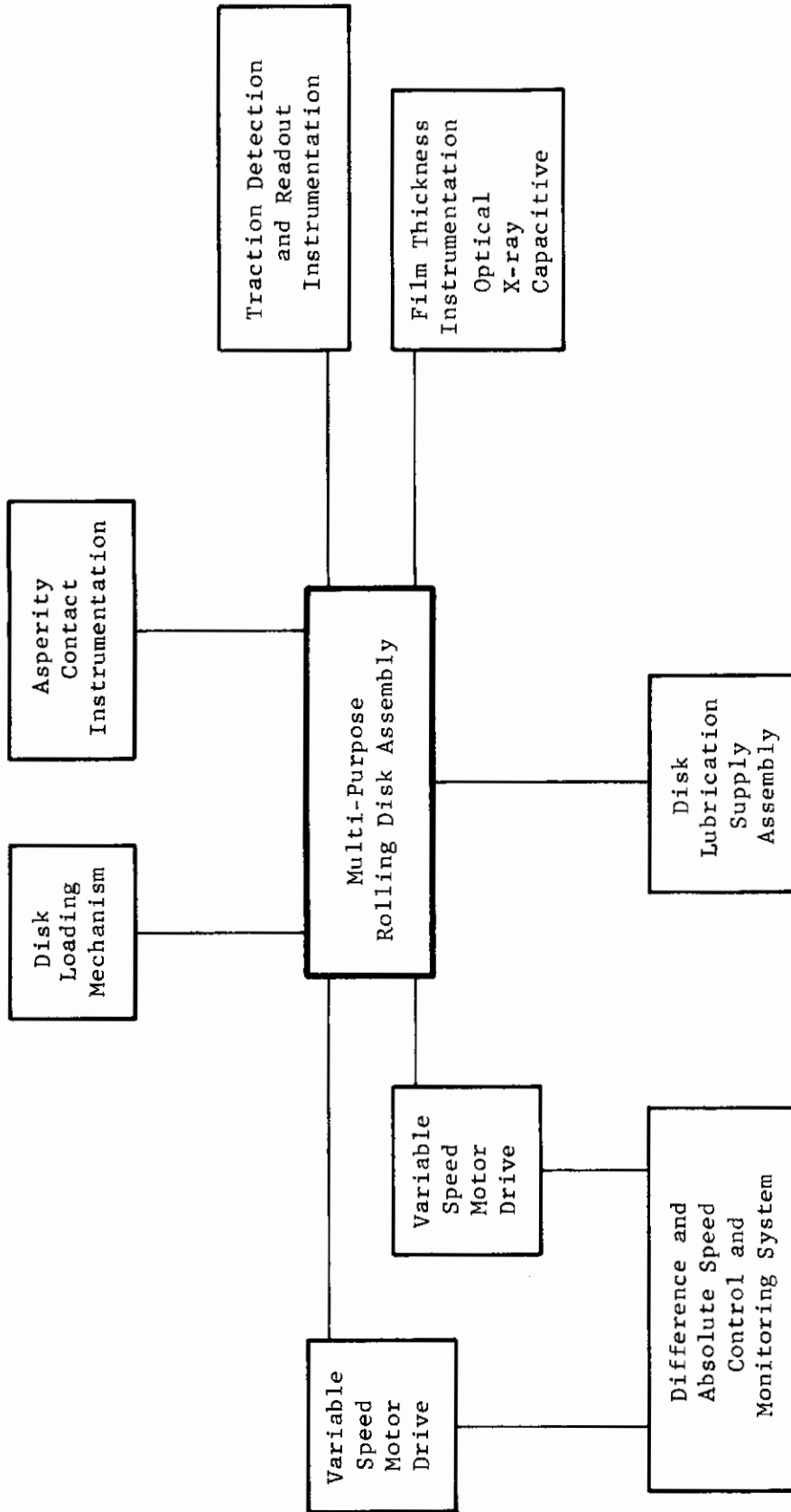


Fig. 2 Elastohydrodynamic Test Facility

Contrails

2. Allows visual observance of the contact zone with the aid of a hollow split shaft and an optically polished quartz disc specimen.
3. Contains access ports in the direction of rolling, which facilitate x-ray detection of lubricant film thicknesses.
4. Has radial loading capability from zero to twelve thousand pounds. Depending upon the specific geometry of the test specimens, this variation in loading can yield Hertz contact pressures up to 500,000 psi.
5. Provides for varying the test disc diameter and material as well as surface finishes and curvatures. The test discs are mounted on split shafts which facilitate interchangeability. Test diameters from a minimum of 2.5 inches to a maximum of 6.0 inches can be run on the machine.
6. Contains two variable speed twenty horsepower drives which can turn the specimens at any selected rotational frequency between 500 rpm and 15,000 rpm. With a three inch diameter disc one could investigate tractions, using rolling velocities from 100 in./sec to 2400 in./sec, with the turn of a knob. Additional test specimen diameters can be chosen for extended studies into higher and lower speed ranges. A six inch specimen would allow 4800 in./sec rolling speeds whereas a 2.5 inch diameter would permit studies as slow as 80 in./sec.
7. Allows the test lubricant to be varied over a wide range of temperatures and maintained for extended test periods of a day or more. The test lubricant is also used for the main shaft support bearings and can be operated normally with all seals and bearing materials to 300° F. A large reservoir (40 gal.) is used to insure controlled temperature stability of $\pm 1^{\circ}$ F for periods of thirty minutes or less and $\pm 3^{\circ}$ F over longer periods even while supplying one-half gallon per minute to the contact zone.
8. Has an internally mounted torque sensor capable of detecting positive and negative torques up to 200 inch-pounds with an output resolution of .1 inch pounds (See Figure 1).
9. Provides electrical isolation for one test roller specimen for electrical asperity contact measurements across the contact zone.
10. Contains one shaft mounting plate which allows nineteen skewed test rolling directions up to 90° in 5° steps.
11. Has individual magnetic speed pickups with toothed wheels mounted on each rotating shaft for precise speed monitoring and/or control. An electronic speed controller is attached to a pair of these for accurate maintenance of speed differentials between the rotating shafts.
12. Contains twenty-four copper-constantan thermocouples which are continuously monitored and recorded during all test runs. Fourteen points of temperature detection, within six inches of the contact zone, are monitoring inlet and outlet lubricant temperatures as well as that of the support bearings.
13. Has a four ton base upon which the mechanical components are mounted

for reducing inherent vibrations from the drive motors.

A front view of the mechanical assembly is pictured during the construction phase in Figure 3. A cross-sectional view of the rig taken through the upper and lower shaft centers is shown in Figure 4.

A detailed review of each aspect of the mechanical and instrumented set-up is presented in the following paragraphs. Explained in separate sub-sections are features of the traction detection, optical, capacitive, and x-ray film thickness measuring concepts as well as asperity contact methods.

3. ROLLING DISC MACHINE DETAILS

The rolling disc machine used during the initial test period reported here is a large device (fills a ten foot square test cell) and has many parts which must be handled with an overhead chain hoist. A list of the MTI rolling disc design drawings is presented in Appendix I. Included in Appendix II is a list of test components and commercially available instrumentation used during the testing.

a. Base Plate and Pedestal

The bottom plate for the rolling disc machine as depicted in Figure 4 was made from a single grey metal casting which weighed approximately one thousand pounds. In order to insure vibration free running, the bottom plate is mounted on a concrete pedestal also shown in Figure 5. The seismic mass pedestal, isolated from the concrete floor of the test cell, holds the twin motor drives for the upper and lower shafts of the rig.

The concrete pedestal is topped off with a Blanchard ground mounting plate which is level to within $\pm .002$ inches over the ten square feet of mating upper surface. This is necessary since the grey iron, when cast in the length to thickness ratio as used in the bottom plate of the test rig, will bend or flex if placed upon a curved irregular surface. In addition, the alignment of the lower shaft bearing supports is necessary since they were machined into the casting. This alignment must be maintained for precise high speed operation.

The basic assembly is a very large structure with many precise components which required careful handling during build up. The base plate, though ground with a flatness of two mils on the bottom, had to be hand scraped in order to insure uniform surface contact over the total base mounting plate of the concrete pedestal.

The machine bores which house the upper and lower shaft bearings were done with extreme care. An on-site inspection during machining indicated the lower shaft bores to be within one half of a mil of perfect alignment over the total thirty-six-inch space. The upper shaft bores were found to be within three-tenths of a mil of perfect alignment.

During assembly, dial indicator measurements were taken to assure the

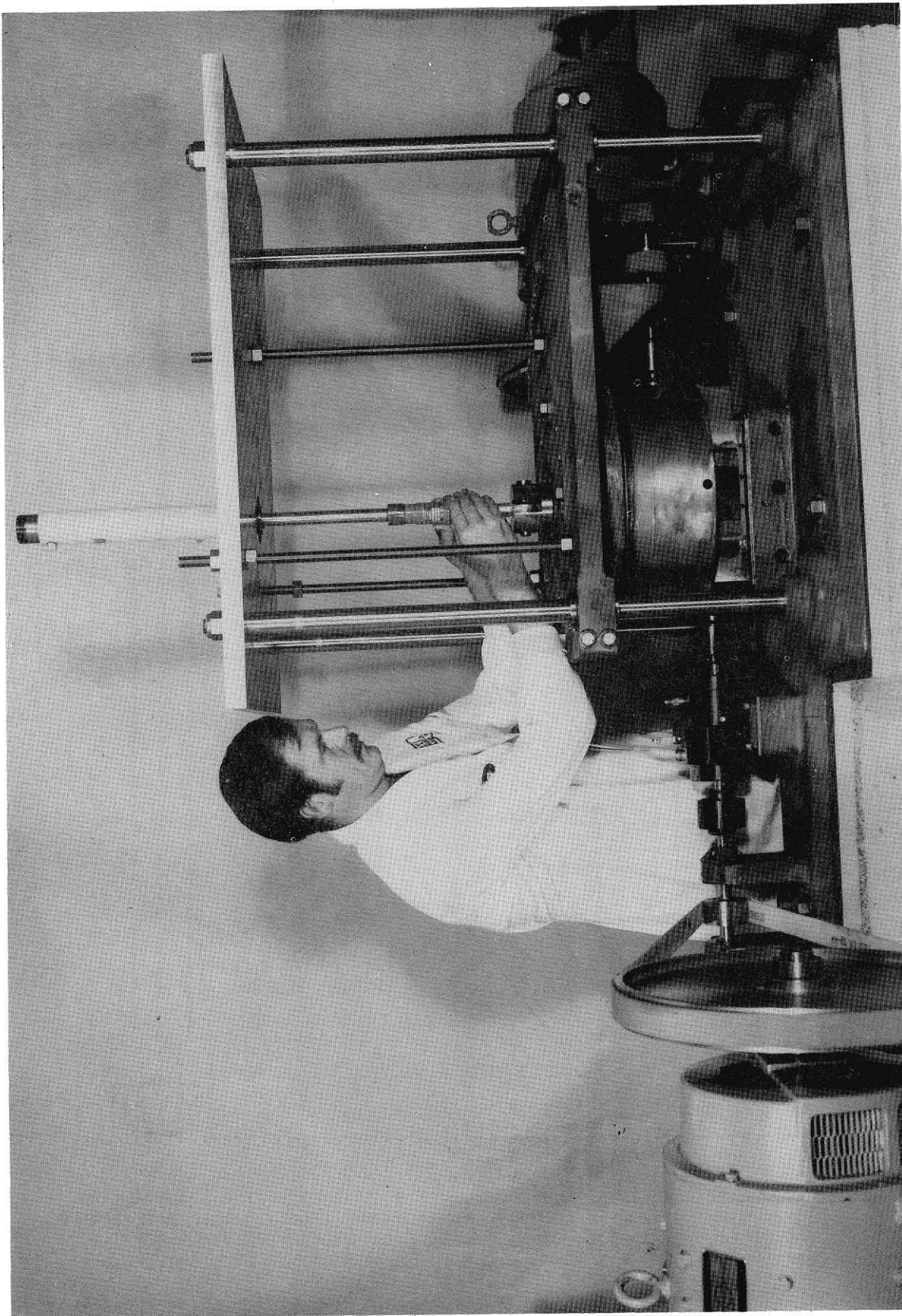


Fig. 3 Rolling Disc Machine During Construction

**HIGH-SPEED HIGH-LOAD
ELASTOHYDRODYNAMIC
ROLLING DISK ASSEMBLY**

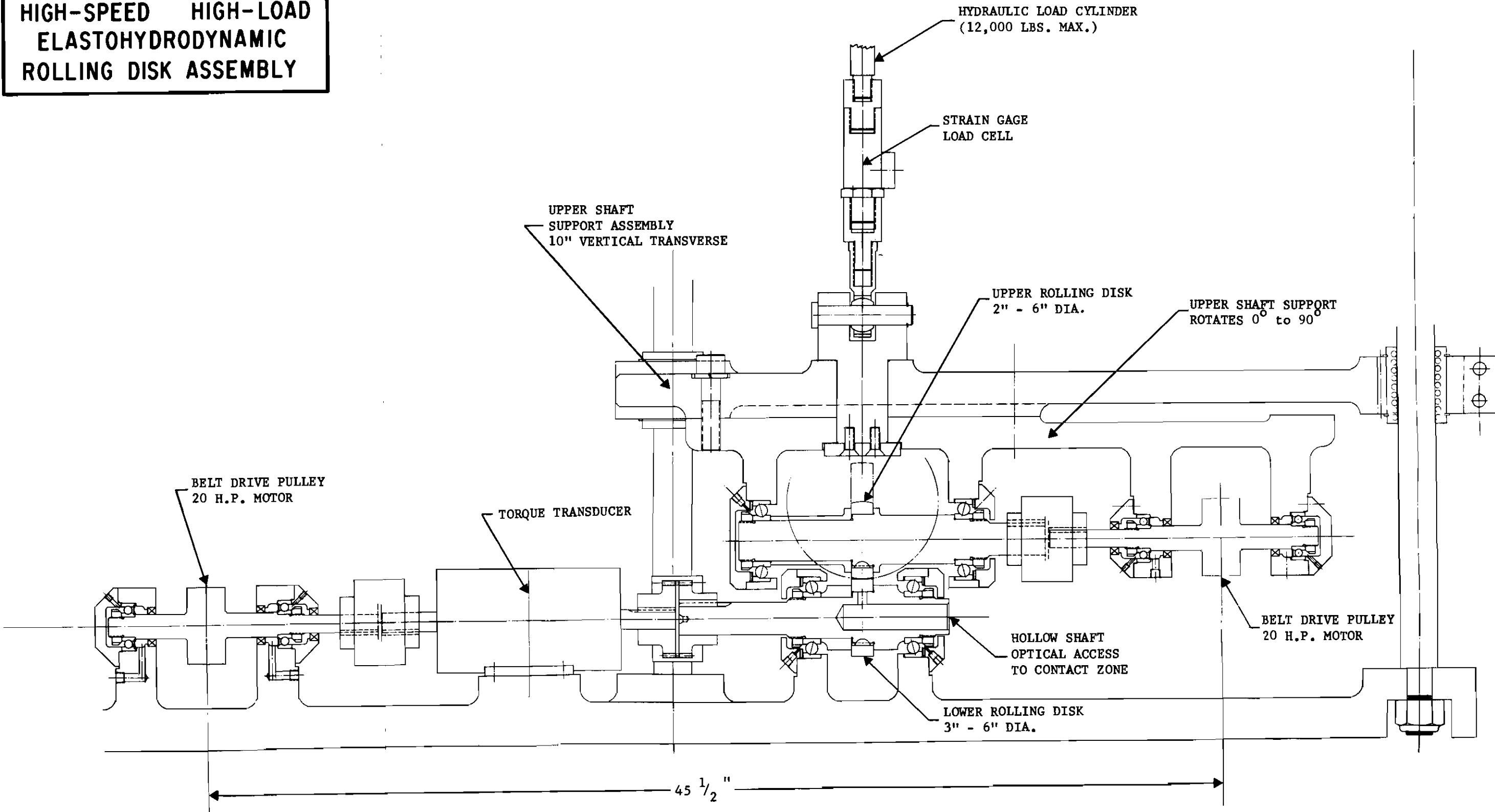


Fig. 4 Rolling Disc Machine: Front View Cross Section

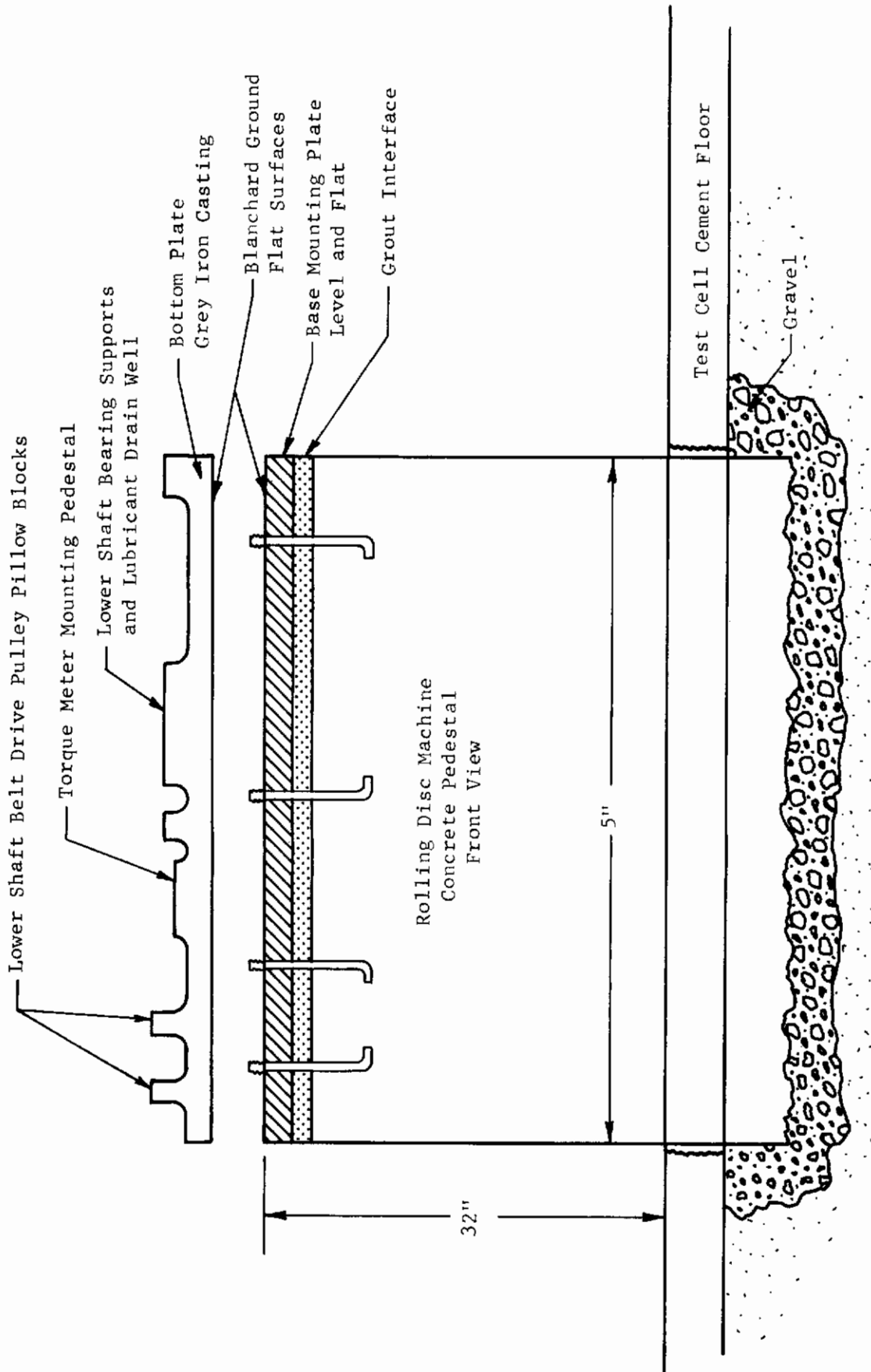


Fig. 5 Front View of Rolling Disc Machine Base Pedestal Assembly

Contrails

alignment of the pulley shafts with the respective specimen carrying shafts. A run out of plus or minus one mil was maintained on the mounted upper shaft while a tolerance of plus or minus two mils was obtained on the assembled lower shafting.

Each twenty horsepower variable speed motor was fixed to the floor of the test cell in proper alignment for operation on its own isolation pedestal. The relative positioning of the drive motors and rolling disc machine are sketched in Figure 6. The result of this care in mounting construction is a smooth operating pair of shafts over the full range of speeds to 15,000 rpm. The largest source of noise in the running assembly (which is by no means transmitted at undesirable levels during operation) is the windage of the belt as it moves with speeds near 2000 in./sec.

b. Temperature Detection

The detection and control of the lubricant temperature in any elastohydrodynamic study is essential. No attempt was made during the past year to experimentally pinpoint the temperature in the contact zone itself. Although, with the present set-up, specimens could be made and operated which contain embedded thermocouples or optical paths for infrared sensing, the standard copper-constantan junction was used exclusively for determining the fluid temperatures in the present rig. Twenty-four points as indicated diagrammatically in Figure 7 were monitored during all test periods.

Fourteen points of temperature near the disc contact zone were of special interest and are shown in a full-scale sketch (See Figure 8). All thermocouples were read out and recorded with an accuracy of $\pm 1^{\circ}$ F on a Honeywell, Brown Instruments Division "Elektronik-Continuous Balance Unit." Detection of inlet lubricant temperatures were made with the aid of four copper-constantan junctions placed inside the contact zone lubricant supply tubing. Two small holes were drilled into each tube and were placed at distances of one-quarter and one inch from the end of the lubricant spouts. A thermocouple bead was inserted into each hole and sealed with silicone rubber sealant as depicted in the sketch of Figure 9. Two additional thermocouples were placed in contact with the surface lubricant present on the test specimens during operation. Their circumferential orientation is indicated in Figure 8. The trailing temperature was taken from the midpoint of the polished specimen in the running track of the disc contact zone. It was strictly a qualitative indication of the increase in temperature of the lubricant which has passed through the pressurized zone of the loaded discs. Temperature increases of 15° F have been observed in the outlet stream during some of the test runs made.

c. Speeds Monitored and Controlled

Shaft rotational frequency monitor and control was accomplished with the aid of toothed wheels and magnetic probes. Four such pickups

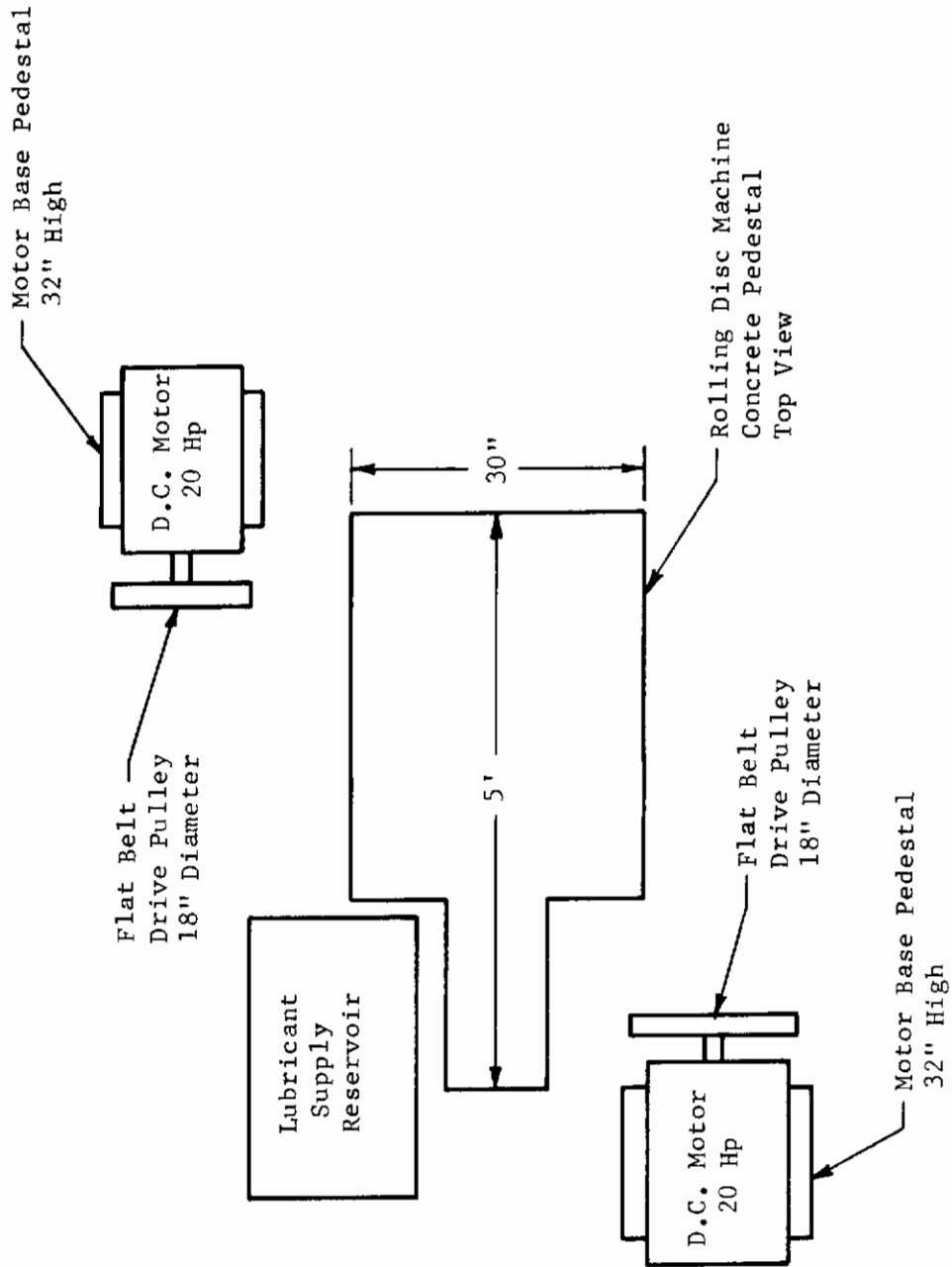


Fig. 6 Top View of Rolling Disc Machine Base and Motor Drive Layout

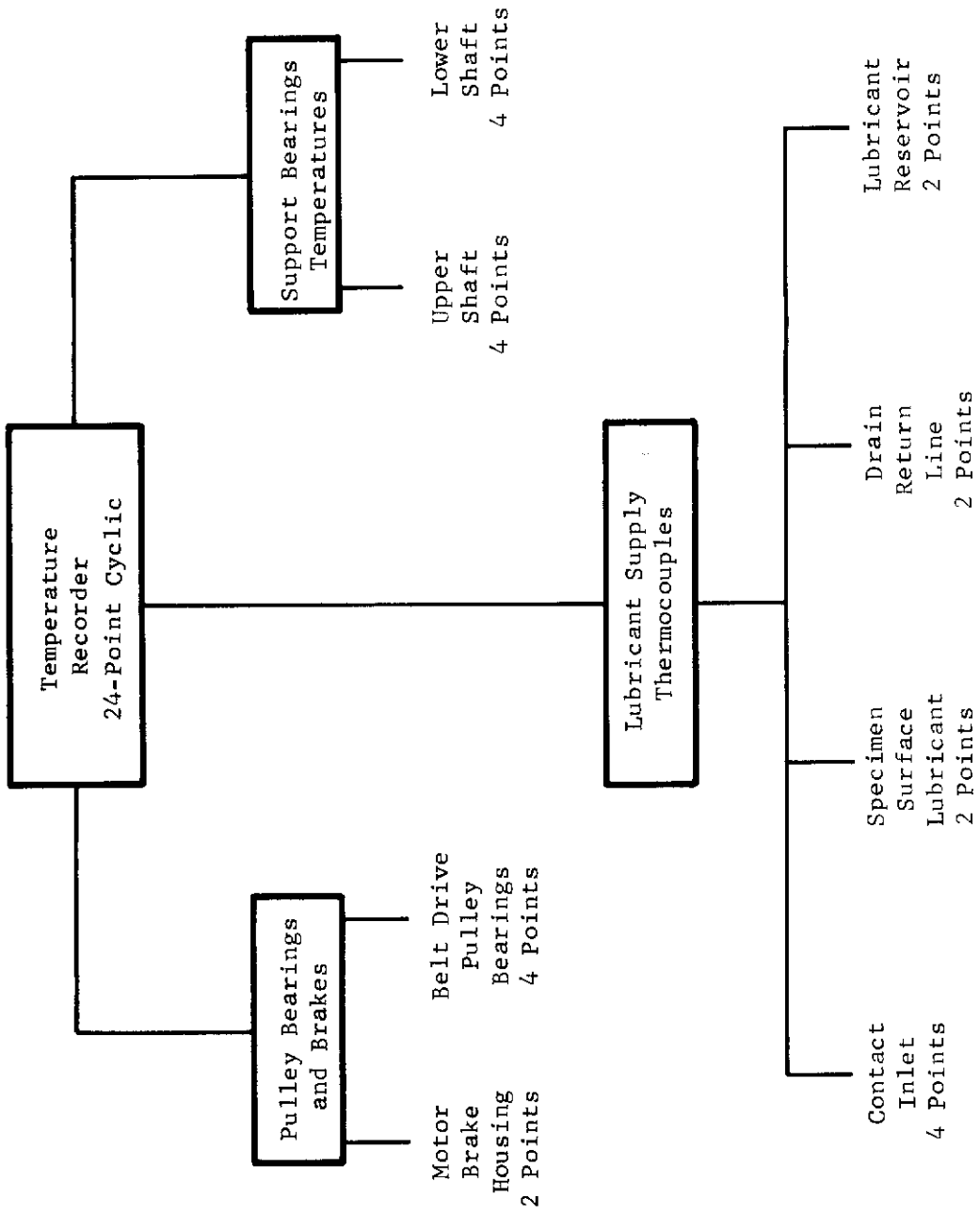


Fig. 7 Thermocouple Detection Points in Rolling Disc Machine

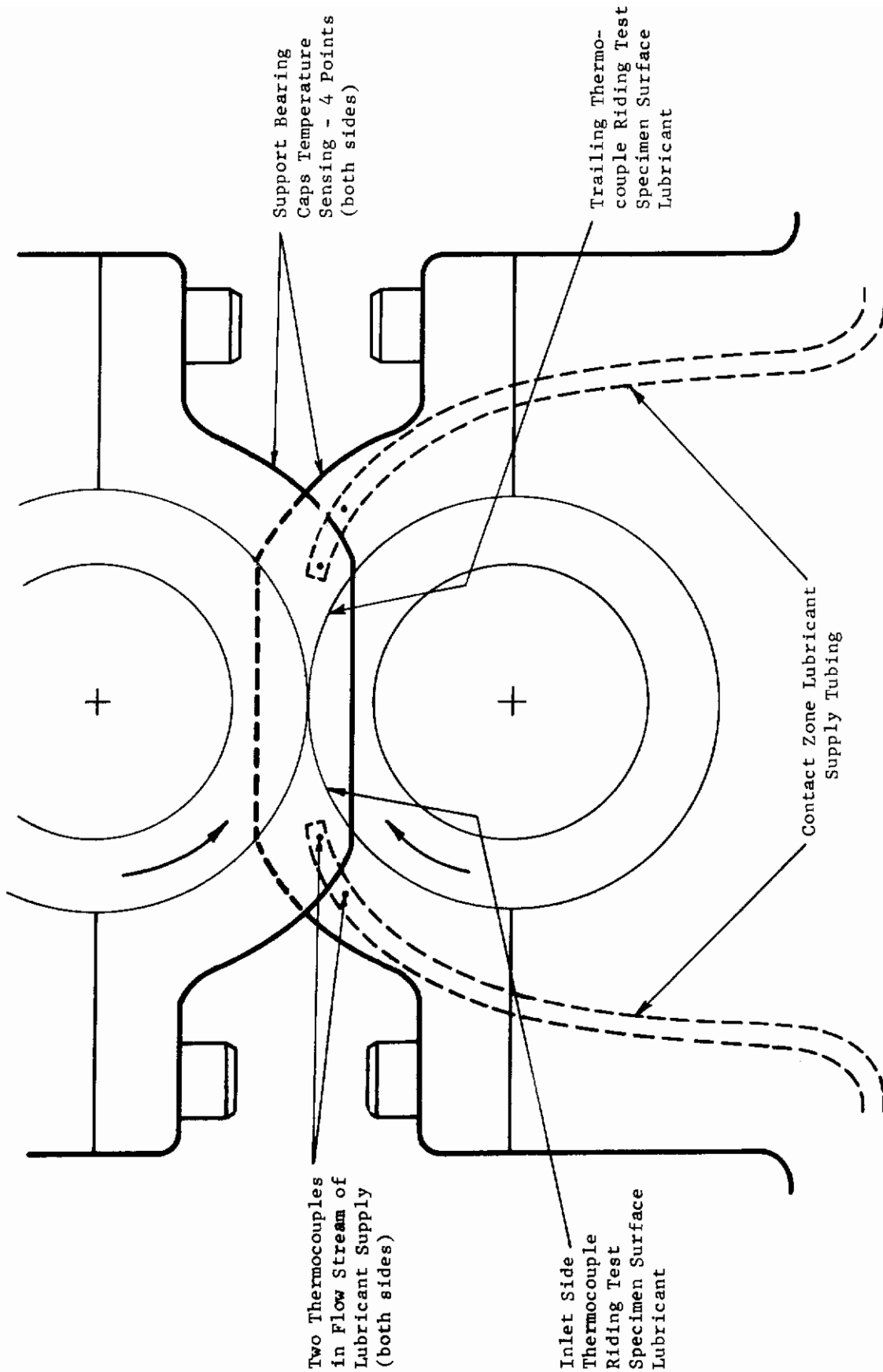


Fig. 8 Full Scale Side View of Mounted Rolling Disc Specimens Showing Thermocouple Placement Near Contact Zone

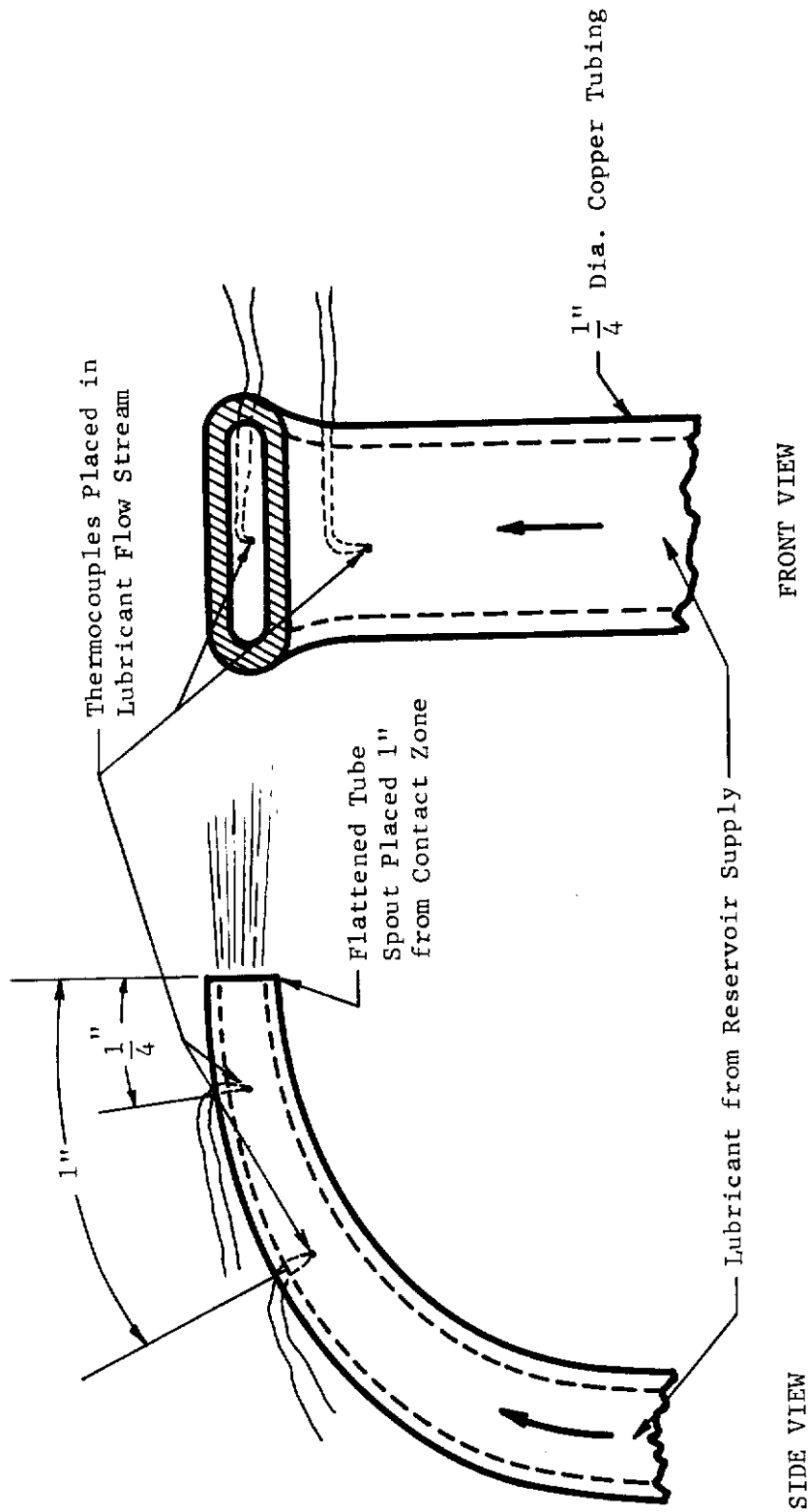


Fig. 9 Temperature Sensing Details of Contact Zone Supply Lubricant

Contrails

were incorporated in the present system. Two magnetic pickups are contained in the twin motor drives and speed ratio controller system. The two additional magnetic sensors are placed directly on the test upper and lower rotating shafts. A schematic of the motors rotational frequency sensing, shaft monitoring, and ratio control system is presented in Figure 10.

In setting the base rolling speed for testing, the reference motor is manually pre-adjusted by a potentiometer on the drive power supply. The second shaft can be manually adjusted through various disc slip speeds or fixed with electronic feed back control to any differential speed relative to the reference motor speed setting. This second mode of operation is desirable whenever constant slip rates must be maintained for long periods of time. Traction dependence upon contact lubricant feed methods, lubricant temperature, and rolling speed changes can be examined with the constant differential speed control system.

As shown in Figure 10 the speed differential monitoring system and motor control system are separately operated units. The tachometer monitoring system designed to measure the differential frequency of two rotating shafts, using individual 60 toothed gears and magnetic pickups located on each shaft (see details of electrical hook-up in Figure 11).

In addition to plotting the speed differential on the x-y recorder, two points of speed are noted during the testing from the components shown in Figure 11. The speed pickup signals are placed into the horizontal and vertical axes of an oscilloscope. The circular Lissajous figure produced is used for precise referencing of the pure rolling state of the test specimens. The absolute rolling speed of the reference motor is also obtained with the parallel connection of a digital frequency indicator accurate to ± 1 rpm.

The tachometer was built by Mechanical Technology Incorporated personnel and was designed to be insensitive to component degradation or temperature changes. It consists of two matched tachometers one of which produces a positive DC voltage proportional to test shaft rotational frequency while the other is negative. The outputs are then summed and amplified to produce a DC signal voltage which is equal to one volt per one hundred rpm of differential frequencies in the operating rolling disc machine shafting. A block diagram of the device is presented in Figure 12. The magnetic pickup which views the toothed gear on the shaft produces a quasi-sinusoidal voltage with an amplitude which is proportional to the shaft rotational frequency. Since only the sinusoidal frequency is desired for detection the first stage of the tachometer contains an integrator which maintains a constant voltage output for any running speed of the rolling disc machine between one and fifteen thousand rpm.

The constant amplitude output of the first stage integration is applied to a comparator to produce a square wave which is subsequently

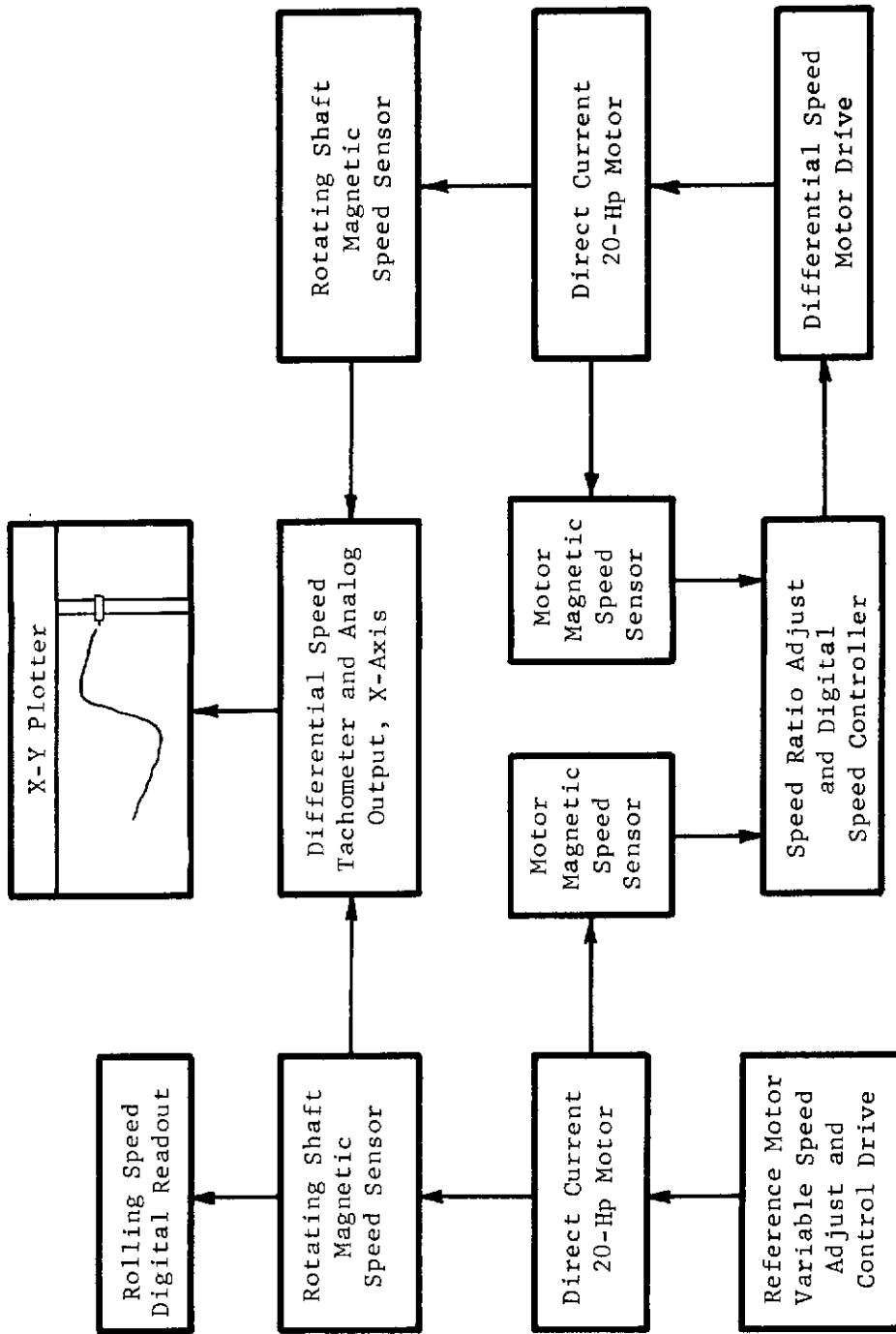


Fig. 10 Motor Speed Sensing, Shaft Rotational Frequency Monitoring and Control Schematic

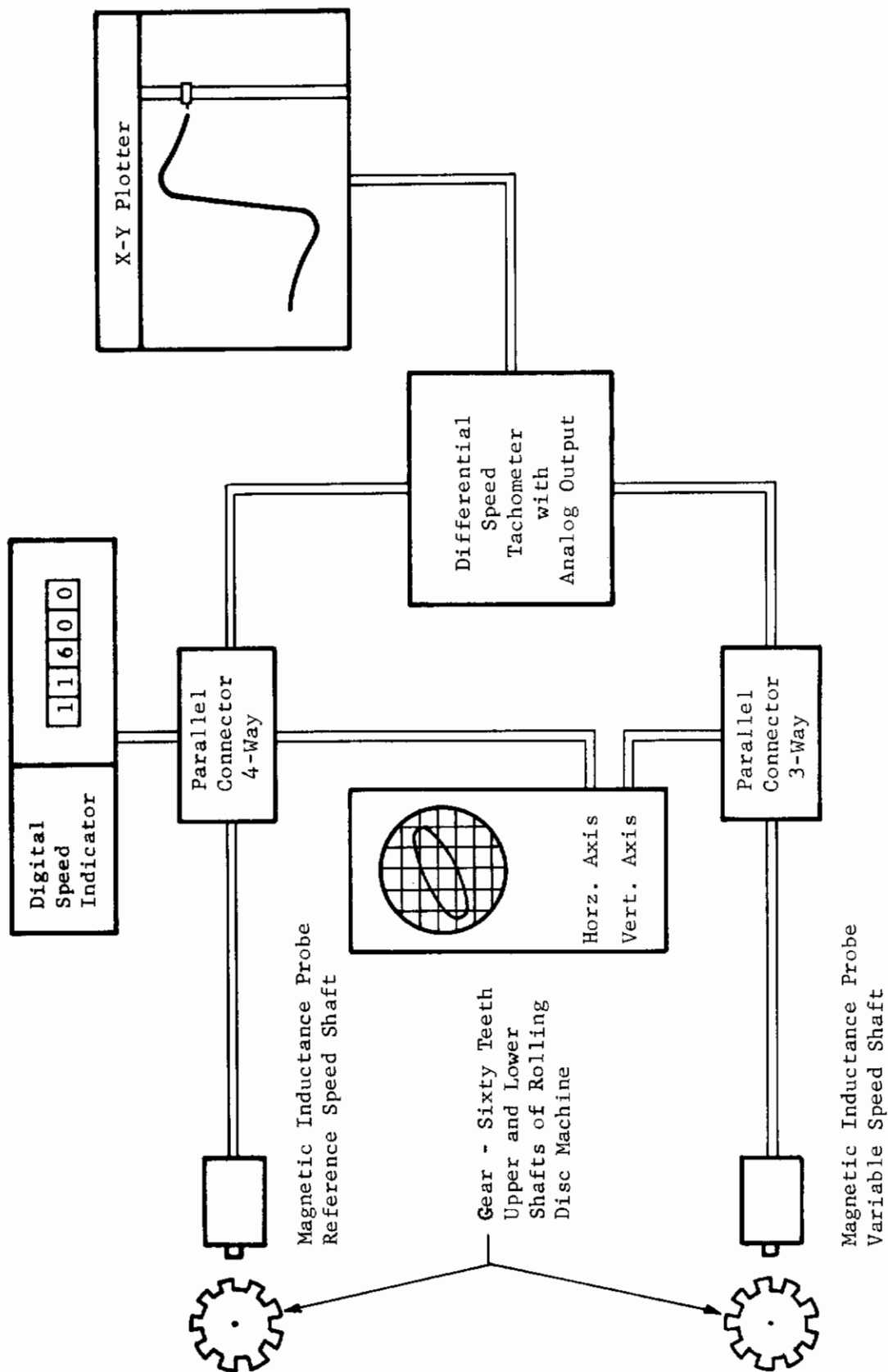


Fig. 11 Details of Speed Monitoring Electrical Hook-Up with Oscilloscope for Precise Pure Rolling Speed Check.

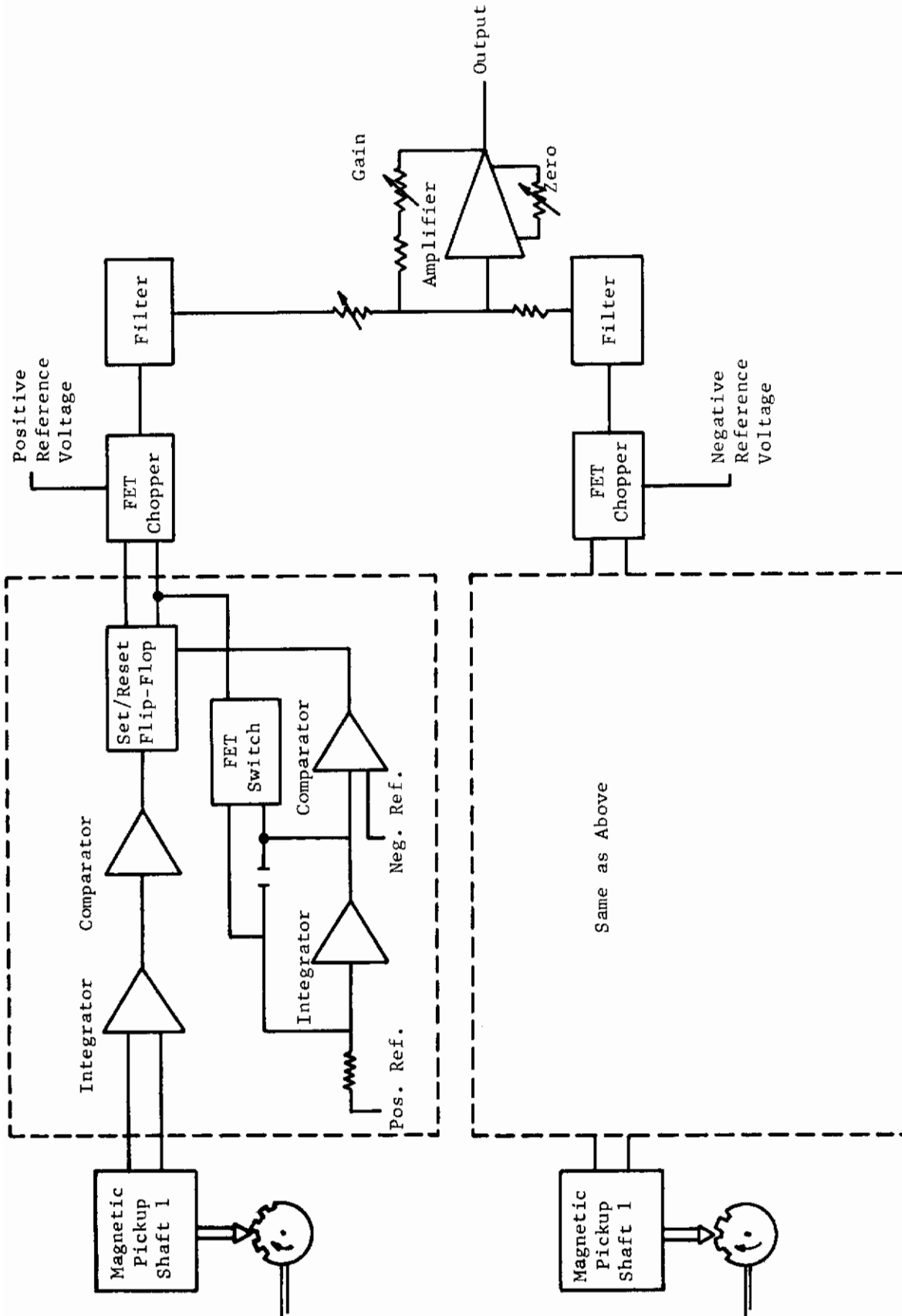


Fig. 12 Electronic Tachometer with Direct Current Analog Voltage Output

Contrails

differentiated and used to operate one side of a set/reset flip-flop. The other side of the set/reset flip-flop is operated from a second integrator. For example, assume that the flip-flop is in the reset state and the integrator switch is closed. A pulse from the input comparator sets the flip-flops, thus opening the switch on the integrator and allowing the output to begin a linear ramp voltage. When the output ramp reaches the reference limit on the comparator, the change of state of the comparator resets the flip-flop which closes the switch and resets the integrator. The circuit is now in the original state, so that the next pulse from the input comparator will restart the cycle.

The circuitry to this point has produced a pulse whose width is precisely known and which depends only upon the product of the resistance-capacitance (RC) value of the second integrator in the network. Since these are precision components, the pulse width is very stable for long periods of time (weeks) and over a wide range of operating temperatures ($\pm 20^{\circ}$ F).

In addition to controlling the internally generated pulse width, the amplitude of the signal must also be closely controlled in order that the tachometer may work with accuracy. This is accomplished by using the flip-flop output to drive a FET chopper which is connected to a precision reference voltage. The output of the FET switch is thus a pulse with the amplitude and width closely controlled. This output is applied to a filter to produce a DC voltage that is proportional to input frequency.

The filtered outputs are then connected to a summing amplifier which produces a signal proportional to the difference in speeds of the observed rotating shafts. The output amplifier contains adjustments to match the slopes of the two circuits, a zero offset, and a gain adjust.

The differential frequency tracking capability of the tachometer depends upon the rate at which the inertial rotating system can fluctuate as well as the electronic time response of the system. In the present case, differential speed resolution capability of the tachometer is at least ten times better than what can be maintained in the mechanical system. As the load on the contact zone is increased, the torsional feedback from motor to motor across the contact zone increases and slip versus traction curves can be drawn with smaller and smaller slip rates on the abscissa of the x-y plotter.

Typical traction versus slip curves, with the abscissa in engineering units of ten revolutions per minute of differential rotational frequency for each inch of x-y plotter pen travel, have been taken. These curves have been plotted with very light Hertzian loads (80,000 psi) over the full range of rotational frequencies from 5000 rpm to 12,000 rpm. Curves with units of two revolutions per minute of differential frequency have been obtained with loads of 140,000 psi Hertzian contact loading over the same range of rolling speed changes. As the contact loading is increased, the differential speeds between

Contrails

the discs can be detected with increasing accuracy. Resolved speed differences of .5 rpm out of 10,000 rpm are typical with the present tachometer system.

Precise long term speed regulation in the rolling disc assembly cannot be obtained with accuracies approaching the output resolution of the speed monitoring system mentioned above. Factors such as variations in line voltages, temperature excursions, generated variable motor loads, bearing wear, and servo-loop feedback time delay all play a part in limiting the ability to control the rolling disc speeds.

Relative disc rotational speed differences were considered as the most important speed parameter to regulate in the present system. As previously shown in Figure 10, speed regulation is maintained with the speed controller whose output is determined from magnetic input pulse generators placed on each motor. Basically, the controller compares the two incoming magnetic pulse rates and produces a correction voltage proportional to the difference between a pre-selected value and the observed ratio of incoming pulses. One motor is used as a reference while the other is made to follow with a selected preset differential speed. This type of speed control allows testing under conditions which require constant slip rates to be maintained with high accuracy for periods ranging from several minutes to an hour or more regardless of the variations in test environment.

The reference motor, which determines the rolling speed in any test, is driven and controlled by a standard silicon controlled rectifier (SCR) unit which maintains the base speed within $\pm 1\%$ of the running speed. Under high loading (more than 10 horsepower) the base speed has been observed to shift by as much as $\pm 3\%$. Some of this error can be attributed to the present SCR units since they are only capable of driving the motors in the direction of increasing speeds. Whenever the traction at the test specimen contact zone becomes large, due to loading and/or slip, the slowest motor might be overdriven and out of control. This condition has been circumvented in the present rig with the aid of two air disc brakes. Each motor is "artificially" loaded with a torque higher than that which can be transmitted by the contact zone and only requires the unidirectional drive control.

The present rolling disc facility has differential speed control to within $\pm .1\%$ of the base running speed for extended periods of an hour or more under light load conditions (100,000 psi or less). With higher loads on the test specimens the torsional feedback between motors produces a stabilizing effect which results in even greater accuracy. This means that shaft frequencies within 10 rpm of any selected difference may be maintained at a running speed of 10,000 rpm while varying parameters such as lubricant flow to the contact zone or temperature of the inlet lubricant.

d. Lubricant Supply

The rolling disc assembly, as designed, was not intended for testing with small volumes of lubricant (i.e., one gallon or less). It was assumed from the start that most testing would require a minimum of thirty-five gallons for normal operation. The primary concern was to obtain a stabilized thermal test assembly with minimum heat exchange required. The dispensing system is shown in Figure 13. It is a commercially available unit with lubricant supply reservoir, heating coils, and heat exchanger included. The seals throughout the lubrication network are Viton-A. This includes those for the gear pump assembly, the heat exchanger, and the lubricant filter mechanism.

The test lubricant supplied to the contact zone is also used in the main support bearings of the disc machine. As the lubricant leaves the heated sump, it passes through the pump, heat exchanger and filter and is then fed through copper tubing to the contact zone or support bearings. The output capacity of the pump which is viscosity dependent is greater than 2.6 gallons per minute with a back pressure of 35 psi. The specific volumetric flow to the contact zone is shown in Figure 14. A needle valve was used to control the amount of lubricant supplied to the contact zone which could be regulated from very small amounts to 1000 milliliters per minute at 140° F or 2000 milliliters per minute at 200° F operating temperature.

Flow to the contact zone was shown on a previous figure (Figure 8) in a full scale side view of the outlet end of the supply tubing. The positioning of the tubing was such that the outlet stream was aligned with the rolling direction of the test specimens. Initial placement of the tubing was at an angle to the rolling direction which resulted in the traction data varying with lubricant supplied. This led to some preliminary studies of the dependence of traction on flow supplied to the contact zone. (See the section on Traction).

Lubricant at the test temperature is also pumped into the four main shaft support bearings. These are unsealed, preloaded, angular contact bearings which are mounted in pedestals of the upper and lower casting (shown previously in Figure 4). Each bearing is supplied with lubricant through ports in the casting pedestal supports. This arrangement insures a positive flow of lubricant on either side of the test specimen on the ends of the support shaft. The shaft supports with this lubricant supply arrangement were never more than 20° F cooler than the test contact zone and in most cases were within 10° F of the test operating temperature.

e. Torque Detection

A schematic of the torque detection, signal conditioning and readout method is shown schematically in Figure 15. The main sensing unit was an in-line rotating torque detector consisting of a square metal shaft to which is attached a Wheatstone Bridge strain gage circuit.

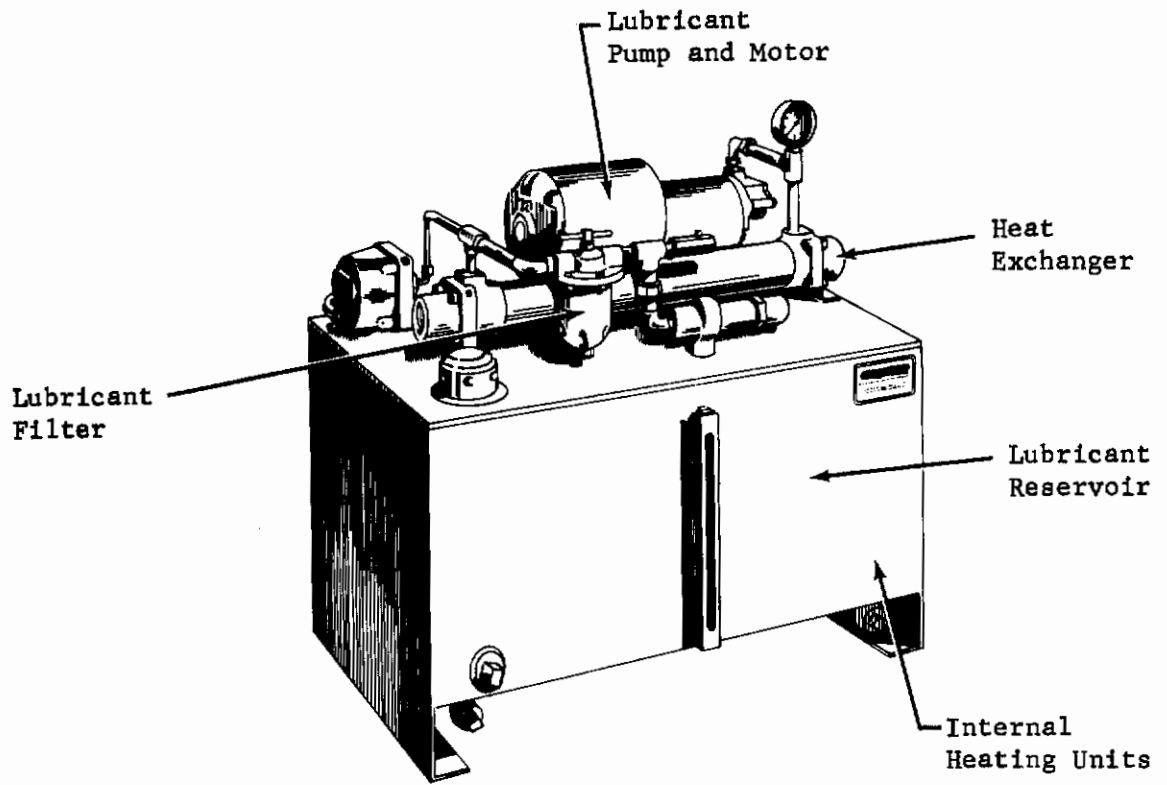


Fig. 13 Rolling Disk Assembly Lubricant Dispensing System with Heat Exchanger

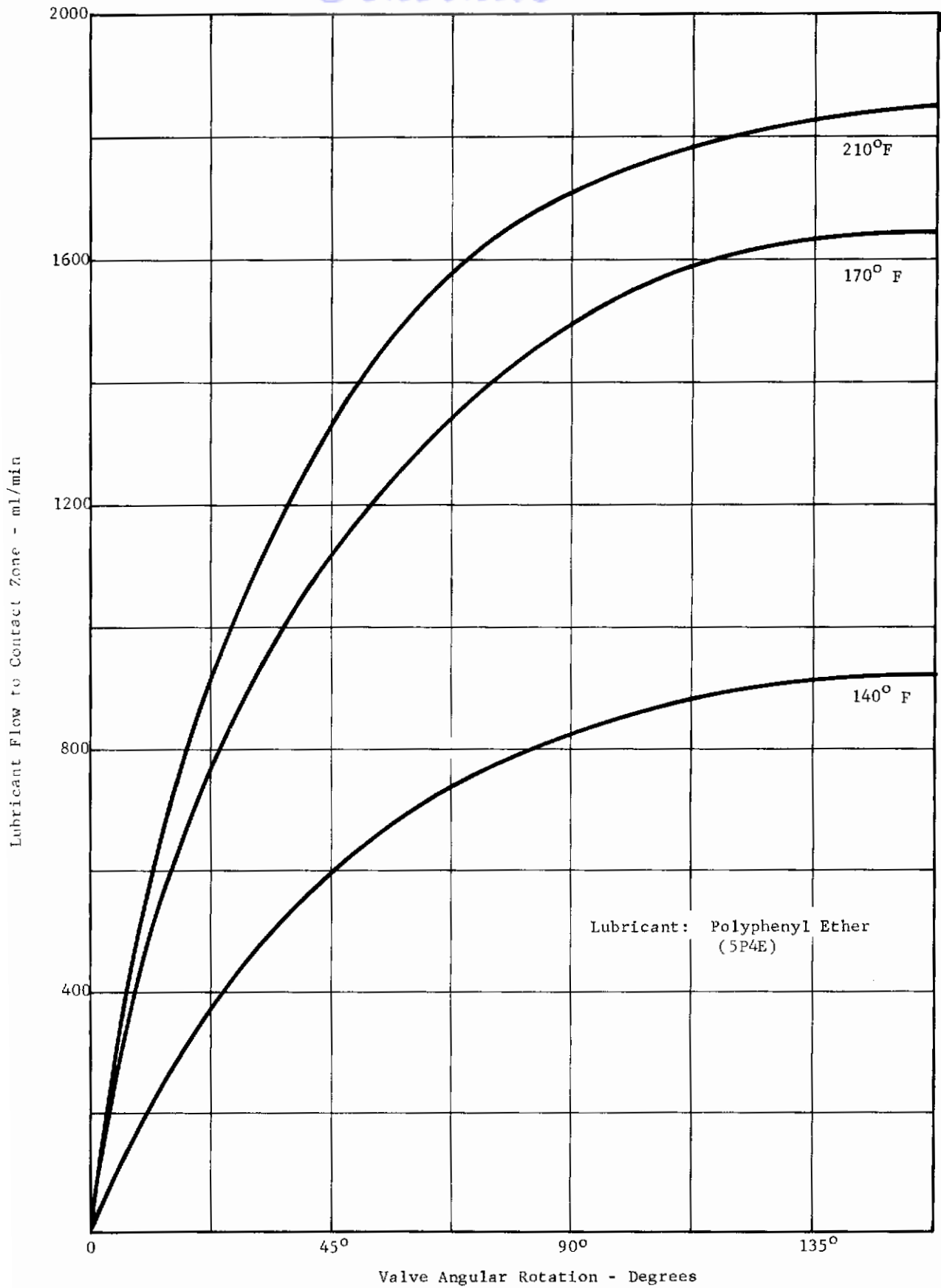


Fig. 14 Contact Zone Lubricant Flow From Needle Valve Control for Three Operating Temperatures

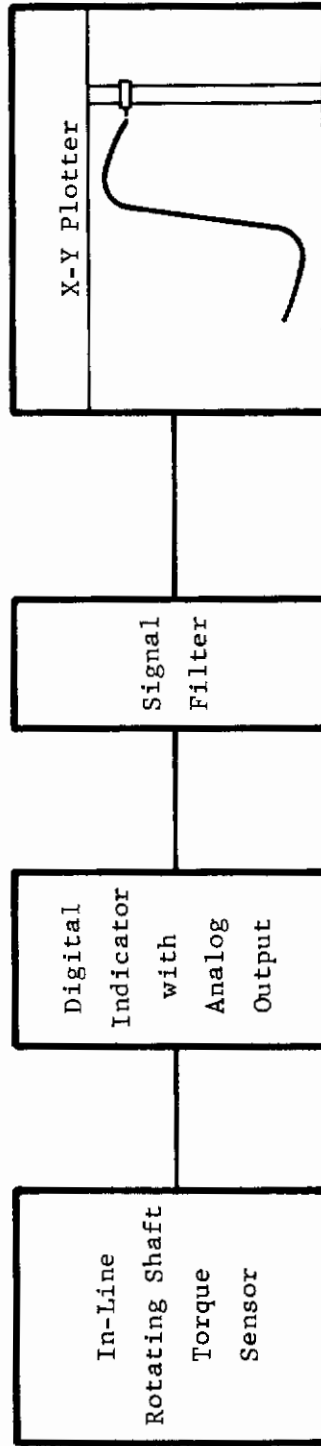


Fig. 15 Torque Detection, Signal Conditioning, and Readout Display Set-Up

Contrails

The shaft was inserted between the mechanical flat belt pulley assembly and the specimen carrying shaft as depicted previously (Figure 1). The bridge is connected to silver graphite brushes which ride on slip rings mounted on the rotating shaft for incoming and outgoing bridge excitation voltages. When the shaft is twisted during traction measurement the strain gage resistance variations produce an output voltage directly proportional to torque present in the shaft.

The unit used has a two hundred inch-pound maximum capacity with a .1 inch-pound signal resolvability. The bridge signal from the torque sensor is read with a six place digital indicator which contains an unfiltered analog signal output. The indicator provides internal calibration for positive and negative torque directions. For each test running day the output of the torque sensor was checked for linearity and accuracy with a known "dead weight" arrangement. The calibrated weights being in the range of the desired output signals for the days testing.

The analog output of the torque indicator contain some AC components which cause excessive pen chatter if recorded directly and was filtered for smooth plotting. Shown in Figure 16 is a photograph of a typical traction versus slip curve which is a direct output on the x-y plotter used with the rolling disc machine. Graphically displayed is the amount of resolution one gets from the set-up along both the abscissa and ordinate. It can be clearly seen that the traction is a widely varying function of the slip range of $\pm 1.8\%$ displayed. For further discussion of the details included in the plot, refer to the section on Traction Measurement Techniques.

f. Loading Mechanism

The present rolling disc machine can be run with test specimens which operate with radially applied loads from zero to twelve thousand pounds. Since discs with diameters of three to six inches were to be operated on the machine, a simple loading mechanism was sought. The nut cracker arrangement which is common for heavy loads was considered undesirable for light loads. In addition, it requires the precise knowledge of loading arm lengths for accurate loading.

The sliding carriage as shown in several figures (Figures 3 and 4) from different angles, was chosen as the best overall scheme for the versatility and accuracy required. It is a cast iron unit which contains the upper rotating shaft, flat belt drive pulley, four Thomson ball bushings for sliding, and a swivel connection for the attachment of a hydraulic cylinder. The hydraulic cylinder, which is used for lifting the carriage or adding a downward load, is attached in series with a commercial load cell (see Figure 17 for details of the assembly). The total weight of the carriage is seven hundred fifty-eight pounds; therefore, it must be added to or subtracted from any loading applied by the hydraulic system. The load cell used in determining the actual test loads is a one thousand pound push or

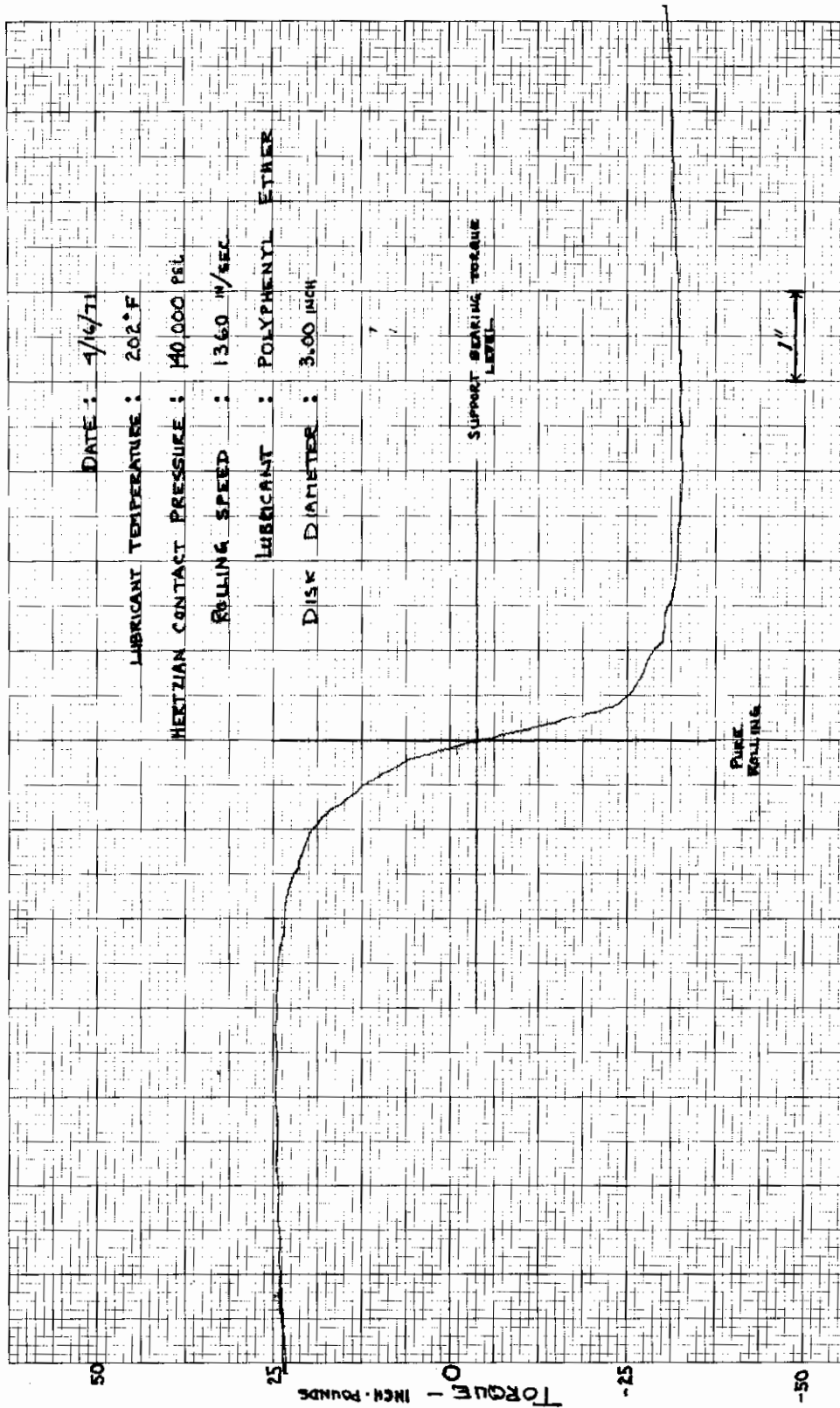


Fig. 16 Traction Versus Slip Curve
 Plotted by X-Y Plotter

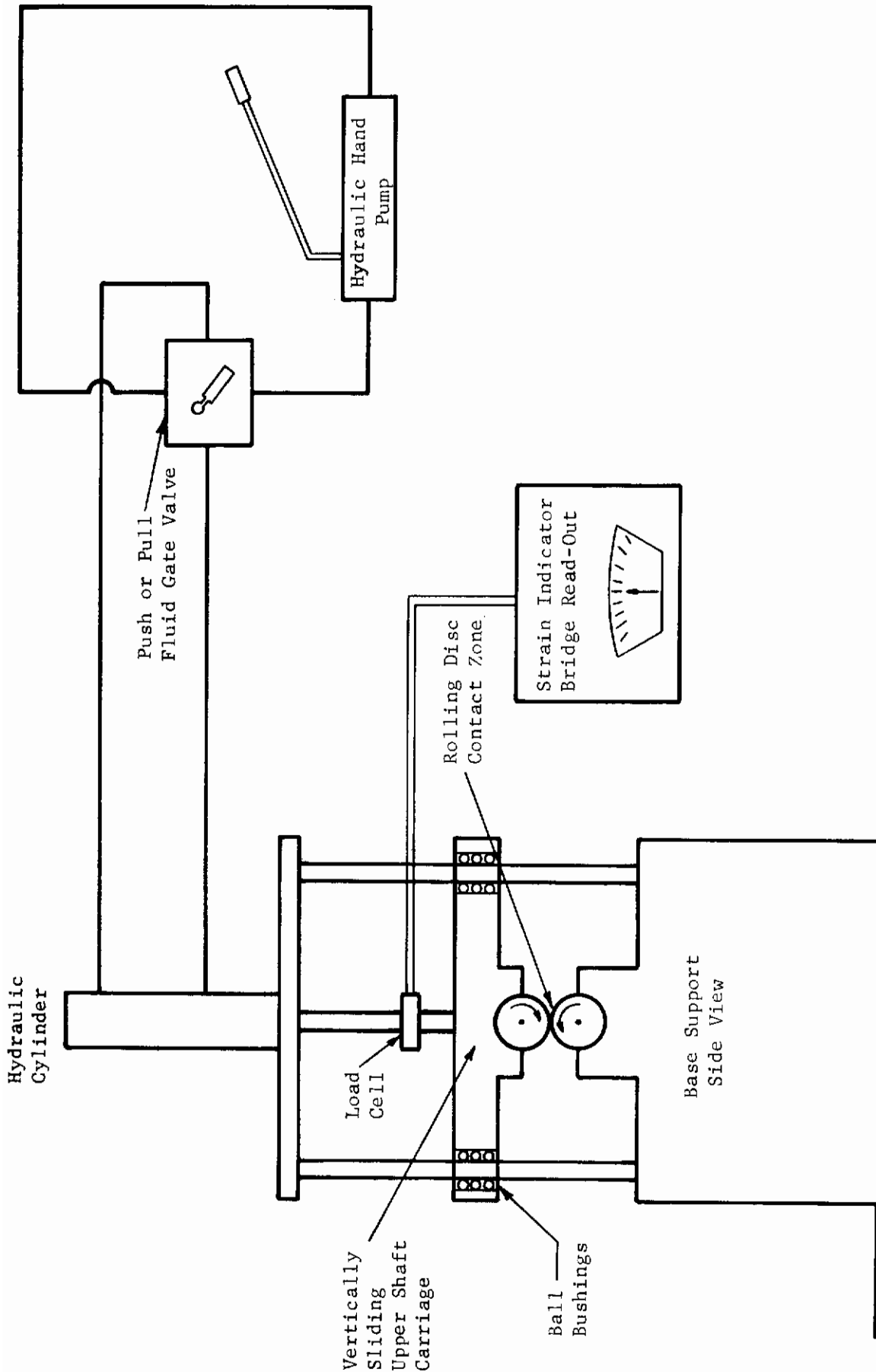


Fig. 17 Hydraulic Loading and Contact Load Indication Read-Out Assembly Schematic of the Rolling Disc Machine.

Contrails

pull, moment compensated, load cell with a four-arm bonded strain gage bridge circuit. The strain present in the load cell is determined with a standard micro-strain bridge null indicator which has a resolution of better than one pound of load. However, due to the drive belt connection to and from the sliding carriage, a repeatability of any load placed on the contact zone can only be done with an accuracy of ± 5 lbs. This means that the heavier loads can be more accurately determined.

Although the present facility is designed for loads up to twelve thousand pounds, two separate upper shafts have been designed for test use. The bending moments for long term high speed operation in the ten inch long upper shaft were too large for a single split unit which could receive all test diameters and all proposed loads. The two inch diameter (ten inch long) shaft used in the present design can be maintained at full speed with loads sufficient for a 250,000 psi Hertzian contact pressure (see Figure 18). The larger diameter shaft (3.5 in.) can be used with the full 12,000 pound load capability.

In order to insure that no moments were applied to the sliding ball bushings in the upper carriage, the total sliding assembly was balanced about the contact zone in the horizontal plane. Test weights and a level arm plate were added to the upper carriage until mass balance was obtained in two orthogonal directions about the contact zone. The assembly was then weighed and found to contain a total mass equal to seven hundred and fifty-eight pounds.

g. Motor Drive System

The variations in speed of the test assembly discs are obtained with a dual DC motor drive system. The twenty horsepower motors, one for each shaft of the assembly, are independently and/or slave controlled for data collection purposes. Each variable speed motor consists of a solid state controlled rectifier, a DC motor, and a flat belt speed-up pulley arrangement. Motor speeds can be controlled over a range of thirty to one with a maximum speed of 15,000 rpm. The motor and disc speed combinations which can be placed into operation with the present test facility are shown in Figure 19. This nomogram shows the relationship between disc surface speed, rotational frequency, and acceptable disc diameters. For additional information, related to the accuracy and maintained operational speeds, refer to the subsection on Speeds Monitored and Controlled.

Since the two motors used in driving the rolling disc test specimen are power limited, the torque available for experimentation is primarily a speed dependent function. Shown in Figure 20 are the available ranges of system torques as a function of disc rotational frequency in the test rig. The torque available at the contact zone is only a portion of that shown for any operational frequency since some torque is used to drive the support bearings, pulleys, and brakes within the drive system. The dotted line in the figure shown represents the torque available at the contact zone after subtracting the

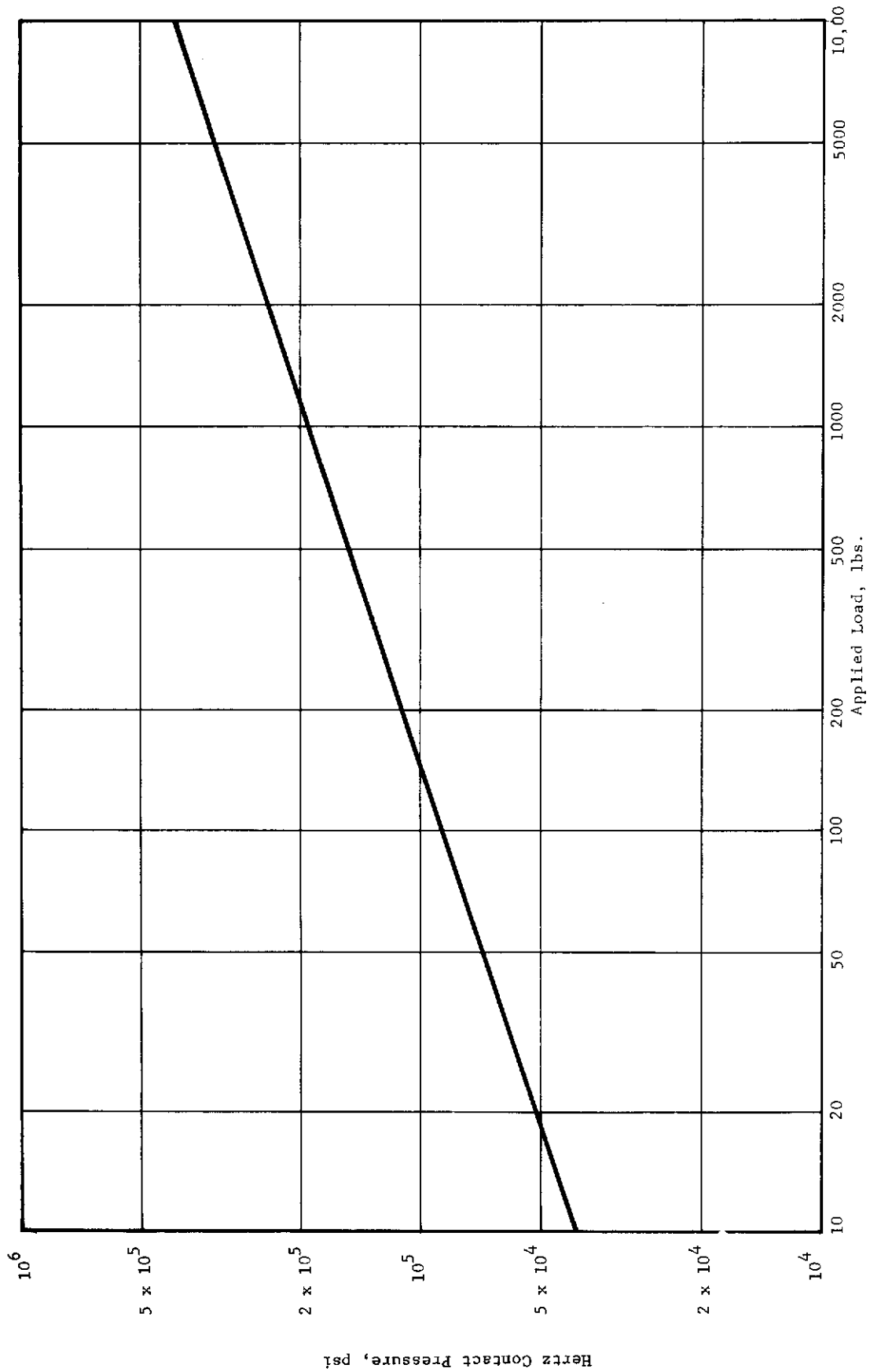


Fig. 18 Hertz Contact Pressure vs. Load for Identical 3 Inch Diameter Crowned Steel Discs; Crown Radius = 36 in.

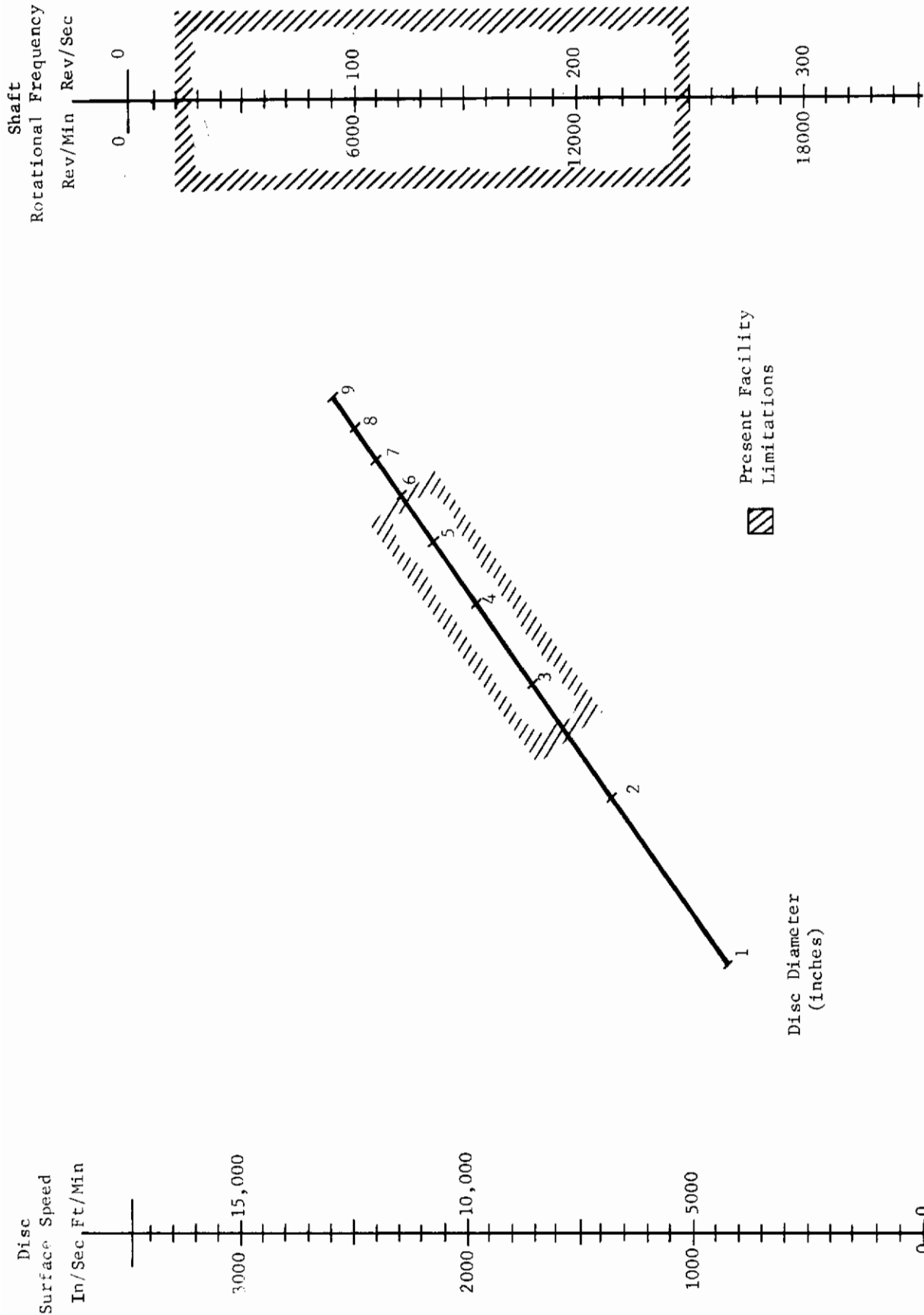


Fig. 19 Nomogram Relating Disc Surface Velocity Rotational Frequency, and Disc Diameter Capability of the Present Test Facility

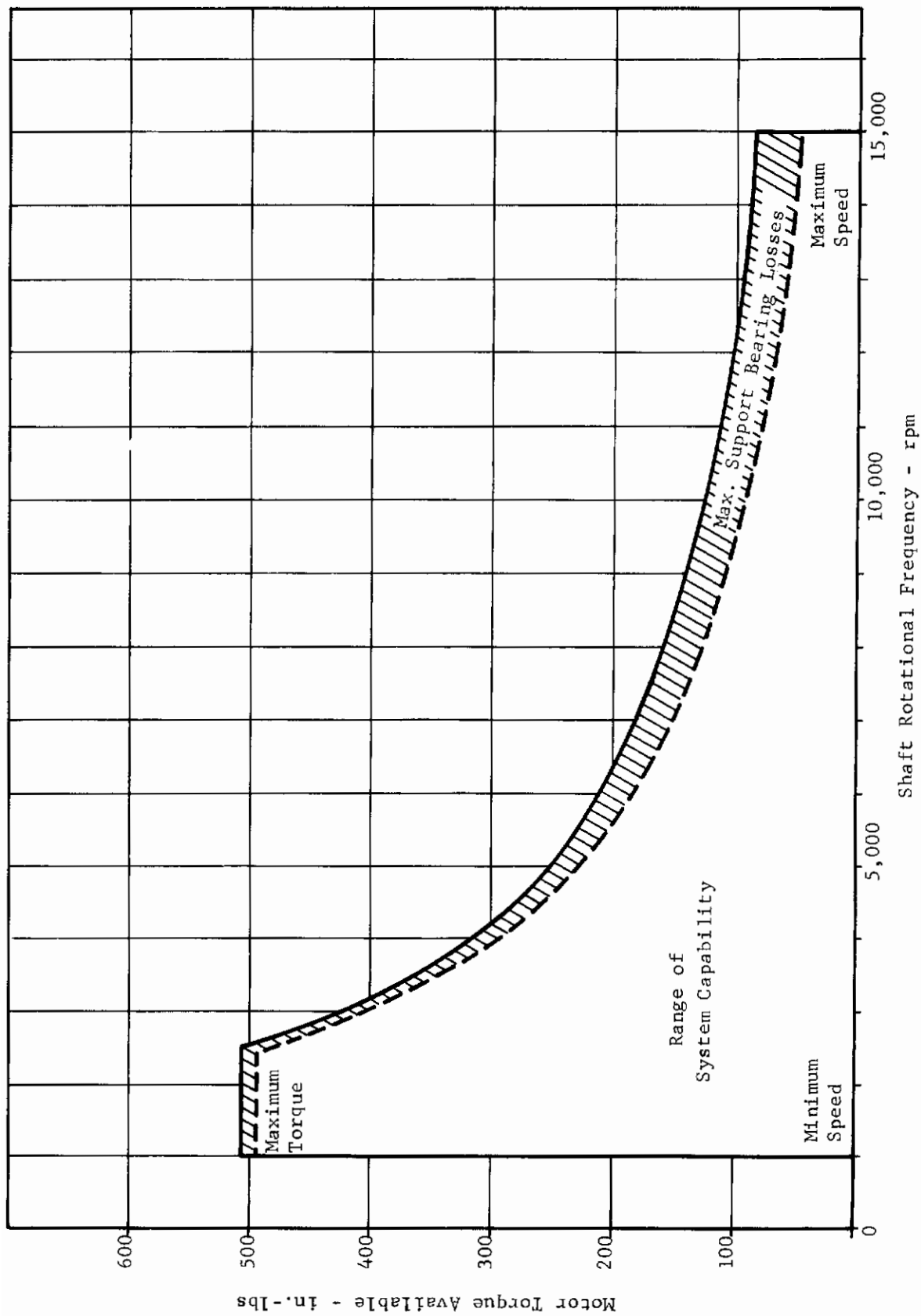


Fig. 20 Torque Output Range of Twenty HP Rolling Disc Motors

maximum loss expected in the support bearing system.

An overall view of the completed rolling disc test facility is shown in Figure 21. The motors are shown bolted to the floor mount in the normal operating positions relative to the concrete base, and rotating shaft assembly. If desired, the motor and belt assembly attached to the upper sliding carriage may be moved for skewed axis operation of the disc rig.

4. TRACTION MEASUREMENT

The previous discussion was concerned with the construction of a rolling contact disc machine which has continuously adjustable sliding speeds and direct electronic plotting of the traction versus slips observed. Presented in Figure 16 was a photographic reproduction of a typical curve with a slip variation of $\pm 1.8\%$ at the rolling speed of 1360 inches/second. Contained in the following paragraphs is a description of the procedures used in obtaining the traction versus slip curves as well as a review of the steps used in processing them for computer handling of the data.

In order to obtain data from the disc machine, approximately two hours are taken for initial set-up and temperature stabilization of the metal in and around the contact zone as well as in the lubricant reservoir. The rig is brought to the operating temperature by pumping the lubricant through the support bearings and contact supply tubing during the set-up procedure. While the lubricant is circulating air pressure is maintained to all labyrinth seals on the rotating shafts for lubricant containment. A coil heater around the lubricant return line to the reservoir is turned on in order to maintain the temperature level required for testing.

Calibration of the differential speed monitor is obtained by putting known frequency signals into both halves of the tachometer and setting the span of the x-y plotter. Frequency signals equal to that in both magnitude and difference expected during the test run are used for calibrating the tachometer. The torque output is handled in much the same way for calibration. A known static load is applied to the torque sensor and the calibration is checked for both linearity and magnitude while the span on the recorder is adjusted to the proper level.

The brakes of each motor are set for a level of torque greater than expected at the contact zone for the test to be made. The absolute magnitude of the setting has been shown experimentally to not affect the output readings as long as a torque level greater than that experienced by the contact zone is used. The motors are run-up with the discs separated in order to attain temperature stability. The support bearing torque level for the range of slips to be investigated is plotted, and the rolling speed of each disc is set to an equivalent value. At this point, the motors are stopped and a selected level of Hertzian load is applied to the test specimens.

After adjusting the lubricant flow to a level of approximately 2,000 milliliters per minute, both motors are started simultaneously. The pure rolling speed is checked and then a plot of the traction versus slip is taken by

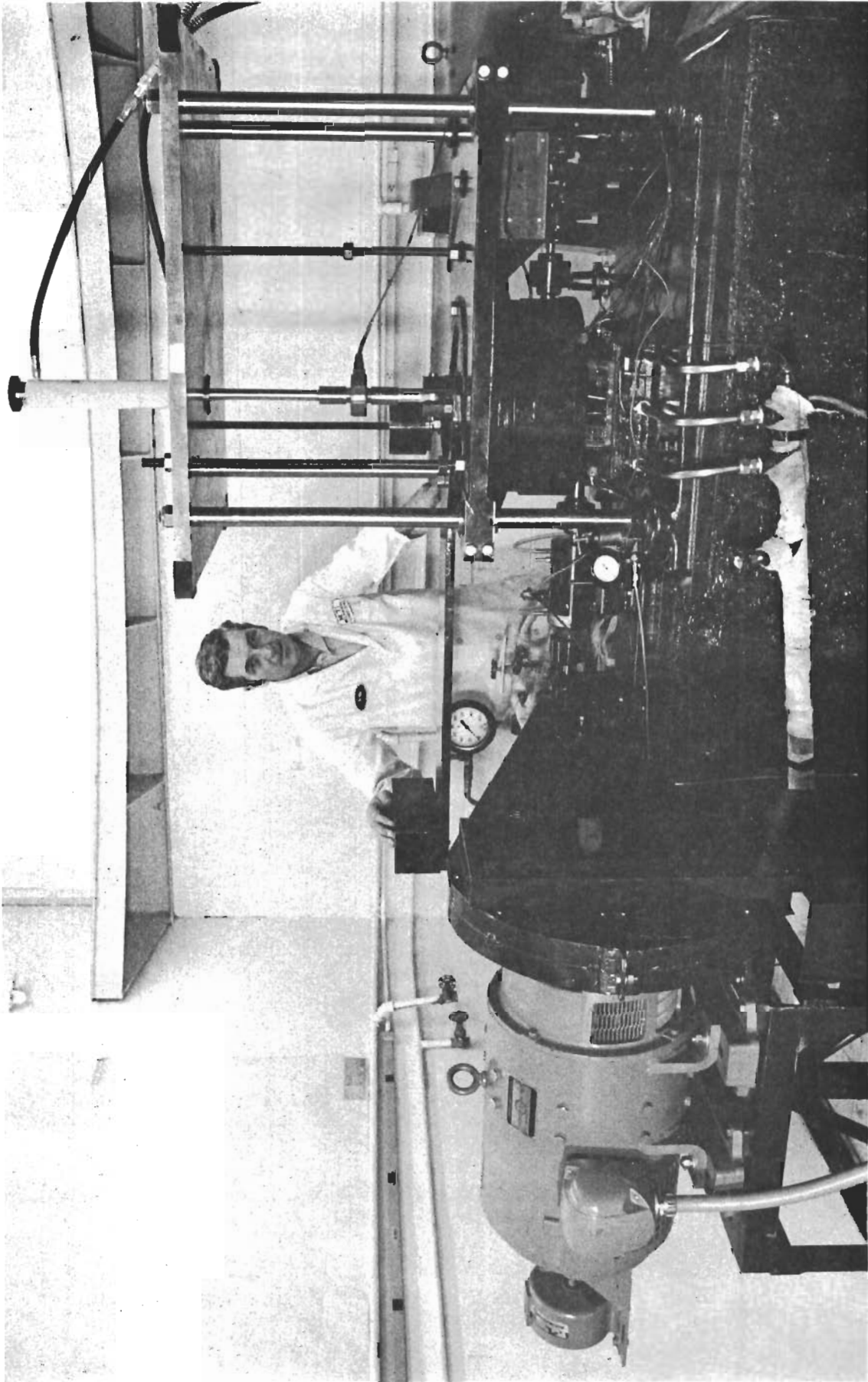


Fig. 21 Front View of Completed Rolling Disc Test Facility Showing Concrete Base, Motor Drives, and Upper Sliding Carriage with Load Cylinder Attached

MTI-11760

Contrails

manually adjusting the speed of one motor through the slip variation desired. The x-y plotter automatically follows the dialed speed settings. Once the traction curve has been drawn, the load (which up to this time has been monitored) is released as the discs are separated. This procedure allows both a minimum amount of contact time on the discs as well as a second check of the support bearing torque level. This level has been observed to remain constant before and after plotting the curves except when temperature stability of the rig was not achieved. After the motors have been shut-off, the procedure of loading the discs and obtaining a new traction curve may be repeated.

The plotting of a total traction curve of $\pm 2\%$ for any setting of initial parameters is accomplished in less than one minutes time and may be retraced over and over as desired. Typically two or three runs are made with the same initial parametric settings just for repeatability.

Shown in Figure 22 are traces of traction versus slip for two lighter loads than displayed previously in Figure 16. Although the majority of curves have been taken with an expanded differential disc rotational frequency of 20 rpm per linear inch of pen travel along the abscissa, these were taken with a scale setting of 100 rpm per inch of pen travel. The highly sloped curvature near the pure rolling speed is clearly evident. Approximately $\pm 2.6\%$ slip is plotted around the rolling speed rotational frequency of 5,720 rpm.

Since the slip rate is small for even the extreme ends of each curve, the support bearing level of torque is seen to remain constant. These bearings are preloaded 5,500 lbs. capacity angular contact bearings and are essentially lightly loaded for the cases shown. Using very high slip rates the slope of the torque level in the support system has been shown to vary with a weaker dependence than

$$\left[\text{Torque} \right]_{\substack{\text{angular contact} \\ \text{support bearings}}} \propto \left[\text{Rotational Frequency} \right]^{.5}$$

as normally taken for such a system. For all practical purposes, support bearing torque changes are insignificant over the speed variations plotted and do not enter in as a variable in the plotting of any of the traction curves presented in this paper.

Another notable feature of the traction curves is the undulation in the torque level at the peak traction of the lighter loaded traces. This phenomenon, though present in the test facility, was not particularly objectionable. A similar output was observed by Jefferies and Johnson (6) and had to be compensated for in their rig. Apparently the oscillatory nature of the curves in the peak region is caused by the negative damping presented to the mechanical system by the reduced traction of the back side of the curve. The displayed oscillatory nature of the peaks shown has limited data taking on the present test facility to Hertzian loads greater than 80,000 psi.

The symmetry point between the traction peaks in all plots was very near or coincident with the plotted support bearing torque level line and coincided for all runs made with loads greater than 120,000 psi Hertzian. Using the

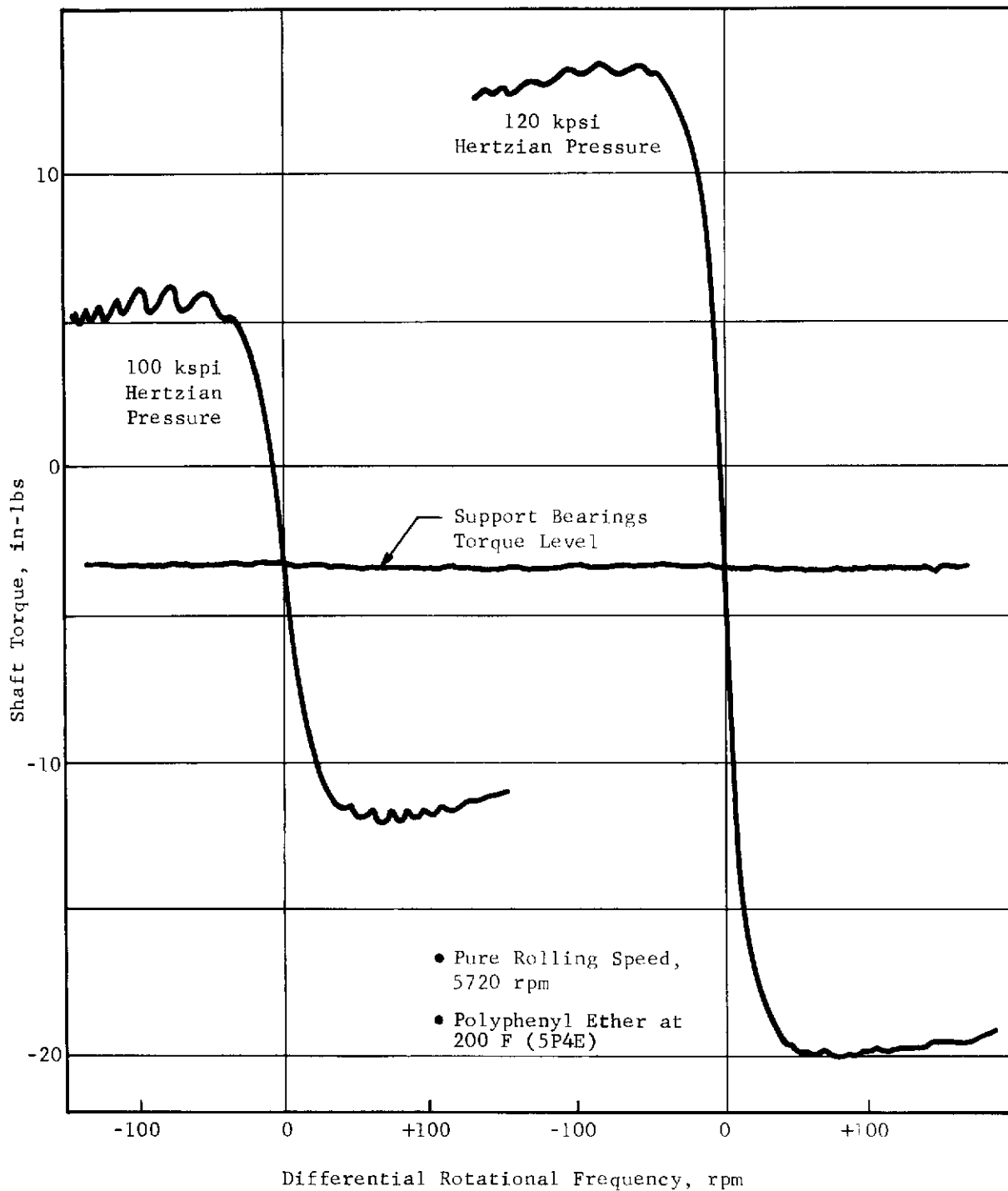


Fig. 22 Full Scale Plot of Total Traction vs. Slip Curve as Received on X-Y Plotter for Two Separate Loads Showing Relative Torque Levels and Support Bearing Losses.

symmetry point between traction peaks, all the plots were doubly folded across the pure rolling speed position of the abscissa and the true off-set torque level present in the support system. The results as shown with the analytical data presentation are a single average curve which begins at zero and proceeds to greater values of traction and slip.

The present rolling disc machine also permitted a preliminary evaluation of the dependence of traction on the volumetric rate of supply of fluid to the contact zone inlet. The traction dependence upon decreasing fluid supply is shown in Figure 23 for an electronically maintained slip rate of 7 ips at a rolling speed of 900 in./sec. When the flow to the contact was reduced below 900 milliliters per minute, a sudden increase in the traction was obtained. Upon restoring the level of flow the lower limit of traction was regained and this response could be repeated over and over again.

Although the conclusions of such a test appear to indicate possible starvation effects, the true origin of the observed data has not been fully established experimentally. It is possible that temperature variations in the supply lubricant and/or support bearing torque level alterations have occurred and could account for some or all of the traction dependence observed. Further experimentation is planned to investigate the effects of lubricant supply rate under more closely controlled conditions.

5. ASPERITY CONTACT AND CAPACITANCE FILM THICKNESS TECHNIQUES

The present work phase has included the design and construction of an electronic asperity detector as well as a feasibility study of the capacitive film thickness measurements on the rolling disc machine. To date, the asperity detector described below has been checked out on a conventional rolling element bearing and the components necessary for measuring contact capacitance have been procured.

The methods of measuring contact continuity and capacitance requires that one of the test specimens be electrically isolated from ground. The lower shaft now in use on the rolling disc assembly is designed to allow electrical isolation of the lower rolling specimen. The sketch of Figure 24 shows how this is accomplished. The lower disc is mounted on a pair of plexiglass inserts which are thick enough to minimize the capacitance of the disc to ground.

The capacitance variation within the contact zone will be measured with a standard carrier frequency capacitance bridge. The bridge to be used has seven decade ranges from micro-farads (10^{-6}) to pico-farads (10^{-12}). Each decade range provides digital capacitances to five significant places or analog voltage outputs with less accuracy for measured capacitances.

For design purposes, the total expected capacitance was calculated from the two dominate sources; the capacitance of the isolated disc to ground through the plexiglass insert (see Figure 24), and the capacitance present at the contact zone during pure rolling. Thus, since these capacitances are in parallel

$$C_{\text{total}} = C_{\text{to ground}} + C_{\text{contact}}$$

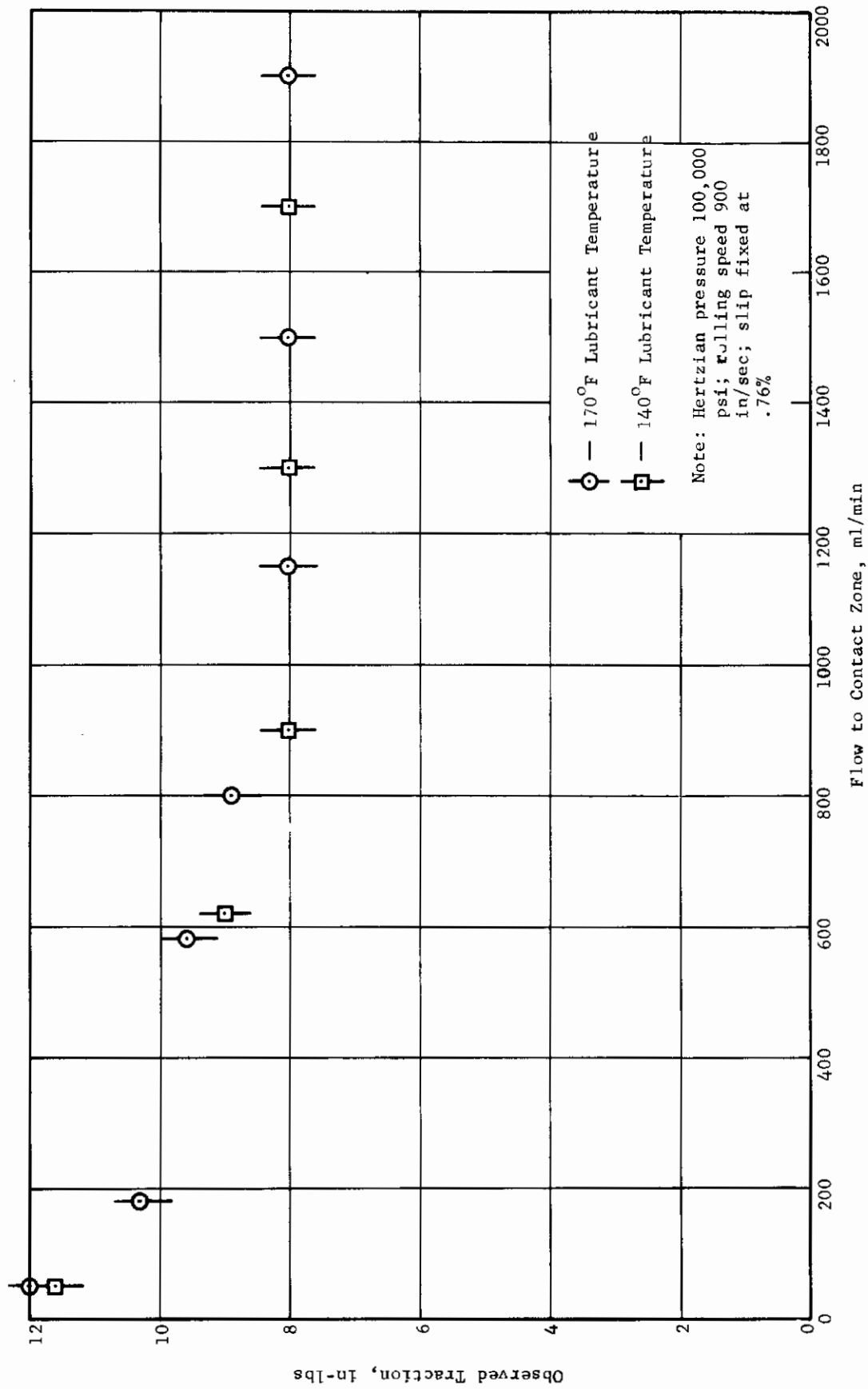


Fig. 23 Traction for a Constant Slip Setting and a Variable Rate of Fluid Supplied to the Contact Zone

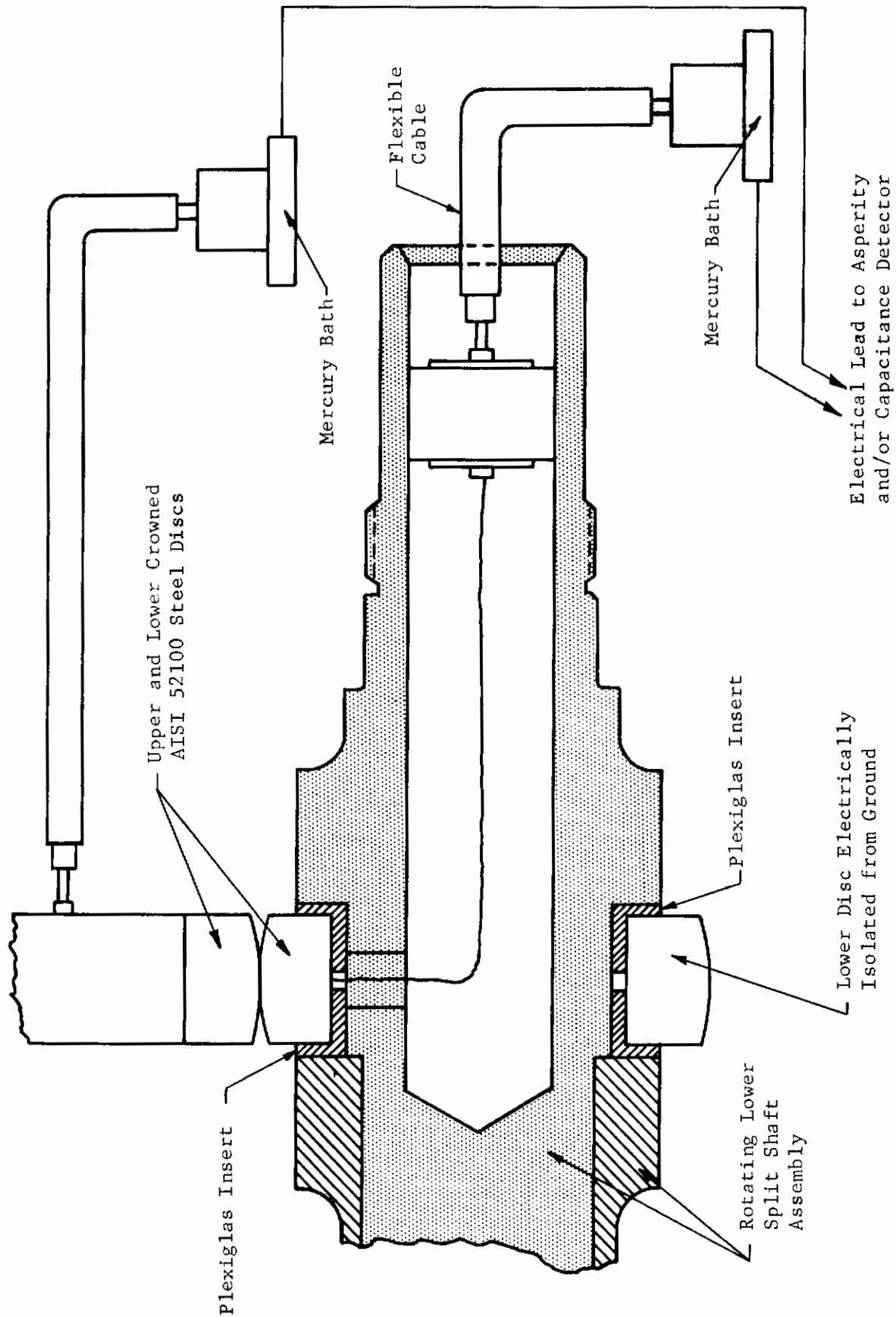


Fig. 24 Test Specimen Mounting Assembly for Contact Zone Asperity and/or Capacitive Detection

MTI-12162

Contrails

where,

$$C = K \epsilon_0 \int \frac{dA}{h_A}$$

Any accurate measurements of the contact capacitance should be made with a minimum constant capacitance to ground. Since the area to ground seen by the mounted disc is fixed, a large separation to ground was the only way to minimize the contribution of capacitance from electrical isolation of one of the discs. Eighty-mils of plexiglass was chosen as the optimum thickness for isolating electrically one disc from ground. A calculation of the expected capacitance to ground yields a value of 200 ± 50 pico-farads.

An expected level of capacitance can also be calculated for the contact zone between the discs. The exact evaluation of the contact capacitance depends on a knowledge of the disc separation distribution and the way in which the dielectric coefficient of the lubricant varies with pressure and temperature. Thus,

$$C_{\text{contact}} = C(h, T, P_{\text{HZ}})$$

For design purposes, the variations of capacitance with temperature and pressure as well as fringing effects were neglected. Typical separations of ten to one-hundred micro-inches between the two crowned discs result in a capacitance from fifty to five hundred pico-farads to be expected from the contact zone of the discs. Temperature variations would alter the expected capacitances by as much as 10%, whereas, pressurization of a non-polar lubricant might change the calculated level by as much as 25%. A rise in temperature tends to lower the contact capacitance while an increase in pressure tends to increase the capacitance.

The deformation of the discs under increasing loads increases the contact capacitance appreciably since

$$\text{Area}_{\text{contact}} \propto \text{Load}^{2/3}$$

These increases, however, can be evaluated both numerically as well as experimentally and will be determined in the coming year.

Measurements of electrical contact resistance have been reported for several years (7). Two metal solids separated by a lubricant can be brought into Hertzian contact and still remain electrically isolated from one another. The degree of isolation and the observed variations in electrical contact resistance depends on many parameters such as: surface finish of the contacted material, load on the contact, lubricant properties, geometric dimensions of the metal parts, the relative velocity between the contacting surfaces,

Contrails

applied voltage, and the percent of elastohydrodynamic lubrication which exists between the contacts.

Attempts to correlate (8,9) variations in the contact resistance with typical bearing parameters such as lubricant viscosity and frictional forces (torque) within ball and flat contacts have been published.

The qualitative results of past studies are:

1. Metal-to-metal contact is reduced when higher viscosity oils are used for interfacial lubrication.
2. High contact loads increase while high speeds decrease percent metal-to-metal contact.
3. Oil additives affect the percent of metal contact in a way that changes with time.

Shown in Figure 25 are two oscilloscope photographs from the asperity detector developed, of typical contact resistance versus time plots. For any metal-to-metal contact the resistance would simply be 10^{-6} ohms or very near zero as a function of time. When a lubricant is placed between the contacts the junction resistance rises from 10^6 to 10^{10} times what it is observed to be without lubricant. In addition, as noted in Figure 25, the resistance can fluctuate over the full range from infinity to zero if the contacts are placed under relative motion to one another.

The number of contacts per unit time is a strong function of the micro topology present in the Hertzian contact area and the hydrodynamic film thickness. A typical observation time as shown in Figure 25 is 100 milliseconds real time. The percent of time the resistance is low (as is the case with metal-to-metal contact) may be anywhere from zero to one hundred, depending upon the area of contact zone and lubricant film thickness present.

With extreme variations in observable contact resistances in hand, MITI has developed a real time electronic device, the Asperitac, which can determine the percent metallic contact, number of contacts per unit time, and average asperity pulse height and width. In addition, the applied test voltage, resistance scale magnification, and test observation time can be widely varied at the discretion of the experimentalist. The preselected settings depend upon the contact or bearing conditions under observation (see Figure 26 for Asperitac functions).

The Asperitac has an adjustable preselected time of observation from one millisecond to one thousand seconds in seven decade steps. Asperity resistance variations in rolling and sliding contacts as well as boundary lubricated bearings can be observed with such a change in time scale.

Applied DC contact voltages can be fixed from a minimum of 10 millivolts to 1 volt in one millivolt increments. Resistance variations in contacts with oils which have low dielectric constant and small breakdown voltages can be analyzed with these excitation voltages.

Contrails

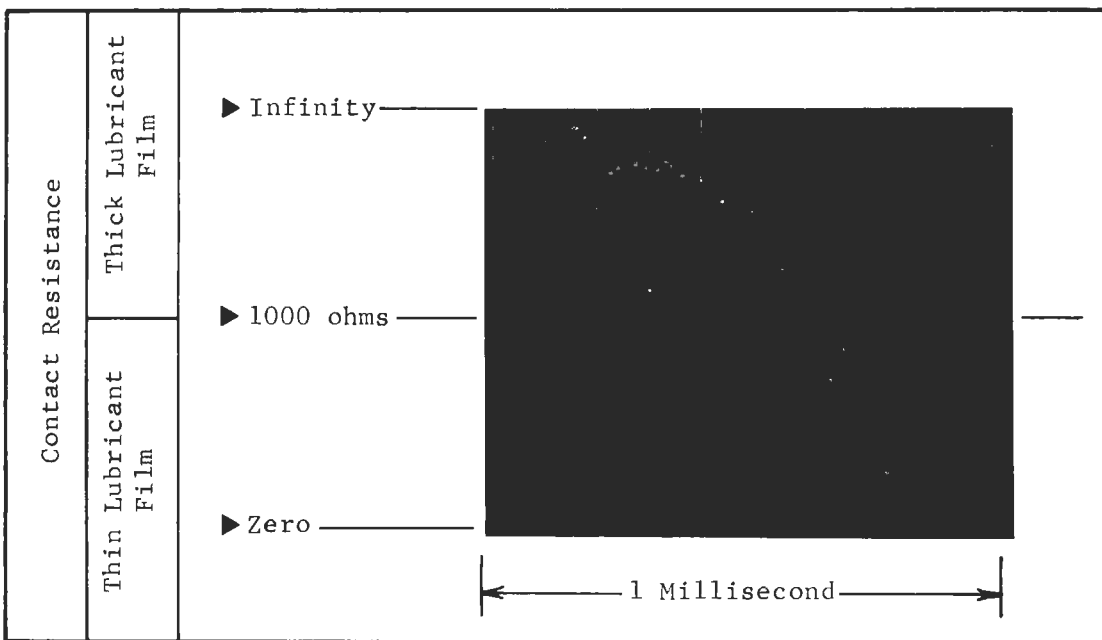
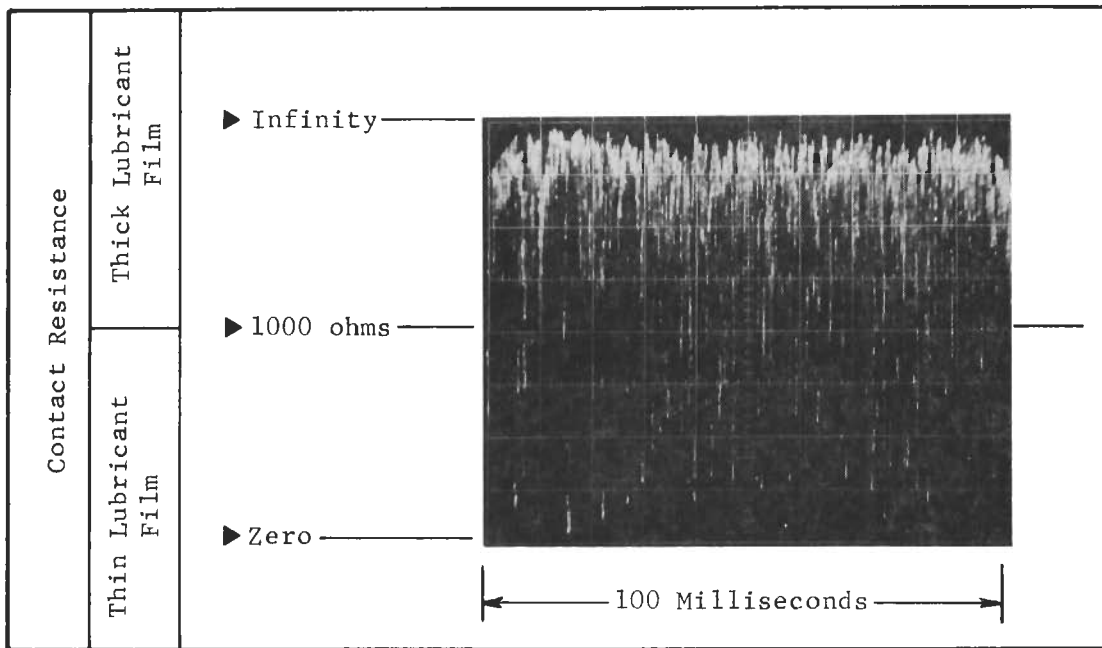


Fig. 25 Typical Contact Resistance Variations as a Function of Time. Ten Percent Contact Over One Second of Observation with Contact Resistance Dropping Below 1000 ohms 1500 Times Per Second.

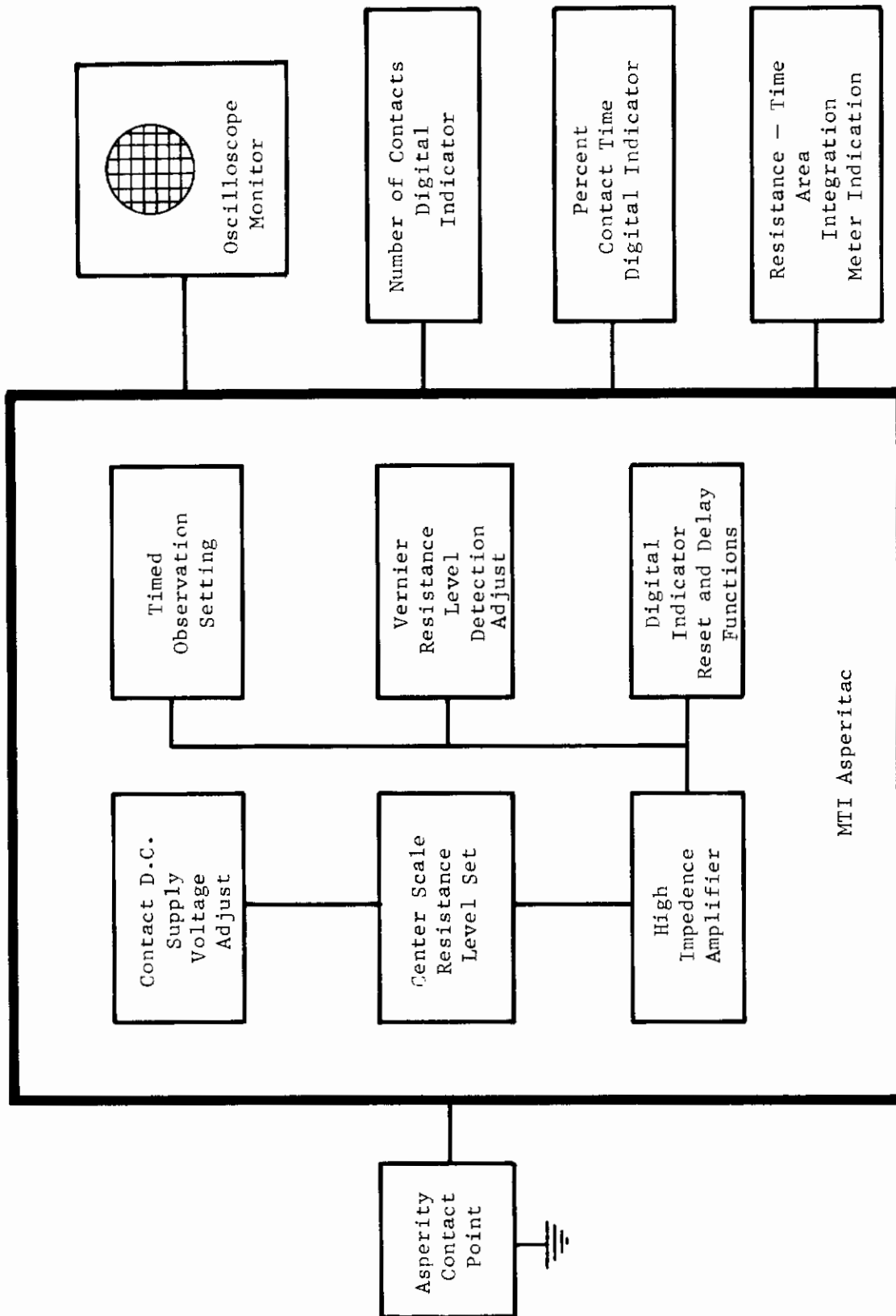


Fig. 26 Functional Diagram of Input-Output Operations Available on Asperitac

Contrails

If certain contacts warrant extensive observation in the zero to 10,000 ohm range the mid-scale resistance of the discrimination level can be decade stepped to as low as ten ohms for highly refined studies of the variations in the low level contact resistance.

The percent of metal-to-metal contact which can be theoretically calculated for certain contact profiles is obtained in real time with the Asperitac by taking the ratio of the time the resistance is below the discrimination level to the total observation time. A counter and summation circuit performs this task for observation times from .1 millisecond to 1000 seconds.

The number of asperity interactions is determined by electrically counting in any observation period the number of times the resistance passes below the discrimination value selected.

The average metal-to-metal contact pulse height and width is found with the Asperitac when a knowledge of the contact or set of contacts such as in a rolling element bearing, require it. The average asperity pulse width is obtained by dividing the detector's display of actual time in contact by the number of asperities counted during the observation time. Average asperity pulse height may be obtained from the detected area of the resistance-time variations and the average pulse width.

6. OPTICAL FILM THICKNESS TECHNIQUES

Precise knowledge of the film thickness existent between two lubricated surfaces has been the quest of many research studies since the early part of the twentieth century. In more recent years the technique of using optical interferometry has emerged as the most promising method of accurately producing film thickness data in and around the so-called contact zone. The first reported interference patterns existing between two surfaces go back as far as Newton.

A study made by Cameron and Gohar (10) was the first to indicate significant success in using interference patterns in lubrication experimentation for mapping the complete contact film.

The majority of tests have been performed with point contacts involving a lubricated rotating ball on a flat loaded transparent plate. Some experiments (11) also done by Cameron have been performed with rollers on optical flats. The principles of the measurement technique in general are discussed in a recent report (12) and only those related to the specific set-up used during the present work phase will be discussed here. Present testing with the designed and constructed system described herein has been limited to preliminary optical check-out with no surface speeds being used in the initial phase of work.

a. The Experimental Assembly

In order that successful optical interference patterns can be observed and used analytically, several prerequisites must be fulfilled:

Contrails

1. The refractive index of the test fluid under the varying pressure and temperature parameters must be known.
2. The optical set-up must be free of aberrations and contain a well defined surface for reference measurements of film distortion under load and/or speed changes.
3. The interference pattern must be stable during the observation period as well as have a high contrast for proper detection.

The present assembly uses a surface geometry which is different than any used to date in optical lubrication experimentation. The mating discs are shown in Figure 27. The transparent reference disc is a section of a cylinder with thick walls constructed of optical grade quartz. The outside and inside diameters have been ground concentric and free of distortion in order that the contact zone may be observed from the central axis of the cylinder. The outside diameter of the quartz disc is coated with a 20% reflective coat of chromium (slightly more than 100 angstroms have been vapor deposited). The coating provides a well defined Newton ring structure at the contact interface which is quite suitable for observation or photographing (see Figure 28). In addition, the chromium has wetting properties which are similar to smooth steel.

In the running position the quartz cylinder is mounted on the split lower shaft of the rolling disc machine. A cross-section view of the lower shaft and the mounted discs is shown in Figure 29. The transparent cylinder is fixed on the hollow shaft which contains three radial holes (one of which is shown in the figure) for viewing the contact zone from the center of the shaft. The contact zone is seen from the open end of the hollow shaft via the microscope extension tube and the stationary front silvered 45 degree mirror.

The microscope assembly consists of the extension tube, a 1X objective lens, right monocular head, and an illuminator access housing. The access housing allows either filtered incandescent light, stroboscopic, or laser light to illuminate the contact zone from the body of the microscope. The unit is a combination of commercially available components especially suited for the required long stand-off distance needed for viewing the contact zone. The working length from the end of the objective lens is approximately seven inches and is used with either a 10X or 15X eyepiece.

The contact zone image shown, as in Figure 28, may be photographed or observed with the aid of a laterally traveling filar micrometer. The filar used has a traveling resolution of one ten-thousandth of an inch across the field of view. In order to properly align the image of the interference fringes in the view finder, the microscope assembly was mounted on a three-way adjustable pedestal. The test set-up without the rotating shafts is shown in the photograph of Figure 30. The tubular extension with 45° mirror is shown in the proper orientation for photographing the contact zone between the

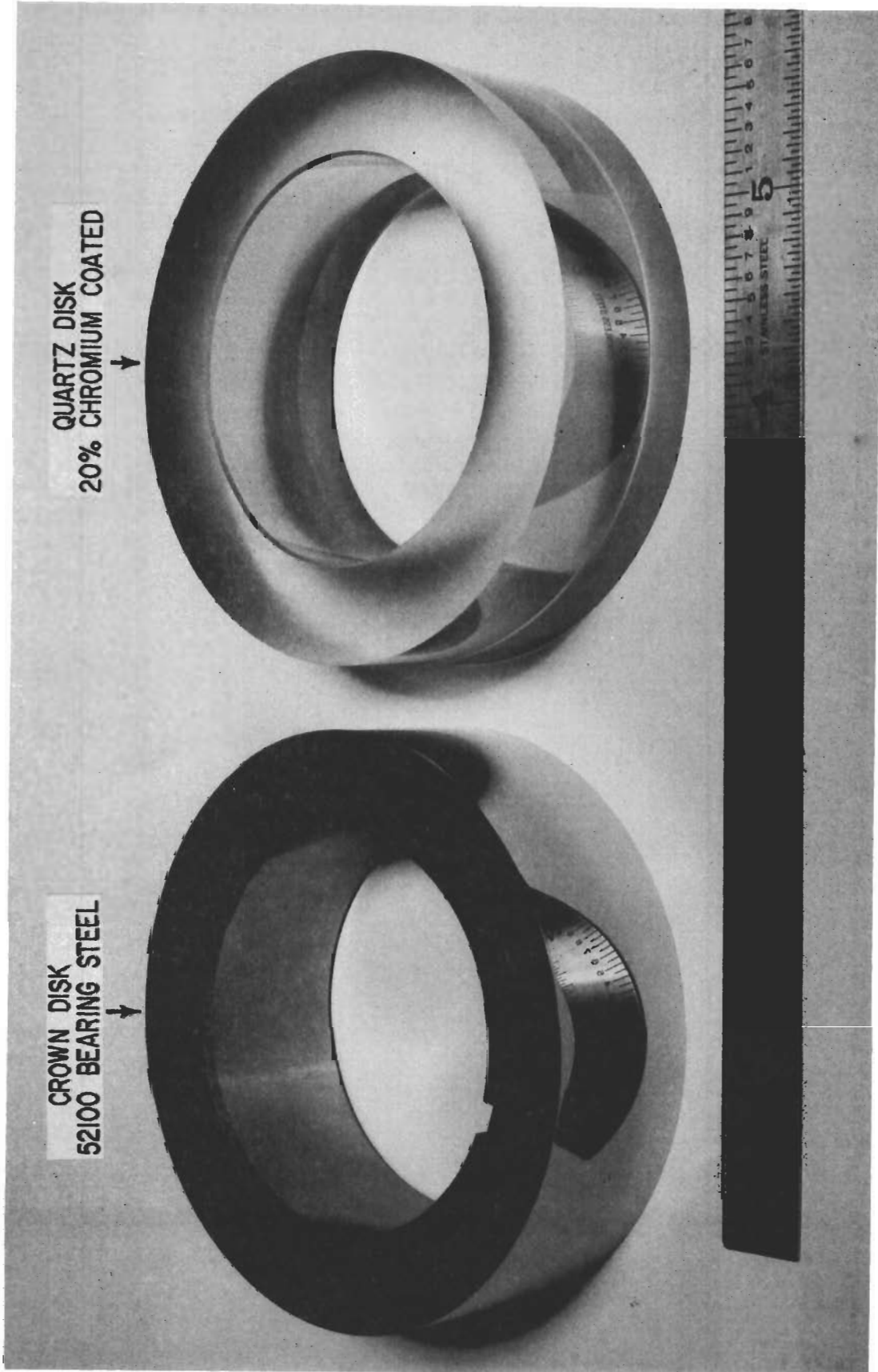


Fig. 27 Rolling Disc Specimens

MTI-12178

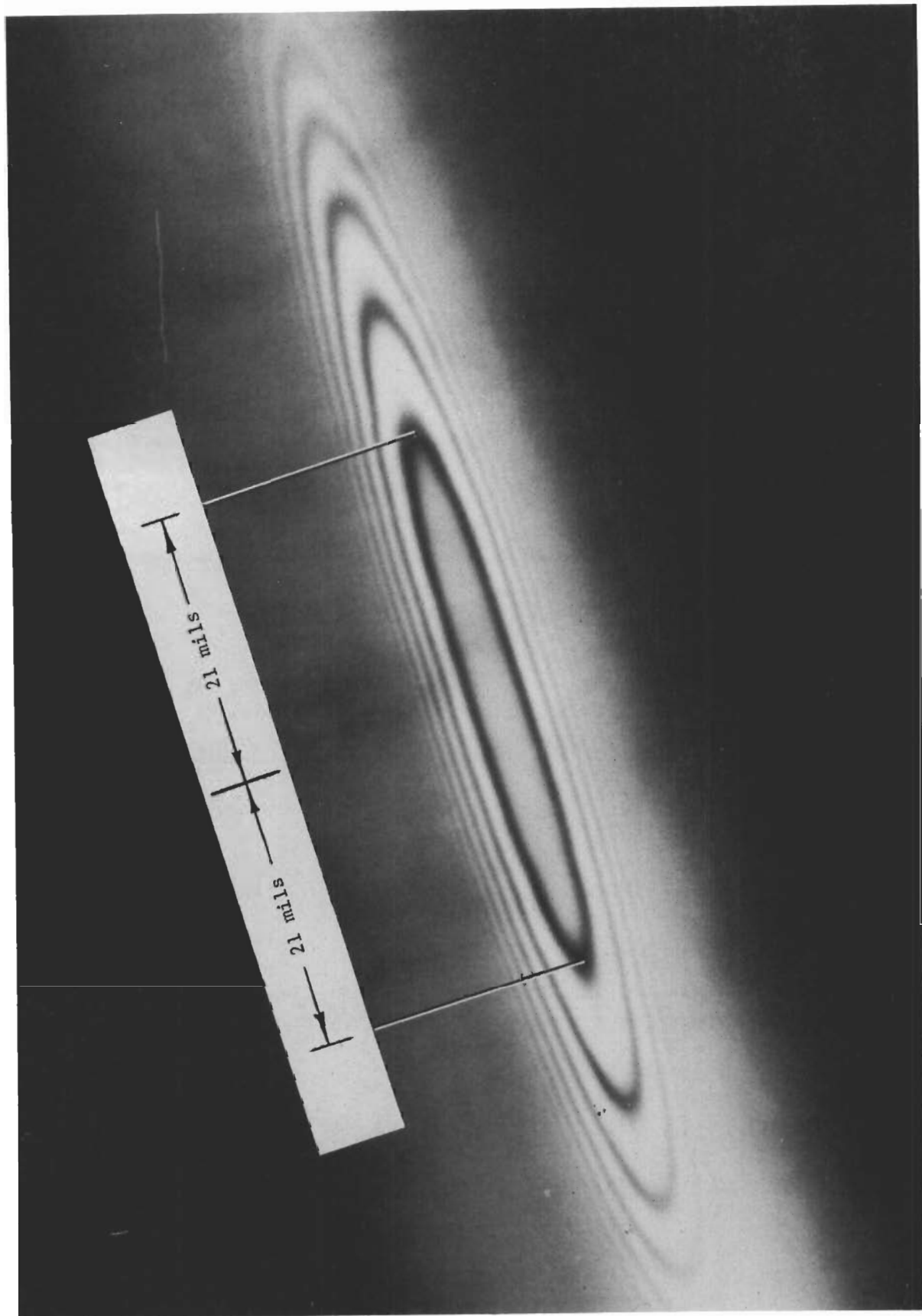


Fig. 28 Optical Interference Pattern Between Cylindrical Quartz Disc and Polished Steel Crowned Disc of the Same Diameter

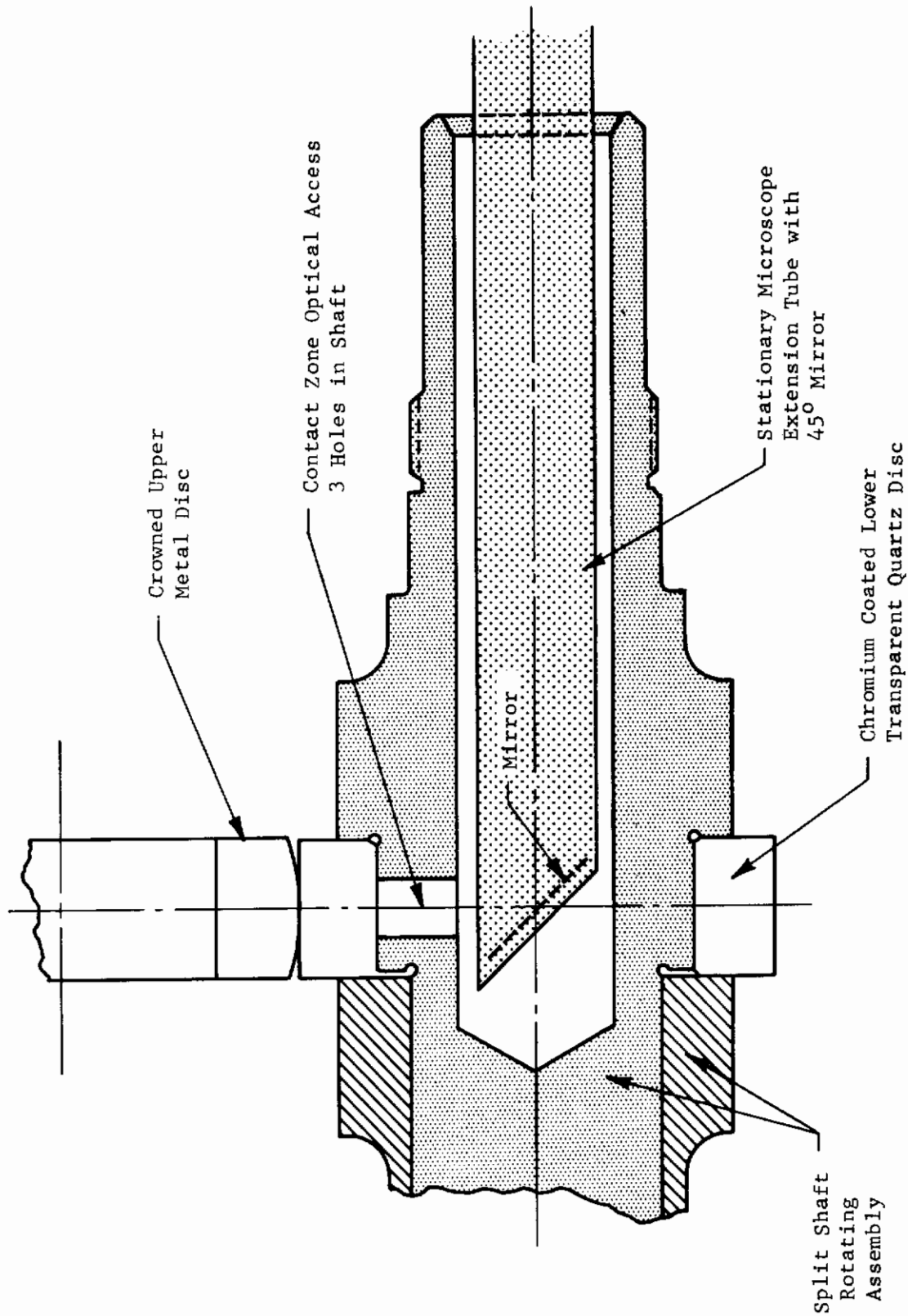


Fig. 29 Lower Disc Specimen Shaft Showing Mounting Arrangement and Optical Access.

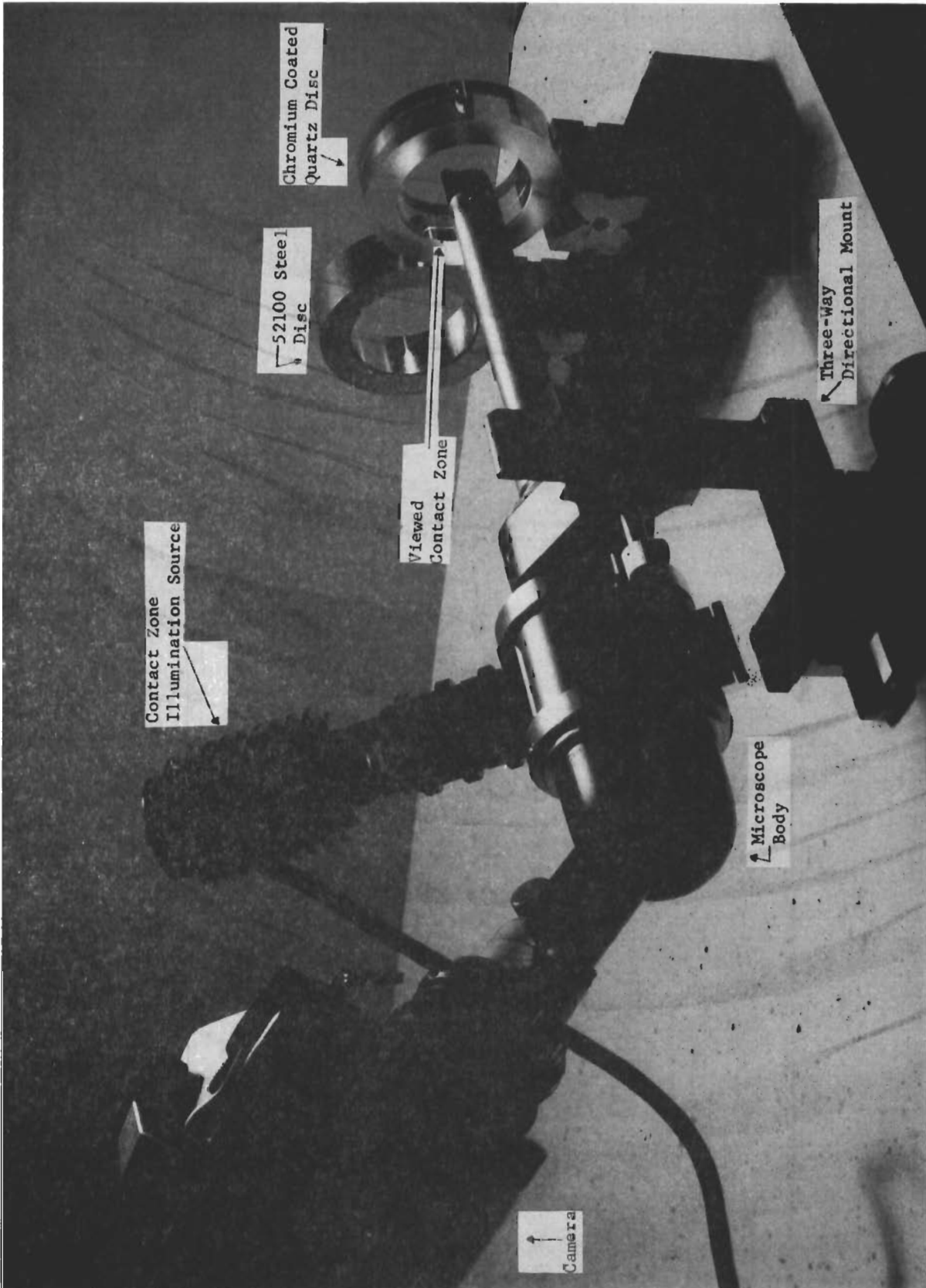


Fig. 30 Optical Assembly Positioned for Viewing Contact Zone Interference Fringes. Test Specimens Shown Unmounted.

Contrails

two disc specimens.

Preliminary optical results have been obtained for static contact between a crowned steel disc and a quartz disc with a partially reflecting coating. Several fringe patterns were obtained under lightly loaded conditions. In order to interpret and evaluate the fringe patterns under static contact, an analysis has been undertaken and completed for predicting the spacing between two bodies in elliptical Hertzian contact.

The equations originally put forth by Hertz are expressed in a convenient manner for numerical computation in Appendix IV. Computer programs have been written for calculating separations at a given position as well as for calculating positions at which the separation is constant to predict location of interference fringes. The output of this program yields loci of constant separation between the discs as shown in Figure 32.

The centers of the dark bands in Figure 28 correspond to separations of approximately 4, 12, 20 and 28 micro-inches from the center respectively. The major axis of the inner most dark band is approximately 41 mils. The fringes were produced by a 3 in. diameter cylindrical quartz disc loaded lightly against a 3 inch diameter crowned steel disc having a 36 inch crown radius (see Figure 27). The precise loading for these preliminary experiments was not measured, however, a load of .09 lbs. places the analytical and the measured value of the major axis of the first dark band in coincidence.

Comparison of predicted and measured separation in the axial direction is shown in Figure 31. Although good agreement is shown to exist along the major axes of the fringes (axial direction), the predicted ratios of the minor to major axes of the fringes as determined from Figure 32 are somewhat larger than the experimental values as determined from Figure 28. This discrepancy could be caused by an error in the assumed crown radius or by possible phase shift effects observed by Holden (13) resulting from the chrome layer on the disc surface. These effects will be investigated more thoroughly under more controlled conditions.

The comparisons between experiment and theory shown here are highly preliminary. They are intended in part to illustrate the use of the analysis performed here as a valuable tool which will be used for interpreting subsequent dynamic optical film thickness data.

7. X-RAY FILM THICKNESS TECHNIQUES

Until 1960 the only reliable methods of measuring film thickness in a lubricated interface between two metal bodies was by using electrical capacitance techniques. At that time, the Battelle x-ray technique was developed. The result at that time was the first valid proof of the existence of very thin lubricating films (less than 100 micro inch) in rolling contacts.

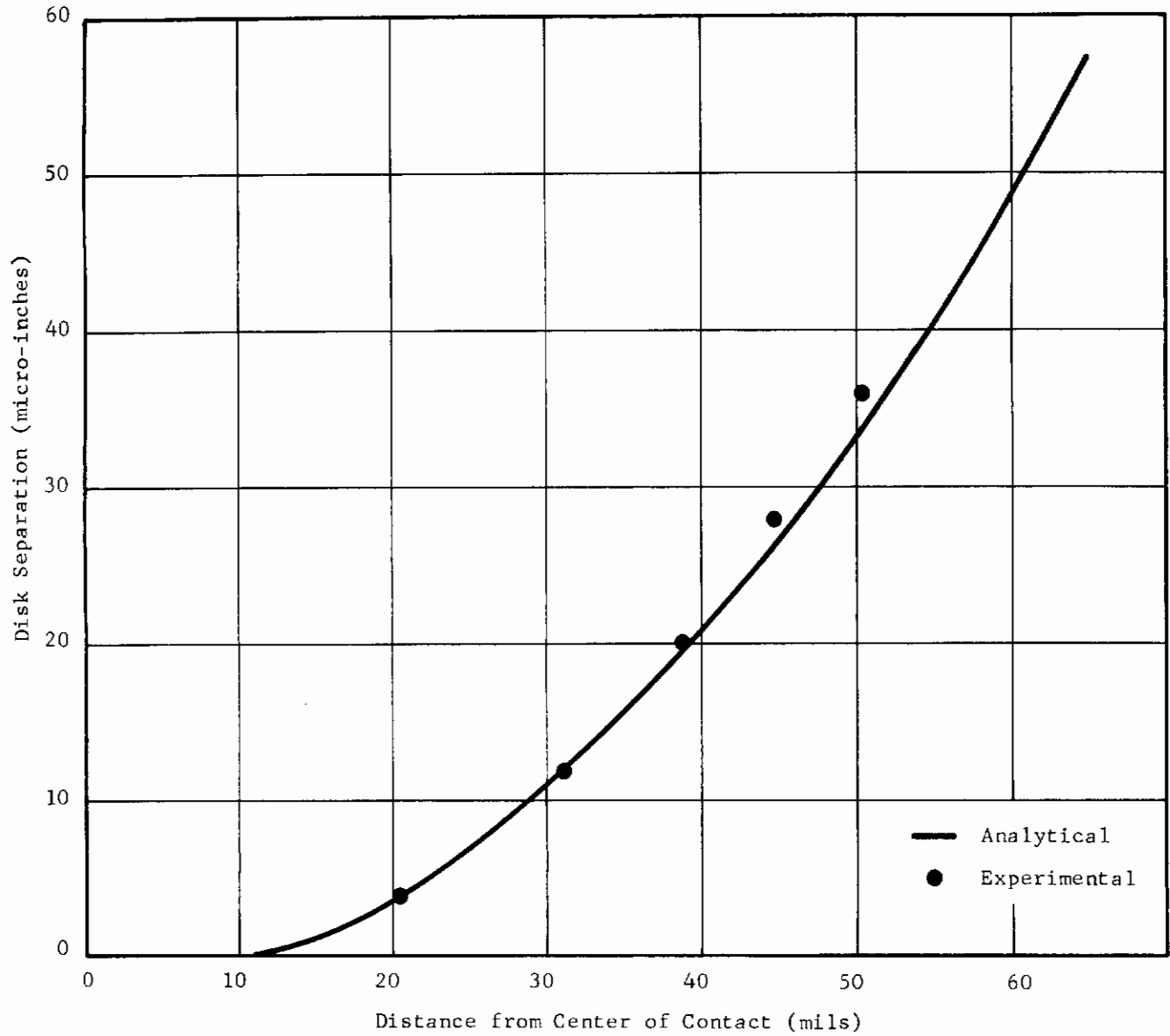


Fig. 31 Measured and Predicted Separations in Axial Direction

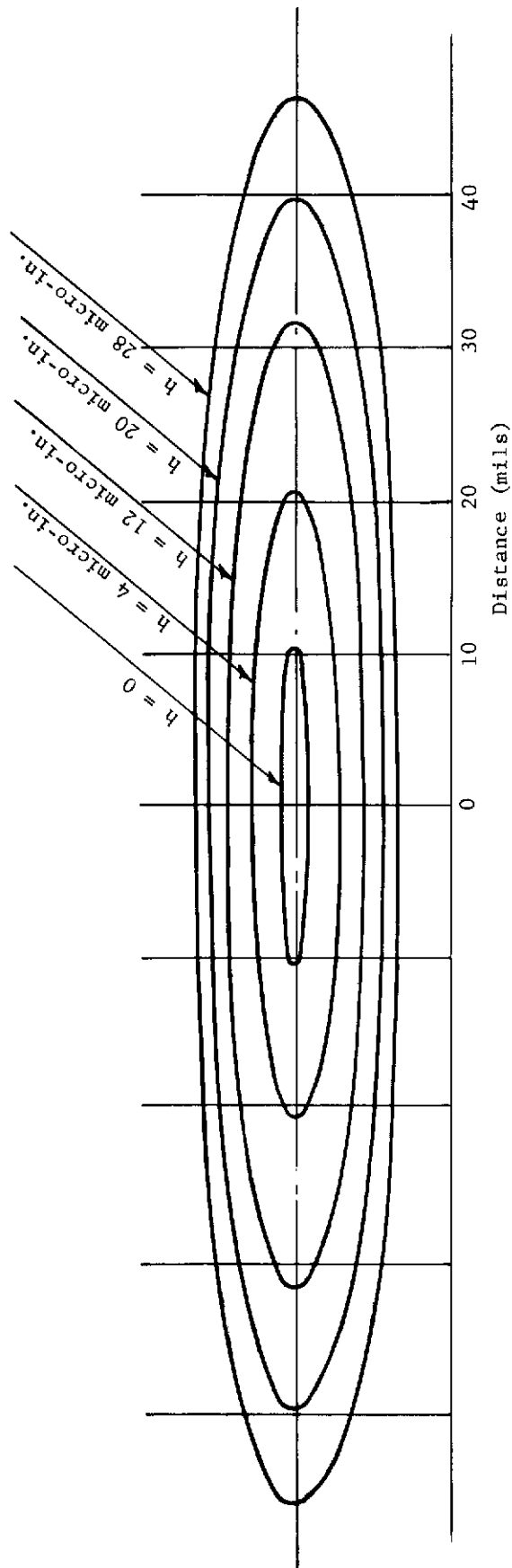


Fig. 32 Theoretical Fringe Pattern

Contrails

A set of x-ray film thickness measurements are being planned for the next phase of work at Mechanical Technology Incorporated on the rolling disc machine described in this document. The tests to be performed will be similar to those originally performed except that only the film thicknesses in the rolling direction will be examined. The present rolling disc facility design has not provided for side viewing the rolling test specimen contact zone.

The sketch of Figure 33 shows the layout of components which will be used for determining the lubricant film thickness between the rollers with x-rays. Two principle items are different from the originally performed classical experiment. Instead of generating the x-rays to be used with a high voltage electron tube a natural radiation source of cadmium-109 will be used. The source will be housed in a special lead container which will allow optical alignment of the beam with the aperture, contact zone, and crystal detector on the photomultiplier tube. In addition, the present set-up will make use of a laterally traveling slip for scanning the contact zone in lieu of moving the rolling disc test machine which was done in the original experiment.

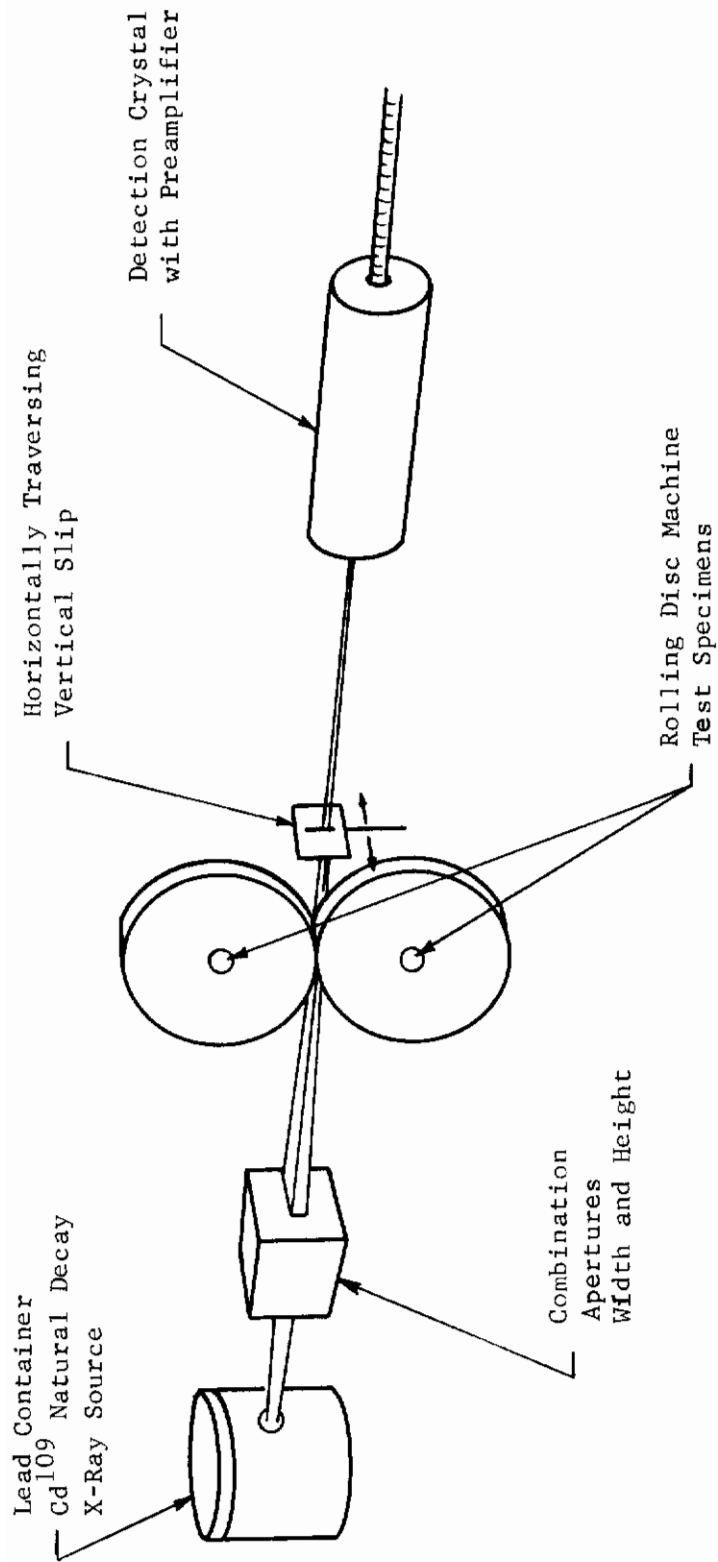


Fig. 33 X-Ray Film Thickness Measurement Assembly Showing the Path of the Radiation Through the Contact Zone of Rolling Discs.

Contrails

SECTION III

TRACTION DATA AND ANALYSIS

The methods by which traction data have been obtained have been described in detail in the preceding sections. In the following sections, the traction data obtained with our test apparatus for 5P4E polyphenyl ether will be presented in the form of traction versus slip rate curves. Traction curves have been obtained at loads corresponding to Hertz maximum pressures between 100,000 psi and 140,000 psi. The rolling speed varies from 900 in./sec to 1,820 in/sec and temperatures range from 175 F to 215 F. Most of the test data were obtained at low slip rates so that comparisons can be made between the MTI data and the traction data obtained at Battelle (1).

Comparisons will also be made between measured data and the data predicted by the MTI elastohydrodynamic performance code given in Reference 2. The elastohydrodynamic performance code tractions are predicted by means of a quasi-empirical method which attempts to relate traction data to the data obtained by Johnson and Cameron (14) for Shell turbo-33 oil. This method which is described in detail in Reference 2, generalizes Johnson and Cameron's data with the use of three dimensionless parameters which were first put forth by A.W. Crook (15) in his analysis of elastohydrodynamic tractions.

An attempt has also been made to predict tractions directly from the existing viscosity-temperature and -pressure data obtained by Midwest Research Institute (16) for polyphenyl ether. These data unfortunately do not extend to the 100,000 to 140,000 psi pressure range covered here. A hypothetical extrapolation of the Midwest data is also presented. This extrapolation was obtained by means of an assumed viscosity-pressure-temperature relationship which resulted in a reasonable fit to our measured data and has been used as a means of correlating the data.

1. TRACTION DATA

Chart recordings of traction data in the form of torque versus slip rate have been smoothed and fed digitally onto computer tape files where they are currently stored. A matrix of traction versus slip rate data is shown in Figures 34 through 36. These data have all been obtained at a temperature of approximately 200 F. The data shown in Figure 34 correspond to a rolling speed of 900 in/sec; Figure 35, 1,360 in/sec; and Figure 36, 1,820 in/sec. These are the same speeds used by Battelle (1). Tractions are found to increase markedly with load and to decrease with increasing speed.

The extent to which traction varies with load can be seen from Figure 37, which is a plot of traction coefficient (traction force divided by load) as a function of slip rate for a rolling speed of 900 in/sec. The spread of these traction coefficient curves at the three different loads indicates that a ceiling friction coefficient has not been reached. This is to be expected in that we are operating at very high rolling speeds in comparison with those given by Johnson and Cameron who observed the ceiling coefficient of traction behavior.

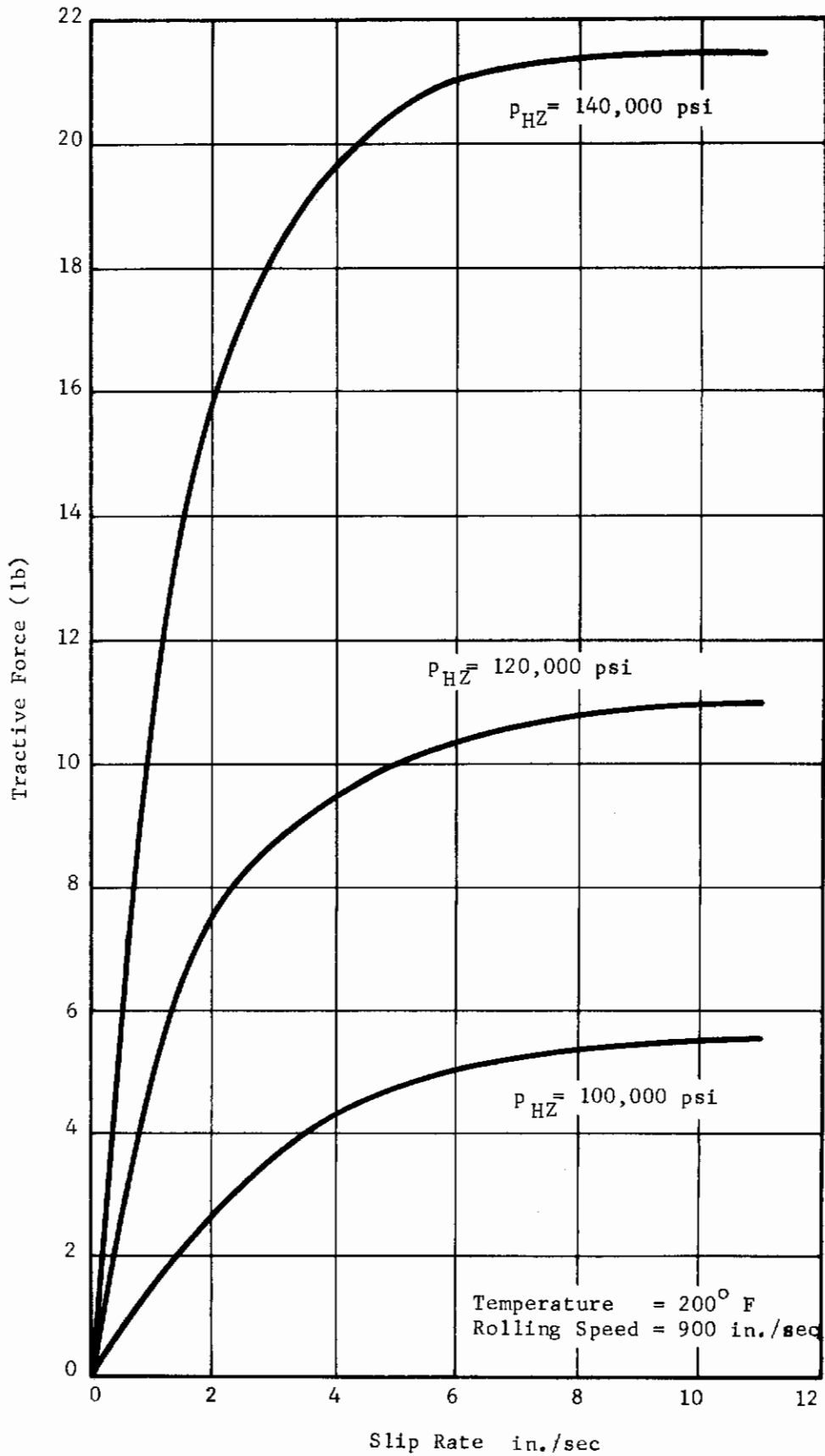


Fig. 34 Traction Data at 200° F at a Rolling Speed of 900 in./sec

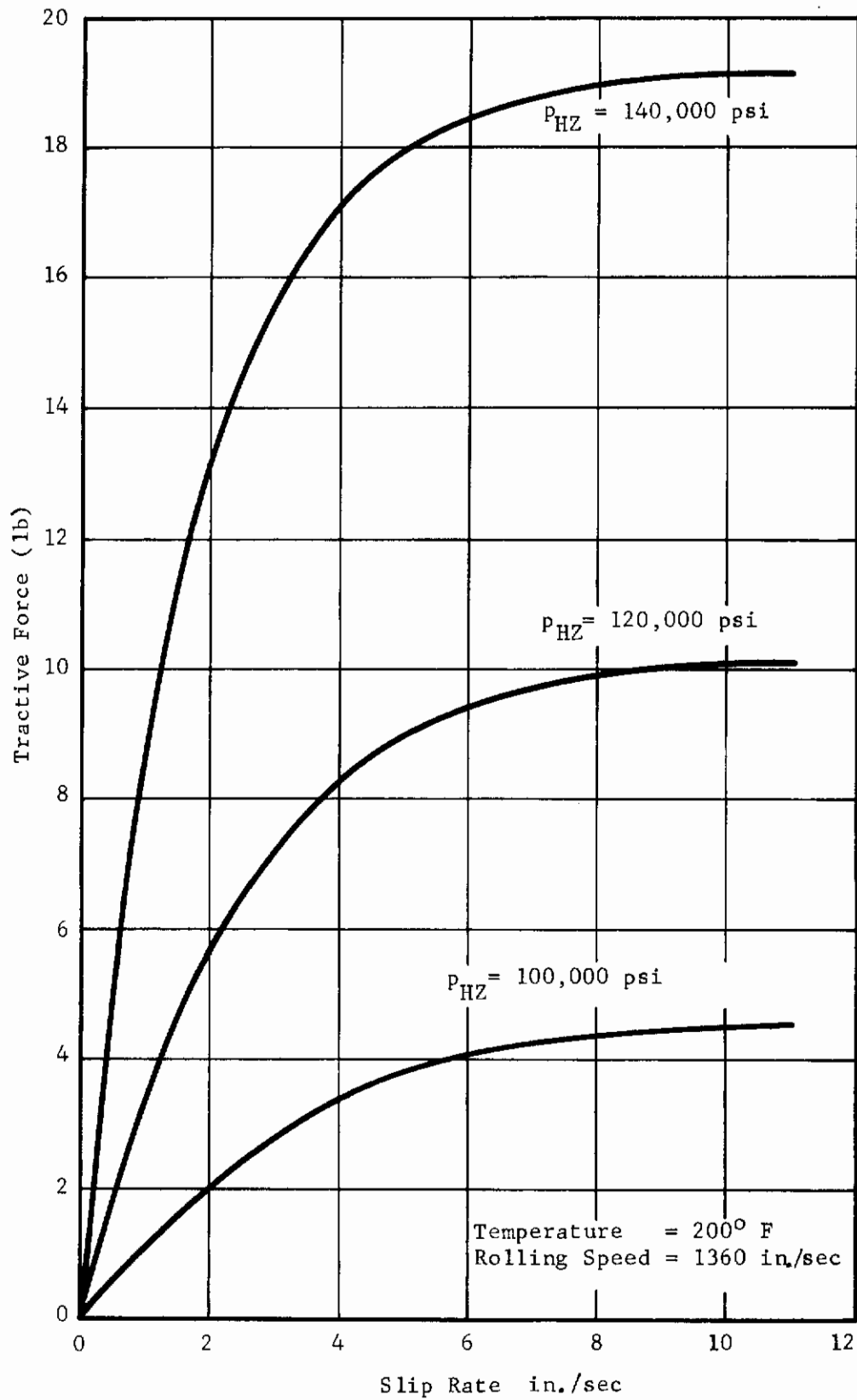


Fig. 35 Traction Data at 200° F at a Rolling Speed of 1360 in./sec

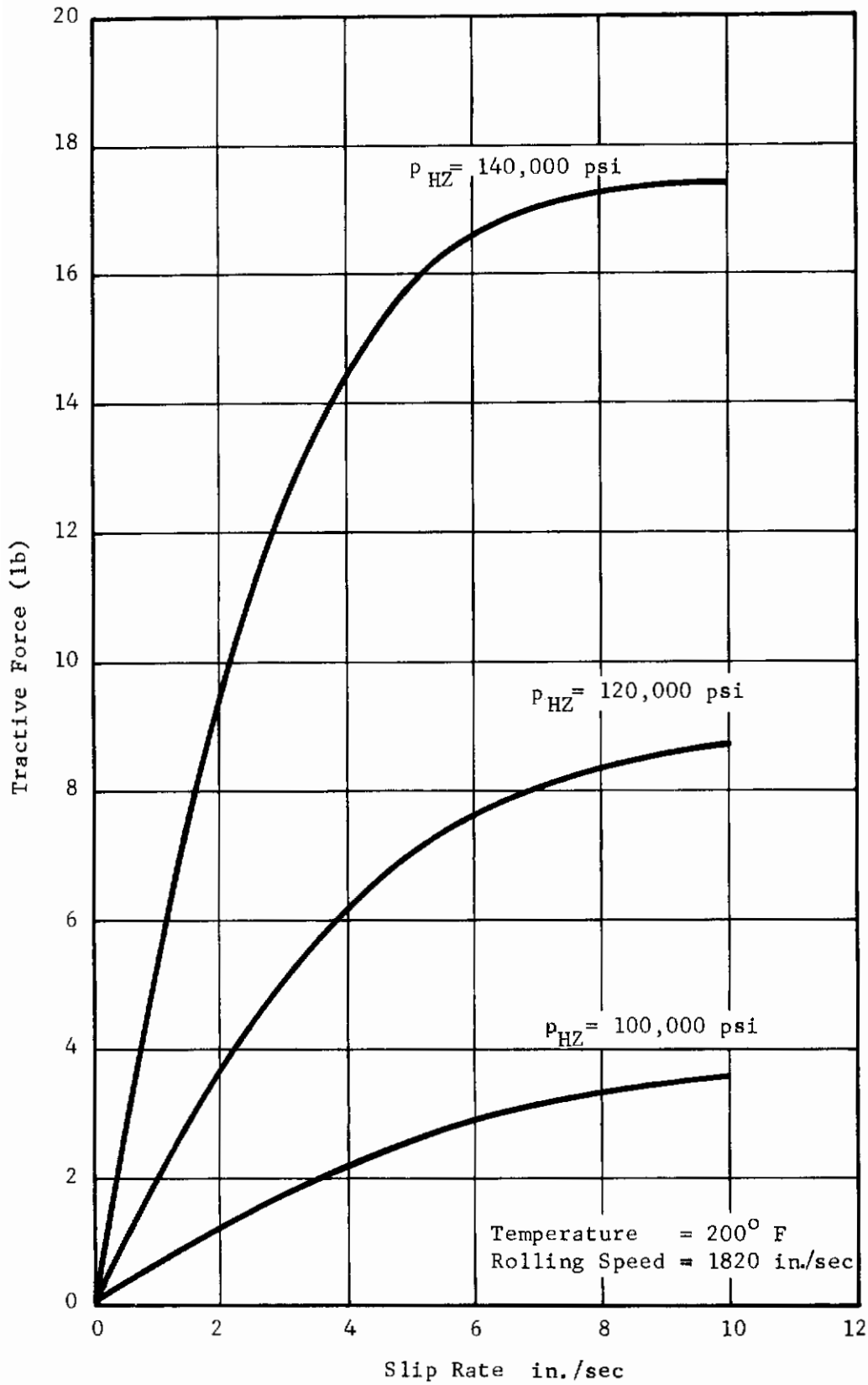


Fig. 36 Traction Data at 200° F at a Rolling Speed of 1820 in./sec

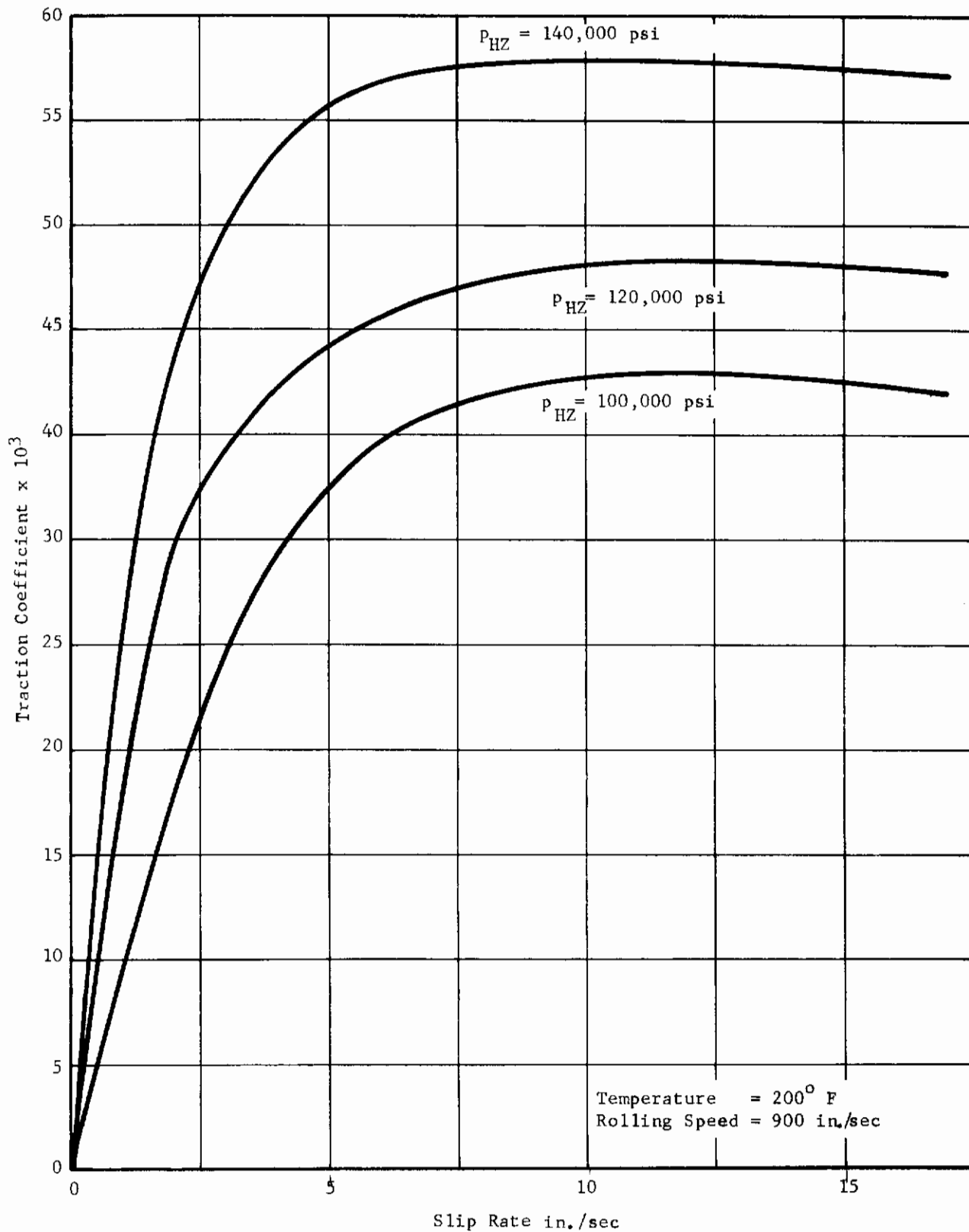


Fig. 37 Traction Coefficient at 200° F and 900 in./sec

Contrails

The variation in traction with rolling speed can in part be explained by the increase in film thickness with rolling speed. However, based upon calculations to be discussed later, the tractions seem to vary more than one would expect solely as a result of changes in film thickness.

The variation of traction with slip rate is quite similar to that reported by most other investigators. Tractions are found to first increase linearly with slip rate in the very low slip region, then the curves tend to bend over as thermal effects become more predominant; and then finally in the higher slip region where thermal effects are dominant, the tractions decrease with increasing slip rate. The data shown in Figures 34 through 37 extend to the vicinity of the peak tractions. Special emphasis is placed on the low slip region for purposes of comparison with Battelle data. However, several cases were run to show the behavior of traction as a function of slip rate at much higher slip. Two such curves are shown in Figure 38 for a rolling speed of 900 in/sec at loads corresponding to Hertz pressures of 100,000 and 120,000 psi. These are extensions of the curves shown in Figure 34. The decreasing portions of the traction curves are clearly seen here.

2. COMPARISON WITH BATTELLE DATA

The Battelle traction data was presented in the form of tractions in pounds versus shear rate in reciprocal seconds. The shear rates were obtained by dividing the slip rates by the measured film thicknesses that were measured by Battelle's x-ray technique (1). In order to make a direct comparison between our data and Battelle's the shear rates were converted back to slip rates based upon the Battelle measured film thickness data reported in Reference 1.

A major discrepancy between MTI data and Battelle data is the variation in tractions with temperature. MTI data is almost completely insensitive to temperature, whereas Battelle reported marked variations in traction with temperature. A direct comparison between MTI and Battelle data at two different temperatures at a rolling speed of 1,820 in/sec and a Hertz maximum pressure of 100,000 psi, is shown in Figure 39. The Battelle data obtained at 220 F appears at least in the lower slip range to be very similar to MTI data. The MTI data at 175 F falls slightly, although not significantly, below the 215 F data, whereas the Battelle 175 F data lies more than a factor of 2 above the 220 F data. In light of this discrepancy in the temperature dependence of tractions it will be somewhat difficult to make absolute comparisons of the variation in tractions with other parameters such as load and rolling speed. If quantitative agreement is observed at a particular temperature, then discrepancies will arise at other temperatures.

An attempt has been made, however, to make relative comparisons between trends in the traction data by comparing variations with rolling speed and load

* No definite temperature trend was apparent. In some cases traction appeared to increase slightly with increasing temperature and in other cases it was found to decrease. In all cases, the scatter was relatively small.

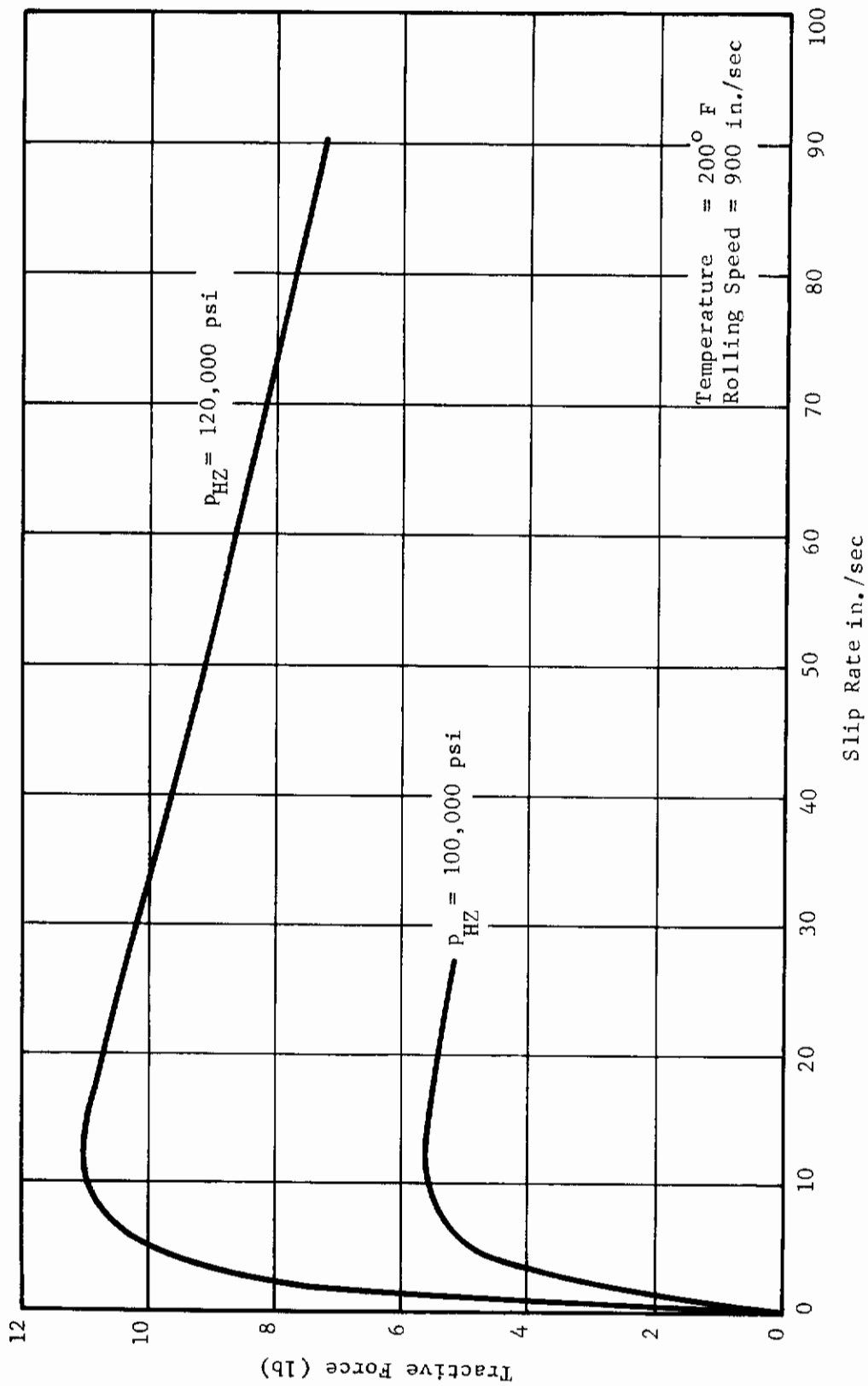


Fig. 38 High Slip-Rate Data at 200° F and a Rolling Speed of 900 in./sec

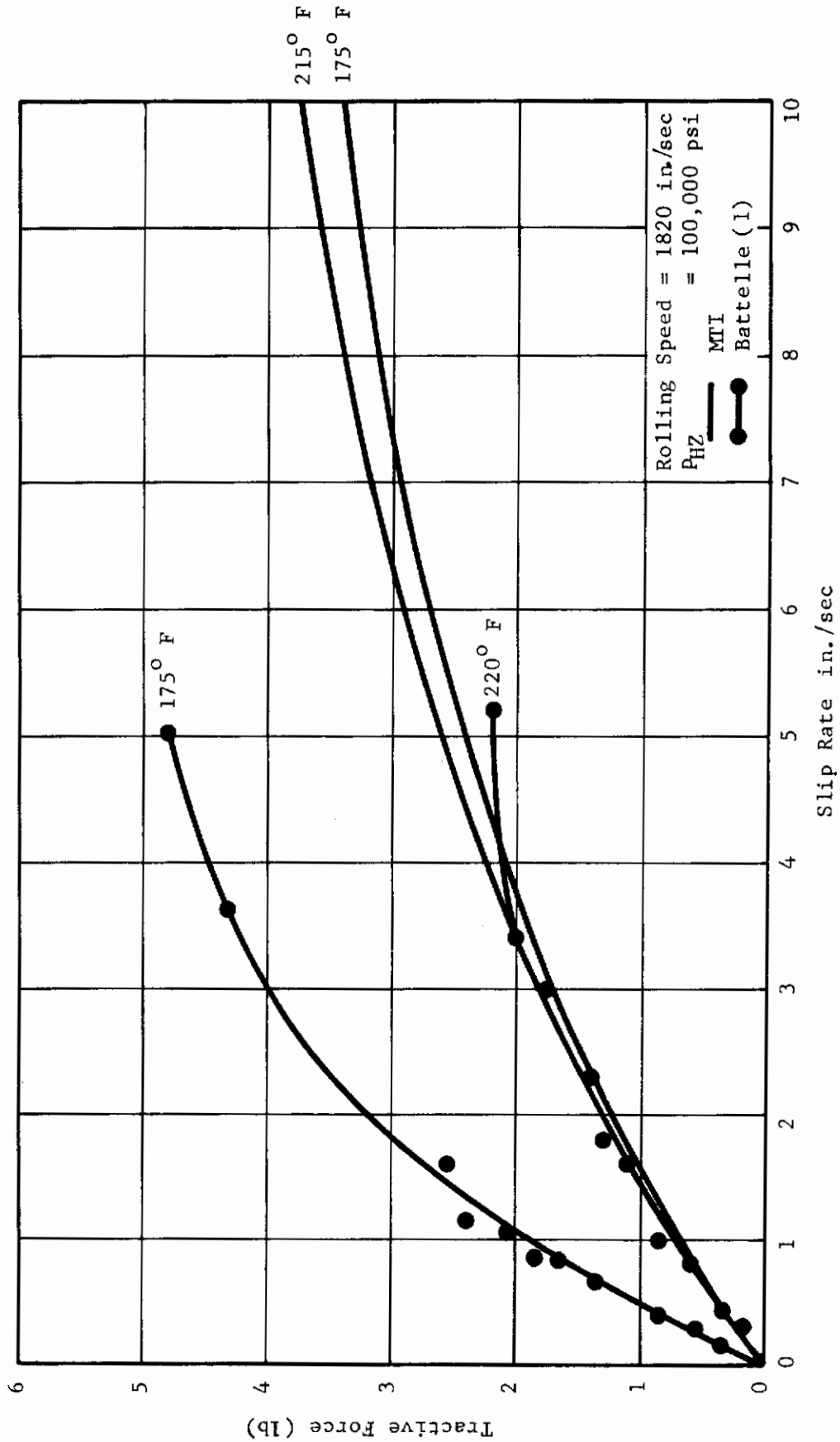


Fig. 39 Comparison Between MTI and Battelle Traction Data at Different Temperatures

between MTI data at 200 F and Battelle data at 220 F. Since these data agree at 1,820 in/sec and 100,000 psi, differences in trends may be observed at other loads and speeds.

Comparisons between 220 F Battelle data and 200 F data at a Hertz maximum pressure of 100,000 psi and rolling speeds of 900 and 1,820 in/sec are shown in Figure 40. Both Battelle and MTI data exhibit tractions which decrease with increasing rolling speed, however, the variations with slip rate appear to be somewhat different between the two sets of data. The Battelle data appears to exhibit a steeper slope at very low slip rates and to level off at somewhat lower slip rates than the MTI data. A comparison between Battelle and MTI traction data at 140,000 psi is shown in Figure 41. The Battelle data appear to exhibit an even stronger sensitivity to load than MTI data.

As a result of this study it can be concluded that although the MTI and Battelle traction data lie within the same overall range and exhibit qualitative similarities with respect to relative behavior as functions of slip rate, rolling speed and load (although not temperature), they do not in any sense agree well quantitatively. Tractions are believed to be extremely sensitive to rheological properties of the lubricant and the Battelle data were taken nine years earlier with lubricant obtained from a different batch than that used by MTI. Hence, it is quite possible that some structural differences or possibly additives could account for some of the observed discrepancies.

3. COMPARISON OF TRACTION DATA WITH PERFORMANCE CODE PREDICTIONS

The elastohydrodynamic performance code (2) predicts tractions based upon the data of Johnson and Cameron (14), together with a method of generalization based on dimensionless parameters evolved by A.W. Crook (15).

Traction coefficients (F_x/P) are assumed to be functions of the inlet temperature and the three parameters G_1 , G_2 , and G_3 are defined below:

$$G_1 = \frac{\mu_o u_s}{p_{HZ} h}, \quad G_2 = \frac{\beta_1 \mu_o u_s^2}{8K_f}, \quad G_3 = \alpha p_{HZ}$$

where μ_o is the viscosity at the inlet oil temperature T_o , u_s is the slip rate, h is the lubricant film thickness, p_{HZ} is the maximum Hertz pressure, and K_f is the thermal conductivity of the fluid. The quantities α and β_1 are viscosity pressure and temperature coefficients based on the viscosity pressure and temperature relationship

$$\mu = \mu_o e^{\alpha p - \beta_1 (T - T_o)} \quad (1)$$

where p denotes pressure and T is temperature.

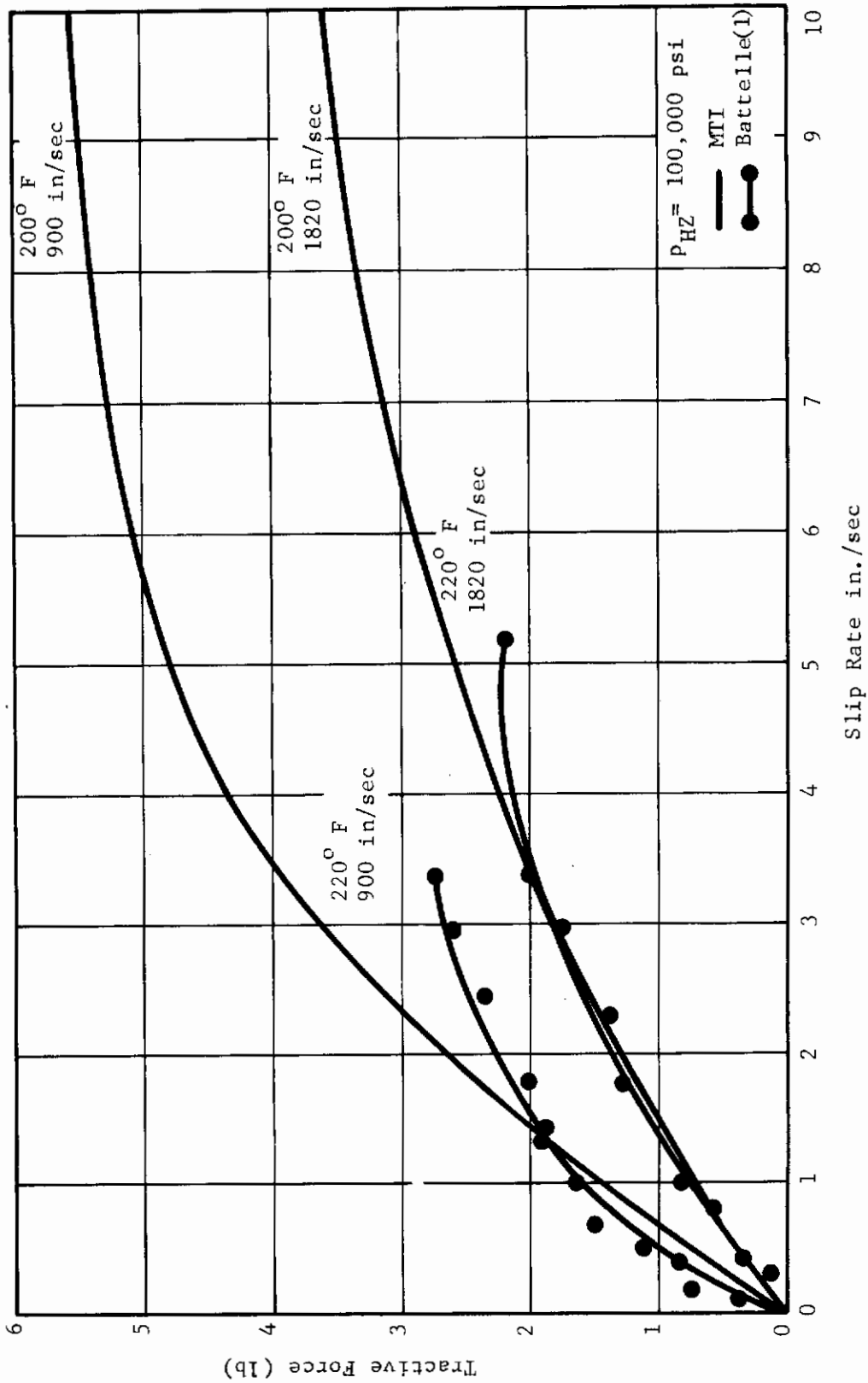


Fig. 40 Comparison Between MTI and Battelle Traction Data at Different Rolling Speeds

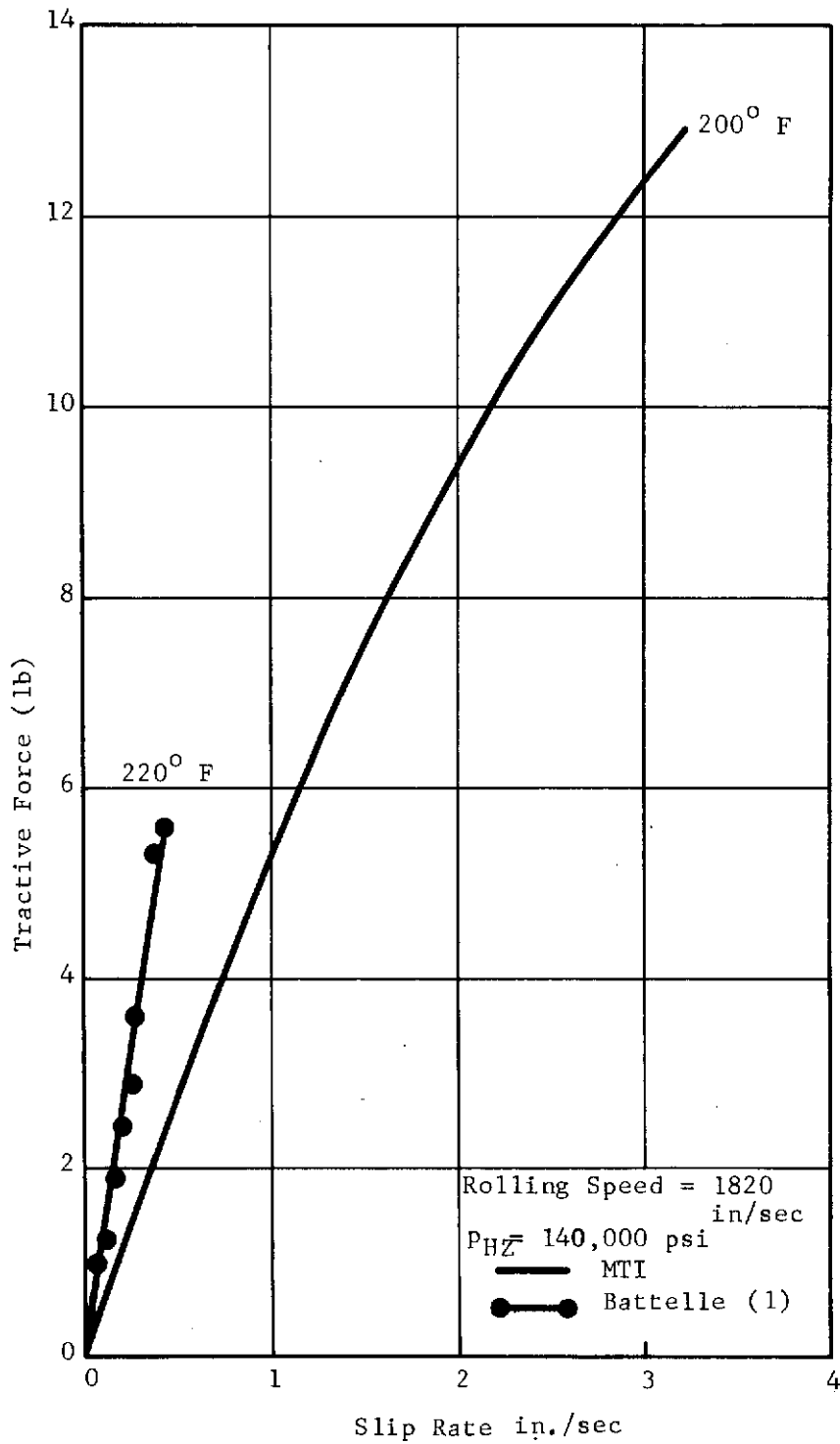


Fig. 41 Comparison Between MTI and Battelle Data at a Hertz Pressure of 140,000 psi.

Contrails

The film thickness, h , appearing in the above parameters is calculated by means of Dowson and Higginson's formula (17) and modified by the thermal correction factor for viscous and compressive heating in the inlet zone given in Reference 2. Traction is calculated for an equivalent line contact which preserves the Hertz maximum pressure and minor half width of the elliptical contact.

Comparisons between performance code predictions and measured tractions at an inlet temperature of 200 F and a rolling speed of 1,820 in/sec and pressures ranging from 100,000 to 140,000 psi are shown in Figure 42. It can be seen that both performance code predictions and experimental data indicate that the traction coefficients will vary with load and that the predicted values of peak tractions lie within a factor of 2 above measured values. The behavior between performance code predictions and MTI experiments is radically dissimilar in the low slip range. Performance code predictions indicate a much more rapid rate of climb of traction coefficients with slip rate and lower values of the slip rates at which peak tractions occur than measured experimentally. In that the performance code attempts to relate data taken with one lubricant (Shell turbo-33 oil) over a range of loads and rolling speeds to a radically different lubricant (5P4E polyphenyl ether) at considerably higher speeds, it is not surprising that dissimilarities exist. Predictions do, however, fall within the right order of magnitude, and have some qualitative similarity with the data.

It is also interesting to note that the performance code predictions are qualitatively in accord with the data regarding sensitivity of traction coefficients to temperature as shown in Figure 43. It can be seen that the tractions predicted at 175 F lie only slightly above those predicted to occur at 220 F.

4. COMPARISON BETWEEN MEASURED TRACTIONS AND PREDICTIONS BASED UPON EXISTING VISCOSITY DATA

Viscosity data for 5P4E polyphenyl ether has been obtained by Midwest Research Institute (16) over a range of pressures and temperatures. The results of their measurements are shown in Figure 44. The viscosity data extend up to 70,000 psi at 300 F, 50,000 psi at 210 F, and 10,000 psi at 100 F.

It should be noted that the viscosity-pressure data at 210 F and 300 F are concave upward on the semi-log scale used in Figure 44. If the lubricant is to behave as a liquid over the entire range of pressures and shear rates of interest then the viscosity-pressure curves should eventually inflect and the viscosities should level off. The curvature of the viscosity-pressure curves was thus not used in extrapolating viscosities to the 100 to 150,000 psi pressure range, but instead it was decided to use the straight lines (on a semi-log scale) which best approximate the viscosity behavior in the lower pressure range.

These lines are shown on Figure 44 and were obtained by fitting the low pressure viscosity as functions of pressure and temperature with the formula

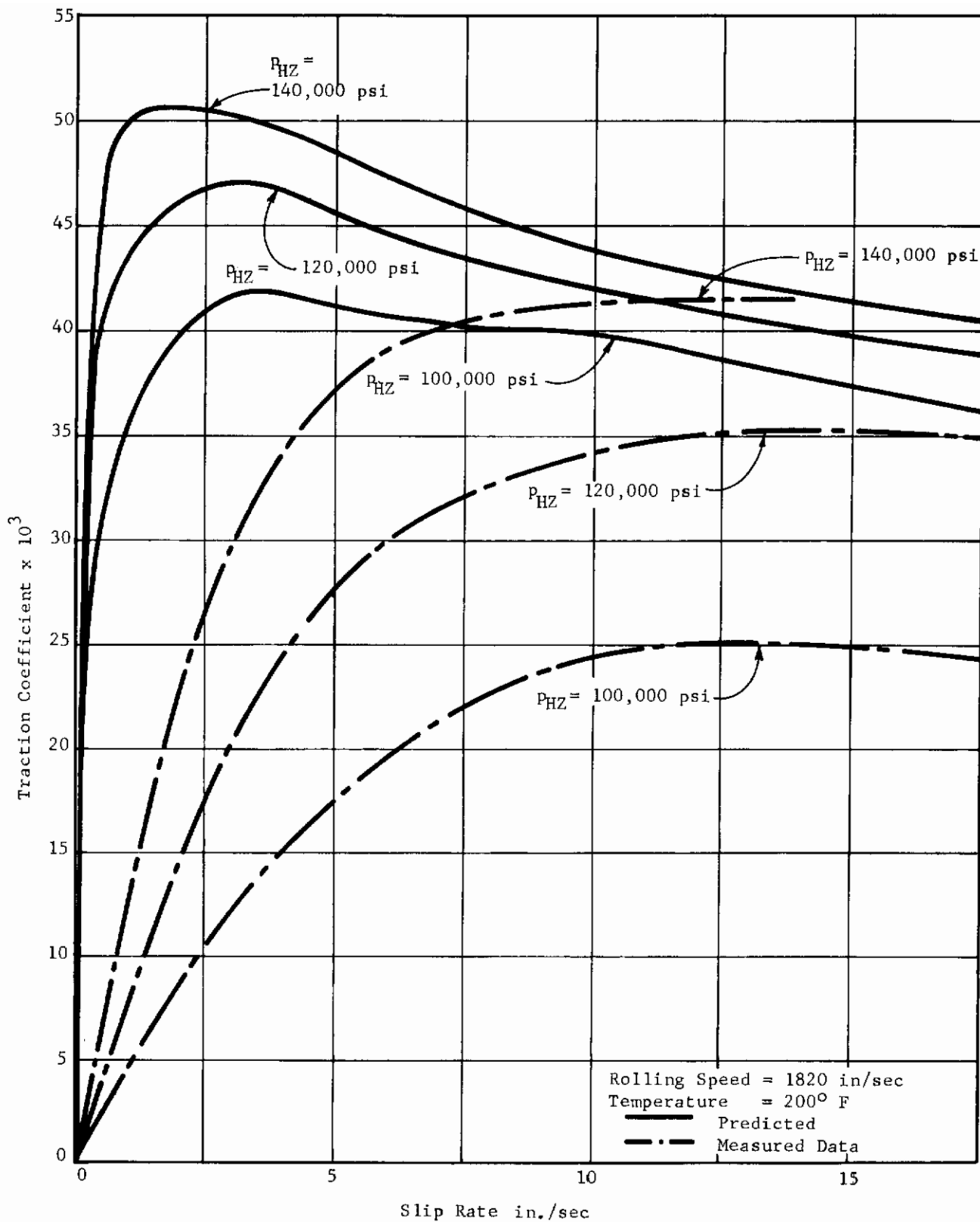


Fig. 42 Comparison Between Measured Traction Coefficients and Performance Code Predictions

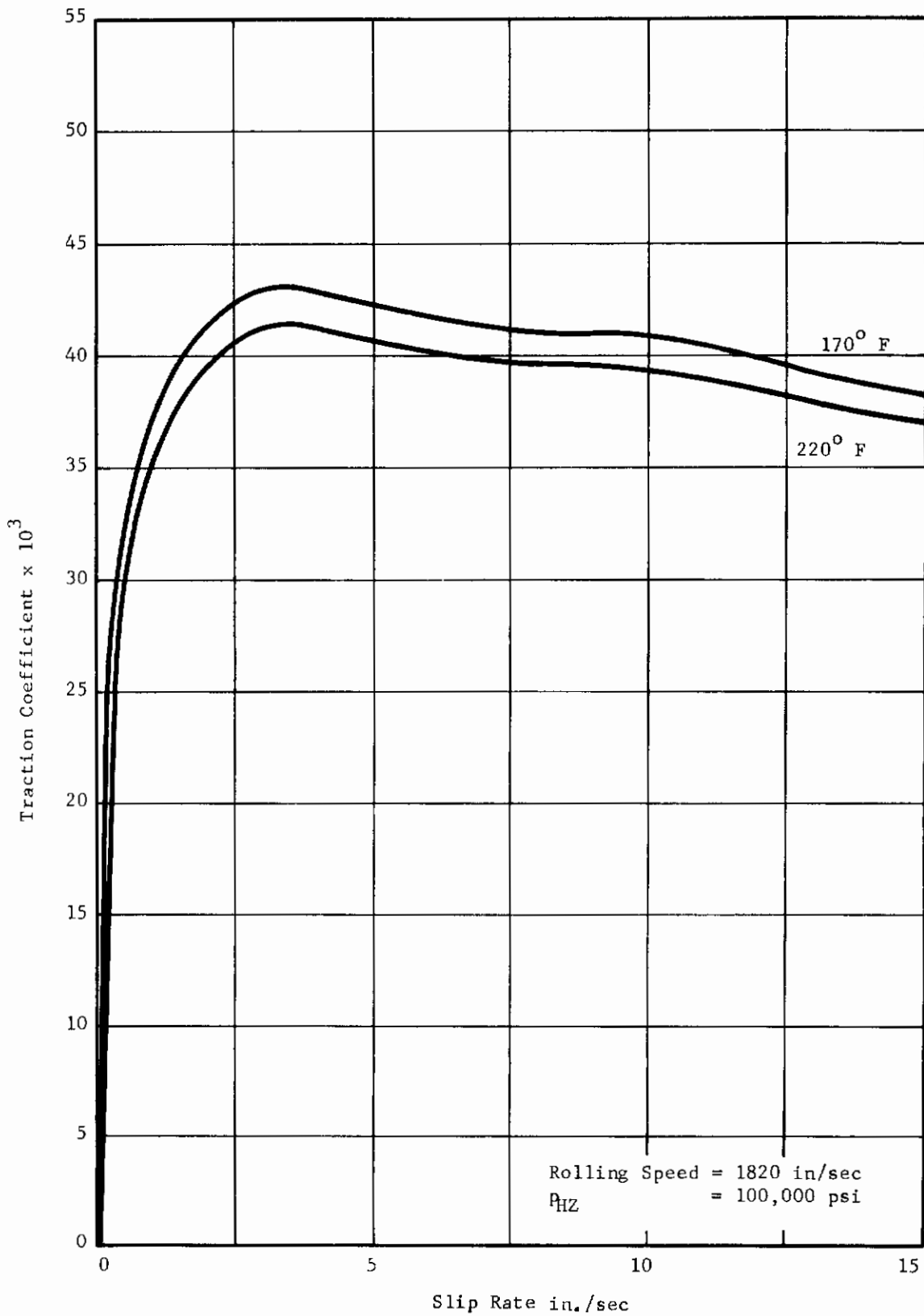


Fig. 43 Performance Code Prediction of the Effect of Lubricant Temperature on Traction Coefficients

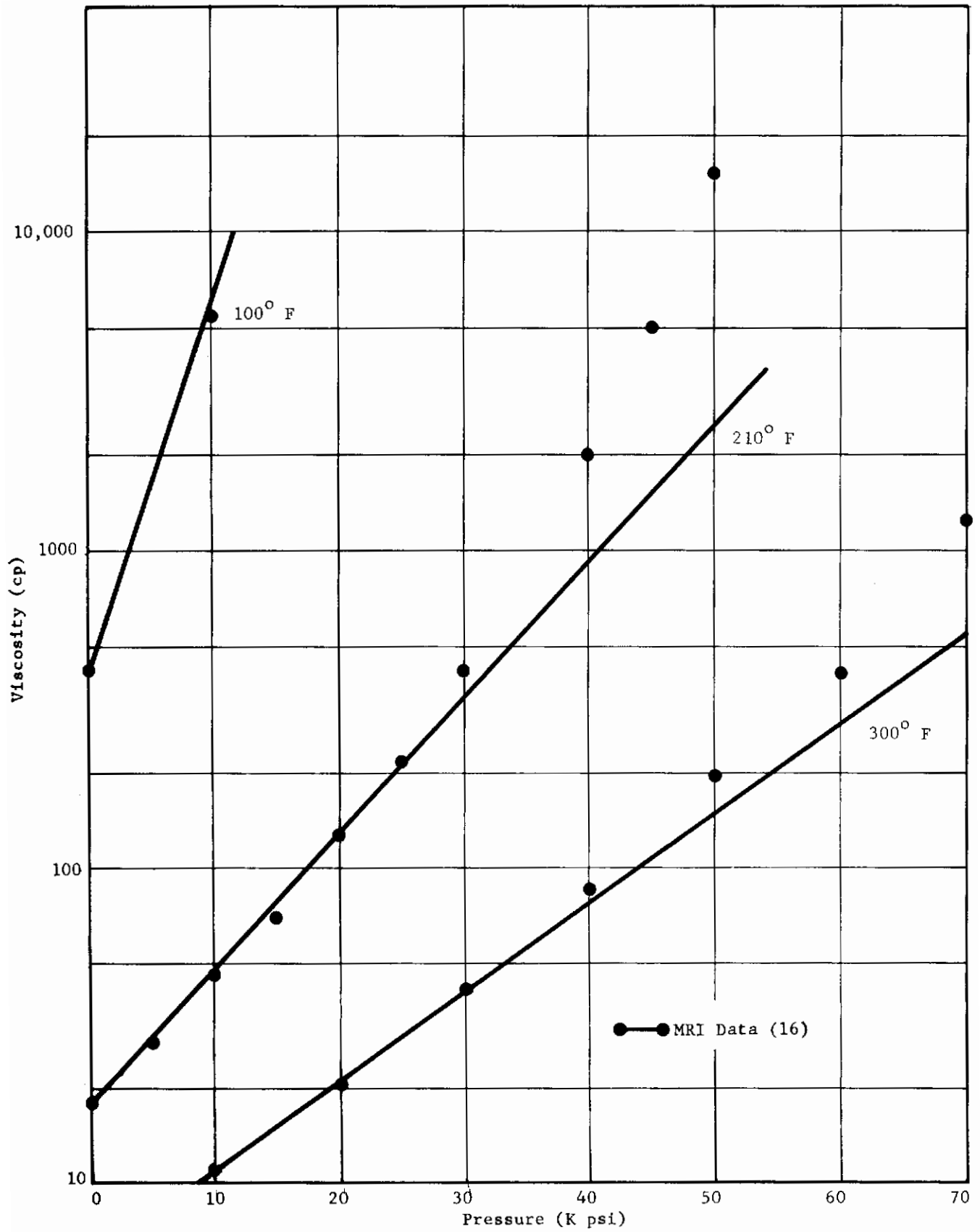


Fig. 44 Viscosity Data for Polyphenyl Ether (5P4E)

$$\mu = \mu_r e^{\alpha p + (\beta + \gamma p) \left(\frac{1}{T+C} - \frac{1}{T_r+C} \right)} \quad (2)$$

where μ_r is a reference viscosity at atmospheric pressure and reference temperature T_r . Values of the parameters in obtaining the fit are

$$\begin{aligned} \alpha &= 1.116 \times 10^{-4} \text{ in}^2/\text{lb} \\ \beta &= 736.1^\circ \text{ F} \\ \gamma &= 3.338 \times 10^{-2} \text{ in}^2\text{-}^\circ\text{F}/\text{lb} \\ C &= 12^\circ \text{ F} \\ \mu_0 &= 2.798 \times 10^{-6} \text{ lb-sec/in}^2. \end{aligned}$$

The traction theory put forth by A.W. Crook (15) predicted tractions for line contact for a viscosity pressure-temperature relationship given by Equation (1). This theory was later modified by Kannel and Walowit (18) to make it amenable to predicting tractions for any prescribed viscosity pressure-temperature relationship for a line contact. This theory for predicting shear stresses has been used in conjunction with the viscosity relationship given by Equation (2) and the shear stresses in turn have been integrated over the entire elliptical contact to predict tractions.

Predictions obtained with the use of this analysis are shown together with the experimental data corresponding to a rolling speed of 1,820 in/sec and a temperature of 200 F in Figure 45. It can be seen that the agreement between theory and experiment, particularly at 140,000 psi, is not good. The ascent rate is too steep, the peak traction occurs at too low a slip rate, and the descending portion of the curve is far too steep. It is believed that a partial explanation of the discrepancy between theory and experiment, particularly at higher loads and in the low slip range, results from the fact that the actual viscosities at the center of contact which are the dominant viscosities in determining tractions are greatly over predicted by the representation used to extrapolate viscosity data up to 140,000 psi. This problem will be dealt with further in the following section.

5. APPARENT VISCOSITY RELATIONSHIPS BASED UPON TRACTION DATA

As a result of the exponential behavior of viscosity with pressure it is to be expected that the dominant tractive forces will arise near the center of contact where the pressures and hence the viscosities are the highest. The pressures at the center of contact extend up to 140,000 psi and are far out of range of the pressures over which viscosity data were taken. In addition, high rolling speeds and shear rates are prevalent which could give rise to non-newtonian and short time effects hence it is not surprising that traction predictions based on these low pressure, low shear, long time data, fall short of providing adequate predictions of measured tractions.

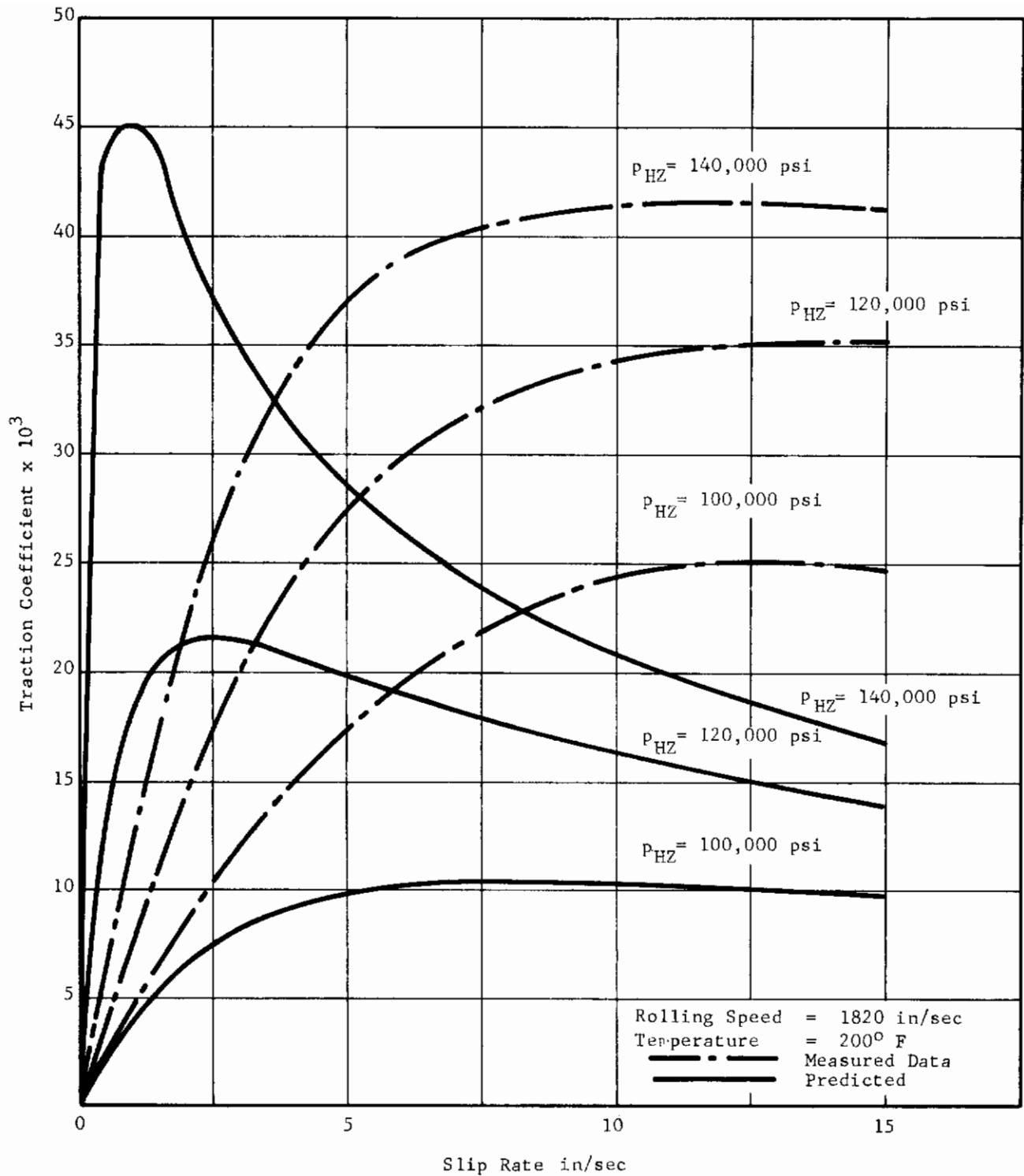


Fig. 45 Comparison Between Measured Traction and Theoretical Prediction

Conrails

In this section attempts will be made to work backwards from measured data to obtain a hypothetical apparent viscosity relationship as a function of pressure and temperature and to use it to correlate traction measurements.

To carry out this objective without introducing undue complexities, a hypothetical viscosity-pressure-temperature relationship of the form given by Equation (1) will be used to describe the behavior of polyphenyl ether in the high pressure region. We may write this equation as

$$\mu = \mu_o^* e^{\alpha^* p - \beta^* (T-T_o)} \quad (3)$$

Here, the three constants μ_o^* , α^* , and β^* refer to the effective high pressure viscosity behavior of polyphenyl ether and will be numerically different from the coefficients μ_o , α , and β given in Equation (1).

These constants could, in principal, be determined from one traction versus slip rate curve and then fixed values of these constants could be used to predict variations of traction with load, slip rate, and rolling speed. If indeed a simple three constant fit of this nature could actually describe a series of curves taken over a range of loads and rolling speeds, it would go a long way toward both correlating the data and providing a means for interpolating and possibly, extrapolating the data.

A plot of a hypothetical viscosity-pressure-temperature relationship is shown in Figure 46. The circled points represent the Midwest Research Institute data at 210 F. Predicted tractions should be relatively insensitive to the shape of the lower portion of the viscosity curve and should be determined primarily by the "high pressure line" shown in Figure 46. Film thickness is determined largely in the inlet zone where the pressures are somewhat lower. Hence, the effective pressure coefficient of viscosity and base viscosity used in calculating film thickness will be taken from the slope and intercept of the "low pressure" line in Figure 46.

The equations for predicting shear stress τ resulting from an exponential viscosity function of the form given by Equation 3 are in the literature (15, 18) and are given below in terms of present notation:

$$\tau_x = \frac{\mu_o^* u_s e^{\alpha^* p/2} \sinh^{-1} (\Psi e^{\alpha^* p/2})}{\Psi \sqrt{1 + \Psi^2 e^{\alpha^* p}}}$$

where h denotes the film thickness (assumed constant) in the contact zone and p is the local pressure. The dimensionless parameter Ψ is defined as

$$\Psi = u_s \sqrt{\frac{\mu_o^* \beta^*}{8K_f}}$$

Contrails

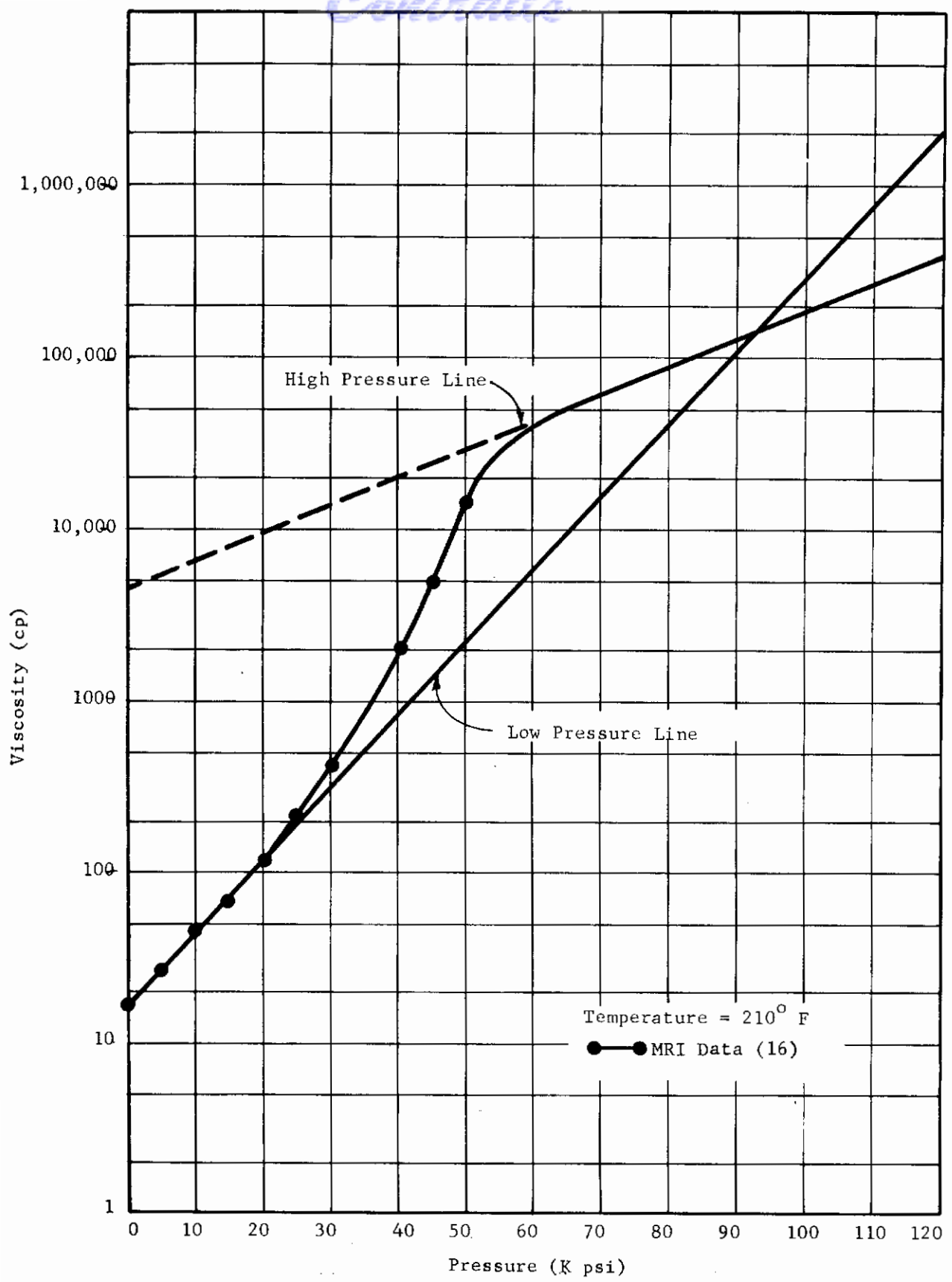


Fig. 46 Hypothetical High Pressure-Viscosity Relationship

Contrails

The pressure p is assumed to be Hertzian in the contact zone (15, 18) and is given by

$$p = p_{HZ} \sqrt{1 - \left(\frac{x}{b}\right)^2 - \left(\frac{y}{a}\right)^2}$$

where a and b represent semi-major and semi-minor axes of the contact ellipse and x and y represent coordinates in the rolling and axial directions respectively.

The total tractive force F_x for elliptic contact is obtained by integrating the shear stress τ_x over the elliptical contact area

$$F_x = 4 \int_0^a \int_0^b \sqrt{1 - (y/a)^2} \tau_x dx dy$$

The above integral may be expressed mathematically as follows

$$F_x = \frac{2P}{\alpha^* p_{HZ} h \Psi} \sqrt{\frac{8K_f \mu_o^*}{\beta^*}} \left\{ \left[\sinh^{-1} (\Psi e^{\alpha^* p_{HZ}/2}) \right]^2 - \left[\frac{2}{\alpha^* p_{HZ}} \left(\Phi(\Psi e^{\alpha^* p_{HZ}/2}) - \Phi(\Psi) \right) \right] \right\} \quad (4)$$

where the function $\Phi(\Psi)$ is given by the relationship

$$\Phi(\Psi) = \int_0^\Psi \frac{[\sinh^{-1}(\Psi')]^2}{\Psi'} d\Psi'$$

which is shown graphically in Figure 47.

Film thicknesses were calculated with the use of Grubin's formula (17) and modified with the use of thermal reduction factors computed from the elastohydrodynamic performance code (2). For the range of conditions used in obtaining the data appearing in Figures 34-36 thermal reduction factors were found to very nearly offset the isothermal (8/11 power) increase in film thickness

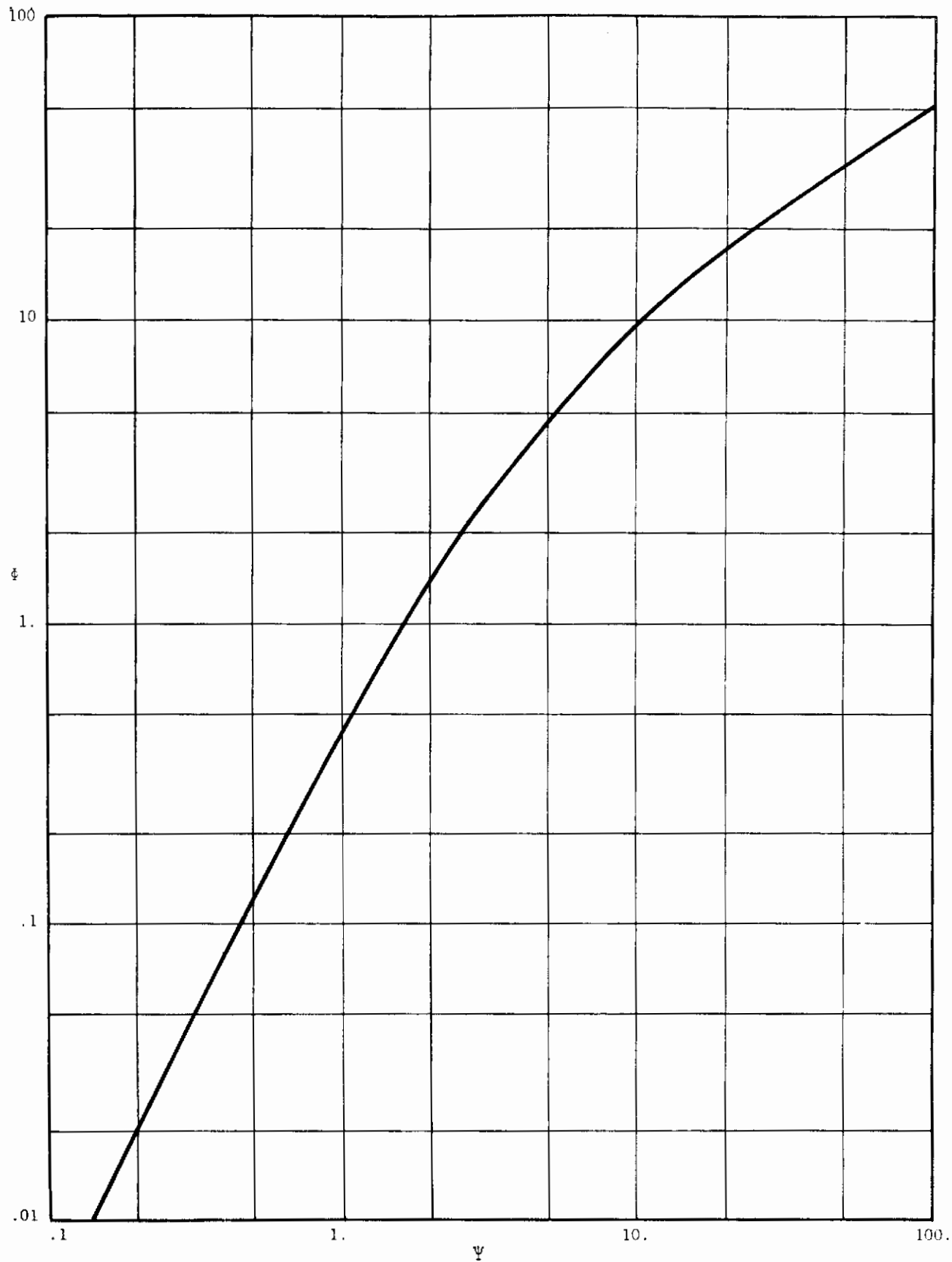


Fig. 47 Function $\phi(\psi)$ Used in Predicting Traction

Conclusions

with speed. Predicted film thicknesses were all found to be within $\pm 10\%$ of 50 micro-inches for the entire range of rolling speeds (900 - 1820 cps) and Hertz pressures (100,000 - 140,000 psi) under consideration.

Tractions were computed with the use of Equation (4) and values of the quantities μ_o^* and α^* were determined by fitting the low slip rate portions of the data shown in Figure 36. The low slip regions were used since the viscous heating will be low there and predicted tractions will be insensitive to the viscosity temperature coefficient (the insensitivity is indicated by the linearity of the traction vs. slip rate curves in the low slip region). It was thus possible to determine values of μ_o^* and α^* independently of β^* . A value of the temperature coefficient β^* was then determined to provide a reasonable fit to the peak tractions for the data shown in Figure 36. It should be noted that no real attempt was made to optimize the constants.

The results of this "viscosity determination process" are shown in Figure 48 for the 1,820 in/sec rolling speed data. It can be seen that the three constant fit can reasonably describe the three curves showing variations of traction versus slip rate over a range of loads. The values of the constants are

$$\begin{aligned}\mu_o^* &= 1.01 \times 10^{-3} \text{ lb-sec-in}^{-2}, \\ \alpha^* &= .377 \times 10^{-4} \text{ in}^2/\text{lb and} \\ \beta^* &= 0.046 \text{ } ^\circ\text{F}^{-1}.\end{aligned}$$

The viscosity isotherm at 210 F corresponding to these values is the "high pressure line" shown in Figure 46. Comparisons between tractions predicted with the values of μ_o^* , α^* , and β^* determined above and the measured data at the other two rolling speeds are shown in Figures 49 and 50. The predicted tractions vary inversely with film thickness hence they vary only slightly with rolling speed because of the insensitivity of the predicted film thickness to rolling speed. The increasing discrepancies between predicted and measured traction at rolling speed 1,360 rps and 900 rps are a result of the rolling speed dependence of the data.

It should be noted that whereas thermal film thickness theory results in traction predictions that are less sensitive to rolling speed than measured data, isothermal theory results in predictions that are considerably more sensitive to rolling speed than the data indicate. It is possible that the true film thickness lies somewhere between the two predictions which might account for the observed rolling speed dependence of tractions.

It is also possible that the film thickness, in fact, is insensitive to rolling speed and that the variation in traction with rolling speed is a result of short time effects on lubricant viscosity or inlet zone heating effects which were not taken into account in arriving at Equation (4). Such effects could be characterized empirically by allowing μ_o^* to vary with rolling speed. The indicated curves appearing in Figures 49 and 50 were obtained by allowing μ_o^* to vary with rolling speed in fitting the data, but keeping α^* and β^* constant. The values of the apparent viscosity coefficient μ_o^* are 1.4×10^{-3}

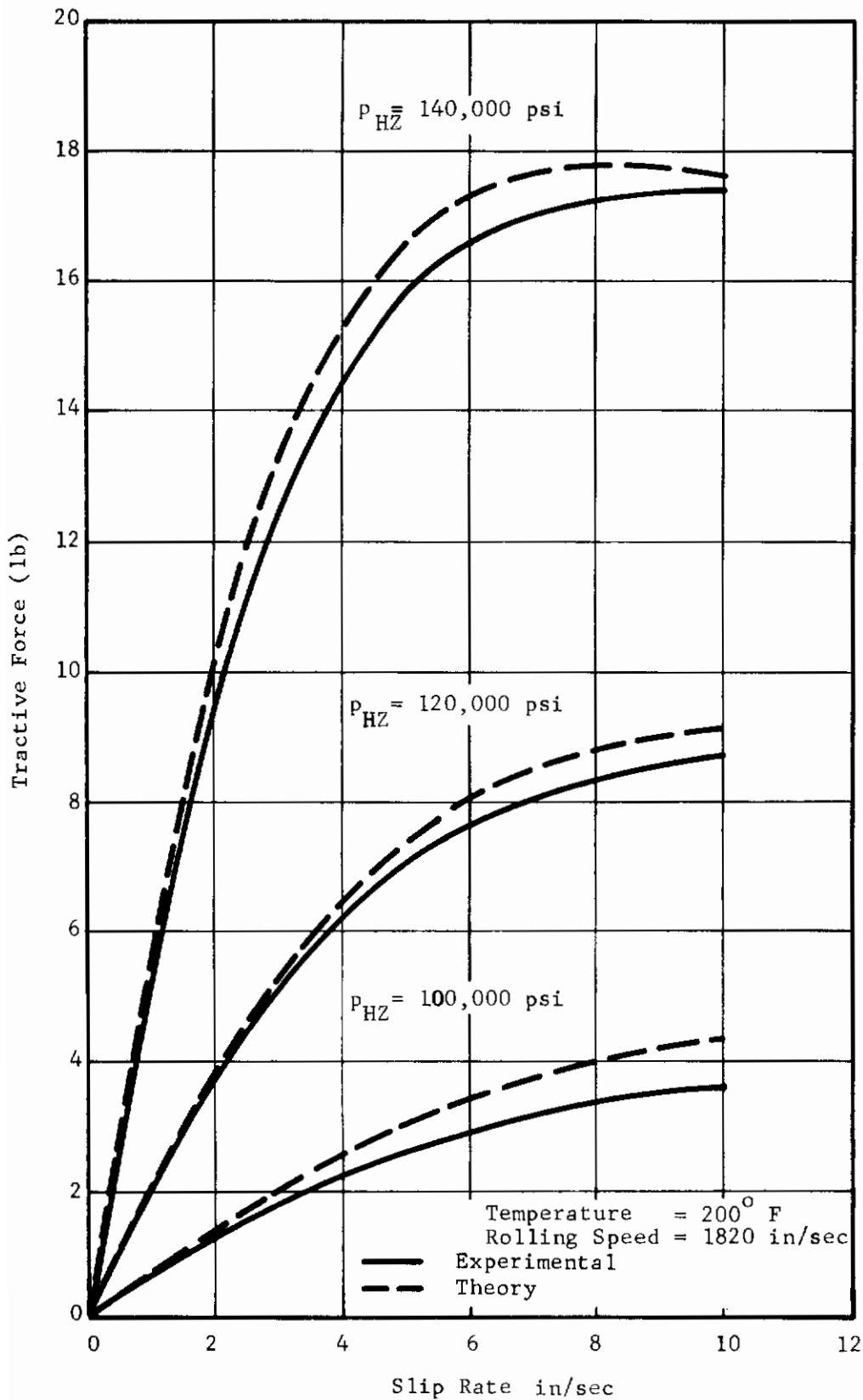


Fig. 48 Comparison Between Predicted Traction Using Hypothetical Viscosity Model and Data at a Rolling Speed of 1820 in/sec

Contrails

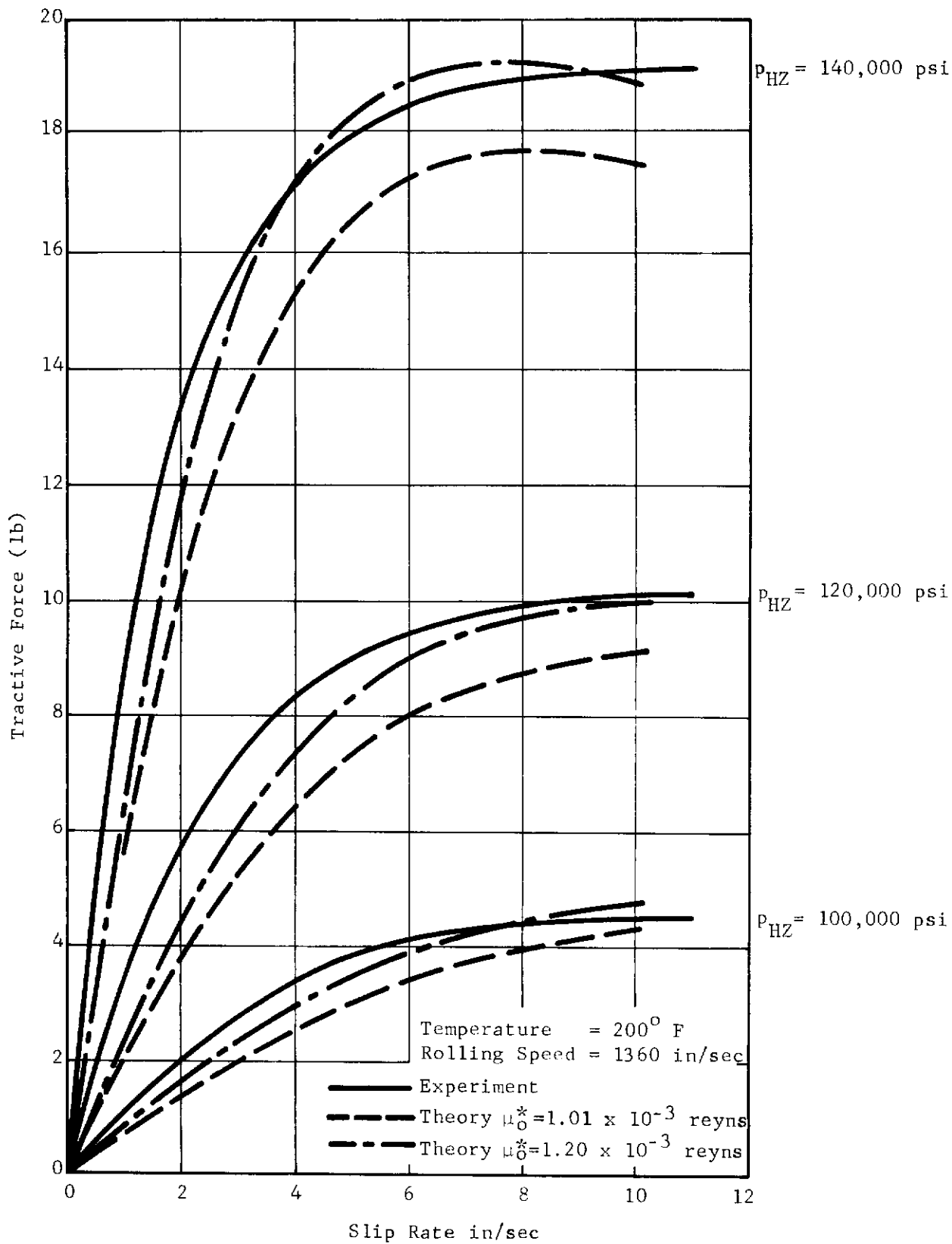


Fig. 49 Comparison Between Predicted and Measured Traction at 1360 in/sec

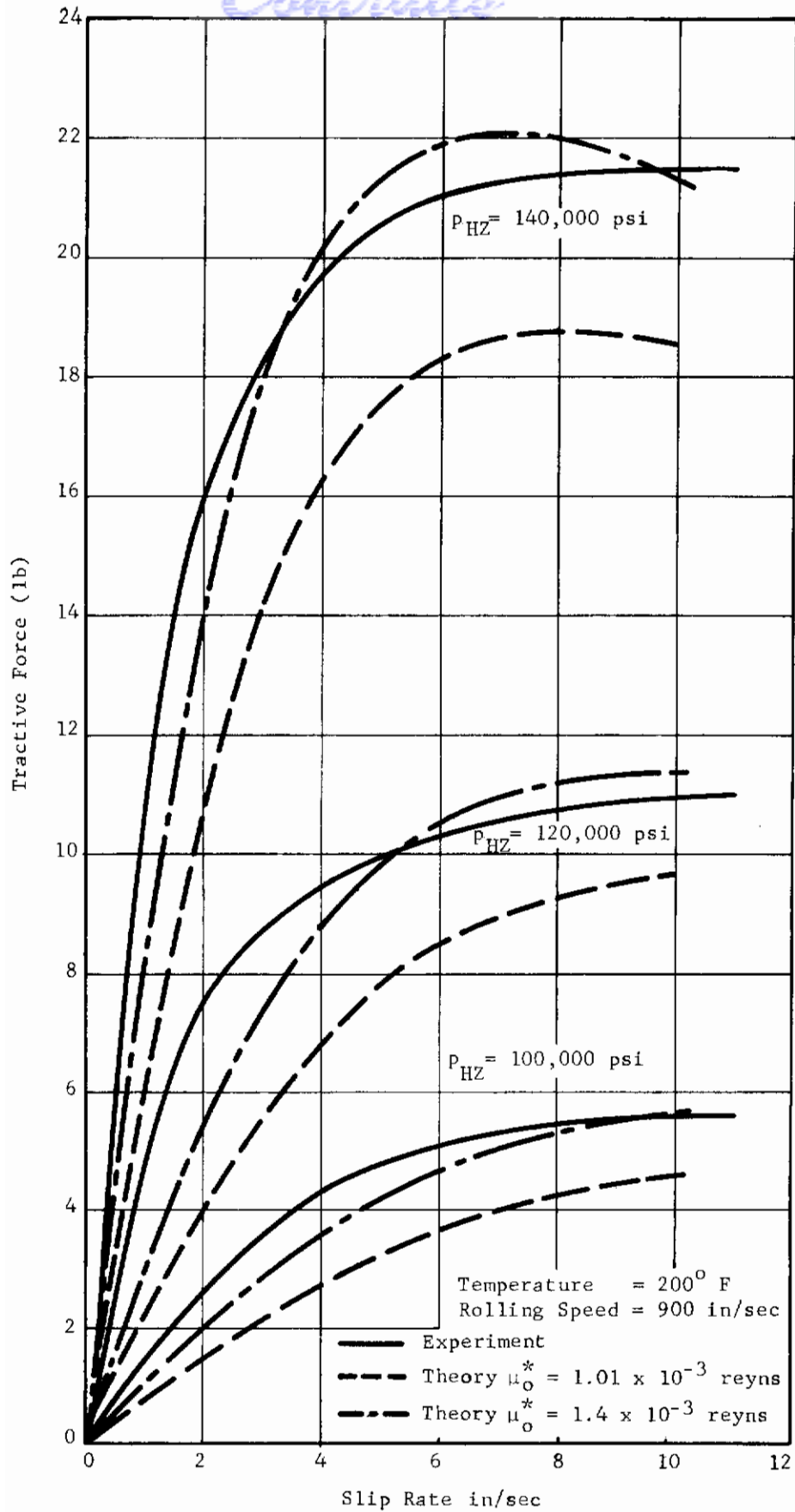


Fig. 50 Comparison Between Predicted and Measured Traction at 900 in/sec

Contrails

reyns at 900 ips, 1.2×10^{-3} reyns at 1,360 in/sec and 1.01×10^{-3} reyns at 1,820 in/sec.

The relationships put forth in this section characterize the variation in traction with load fairly well (even using a single value of μ^*) and speed dependent values of μ_0 can be used to obtain an improved fit of the data at different rolling speeds.

In the absence of better quantitative information regarding the rheological properties of polyphenyl ether at high pressures, high shear rates and short times, it is hoped that an apparent viscosity model of the type advanced here can serve to provide mathematical representation of measured tractions and to relate them to other geometric and dynamic configurations.

Attempts will be made in the near future to investigate the possibility of improving the apparent viscosity model by incorporating measured film thickness data and eventually to extend the model as more rheological data becomes available.

SECTION IV

ASPERITY INTERACTIONS AND PARTIAL ELASTOHYDRODYNAMIC LUBRICATION IN ROLLING ELEMENT BEARINGS

Traction measurements thus far have been obtained over a range of loads, speeds and temperatures where the lubricant film thickness is expected to be of the order of 50 microinches or more. These films should be quite large in comparison with the surface roughness (which was of the order 2 microinches rms at the outset) hence it is anticipated that the data presented here were all obtained in the full elastohydrodynamic regime.

In subsequent investigations however, experiments will be performed at lower speed and higher loads with less viscous fluids so that partial elastohydrodynamic conditions will be prevalent. Under these conditions some asperity contact will occur.

The analysis to be presented here considers the contribution to the total tractive force resulting from the direct interaction of asperities on two surfaces that are sliding with respect to each other. The effect of a lubricant film is assumed to be manifested solely in the determination of the mean spacing between the two surfaces and forces transmitted across the lubricant film are not considered. The analysis represents an extension of the work performed by Gupta and Cook (19, 20) who considered asperity interactions between two flat surfaces in unlubricated sliding contact. The extensions have been performed to include the spacing effects of a lubricant film thickness profile, and a concentrated contact geometry.

A brief review of the analysis will be presented followed by presentation of results of computations applied to a lubricated elastohydrodynamic contact.

1. STATISTICAL ANALYSIS OF ROUGH SURFACES IN SLIDING INTERACTION

Since surface profiles are usually of a random nature it is possible to describe surface topography in terms of statistical properties e.g., distribution of peak heights and radii of curvature at the peaks. With such a description of surface topography it is possible to express the mechanical interactions between mating surfaces in terms of statistics of the surface profiles.

From the experimental analysis of various surface profiles it is found that statistical distribution of peak heights generally approach a Gaussian function (19). The distribution of radius of curvature at the peaks, however, is skewed and the data is best fitted by a log-normal function. Furthermore, statistical correlations between peak heights and radii is negligible. With these statistical results, the analysis may essentially be divided into two independent steps: analysis of individual asperity interactions and distributions of interacting asperities over the entire surfaces.

It is assumed that contact takes place only at the peaks and all asperities are geometrically described as spherical bodies and the junctions formed by

Contrails

individual pairs of asperities do not have any force of displacement interaction among themselves. A justification for these assumptions is described in Reference (21).

Consider two interacting surfaces, 1 and 2, as shown in Figure (51). It is clear that contact between two asperities of peak heights, Z_1 and Z_2 , will take place only if the sum of the peak heights (Z') is greater than the mean separation between mating surfaces (d') which may be expressed mathematically as

$$Z_1 + Z_2 = Z' > d'$$

Since the distributions of Z_1 and Z_2 are normal, the mean M and standard deviation σ of the distribution of sum $Z_1 + Z_2$ may be described in terms of individual means and standard deviations.

$$M = M_1 + M_2$$

$$\sigma = \sqrt{\sigma_1^2 + \sigma_2^2}$$

Sum of the heights Z' and the separation between the mean planes of the surfaces d' may be expressed in non-dimensional form

$$Z = \frac{Z' - M}{\sigma}$$

and

$$d = \frac{d' - M}{\sigma}$$

Since Z is normally distributed with a mean of zero and variance of unity, the numbers of asperity interactions satisfying the condition

$$Z > d$$

may be easily determined by the shaded area in Figure 52. Furthermore, the maximum geometric interference for mating asperities is described by

$$w_{\max} = Z - d$$

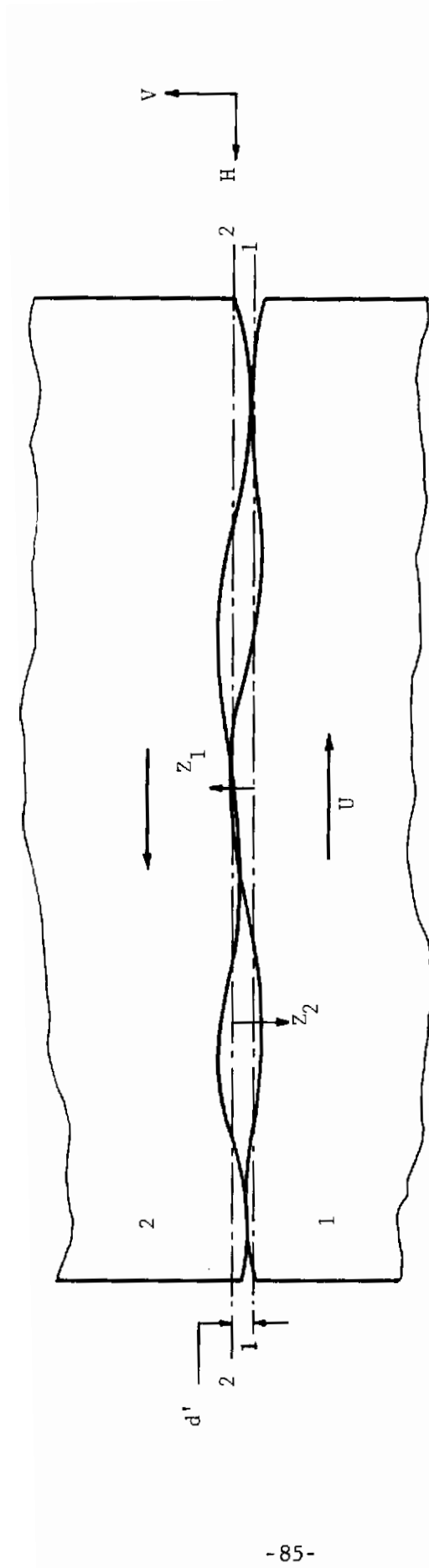


Fig. 51 Contact of a Pair of Rough Surfaces,
Sliding Against Each Other

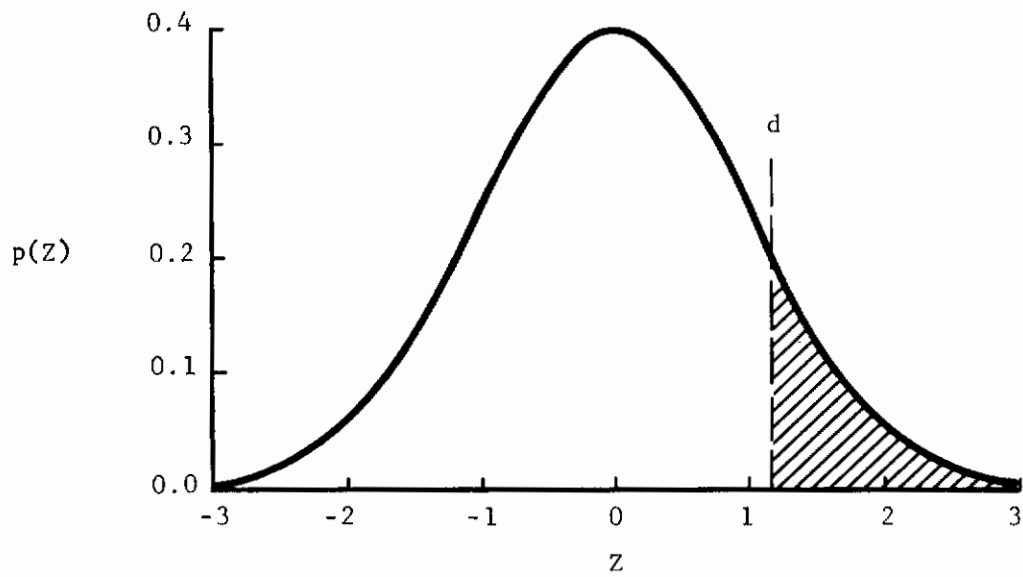


Fig. 52 The Standardized Normal Distribution Function for Z

Contrails

Since the asperities are geometrically described as spherical bodies, the interaction is described by the radii of curvature and w_{\max} . As stated earlier, the radii may be distributed by a log-normal function and may be considered as independent of heights. Thus, if we consider the distributions in discrete form, it is possible to describe all asperity interactions in terms of junctions J_{ijk} each of which may be described geometrically by a set of parameters

$$J_{ijk} = (N_{ijk}, w_{\max_i}, R_{1_j}, R_{2_k})$$

where N_{ijk} is the number of junctions having maximum geometric interference w_{\max_i} . The radii of curvature of the interacting asperities are R_{1_j} and R_{2_k} . Now if we know the force deformation relations for all junctions J_{ijk} , the total interaction between the surfaces may be determined. We shall discuss these models later. For the present, let the average normal and friction forces, V_{ijk} and H_{ijk} , and the average real contact area A_{ijk} for junctions J_{ijk} be described by the relations

$$V_{ijk} = V_{ijk}(w_{\max_i}, R_{1_j}, R_{2_k})$$

$$H_{ijk} = H_{ijk}(w_{\max_i}, R_{1_j}, R_{2_k})$$

$$A_{ijk} = A_{ijk}(w_{\max_i}, R_{1_j}, R_{2_k})$$

Also knowing the size of a junction, the contact resistance C_{ijk} , using Holm's theory (22) may be estimated (21). The total time average forces, real contact area and electrical contact resistance for the interacting surfaces may be obtained by summation

$$V = \sum_i \sum_{j=1}^m \sum_{k=1}^m V_{ijk} N_{ijk}$$

$$H = \sum_i \sum_{j=1}^m \sum_{k=1}^m H_{ijk} N_{ijk}$$

$$A = \sum_i \sum_{j=1}^m \sum_{k=1}^m A_{ijk} N_{ijk}$$

Contraails

$$C = \sum_i \sum_{j=1}^m \sum_{k=1}^m N_{ijk} / C_{ij}$$

where summation over i is carried over all asperity interactions satisfying the condition $Z > d$.

A detailed derivation of various junction models is described in Reference (20). With a given geometric interference the junctions are classified as elastic or plastic depending on the mode of deformation. Elastic junctions are analyzed by using Hertz solutions (23) for normal contact forces and real contact area. Friction force is assumed to be proportional to real contact area at the junction; in other words, constant interfacial shear stress is assumed. Plane strain slip line field solutions are used to analyze fully plastic junctions. The junctions are further classified as "weak" or "strong" depending on the strength of interfacial adhesion. If the interfacial shear stress is equal to the ultimate shear flow stress of the weaker material, the junction is called "strong". A junction is "weak" when interfacial shear stress is less than the shear flow stress of weaker material. Tension in a plastic junction is limited by maximum permissible adhesion stress, which essentially depends on the environmental conditions.

2. RESULTS OF ASPERITY INTERACTION ANALYSIS AS APPLIED TO A LUBRICATED ROLLING-SLIDING CONTACT

Contact forces, real area of contact and the electrical contact resistance were determined for typical ball bearing surfaces. The radius of curvature at all peaks was assumed to be 0.006 in. and the standard derivation of peak height distributions was taken as 1 microinch. These numbers are estimated from the experimental data given in Reference (24). The mean peak height was estimated as one third of the standard derivation (21). The average separations between peaks was assumed to be about one tenth of the radius of curvature, giving a peak density of 2.8×10^6 /sq-in. It should be noted that the purpose of "guessing" these topographic properties, is to just illustrate a typical solution. In a real case, these parameters must be determined by actual profilometric measurements.

A ball bearing steel (hardness ≈ 65 RC) was taken to be the material of both surfaces. Tunnel resistivity for a film thickness of 7 \AA between both steel surfaces was estimated to be $0.55 \mu \Omega \text{ cm}^2$ (21). Under room temperature conditions adhesion stress was assumed equal to the tensile yield stress.

The computer program used in Reference (21) is modified to handle asperity interactions in partial elastohydrodynamic contacts. With the above data, the modified program is used to produce the results shown in Figure 53. For a unit apparent area normal and friction forces supported by interacting asperities, real contact area and electrical contact resistance are plotted as a function of the separation d' , between the mean planes of interacting surfaces. All junctions were found to be elastic in the load range shown in Figure 53. A listing of the computer program and typical output are given in Appendix III.

Contrails

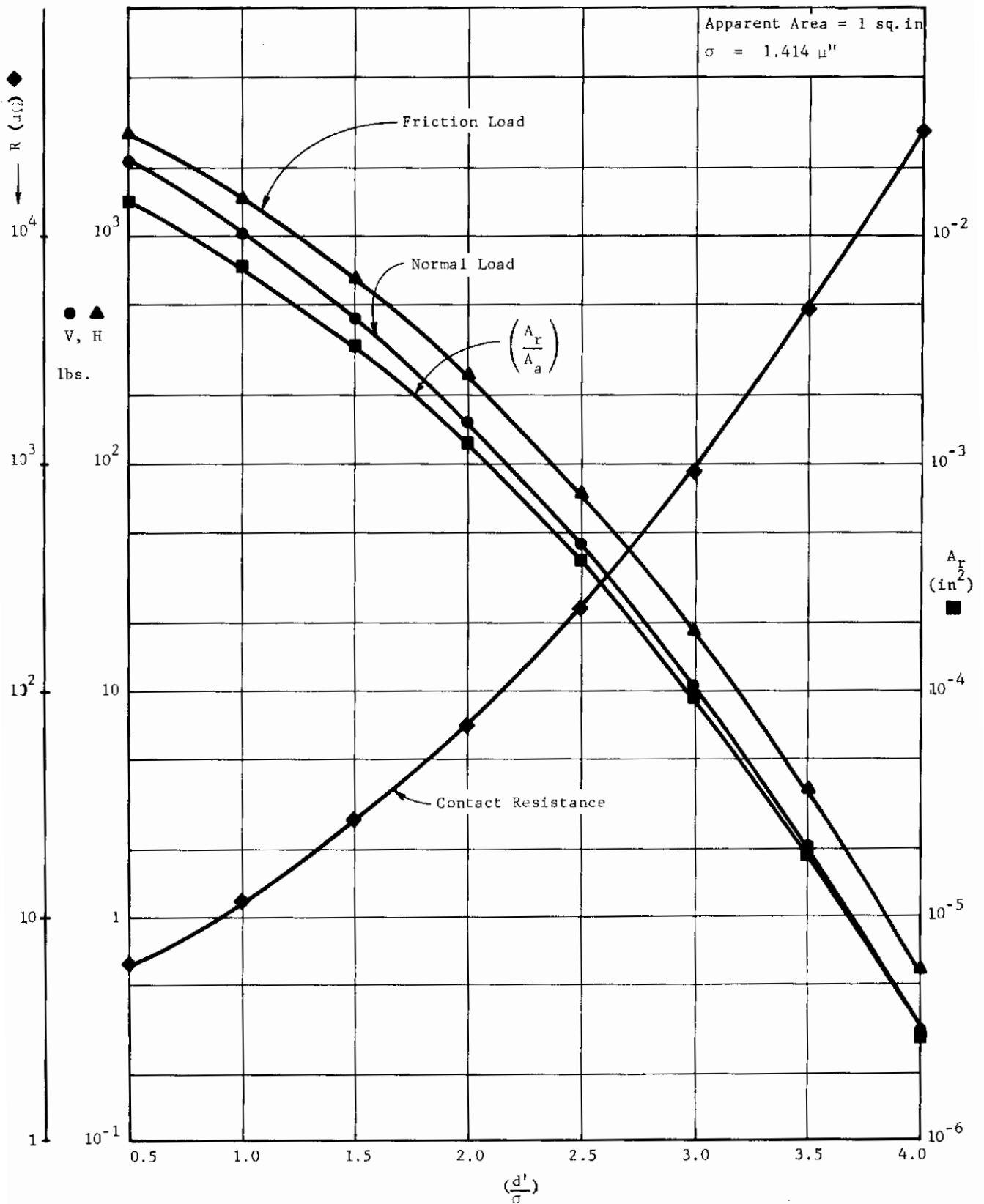


Fig. 53 Typical Solutions as a Function of the Mean Separation Between the Interacting Surfaces

Contrails

The friction contributed by direct asperity interaction in an elastohydrodynamic contact will be analyzed by taking the separation between the surfaces d' to be equal to the lubricant film thickness, h , (in this case assumed to be constant). Metallic interaction will take place when the sum of peak heights on the two surfaces is greater than the lubricant film thickness. Thus, if the film thickness is known, the normal and friction forces supported by the asperities, total average real contact area and electrical resistance due to metallic contact may be determined by solutions similar to the one shown in Figure 53. The procedure may be illustrated by the following specific example.

Consider a pair of discs, 3" diameter and 36" crown radius, in rolling contact at a normal load of 100 lbs. An estimate of the expected lubricant film thickness may be obtained from Grubin's or Dowson and Higginson's (17) formula. Taking typical values for inlet viscosity $\mu_0 = 4.35 \times 10^{-7}$ lb.sec/in² and pressure viscosity coefficient $\alpha = 1.2 \times 10^{-4}$ in²/lb, the film thickness h is estimated for different velocities. Also for the fixed normal load the apparent contact area, i.e., area of Hertzian ellipse may be determined. In the present case, this area is 1.7×10^{-3} in².

Now for a fixed apparent area, the loads supported by the asperities, real contact area and electrical contact resistance may be determined for any film thickness, and therefore for any speed, from the solutions plotted in Figure 53. Figure 54 shows these results plotted as a function of speed. It can be clearly seen from Figure 54 that for the surfaces specified by the topography used in the present analysis, asperity interaction effects occur at velocities less than 100 in/sec.

The friction coefficient as a function of velocity may be determined from Figure 54, where the friction load H , and normal load V , supported by the asperities is plotted as a function of velocity. Thus, for a total applied normal load P , the friction coefficient defined by the friction force supported by the interacting asperities only is determined.

$$f = H/P$$

Figure 55 shows the estimated values of friction coefficient, based on metallic asperity interactions only, as a function of velocity. It is clearly seen that at increasing speeds the contribution of metallic asperity interaction to friction rapidly reduces, essentially due to the increasing film thickness. Hydrodynamic effects will usually dominate the friction behavior at high speeds. At low speeds however, when the film thickness is small, friction will be more strongly dependent on asperity interactions.

The preceding analysis is intended to provide a vehicle for studying the effects of asperity interaction in the partial elastohydrodynamic regime. It will be valid in predicting total tractive forces only when hydrodynamic effects are small. It thus represents the opposite end of the spectrum to the analyses discussed in Section II which are limited to purely hydrodynamic forces. As more information is obtained the asperity interaction analysis should be integrated with the elastohydrodynamic analysis to provide a more complete understanding of the partial elastohydrodynamic process.

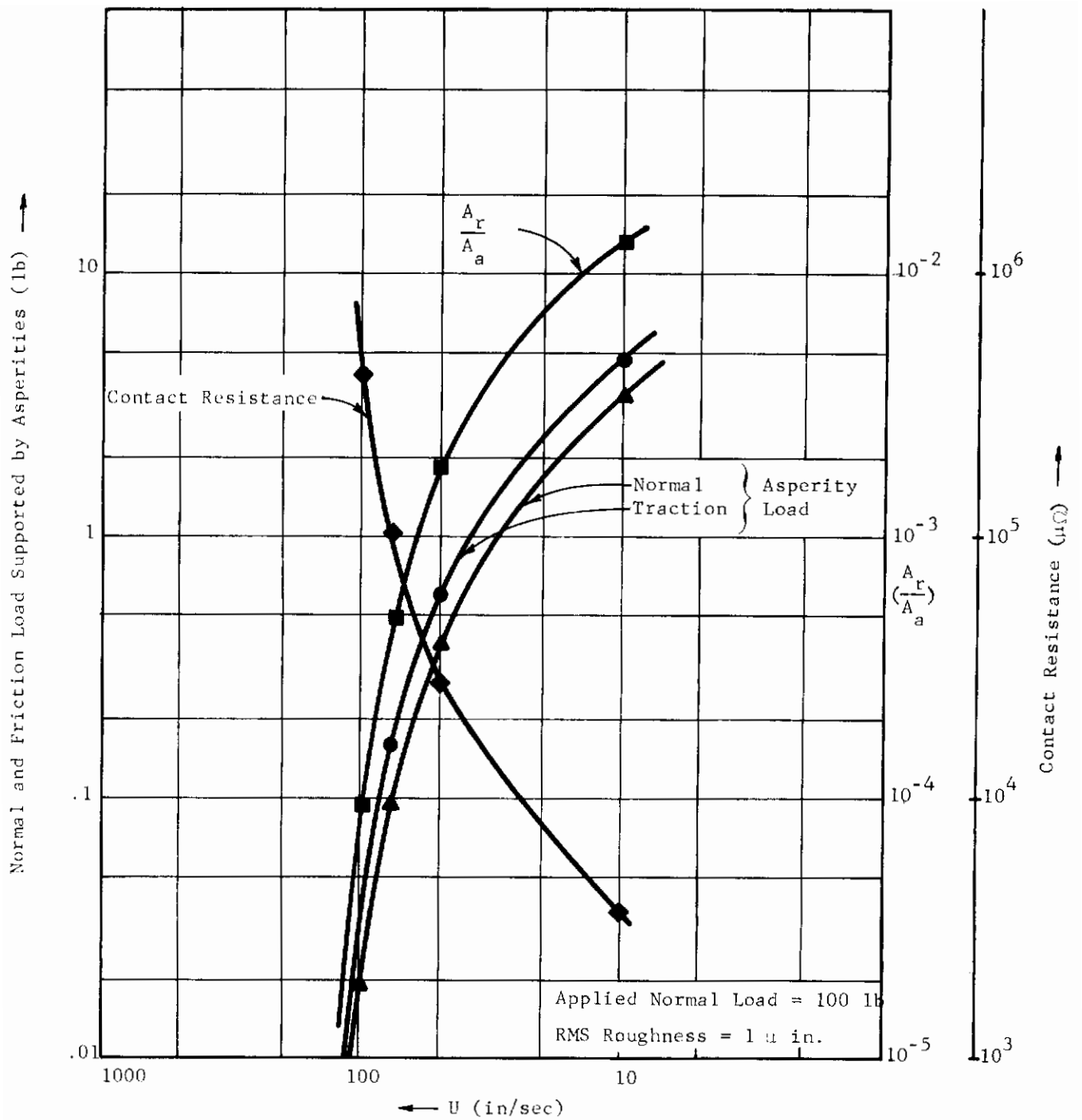


Fig. 54 Effect of Relative Sliding Speed

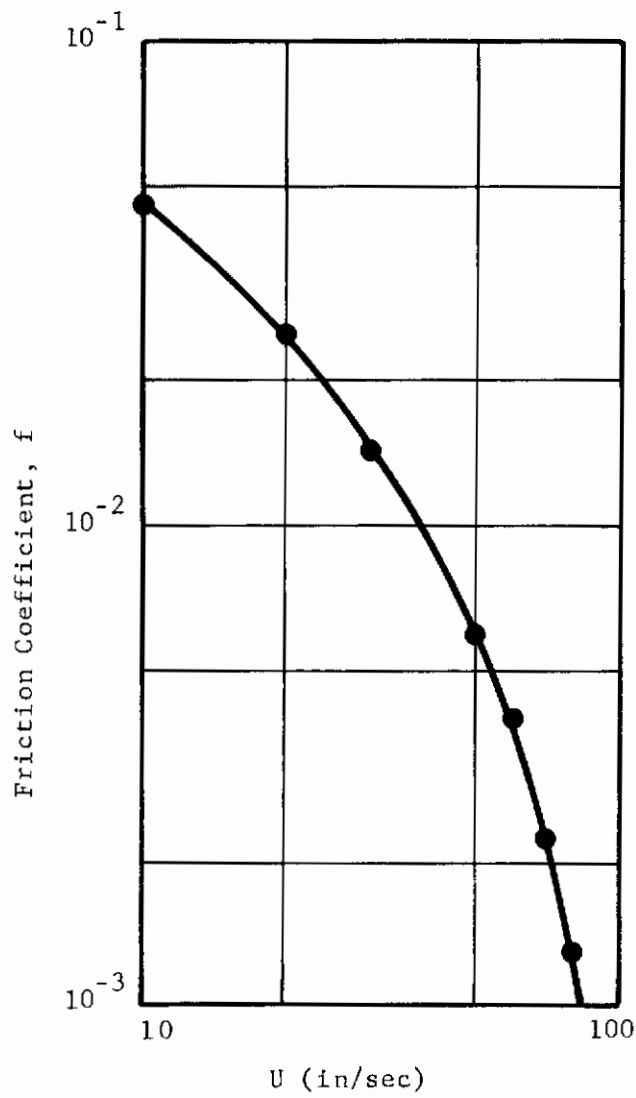


Fig. 55 Variation of Friction Coefficient with Sliding Speed

SECTION V

CONCLUSIONS

The elastohydrodynamic rolling disc test apparatus has been designed and built and a matrix of data covering a range of loads, speeds and temperatures have been obtained for 5P4E polyphenyl ether.

Measured tractions are found to markedly increase with load and decrease moderately with rolling speed. The data show a very weak sensitivity to temperature whereas Battelle data obtained under the same apparent conditions show a very strong decrease in traction with increasing temperature. The precise nature of this discrepancy has not yet been established, however, the two sets of data have been taken ten years apart with different batches of fluids, and since tractions are predicted to be very sensitive to fluid properties, it is possible that additives or structural differences in the lubricant could account for the discrepancies.

Although in many respects qualitative similarity exists, tractions do not compare well quantitatively with either performance code predictions or other existing viscous traction theories. An apparent viscosity model has been advanced which uses an increased base viscosity and a decreased pressure coefficient of viscosity determined from the traction data to correlate the traction data and can provide a reasonable mathematical representation of the data.

Preliminary investigations indicate some variation in traction with lubricant supply rate. Further studies will be performed to determine whether or not these are starvation effects as opposed to thermal effects.

Preliminary optical interference measurements have been obtained which compare reasonably well with predictions of exterior contact separation profiles based upon Hertz theory.

An asperity interaction model has been presented which will be used in our subsequent investigation of partial elastohydrodynamic lubrication. The model facilitates for prediction of real area of contact, frictional contributions resulting from asperity interaction, fraction load supported by asperity contact, and electrical contact resistance.

Contrails

APPENDIX I

MTI ROLLING DISC DESIGN DRAWINGS

<u>DRAWING NUMBER</u>	<u>DESCRIPTION</u>
245-J-01	Layout - Elastohydrodynamic Test Rig
245-J-02	Facility Layout Elastohydrodynamic Test Rig
245-J-03	Assembly - Elastohydrodynamic Test Rig
245-E-04	Sliding Plate
245-E-05	Bottom Plate (2 SH)
245-E-06	Top Plate
245-C-07	Guide Rods
245-E-08	Upper Bearing Housing
245-C-09	Bearing Housing - Upper Half - Large
245-C-10	Bearing Cap - Small
245-C-11	Bearing Cap - Large
245-C-12	Bearing Housing - Upper Half - Small
245-D-13	Labyrinth Seal - Lower
245-D-14	Upper Shaft - Main - Low Load
245-D-15	Labyrinth Seal - Upper
245-D-16	Lower Shaft - Main
245-C-17	Pivot Yoke
245-B-18	Pivot Pin
245-B-19	Bearing Spacer - Lower
245-C-20	Bearing Spacer - Upper
245-B-21	Pivot Plate
245-B-22	Load Cell Adapter
245-B-23	Adapter, Hybrid Cylinder
245-D-24	Oil Guard Upper
245-E-25	Oil Guard Lower
245-C-26	Drive Shaft
245-D-27	Upper Shaft - Main - High Load
245-B-28	Bearing Spacer - Upper - High Load Shaft
245-B-29	Inspection Plate
245-B-30	Support Rods

Contrails

245-C-31	Shaft
245-C-32	Test Specimens
245-B-33	Shim
245-B-34	Basket
245-D-35	Radiation Source Container

APPENDIX II

EQUIPMENT LIST

An itemization of the test hardware and instrumentation used during the period of work described in this report follows.

Rolling Disc Machine Assembly

- Machined parts as indicated in drawings list of Appendix I.
- Two U.S. Electrical motors direct current 20 hp type H.D. P/N x 575644.
- Two Horton Mfg. Co. air disc brakes model HWB.
- Two machined pulleys 18" dia. with extremultis belts.
- Four SKF Inc. angular contact ball bearings cat. #7208/C78 ABEC 7.
- Four New Departure Co. deep groove ball bearings cat. #Z99504-LR5.

Torque Measurement

- One Lebow Associates Inc. torque transducer model 1214-200.
- One Lebow Associates Inc. transducer indicator model 7510.
- One Spencer-Kennedy Labs variable electronic filter model 308A.
- One Hewlett-Packard X-Y recorder model 7004A (torque output on y-axis).

Temperature Measurement

- One Minneapolis-Honeywell, Brown Instruments Division "Elektronik" 24 point continuous balance temperature recorder.
- Twenty-four Copper-Constantan thermocouple junctions.

Speed Monitor and Control

- Two U.S. Electrical Motors speed-a-matic controllers SCR 460 volt, three phase, 60 cycle.
- One Emerson Electric Co. digital process controller model 101 ratio speed controller.
- One Mechanical Technology Inc. EHD differential tachometer, drawing no. 10D000068.
- One Hewlett-Packard digital electronic counter model 5321A.
- One Tektronics Inc. dual beam oscilloscope type 502.
- One Hewlett-Packard X-Y recorder model 7004A (speed difference on x-axis).

Lubricant Supply and Viscosity

- One Oil-Rite Corp. lubrication dispensing system type A-4015 cat. no. YC-191-1.
- Three Cannon viscometers 3-500 centistokes type 100-B896, 200-X870, 350-V82.
- One Variac 220 volt, 10 amp capacity.

Loading System

- One Lebow Associates load cell model 3132-1K
- One Baldwin-Lima-Hamilton strain indicator Model SR-4, Type N

Optical System

- One Nikon shopscope long working distance microscope with illuminator and directional mount, 1x-objective, 15x-eyepiece.
- Two Dell Optics cylindrical quartz disc per MTI Sketch # SK-A-4211.

APPENDIX III

COMPUTER PROGRAM FOR EVALUATION OF ASPERITY INTERACTIONS IN PARTIAL ELASTOHYDRODYNAMIC LUBRICATION

From the given surface profiles (in digitized form) along the direction of rolling, this program computes the mechanical interaction between the rolling elements. Both elastic and plastic deformations are considered at mating asperities. Adhesion and partial or complete welding of the asperities is allowed by specifying some variable stress parameters.

The program is divided into various subroutines. However, all the calculations are performed by calling one "main" subroutine PRADEEP. All the other necessary subroutines are automatically called during the execution of PRADEEP. Except the main subroutine PRADEEP and the subroutine for statistical analysis of rough surface profile, SARP, all the subroutines are free from any input-output statements. SARP needs the surface profile data as the essential input and all the necessary statistical distributions are printed out. There is no input required by PRADEEP, other than the subroutine input parameters. A description of all the input data and the computed results are printed out.

Usage

As mentioned above, the usage of all programs consists of one call statement:

```
CALL PRADEEP(PROP,B,AA,D,DP,DW,NT)
```

All the arguments are input. The definitions are as follows:

PROP = Property vector of length 10, specifying the following properties:

- PROP(1) = Young's modulus of material one (lbs per sq in)
- PROP(2) = Young's modulus of material two (lbs per sq in)
- PROP(3) = Poisson's ratio of material one
- PROP(4) = Poisson's ratio of material two
- PROP(5) = Hardness of softer material (lbs per sq in)
- PROP(6) = Ultimate shear stress of the weaker material
(lbs per sq in)
- PROP(7) = Interfacial shear stress / PROP(6)
- PROP(8) = Adhesion stress / PROP(6)
- PROP(9) = Sum of the specific resistances of the two materials
(micro ohm in)
- PROP(10) = Expected tunnel resistivity for the infacial film
(micro ohm sq in)

Contrails

- B = Hertzian contact size in rolling direction ($\times 10^{-3}$ inch)
- AA = Hertzian contact size perpendicular to rolling direction ($\times 10^{-3}$ inch)
- D = Nominal film thickness ($\times 10^{-3}$ inch)
- DP = Vector specifying protrusion depth values ($\times 10^{-3}$ inch)
- DW = Vector specifying protrusion width values ($\times 10^{-3}$ inch)
- NT = Length of vectors DP and DW (always ≥ 2 ; DP(1) = DW(1) = 0)

DP and DW are two vectors specifying the geometry of protrusion in the interfacial film. DP is the depth vector and DW is the width vector. Reference axes for DP and DW are shown in Figure III-1. When protrusion exists of both interacting surfaces, DP should be such that the effective film thickness in the protrusion zone is given by

$$\text{Effective Film Thickness} = D - DP$$

The main program calling PRADEEP must have a common statement described below:

COMMON/CØNTO/NCT

where NCT is name for any integer specifying the following options:

- NCT = 0 Subroutine SARP is called each time PRADEEP is called and therefore the necessary input for SARP for each call should be provided.
- NCT = 1 SARP is called only at the first call of PRADEEP. For subsequent calls topography is kept fixed and SARP is not called. This option is useful when computation is to be performed for different nominal film thickness for surfaces with given surface topography.

Statistical analysis of the surface profiles is performed in subroutine SARP. Whether this analysis is to be performed or not must be specified by necessary input data cards.

Various input options for executing SARP are available. In case the statistical analysis for the surface profile is readily available, all the parameters may be specified as described in SARP. However, if the statistical analysis for one or two surface profiles is to be performed, data cards containing the digitized surface profile data are necessary. The details of all input data cards are described in SARP. No data cards other than those described in SARP are required.

Output

The output of the program is divided into two parts:

Contrails

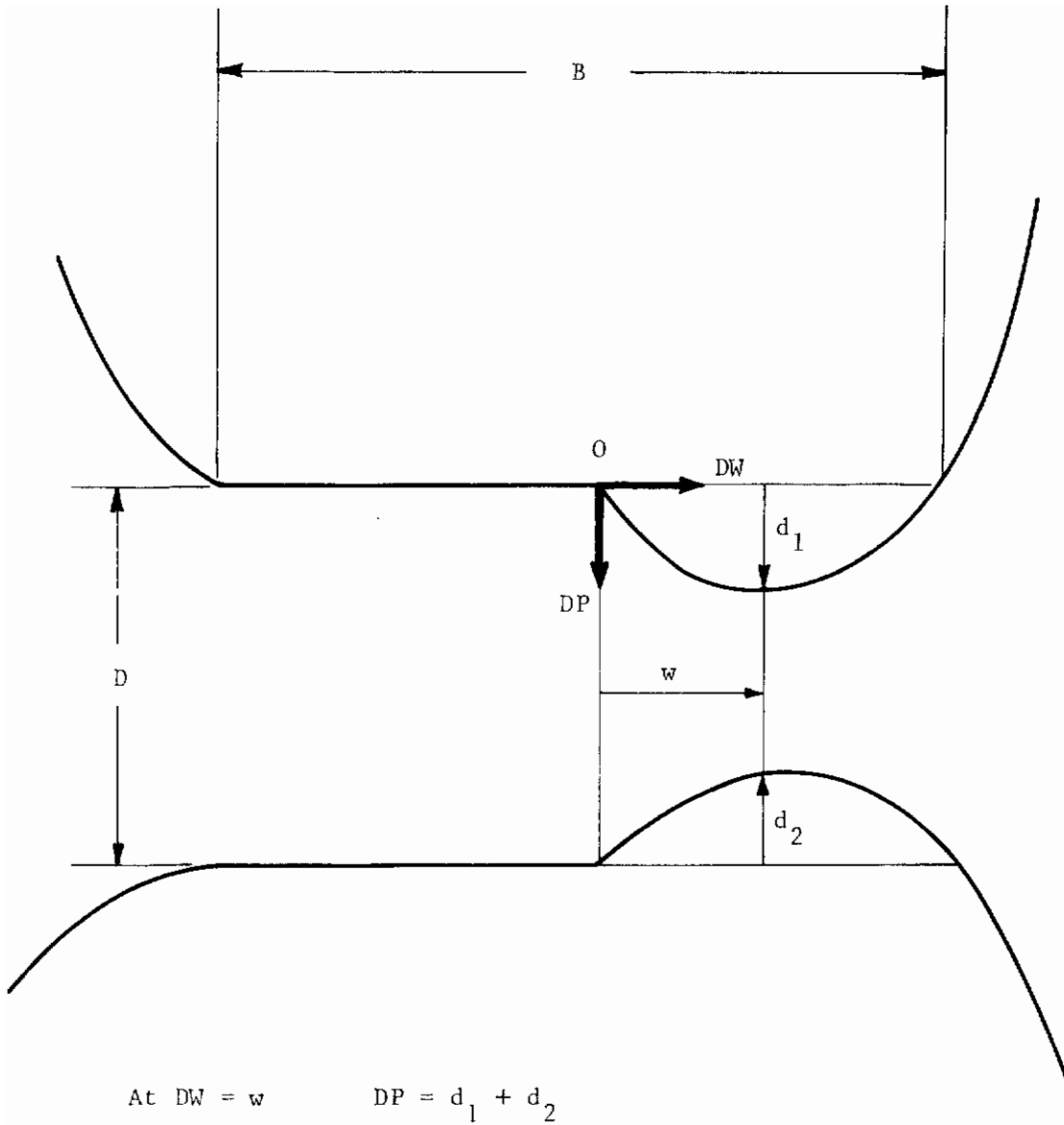


Figure III-1 Specification of Film Profile

Contrails

I

Statistical analysis for each of the surface profiles: histograms and cumulative distribution for the following are printed out for each surface profile:

1. All heights
2. Peak heights
3. Radius of curvature of all peaks
4. Radius of curvature at upper 25% peaks
5. Log (radius of curvature) at all peaks
6. Log (radius of curvature) at upper 25% peaks

Correlation coefficients between peak heights and radii of curvature at the peaks are computed for all peaks and the upper 25% peaks. Density of peaks and a summary of all the above results is printed for each surface profile.

II

Results of asperity interactions: results of metallic contact between asperities are printed in this section. The output consists of the following:

1. Total estimated number of junctions
2. Estimated number of elastic junctions
3. Estimated number of plastic junctions
4. Total normal load supported by the asperities
5. Total friction force due to interacting asperities
6. Friction coefficient due to metal-to-metal contact
7. Average total real area of contact
8. Average maximum geometric interference between interacting asperities
9. Average junctions life
10. Mean junction radius
11. Std. deviation of junction radius distribution
12. Estimated electrical contact resistance

Summary of all External Subroutines

PRADEEP - Main calling subroutine
SARP - Statistical analysis of rough surface profile

Contrails

TABL	- Frequency distribution for a tabulated function
WRTE	- Writing out the histograms and cumulative distributions
ACPR	- Analysis of the contact problem for a pair of rough surfaces
NDIS	- Normal frequency distribution
NDTR	- Normal distribution function (cumulative)
RDIS	- Radii of curvature distribution at the peaks
GUPTA	- Junction deformation model
DQSF	- Integration of a tabulated function
ELJUN	- Elastic junction solution
PSJUN	- Strong plastic junction solution
PWJUN	- Weak plastic junction solution
ANGLE	- Junction angle for strong plastic junction
ASUB	- Solution of a non-linear equation
FCT	- Functions defining the junction angle in terms of incompressibility requirement in case of strong plastic junction

A listing of all the subroutines is given in the following pages along with a typical output.

Contrails

```

SUBROUTINE PRADEEP (PROP,B,AA,D,DP,DW,NT)                                PRAD 010
C                                                                           PRAD 020
C*****                                                                    PRAD 030
C                                                                           PRAD 040
C                                                                           PRAD 050
C THIS SUBROUTINE IS A MAIN ROUTINE WHICH CALLS #SARP# AND #ACPR# TO    PRAD 060
C PERFORM STATISTICAL ANALYSIS OF ROUGH SURFACE PROFILES AND ANALYSIS    PRAD 070
C OF MECHANICAL INTERACTION WHEN THE SURFACES ARE SUBJECTED TO          PRAD 080
C SLIDING. THE PROGRAM IS WRITTEN SUCH DTHAT THE ENTIRE ANALYSIS        PRAD 090
C IS DIRECTLY APPLICABLE TO EHD CONTACTS IN ROLLING ELEMENT             PRAD 100
C BEARINGS. VARIATIONS IN FILM THICKNESS DUE TO PROTUSION HAVE BEEN     PRAD 110
C CONSIDERED. THE OUTPUT, AS IT IS PRINTED OUT IS SELF EXPLANATORY.    PRAD 120
C ALL ARGUMENTS ARE INPUT PARAMETERS.                                     PRAD 130
C                                                                           PRAD 140
C                                                                           PRAD 150
C DESCRIPTION OF ARGUMENTS .....                                         PRAD 160
C PROP = PROPERTY VECTOR OF LENGTH 10, SPECIFYING THE FOLLOWING          PRAD 170
C PROPERTIES.....                                                       PRAD 180
C     PROP(1) = YOUNG'S MODULUS OF MATERIAL ONE (LBS PER SQ IN).         PRAD 190
C     PROP(2) = YOUNG'S MODULUS OF MATERIAL TWO (LBS PER SQ IN).         PRAD 200
C     PROP(3) = POISSON'S RATIO OF MATERIAL ONE.                         PRAD 210
C     PROP(4) = POISSON'S RATIO OF MATERIAL TWO.                         PRAD 220
C     PROP(5) = HARDNESS OF SOFTER MATERIAL (LBS PER SQ IN)             PRAD 230
C     PROP(6) = ULTIMATE SHEAR STRESS OF THE WEAKER MATERIAL             PRAD 240
C               (LBS. PER SQ. IN.).                                       PRAD 250
C     PROP(7) = INTERFACIAL SHEAR STRESS / PROP(6).                     PRAD 260
C     PROP(8) = ADHESION STRESS / PROP(6).                               PRAD 270
C     PROP(9) = SUM OF THE SPECIFIC RESISTANCES OF THE TWO               PRAD 280
C               MATERIALS (MICRO OHM IN).                                  PRAD 290
C     PROP(10) = EXPECTED TUNNEL RESISTIVITY FOR THE INTERFACIAL         PRAD 300
C               FILM (MICRO OHM SQ IN).                                   PRAD 310
C B = HERTZIAN CONTACT SIZE IN THE DIRECTION OF ROLLING (MIL IN).       PRAD 320
C AA = HERTZIAN CONTACT SIZE PERPENDICULAR TO ROLLING DIRECTION         PRAD 330
C      (MIL IN).                                                         PRAD 340
C DP = VECTOR SPECIFYING PROTUSION DEPTH VALUES (MIL IN).              PRAD 350
C      (SEE NOTES FOR DETAILS).                                           PRAD 360
C DW = VECTOR SPECIFYING PROTUSION WIDTH VALUES (MIL IN).             PRAD 370
C      (SEE NOTES FOR DETAILS).                                           PRAD 380
C NT = LENGTH OF VECTORS DP AND DW.                                       PRAD 390
C                                                                           PRAD 400
C CAUTION -- NT MUST BE GREATER THAN 2 FOR ANY PROTUSION.              PRAD 410
C           IF NT IS LESS THAN 2, NO PROTUSION IS ASSUMED.              PRAD 415
C                                                                           PRAD 420
C           WHEN THE PROGRAM CALLS #SARP# CERTAIN DATA CARDS ARE        PRAD 430
C           NECESSARY. MAKE SURE THAT THE REQUIRED DATA IS               PRAD 440
C           AVAILABLE. SEE DETAILS OF THIS INPUT DATA IN #SARP#.        PRAD 450
C                                                                           PRAD 460
C                                                                           PRAD 470
C EXTERNAL SUBROUTINES CALLED .....                                       PRAD 480
C                                                                           PRAD 490
C SUBROUTINES CALLED EITHER DIRECTLY OR INDIRECTLY BY #PRADEEP# ARE     PRAD 500
C SUMMARIZED BELOW ---                                                    PRAD 510
C                                                                           PRAD 520
C SARP  -- STATISTICAL ANALYSIS OF ROUGH SURFACE PROFILE.                PRAD 530
C TAB1  -- FREQUENCY DISTRIBUTION FOR A TABULATED FUNCTION.              PRAD 540
C WRTE  -- WRITING OUT THE HISTOGRAMS AND COMULATIVE DISTRIBUTION.      PRAD 550
C ACPR  -- ANALYSIS OF THE CONTACT PROBLEM FOR A PAIR OF ROUGH          PRAD 560

```

Contrails

```
C          SURFACES. PRAD 570
C NDIS  -- NORMAL FREQUENCY DISTRIBUTION. PRAD 580
C NDTR  -- NORMAL DISTRIBUTION FUNCTION (COMULATIVE). PRAD 590
C RDIS  -- RADII OF CURVATUPE DISTRIBUTION AT THE PEAKS. PRAD 600
C RDIS  -- RADII OF CURVATURE DISTRIBUTION AT THE PEAKS. PRAD 600
C GUPTA -- JUNCTION DEFORMATION MODEL. PRAD 610
C DQSF  -- INTEGRATION OF A TABULATED FUNCTION. PRAD 620
C ELJUN -- ELASTIC JUNCTION SOLUTION. PRAD 630
C PSJUN -- STRONG PLASTIC JUNCTION SOLUTION. PRAD 640
C PWJUN -- WEAK PLASTIC JUNCTION SOLUTION. PRAD 650
C ANGLE -- JUNCTION ANGLE FOR STRONG PLASTIC JUNCTION. PRAD 660
C ASUB  -- SOLUTION OF A NON-LINEAR EQUATION. PRAD 670
C FCT   -- FUNCTION DEFINING THE JUNCTION ANGLE IN TERMS OF PRAD 680
C        INCOMPRESSIBILITY REQUIREMENT IN CASE OF STRONG PLASTIC PRAD 690
C        JUNCTION. PRAD 700
C PRAD 710
C PRAD 720
C FOR A DETAILED SUMMARY OF THE OUTPUT SEE NOTES. PRAD 730
C PRAD 740
C ----- PRAD 750
C N.B. THE UNITS OF ALL PARAMETERS WITH DIMENSIONS OF LENGTH ARE PRAD 760
C GENERALLY WRITTEN AS (MIL IN), WHICH IS DEFINED AS ... PRAD 770
C 1.0 MIL IN = 1.0E-03 INCH. PRAD 780
C PRAD 790
C CAUTION -- A CONTROL COMMON STATEMENT, DESCRIBED BELOW IS NECESSARY PRAD 791
C IN THE MAIN CALLING PROGRAM ... PRAD 792
C PRAD 793
C COMMON/CONT0/NCT PRAD 794
C PRAD 795
C WHERE NCT IS ANY DUMMY INTEGER, IF EQUAL TO 1#SARP# IS PRAD 796
C CALLED ONLY ONCE AND TOPOGRAPHY IS KEPT FIXED. THE PRAD 797
C DEFAULT VALUE OF THE INTEGER IS ZERO, WHEN SARP IS PRAD 798
C CALLED EACH TIME THE MAIN ROUTINE #PRADEEP# IS CALLED. PRAD 799
C PRAD 800
C PRAD 801
C PRADEEP K. GUPTA. PRAD 810
C PRAD 820
C PRAD 830
C ***** PRAD 840
C PRAD 850
000012 DIMENSION RLD(6),PROP(10),TOP(6),DP(1),DW(1) PRAD 860
000012 REAL NN,NEE,NPP PRAD 865
000012 COMMON/CONT0/JCT0 PRAD 867
000012 COMMON/CONT1/JCT1 PRAD 870
000012 COMMON/CONT2/JCT2 PRAD 875
000012 100 FORMAT(45X,43H***** RESULTS OF ASPERITY INTERACTION *****/) PRAD 880
000012 101 FORMAT(10X,36HDESCRIPTION OF INPUT VARIABLES .....//) PRAD 890
000012 102 FORMAT(15X,23HMATERIAL PROPERTIES ---//) PRAD 900
000012 103 FORMAT(20X,65HYOUNG#S MODULUS FOR MATERIALS 1,2 (LBS PEPRAD 910
1R SQ IN) = ,2(E10.4,2X)) PRAD 920
000012 104 FORMAT(20X,65HPOISSON#S RATIO FOR MATERIALS 1,2 PRAD 930
1 = ,2(E10.4,2X)) PRAD 940
000012 105 FORMAT(20X,65HHARDNESS OF SOFTER MATERIAL (LBS PEPRAD 950
1R SQ IN) = ,E10.4) PRAD 960
000012 106 FORMAT(20X,65HULTIMATE SHEAR STRESS OF WEAKER MATERIAL (LBS PEPRAD 970
1R SQ IN) = ,E10.4) PRAD 980
000012 107 FORMAT(20X,65HINTERFACIAL SHEAR STRESS RATIO PRAD 990
1 = ,E10.4) PRAD1000
000012 108 FORMAT(20X,65HADHESION STRESS RATIO PRAD1010
```

Contrails

```

1          = ,E10.4) PRAD1020
000012 110  FORMAT(20X,65HSUM OF SPECIFIC RESISTANCES OF MATERIALS 1,2 (MICRO PRAD1030
10HM IN) = ,E10.4) PRAD1040
000012 111  FORMAT(20X,65HEXPECTED TUNNEL RESISTIVITY (MICRO PRAD1050
10HM SQ IN) = ,E10.4) PRAD1060
000012 112  FORMAT(///15X,26HTOPOGRAPHIC PARAMETERS ---/) PRAD1070
000012 113  FORMAT(20X,14HPEAK DENSITY =,I10,11H PER SQ IN.) PRAD1080
000012 114  FORMAT(20X,58HMEAN RADIUS AT PEAKS SURFACE 1,2 (MIL IN) PRAD1100
1          = ,2(E10.4,2X)) PRAD1110
000012 115  FORMAT(/20X,37HPEAK HEIGHT DISTRIBUTIONS SURFACE 1,2) PRAD1120
000012 116  FORMAT(53X,24HMEAN (MIL IN) = ,2(E12.5,2X)) PRAD1130
000012 117  FORMAT(49X,28HSTD.DEV. (MIL IN) = ,2(E12.5,2X)) PRAD1140
000012 118  FORMAT(/20X,37HLOG(RADIUS) DISTRIBUTIONS SURFACE 1,2) PRAD1150
000012 120  FORMAT(53X,24HMEAN (LOG(MIL IN)) = ,2(E12.5,2X)) PRAD1160
000012 121  FORMAT(49X,28HSTD.DEV. (LOG(MIL IN)) = ,2(E12.5,2X)) PRAD1170
000012 122  FORMAT(/20X,30HUPPER LIMIT ON RADIUS GIVEN BY,F5.2,15H TIMES STD.0PRAD1180
1EV.) PRAD1190
000012 123  FORMAT(///15X,30HEHD CONTACT SPECIFICATIONS ---/) PRAD1200
000012 124  FORMAT(20X,59HHERTZIAN CONTACT SIZE ALONG AND PER. TO ROLLING (MILPRAD1210
1 IN) = ,2(E10.4,2X)) PRAD1220
000012 125  FORMAT(20X,59HFILM PROTUSION WIDTH AND DEPTH (MILPRAD1230
1 IN) = ,2(E10.4,2X)) PRAD1240
000012 126  FORMAT(20X,59HNOMINAL FILM THICKNESS (MILPRAD1250
1 IN) = ,E10.4) PRAD1260
000012 127  FORMAT(///10X,33HSUMMARY OF COMPUTED RESULTS ...../) PRAD1270
000012 128  FORMAT(///15X,30HMICRO CONTACT DESCRIPTIONS ---/) PRAD1280
000012 130  FORMAT(20X,28HTOTAL NUMBER OF JUNCTIONS = ,I8,5X,10HELASTIC = ,I8,PRAD1290
15X,10HPLASTIC = ,I8) PRAD1300
000012 131  FORMAT(20X,61HMEAN AND STD.DEV. OF JUNCTION RADIUS DISTRIBUTION (MPRAD1310
1IL IN) = ,2(E10.4,2X)) PRAD1320
000012 132  FORMAT(20X,61HAVERAGE GEOMETRIC INTERFERENCE AND JUNCTION LIFE (MPRAD1330
1IL IN) = ,2(E10.4,2X)) PRAD1340
000012 133  FORMAT(///15X,47HCONTACT FORCES DUE TO ASPERITY INTERACTIONS ---) PRAD1350
000012 134  FORMAT(/20X,43HAVERAGE NORMAL AND FRICTION FORCES (LBS) = ,2(E10.4PRAD1360
1,2X)) PRAD1370
000012 135  FORMAT(20X,43HESTIMATED FRICTION COEFFICIENT = ,E10.4) PRAD1380
000012 136  FORMAT(20X,43HTOTAL REAL AREA OF CONTACT (SQ IN) = ,E10.4) PRAD1390
000012 137  FORMAT(///15X,54HESTIMATED ELECTRICAL CONTACT RESISTANCE (MICRO OHMPRAD1400
1) = ,E10.4) PRAD1410
000012 138  FORMAT(79X,2(E10.4,2X)) PRAD1420
000012 140  FORMAT(///10X,85HN.B. ALL PEAKS WERE ASSUMED TO HAVE RADIUS OF CPRAD1430
1URVATURE EQUAL TO THE AVERAGE RADIUS.) PRAD1440
000012 141  FORMAT(///10X,80HN.B. LOG-NORMAL DISTRIBUTION OF RADII OF CURVATPRAD1450
1URE AT THE PEAKS WAS CONSIDERED.) PRAD1460
000012 142  FORMAT(20X,43HRATIO OF REAL TO APPARANT CONTACT AREA = ,E10.4) PRAD1470
000012 143  FORMAT(38X,39HMINIMUM SPECIFIED RADIUS (MIL IN) = ,E12.5) PRAD1475
000012 900  FORMAT(1H1) PRAD1480
C PRAD1490
C.... PERFORM STATISTICAL ANALYSIS OF SURFACE PROFILES. ....PRAD1500
C PRAD1510
000012 JCT1=0 PRAD1512
000012 JCT2=0 PRAD1514
000013 IF(JCT0.EQ.1) GO TO 10 PRAD1516
000016 CALL SARP(ND,ICT,TOP,RLD) PRAD1520
C PRAD1530
C.... PRINT INPUT DATA AND COMPUTED TOPOGRAPHIC PARAMETERS. ....PRAD1540
C PRAD1550
000021 10 WRITE(6,900) PRAD1560

```

Contrails

000025		WRITE(6,100)	PRAD1570
000031		WRITE(6,101)	PRAD1580
000035		WRITE(6,102)	PRAD1590
000041		WRITE(6,103) PROP(1),PROP(2)	PRAD1600
000063		WRITE(6,104) PROP(3),PROP(4)	PRAD1610
000105		WRITE(6,105) PROP(5)	PRAD1620
000122		WRITE(6,106) PROP(6)	PRAD1630
000137		WRITE(6,107) PROP(7)	PRAD1640
000154		WRITE(6,108) PROP(8)	PRAD1650
000171		WRITE(6,110) PROP(9)	PRAD1660
000206		WRITE(6,111) PROP(10)	PRAD1670
000223		WRITE(6,112)	PRAD1680
000227		WRITE(6,113) ND	PRAD1690
000235		WRITE(6,114) TOP(5),TOP(6)	PRAD1700
000245		WRITE(6,115)	PRAD1710
000251		WRITE(6,116) TOP(3),TOP(4)	PRAD1720
000261		WRITE(6,117) TOP(1),TOP(2)	PRAD1730
000271		IF(ICT.EQ.0) GO TO 8	PRAD1735
000276		WRITE(6,118)	PRAD1740
000301		WRITE(6,120) RLD(1),RLD(3)	PRAD1750
000311		WRITE(6,121) RLD(2),RLD(4)	PRAD1760
000321		WRITE(6,143) RLD(5)	PRAD1765
000327		WRITE(6,122) RLD(6)	PRAD1770
000335	8	WRITE(6,123)	PRAD1780
000341		WRITE(6,124) B,AA	PRAD1790
000355		WRITE(6,125) DW(1),DP(1)	PRAD1800
000377		IF(NT.LT.2) GO TO 4	PRAD1805
000405		DWS=DW(1)	PRAD1810
000407		DO 9 I=2,NT	PRAD1820
000410		DWS=DWS+DW(I)	PRAD1830
000413	9	WRITE(6,138) DW(I),DP(I)	PRAD1840
000441	4	WRITE(6,126) D	PRAD1850
000447		B=B*(1.0E-03)	PRAD1860
000454		AA=AA*(1.0E-03)	PRAD1870
000455		DWS=DWS*(1.0E-03)	PRAD1880
		C	PRAD1890
		C.... COMPUTE ASPERITY INTERACTIONS IN CONTACT ZONE OF UNIFORM FILM. ...	PRAD1900
		C	PRAD1910
000456		AX=B*AA	PRAD1920
000457		Y=D	PRAD1930
000460		IF(NT.GT.1) GO TO 5	PRAD1932
000464		AX1=AX	PRAD1934
000465		GO TO 6	PRAD1936
000465	5	AX1=(B-DWS)*AA	PRAD1940
000470	6	CONTINUE	PRAD1945
000470		CALL ACPR(ICT,ND,PROP,TOP,RLD,Y,N,V,H,NE,NP,W,A,X,C,R,RS)	PRAD1950
000511		NN=N*AX1	PRAD1960
000513		NEE=NE*AX1	PRAD1970
000515		NPP=NP*AX1	PRAD1980
000517		VA=V*AX1	PRAD1990
000521		HA=H*AX1	PRAD2000
000522		WA=W*AX1	PRAD2010
000524		AP=A*AX1	PRAD2020
000526		XA=X*AX1	PRAD2030
000527		CR=AX1/C	PRAD2040
000531		RM=R*AX1	PRAD2050
000532		RS1=RS*AX1	PRAD2060
000533		IF(NT.LT.2) GO TO 7	PRAD2065

Contrails

	C	PRAD2070
	C.... COMPUTE ASPERITY INTERACTIONS IN THE PROTUSION ZONE	PRAD2080
	C.... AND OBTAIN TOTAL EFFECTS.	PRAD2090
	C	PRAD2100
000542	DO 99 I=2,NT	PRAD2110
000544	Y=D-DP(I)	PRAD2120
000546	AX2=(DW(I)-DW(I-1))*AA*(1.0E-03)	PRAD2130
000553	CALL ACPR(ICT,ND,PROP,TOP,RLD,Y,N,V,H,NE,NP,W,A,X,C,R,RS)	PRAD2140
000574	NN=NN+N*AX2	PRAD2150
000577	VA=VA+V*AX2	PRAD2160
000602	HA=HA+H*AX2	PRAD2170
000604	NEE=NEE+NE*AX2	PRAD2180
000610	NPP=NPP+NP*AX2	PRAD2190
000613	WA=WA+W*AX2	PRAD2200
000615	AR=AR+A*AX2	PRAD2210
000620	XA=XA+X*AX2	PRAD2220
000623	CR=CR+AX2/C	PRAD2230
000625	RM=RM+R*AX2	PRAD2240
000630	RS1=RS1+RS*AX2	PRAD2250
000633	99 CONTINUE	PRAD2260
000641	7 CONTINUE	PRAD2265
000641	RS=RS1/AX	PRAD2270
000643	R=RM/AX	PRAD2280
000644	RMS=SQRT(RS-R*R)	PRAD2290
000651	N=NN	PRAD2300
000653	NE=NEE	PRAD2310
000655	NP=NPP	PRAD2320
000657	W=WA/AX	PRAD2330
000661	X=XA/AX	PRAD2340
000663	F=HA/VA	PRAD2350
000665	C=1.0/CR	PRAD2360
	C	PRAD2370
	C.... PRINT OUT FINAL RESULTS.	PRAD2380
	C	PRAD2390
000667	WRITE(6,900)	PRAD2400
000673	WRITE(6,127)	PRAD2410
000677	WRITE(6,128)	PRAD2420
000703	WRITE(6,130) N,NE,NP	PRAD2430
000715	WRITE(6,131) R,RMS	PRAD2440
000725	WRITE(6,132) W,X	PRAD2450
000735	WRITE(6,133)	PRAD2460
000741	WRITE(6,134) VA,HA	PRAD2470
000751	WRITE(6,135) F	PRAD2480
000757	WRITE(6,136) AR	PRAD2490
000765	AR=AR/AX	PRAD2500
000767	WRITE(6,142) AR	PRAD2510
000774	WRITE(6,137) C	PRAD2520
001002	DO 19 I=1,NT	PRAD2530
001007	19 DW(I)=DW(I)*(1.0E+03)	PRAD2540
001014	B=B*(1.0E+03)	PRAD2550
001014	AA=AA*(1.0E+03)	PRAD2560
001015	IF(ICT)1,1,2	PRAD2570
001017	1 WRITE(6,140)	PRAD2580
001023	GO TO 3	PRAD2590
001027	2 WRITE(6,141)	PRAD2600
001033	3 CONTINUE	PRAD2610
001033	RETURN	PRAD2630
001034	END	PRAD2640

Contrails

```

SUBROUTINE SARP(IPD,ICT,TOP,RLD)
C
C SARP 010
C SARP 020
C*****SARP 030
C SARP 040
C THIS SUBROUTINE IS A MODIFIED FORM OF THE PROGRAM #STATISTICAL SARP 050
C ANALYSIS OF ROUGH SURFACE PROFILE# AS DESCRIBED IN THE FOLLOWING SARP 060
C REFERENCE ... SARP 070
C SARP 080
C #TOPOGRAPHIC ANALYSIS OF FRICTION BETWEEN A PAIR OF ROUGH SARP 090
C SURFACES# BY... PRADEEP K. GUPTA SARP 100
C SC.D THESIS (1970), DEPT. OF MECH. ENGG., M.I.T.,CAMBRIDGE SARP 110
C MASSACHUSETTS, U.S.A. SARP 120
C SARP 130
C SARP 140
C THE PROGRAM HAS BEEN WRITTEN FOR THE COMPUTATION OF THE VARIOUS SARP 150
C STATISTICAL DISTRIBUTIONS FOR A ROUGH SURFACE PROFILE. DIGITIZED SARP 160
C DATA OF A SURFACE PROFILE PUNCHED IN FORMAT(18I4) IS ACCEPTABLE SARP 170
C BY THIS SUBROUTINE. VARIOUS OPTIONS OF EXECUTION OF THIS PROGRAM, SARP 180
C WHEN USED WITH THE MAIN SUBROUTINE #PRADEEP#, ARE EXPLAINED IN SARP 190
C THE INPUT DESCRIPTION. SARP 200
C SARP 210
C SARP 220
C DESCRIPTION OF THE ARGUMENTS ..... SARP 230
C SARP 240
C ALL THE ARGUMENTS OF THIS SUBROUTINE ARE EITHER OUTPUT SARP 250
C OR READ IN FROM THE INPUT DATA DECK TO THIS SUBROUTINE. THE SARP 260
C DEFINITION OF THE VARIOUS PARAMETERS IS AS FOLLOWS ... SARP 270
C SARP 280
C IPD = COMPUTED PEAK DENSITY (NUMBER PER SQ IN). SARP 290
C ICT = AN INTEGER SPECIFYING THE HEIGHTS TO BE USED IN COMPUTATION. SARP 300
C IF ICT=1, ALL HEIGHTS ARE SELECTED, IF ICT=2, ALTERNATE SARP 310
C HEIGHTS ARE CONSIDERED, AND SO ON. SARP 320
C TOP = TOPOGRAPHY VECTOR OF LENGTH 6, SPECIFYING THE FOLLOWING SARP 330
C TOPOGRAPHIC PARAMETERS..... SARP 340
C TOP(1) = STD. DEV. FOR PEAKS ON SURFACE ONE (MIL IN). SARP 350
C TOP(2) = STD. DEV. OF LOG-NORMAL DIS OF RADII FOR SURFACE SARP 360
C ONE (LOG(MIL IN)). SARP 370
C TOP(3) = MEAN FOR PEAKS ON SURFACE ONE (MIL IN). SARP 380
C TOP(4) = MEAN FOR PEAKS ON SURFACE TWO (MIL IN). SARP 390
C TOP(5) = MEAN RADIUS OF CURVATURE AT PEAKS OF SURFACE ONE SARP 400
C (MIL IN). SARP 410
C TOP(6) = MEAN RADIUS OF CURVATURE AT PEAKS OF SURFACE TWO SARP 420
C (MIL IN). SARP 430
C RLD = VECTOR OF LENGTH 6, SPECIFYING REDII OF CURVATURE DISTRIBU- SARP 440
C TION AT THE PEAKS..... SARP 450
C RLD(1) = MEAN OF LOG-NORMAL DIS. OF RADII FOR SURFACE ONE. SARP 460
C (LOG(MIL IN)). SARP 470
C RLD(2) = STD. DEV. OF LOG-NORMAL DIS OF RADII FOR SURFACE SARP 480
C ONE (LOG(MIL IN)). SARP 490
C RLD(3) = MEAN OF LOG-NORMAL DIS. OF RADII FOR SURFACE TWO SARP 500
C (LOG(MIL IN)). SARP 510
C RLD(4) = STD. DEV. OF LOG-NORMAL DIS OF RADII FOR SURFACE SARP 520
C TWO (LOG(MIL IN)). SARP 530
C RLD(5) = LOWER ROUND ON THE VALUE OF RADIUS OF CURVATURE SARP 540
C (MIL IN). SARP 550
C RLD(6) = NUMBER SPECIFYING VARIATION ON LOG(RAD OF CUR) IN SARP 560
C TERMS OF MULTIPLE OF STD. DEV. OF DISTRIBUTION SARP 570
C OF RAD OF CUR. SARP 570
```

Contrails

```
C
C
C INPUT TO THE PROGRAM ..... SARP 580
C SARP 590
C SARP 600
C SARP 610
C VARIOUS OPTIONS FOR THE NECESSARY INPUT ARE AVAILABLE SARP 620
C AND ARE DEFINED BY THE HEADER CARD, WHICH IS THE FIRST CARD IN SARP 630
C THE INPUT DATA DECK. THE DECK SET-UP IS AS FOLLOWS ... SARP 640
C SARP 650
C FIRST CARD IN DATA DECK ----- SARP 660
C COLS. 1- 2, IZ =90,91 OR 92. SARP 670
C THIS IS A HEADER CARD. THE THREE INTEGERS SARP 680
C PROVIDE THE FOLLOWING OPTIONS ... SARP 690
C =90, SURFACE PROFILES FOR BOTH SURFACES IN SARP 700
C CONTACT ARE PROVIDED AS INPUT AND STATISTICAL SARP 710
C DISTRIBUTIONS ARE TO BE COMPUTED FOR BOTH SARP 720
C PROFILES. THE COMPUTED PARAMETERS ARE PASSED SARP 730
C FOR FURTHER ANALYSIS. SARP 740
C =91, ONLY ONE SURFACE PROFILE IS IN THE INPUT SARP 750
C DECK AND SURFACE TOPOGRAPHY IS ASSUMED TO BE SARP 760
C IDENTICAL FOR BOTH MATING SURFACES. SARP 770
C =92, THE NECESSARY STATISTICAL DISTRIBUTIONS SARP 780
C HAVE ALREADY BEEN COMPUTED AND THE NECESSARY SARP 790
C PARAMETERS ARE READILY AVAILABLE. SARP 800
C SARP 810
C **** THE DATA CARDS FOLLOWING THE HEADER CARD, ARE DESCRIBED BY THE SARP 820
C VALUE OF THE OPTION INTEGER, IZ. SARP 830
C SARP 840
C***** FOR IZ = 90 OR 91 ***** SARP 850
C SARP 860
C SECOND CARD IN DATA DECK ----- SARP 870
C COLS. 1- 2, ICT=AS DESCRIBED ABOVE. SARP 880
C COLS. 3-14, VERT=VERTICAL MAGNIFICATION OF TALYSURF. SARP 890
C COLS. 15-26, HORZ=HORIZONTAL MAGNIFICATION OF TALYSURF. SARP 900
C COLS. 27-38, DF=DIGITIZING FREQUENCY (CYCLES/SEC). SARP 910
C COLS. 39-40, NR=EXPT. NO., FOR REFERENCE ONLY. SARP 920
C COLS. 41-44, MR=NUMBER OF DIGITIZED DATA CARDS. SARP 930
C SARP 940
C THIRD CARD IN DATA DECK ----- SARP 950
C COLS. 1- 4, N=#OF INTERVALS DESIRED IN THE HISTOGRAMS. SARP 960
C (INCLUDE TWO BOXES FOR UNDER AND OVER FLOW.) SARP 970
C COLS. 5-16, UB(1)=LOWER LIMIT ON ALL HEIGHTS AND PEAKS SARP 980
C (MIL IN). SARP 990
C COLS. 17-28, UB(2)=UPPER LIMIT ON ALL HEIGHTS AND PEAKS SARP1000
C (MIL IN). SARP1010
C COLS. 29-40, UB(3)=LOWER LIMIT ON RAD. OF CURVATURE SARP1020
C (MIL IN). SARP1030
C COLS. 41-52, UB(4)=UPPER LIMIT ON RAD. OF CURVATURE SARP1040
C (MIL IN). SARP1050
C COLS. 53-64, UB(5)=NUMBER SPECIFYING VARIATION ON LOG(RAD OF SARP1060
C CUR) IN TERMS OF MULTIPLES OF STD. DEV. OF SARP1070
C LOG(RAD OF CUR) DISTRIBUTION. SARP1080
C SARP1090
C N.B. - IF UPPER AND LOWER LIMITS ARE SET EQUAL SARP1100
C THEN THE MAXIMUM AND MINIMUM VALUES ARE SARP1110
C TAKEN AS UPPER AND LOWER LIMITS. SARP1120
C SARP1130
C DIGITIZED DATA DECK. ***** SARP1140
C SARP1150
```


Contrails

```

C                                     PRADEEP K. GUPTA.                SARP1740
C                                     SARP1750
C*****SARP1760
C                                     SARP1770
C                                     SARP1780
C                                     SARP1790
000007  DIMENSION IRI(9000),A(9000,3),G(500)                SARP1800
000007  DIMENSION S(9000),STATS(5),UBO(3),FREQ(102),PCT(102),UB(5)  SARP1810
000007  DIMENSION TOP(6),RLD(6)                                SARP1820
000007  100  FORMAT(12,3F12.2,12,14)                          SARP1830
000007  101  FORMAT(25X,55H***** STATISTICAL ANALYSIS OF ROUGH SURFACE PROFILE SARP1840
          1-- .12,1X,5H*****/)
000007  102  FORMAT(10X,37HSTATISTICAL ANALYSIS FOR ALL HEIGHTS.,5X,7HVMAG = F1 SARP1850
          12.6,2X,7HMMAG = ,F12.6/)
000007  103  FORMAT(28X,12H(ALL POINTS),15X,7HMODE = ,E12.5,1X,6HMIL IN)  SARP1870
000007  104  FORMAT(53X,9HMEDIAN = ,E12.5,1X,6HMIL IN)        SARP1880
000007  105  FORMAT(10X,71HDISTRIBUTION OF LOG(RADIUS OF CURVATURE) AT THE UPPE SARP1890
          1R 25 PERCENT PEAKS.//)
000007  106  FORMAT(10X,36HSTATISTICAL ANALYSIS FOR PFAK HEIGHTS.,5X,7HVMAG = FSARP1910
          112.6,2X,7HMMAG = F12.6/)
000007  107  FORMAT(10X,46HSTATISTICAL ANALYSIS FOR RADIUS OF CURVATURE. ,5X,7HSARP1930
          1VMAG = ,F12.6,2X,7HMMAG = F12.6/)
000007  108  FORMAT(//10X,58HCORRELATION COEFFICIENTS BETWEEN PEAK HEIGHTS AND SARP1950
          1PADII = ,2(FR.3,2X),15HPEAK DENSITY = ,112,1X,9HPER SQ IN//)
000007  110  FORMAT(10X,52HPEAK HEIGHTS ---- MEAN = SARP1970
          1,E12.5,1X,6HMIL IN,5X,11HSTD.DEV. = ,E12.5,1X,6HMIL IN//)
000007  111  FORMAT(//30X,29H*** SUMMARY OF RESULTS.,RUN .12,1X,3H****//)  SARP1990
000007  112  FORMAT(10X,52HPEAK OF CUR... LOG-NORMAL DISTRIBUTION---- MEAN = SARP2000
          1,E12.5,12X,11HSTD.DEV. = ,E12.5)
000007  113  FORMAT(14,5F12.6)                                SARP2020
000007  114  FORMAT(55X,7HMEAN = ,E12.5,1X,6HMIL IN)        SARP2030
000007  115  FORMAT(28X,12H(UPPER .25 POINTS),9X,7HMODE = ,E12.5,1X,6HMIL IN) SARP2040
000007  116  FORMAT(10X,56HDISTRIBUTION OF RAD. OF CUR. FOR UPPER 25 PERCENT PE SARP2050
          1AKS.//)
000007  117  FORMAT(10X,50HDISTRIBUTION OF LOG(RADIUS OF CURVATURE) AT PEAKS.//SARP2070
          1)
000007  118  FORMAT(10X,91H(N.B. ALL UNITS STATED AS MIL IN ARE, IN FACT, LOG(MSARP2090
          1IL IN) IN THE FOLLOWING DISTRIBUTIONS.))//)
000007  120  FORMAT(10X,52HALL HEIGHTS ---- CLA = SARP2110
          1,E12.5,1X,6HMIL IN,10X,6HRMS_ = ,E12.5,1X,6HMIL IN//)
000007  121  FORMAT(18I4,48)                                  SARP2130
000007  122  FORMAT(//10X,42HSEQUENCE NUMBERS OF DATA CARDS READ IN ---/)  SARP2140
000007  123  FORMAT(12(2X,48))                                SARP2150
000007  124  FORMAT(//10X,83HEXECUTION TERMINATING DUE TO INVALID HEADER CARD OSARP2160
          1F INPUT DECK FOR SUBROUTINE SARP.//)
000007  125  FORMAT(18,6E12.5)                                SARP2180
000007  126  FORMAT(12,6E12.5)                                SARP2190
000007  800  FORMAT(12,14)                                    SARP2200
000007  900  FORMAT(1H1)                                       SARP2210
C                                     SARP2220
C.... READ HEADER CARD AND DETERMINE INPUT OPTIONS. ....SARP2230
C
000007  READ(5,800) IZ                                         SARP2250
000014  IF(IZ.EQ.90) GO TO 1                                    SARP2260
000021  IF(IZ.EQ.91) GO TO 1                                    SARP2270
000023  IF(IZ.EQ.92) GO TO 25                                  SARP2280
000025  WRITE(6,124)                                           SARP2290
000030  STOP                                                    SARP2300
000032  25  READ(5,125) IPD,(TOP(I),I=1,6)                     SARP2310

```

Contrails

```

000052      READ(5,126) ICT,(RLD(I),I=1,6)                                SARP2320
000073      WRITE(6,900)                                                SARP2330
000077      WRITE(6,125) IPD,(TOP(I),I=1,6)                            SARP2340
000117      WRITE(6,126) ICT,(RLD(I),I=1,6)                            SARP2350
000140      RETURN                                                       SARP2360
000141      1  READ(5,100) ICT,VERT,HORZ,DF,NR,MR                       SARP2370
000164      READ(5,113) N,(UB(I),I=1,5)                                SARP2380
000200      WRITE(6,900)                                                SARP2390
000204      WRITE(6,101) NR                                             SARP2400
000212      WRITE(6,100) ICT,VERT,HORZ,DF,NR,MR                       SARP2410
000235      WRITE(6,113) N,(UB(I),I=1,5)                                SARP2420
000251      RLD(5)=UB(3)                                               SARP2430
000255      RLD(6)=UB(5)                                               SARP2440
C                                                                 SARP2450
C.... READ PROFILE DATA AND PRINT OUT THE SEQUENCE NUMBERS. .... SARP2460
C                                                                 SARP2470
000257      J1=1                                                       SARP2480
000260      J2=1#                                                       SARP2490
000261      I=1                                                         SARP2500
000262      MR=MR*18                                                    SARP2510
000264      20 READ(5,121) (IRT(J),J=J1,J2),G(I)                       SARP2520
000301      J1=J2+1                                                     SARP2530
000303      J2=J2+1#                                                    SARP2540
000304      I=I+1                                                       SARP2550
000305      IF(J2.LE.MR) GO TO 20                                       SARP2560
000312      IST=J2-18                                                    SARP2570
000314      IC=I-1                                                       SARP2580
000316      24 IF(IRT(IST))23,22,23                                       SARP2590
000320      22 IST=IST-1                                                 SARP2600
000322      GO TO 24                                                     SARP2610
000322      23 CONTINUE                                                  SARP2620
000322      WRITE(6,122)                                                SARP2630
000326      WRITE(6,123) (G(I),I=1,IC)                                   SARP2640
C                                                                 SARP2650
C.... COMPUTE HORIZONTAL AND VERTICAL MAGNIFICATIONS. .... SARP2660
C                                                                 SARP2670
000341      XMAG=2.0/VERT                                               SARP2680
000343      HINT=233.33333*ICT/(DF*HORZ)                               SARP2690
C                                                                 SARP2700
C.... SELECT HEIGHTS AND FILL COL. 1 OF ARRAY *A#. .... SARP2710
C                                                                 SARP2720
000352      NO=4000                                                     SARP2730
000353      K=1                                                         SARP2740
000354      DO 9 I=1,IST*ICT                                             SARP2750
000355      A(K,1)=FLOAT(IRT(I))                                         SARP2760
000360      K=K+1                                                       SARP2770
000362      9 CONTINUE                                                  SARP2780
000364      NA=K-1                                                       SARP2790
000366      IT=IST-2                                                    SARP2800
000370      K=1                                                         SARP2810
000371      DO 19 I=3,IT                                                SARP2820
000372      PH=A(I-2,1)                                                 SARP2830
000374      PA=A(I-1,1)                                                 SARP2840
000375      P=A(I,1)                                                    SARP2850
000377      PAA=A(I+1,1)                                                SARP2860
000400      PAB=A(I+2,1)                                                SARP2870
C                                                                 SARP2880
C.... PEAK DEFINITIONS AND COMPUTATION OF CURVATURE AT PEAKS. .... SARP2890

```

Contrails

```

C
000402      IF(PAA-PAB) 19,7,7          SARP2900
000404      7  IF(P-PA) 19,4,5          SARP2910
000407      5  IF(P-PAA) 19,19,6       SARP2920
000412      6  IF(PA-PB) 19,10,6       SARP2930
000415      4  IF(PA-PB) 19,19,3       SARP2940
000420      3  IF(P-PAA) 19,10,8       SARP2950
000423      10 CUR = (2.0*P-PB-PBB)/4.0 SARP2960
C
C..... SPACING BETWEEN THE POINTS IS TAKEN TO BE 1.0 HERE. .... SARP2970
C
000430      GO TO 28                    SARP2980
000431      8  CUR = 2.0*P-PA-PAA       SARP2990
C
C..... SET PEAK HEIGHT VALUES IN COL. 2 AND RAD. OF CUR. VALUES ..... SARP3000
C..... IN COL. 3 OF ARRAY #A#. .... SARP3010
C
000435      28  A(K,2)=P                 SARP3020
000437      A(K,3)=1.0/CUR              SARP3030
000441      K=K+1                        SARP3040
000443      19  CONTINUE                 SARP3050
000446      NP=K-1                       SARP3060
C
C..... REARRANGE COLUMNS OF PEAKS AND RAD. OF CUR. IN ..... SARP3070
C..... DECREASING ORDER OF PEAK HEIGHTS. .... SARP3080
C
000450      NI=NP-1                      SARP3090
000451      DO 119 I=1,NI                SARP3100
000452      JJ=I+1                       SARP3110
000454      DO 119 J=JJ,NP              SARP3120
000456      IF(A(I,2)-A(J,2)) 15,119,119 SARP3130
000461      15  D1=A(I,2)                SARP3140
000463      D2=A(I,3)                    SARP3150
000465      A(I,2)=A(J,2)                 SARP3160
000467      A(I,3)=A(J,3)                 SARP3170
000470      A(J,2)=D1                     SARP3180
000472      A(J,3)=D2                     SARP3190
000473      119 CONTINUE                  SARP3200
C
C..... ANALYSIS FOR ALL HEIGHTS. .... SARP3210
C
000500      DO 29 J=1,NO                  SARP3220
000502      IF(J.LE.NA) GO TO 2          SARP3230
000504      S(J)=0.0                      SARP3240
000505      GO TO 29                      SARP3250
000506      2  S(J)=1.00                  SARP3260
000510      29  CONTINUE                  SARP3270
000513      UBO(1)=UB(1)/XMAG             SARP3280
000515      UBO(2)=FLOAT(N)              SARP3290
000516      UBO(3)=UB(2)/XMAG            SARP3300
000520      CALL TAB1(A,S,1,UBO,FREQ,PCT,STATS,NO,3) SARP3310
000530      WRITE(6,900)                   SARP3320
000534      WRITE(6,102) XMAG,HINT        SARP3330
000544      AV=STATS(2)                   SARP3340
000546      NN=NA                          SARP3350
000547      GMAG=XMAG                      SARP3360
000551      CALL WRTE(NN,GMAG,UBO,FREQ,PCT,STATS) SARP3370
000555      RMS=STATS(3)                   SARP3380

```

Contrails

```

C
C..... COMPUTATION OF CLA. .... SARP3480
C..... SARP3490
C..... SARP3500
000557 CLA=0. SARP3510
000560 DO 139 I=1,NA SARP3520
000564 139 CLA=CLA+ABS(A(I,1)-AV) SARP3530
000574 CLA=CLA*XMAG/NA SARP3540
C..... SARP3550
C..... ANALYSIS FOR PEAK HEIGHTS. .... SARP3560
C..... SARP3570
000576 DO 59 J=1,NO SARP3580
000600 IF (J.LE.NP) GO TO 13 SARP3590
000602 S(J)=0.000 SARP3600
000603 GO TO 59 SARP3610
000604 13 S(J)=1.00 SARP3620
000606 59 CONTINUE SARP3630
000611 CALL TAB1(A,S,2,UBO,FREQ,PCT,STATS,NO,3) SARP3640
000621 WRITE(6,900) SARP3650
000625 WRITE(6,106) XMAG,HINT SARP3660
000635 A1=STATS(2) SARP3670
000637 S1=STATS(3) SARP3680
000640 NN=NP SARP3690
000642 GMAG=XMAG SARP3700
000643 CALL WRTE(NN,GMAG,UBO,FREQ,PCT,STATS) SARP3710
C..... SARP3720
C..... ANALYSIS FOR RADIUS OF CURVATURES AT THE PEAKS. .... SARP3730
C..... SARP3740
000647 GMAG=HINT*HINT/XMAG SARP3750
000651 URO(1)=UR(3)/GMAG SARP3760
000653 URO(3)=UR(4)/GMAG SARP3770
000654 CALL TAB1(A,S,3,UBO,FREQ,PCT,STATS,NO,3) SARP3780
000665 WRITE(6,900) SARP3790
000671 WRITE(6,107) XMAG,HINT SARP3800
000701 A2=STATS(2) SARP3810
000703 S2=STATS(3) SARP3820
000704 CALL WRTE(NN,GMAG,UBO,FREQ,PCT,STATS) SARP3830
C..... SARP3840
C..... DISTRIBUTION OF RAD. OF CUR. FOR THE UPPER 25% PEAK HEIGHTS. .... SARP3850
C..... SARP3860
000710 NN=NP/4 SARP3870
000712 DO 129 J=1,NO SARP3880
000716 IF (J.LE.NN) GO TO 16 SARP3890
000720 S(J)=0. SARP3900
000721 GO TO 129 SARP3910
000722 16 S(J)=1.0 SARP3920
000724 129 CONTINUE SARP3930
000727 CALL TAB1(A,S,3,UBO,FREQ,PCT,STATS,NO,3) SARP3940
000737 WRITE(6,900) SARP3950
000743 WRITE(6,116) SARP3960
000747 A22=STATS(2) SARP3970
000751 S22=STATS(3) SARP3980
000752 CALL WRTE(NN,GMAG,UBO,FREQ,PCT,STATS) SARP3990
C..... SARP4000
C..... ESTIMATION OF MEAN AND VARIANCE OF UPPER 25% PEAK HEIGHTS. .... SARP4010
C..... SARP4020
000756 URO(1)=UR(1)/XMAG SARP4030
000760 URO(3)=UR(2)/XMAG SARP4040
000762 CALL TAB1(A,S,2,UBO,FREQ,PCT,STATS,NO,3) SARP4050

```

Contrails

```

000772      A11=STATS(2)                                SARP4060
000774      S11=STATS(3)                                SARP4070
C                                                    SARP4080
C..... CALCULATION OF CORRELATION BETWEEN PEAKS AND RAD OF CUR. .... SARP4090
C                                                    SARP4100
000775      PSUM=0.0                                    SARP4110
000776      DO 109 J=1, NP                             SARP4120
001002      109 PSUM=PSUM+A(J,2)*A(J,3)                SARP4130
001011      PSUM=PSUM/(NP-1) - (NP/(NP-1))*A1*A2      SARP4140
001022      R=PSUM/(S1*S2)                             SARP4150
C                                                    SARP4160
C..... CORRELATION COEFFICIENT FOR UPPER 25+ PEAKS AND RAD. OF CUR. .... SARP4170
C                                                    SARP4180
001024      PSUM=0.                                     SARP4190
001025      DO 89 J=1, NN                              SARP4200
001026      89 PSUM=PSUM+A(J,2)*A(J,3)                SARP4210
001035      PSUM=PSUM/(NN-1) - (NN/(NN-1))*A11*A22   SARP4220
001046      RR=PSUM/(S11*S22)                         SARP4230
C                                                    SARP4240
C..... COMPUTATION OF LOG-NORMAL DISTRIBUTION FOR RAD OF CUR. .... SARP4250
C                                                    SARP4260
001050      DO 39 J=1, NP                             SARP4270
001052      39 A(J,3)=ALOG10(A(J,3)*GMAG)             SARP4280
001064      DO 49 J=1, NO                             SARP4290
001066      IF(J.LE.NP) GO TO 17                      SARP4300
001070      S(J)=0.                                    SARP4310
001071      GO TO 49                                  SARP4320
001072      17 S(J)=1.0                               SARP4330
001074      49 CONTINUE                              SARP4340
001077      UB0(1)=ALOG10(UB(3))                     SARP4350
001102      UB0(3)=ALOG10(UB(4))                     SARP4360
001105      CALL TAB1(A,S,3,UB0,FREQ,PCT,STATS,NO,3) SARP4370
001115      NN=NP                                     SARP4380
001117      GMAG=1.0                                  SARP4390
001120      WRITE(6,900)                              SARP4400
001124      WRITE(6,117)                              SARP4410
001130      WRITE(6,118)                              SARP4420
001134      CALL WRITE(NN,GMAG,UB0,FREQ,PCT,STATS)   SARP4430
001140      ST2=STATS(2)                              SARP4440
001142      ST3=STATS(3)                              SARP4450
001143      R1=STATS(2)-2.3026*STATS(3)*STATS(3)    SARP4460
001146      R1=EXP(R1/0.43429)                       SARP4470
001152      R2=EXP(STATS(2)/0.42439)                 SARP4480
001156      R1=STATS(2)+1.1513*STATS(3)*STATS(3)   SARP4490
001161      R3=EXP(R1/0.43429)                       SARP4500
C                                                    SARP4510
C..... LOG-NORMAL DISTRIBUTION FOR RAD. OF CUR. FOR UPPER 25+ POINTS. ... SARP4520
C                                                    SARP4530
001165      NN=NP/4                                    SARP4540
001166      DO 69 J=1, NO                             SARP4550
001172      IF(J.LE.NN) GO TO 18                      SARP4560
001174      S(J)=0.                                    SARP4570
001175      GO TO 69                                  SARP4580
001176      18 S(J)=1.0                               SARP4590
001200      69 CONTINUE                              SARP4600
001203      CALL TAB1(A,S,3,UB0,FREQ,PCT,STATS,NO,3) SARP4610
001213      WRITE(6,900)                              SARP4620
001217      WRITE(6,105)                             SARP4630

```


Contrails

```
001223      WRITE(6,118)                                     SARP4640
001227      CALL WRITE(NN,GMAG,UBD,FREQ,PCT,STATS)          SARP4650
001233      RL=STATS(2)-2.3026*STATS(3)*STATS(3)          SARP4660
001237      T1=EXP(RL/0.43429)                             SARP4670
001243      T2=EXP(STATS(2)/0.42439)                       SARP4680
001247      RL=STATS(2)+1.1513*STATS(3)*STATS(3)          SARP4690
001252      T3=EXP(RL/0.43429)                             SARP4700
C                                                    SARP4710
C.... CALCULATION OF DENSITY OF PEAKS AND PRINTING DATA SUMMARY. .... SARP4720
C                                                    SARP4730
001256      PD=(0.1E+07)*(NP/(ICT*HINT*NA))**2            SARP4740
001266      IPD=PD                                          SARP4750
001270      AVP=(A1-AV)*XMAG                               SARP4760
001273      SIGP=S1*XMAG                                    SARP4770
001274      WRITE(6,900)                                   SARP4780
001300      WRITE(6,111) NR                                SARP4790
001306      WRITE(6,108) R,RR,IPD                          SARP4800
001322      WRITE(6,120) CLA,RMS                           SARP4810
001332      WRITE(6,110) AVP,SIGP                          SARP4820
001342      WRITE(6,112) ST2,ST3                           SARP4830
001352      WRITE(6,103) R1                                 SARP4840
001360      WRITE(6,104) R2                                 SARP4850
001366      WRITE(6,114) R3                                 SARP4860
001374      WRITE(6,112) STATS(2),STATS(3)                 SARP4870
001404      WRITE(6,115) T1                                 SARP4880
001412      WRITE(6,104) T2                                 SARP4890
001420      WRITE(6,114) T3                                 SARP4900
001426      IF(I72.EQ.1) GO TO 26                           SARP4910
001433      IPD1=IPD                                        SARP4920
001434      TOP(1)=SIGP                                     SARP4930
001435      TOP(3)=AVP                                     SARP4940
001437      TOP(5)=T3                                       SARP4950
001440      RLD(1)=STATS(2)                                 SARP4960
001442      RLD(2)=STATS(3)                                 SARP4970
001443      I77=1                                          SARP4980
001444      IF(I7.EQ.90) GO TO 1                            SARP4990
001446      GO TO 27                                         SARP5000
001447      26 IF(IPD.GT.IPD1) IPD=IPD1                     SARP5010
001452      27 TOP(2)=SIGP                                   SARP5020
001454      TOP(4)=AVP                                       SARP5030
001455      TOP(6)=T3                                       SARP5040
001457      RLD(3)=STATS(2)                                 SARP5050
001460      RLD(4)=STATS(3)                                 SARP5060
001462      WRITE(6,900)                                     SARP5070
001465      RETURN                                          SARP5080
001466      END                                            SARP5090
```

Contrails

```

SUBROUTINE WRTE(NN,GMAG,UBO,FREQ,PCT,STATS)                                WRTE 010
C                                                                           WRTE 020
C*****                                                                    WRTE 030
C                                                                           WRTE 040
C   SUBROUTINE WRTE                                                         WRTE 050
C                                                                           WRTE 060
C   THIS PROGRAM HAS BEEN WRITTEN TO COMPUTE COMULATIVE                   WRTE 070
C   PROBABILITIES AND WRITE OUT THE RESULTS ALONG WITH THE FREQUENCY      WRTE 080
C   DISTRIBUTIONS, AS PRODUCED IN THE MAIN PROGRAMS *STATISTICAL          WRTE 090
C   ANALYSIS OF ROUGH SURFACE PROFILE#.                                     WRTE 100
C                                                                           WRTE 110
C   NO EXTERNAL SUBROUTINES ARE CALLED BY THIS PROGRAM. SINCE            WRTE 120
C   THIS PROGRAM IS BASICALLY DESIGNED TO MATCH THE OUTPUT OF THE         WRTE 130
C   MAIN PROGRAM, SARP, THE PARAMETERS WILL BE OBVIOUS FROM THE MAIN     WRTE 140
C   PROGRAM. OUTPUT OF THIS SUBROUTINE ESSENTIALLY CONSISTS OF THE       WRTE 150
C   WRITE OUT OF THE RESULTS IN THE FORMATS SPECIFIED IN THE PROGRAM.     WRTE 160
C                                                                           WRTE 170
C                                                                           WRTE 180
C                                                                           WRTE 190
C                                                                           WRTE 200
C*****                                                                    WRTE 210
C                                                                           WRTE 220
000011  DIMENSION UBO(3),FREQ(102),PCT(102),STATS(5),CF(102)             WRTE 230
000011 103  FORMAT(/10X,39HHISTOGRAM AND COMMULATIVE DISTRIBUTION.,5X,9HORIGINWRTE 240
          1 = ,E10.3,1X,6HMIL IN 7X,16HINTERVAL SIZE = ,E10.3,1X,6HMIL IN/) WRTE 250
000011 104  FORMAT(2(10X,13,1X,E10.3,1X,15,1X,F8.3,1X,F8.3,10X))          WRTE 260
000011 105  FORMAT(/5X,22HTOTAL NO. OF POINTS = 15,2X,6HTOT = E12.5,2X,6HAVE =WRTE 270
          1 ,E12.5,2X,6HSIG = ,E12.5,2X,6HMIN = E12.5,2X,6HMAX = ,E12.5)   WRTE 280
000011 113  FORMAT(32X,5(12X,8HMIL INS.))//)                               WRTE 290
000011 114  FORMAT(/10X,68HFIRST INTERVAL IS UNDER FLOW BOX AND LAST INTERVAL WRTE 300
          IIS OVER FLOW BOX./)                                             WRTE 310
000011 115  FORMAT(/2(10X,38HINT      MIL IN  FREQ      REL      COM,10X)/) WRTE 320
000011      N=UBO(2)                                                       WRTE 330
000012      IF (UBO(1)-UBO(3)) 1,2,1                                       WRTE 340
000015  2   SIZE=(STATS(5)-STATS(4))*GMAG/(UBO(2)-2.0)                    WRTE 350
000022      ORIGIN=STATS(4)*GMAG                                             WRTE 360
000024      GO TO 3                                                         WRTE 370
000025  1   SIZE=(UBO(3)-UBO(1))*GMAG/(UBO(2)-2.0)                        WRTE 380
000032      ORIGIN=UBO(1)*GMAG                                              WRTE 390
000033  3   CONTINUE                                                       WRTE 400
000033      WRITE(6,103) ORIGIN,SIZE                                       WRTE 410
000043      SUM=0.00                                                         WRTE 420
000044      DO 39 I=1,N                                                     WRTE 430
000051      SUM=SUM+PCT(I)                                                  WRTE 440
000053      CF(I)=SUM                                                       WRTE 450
000055 39  CONTINUE                                                       WRTE 460
000057      WRITE(6,115)                                                    WRTE 470
000062      II=N/2                                                           WRTE 480
000064      DO 139 I=1,II                                                  WRTE 490
000071      J=I+II                                                           WRTE 500
000072      SI=ORIGIN+(I-1)*SIZE                                           WRTE 510
000100      SJ=ORIGIN+(J-1)*SIZE                                           WRTE 520
000104      IIF=FREQ(I)                                                     WRTE 530
000107      JF=FREQ(J)                                                      WRTE 540
000112      WRITE(6,104) I,S1,IIF,PCT(I),CF(I),J,SJ,JF,PCT(J),CF(J)      WRTE 550
000162 139  CONTINUE                                                       WRTE 560
000170      WRITE(6,114)                                                    WRTE 570

```

Contrails

000174		DO 49 J=1,5	WRTE 580
000201	49	STATS(J)=STATS(J)*GMAG	WRTE 590
000205		WRITE(6,105) NN,(STATS(J),J=1,5)	WRTE 600
000223		WRITE(6,113)	WRTE 610
000227		RETURN	WRTE 620
000230		END	WRTE 630

Contrails

SUBROUTINE TAB1(A,S,NOVAR,UBO,FREQ,PCT,STATS,NO,NV)	TAB1 010
.....	TAB1 020
.....	TAB1 030
.....	TAB1 040
.....	TAB1 050
.....	TAB1 060
.....	TAB1 070
.....	TAB1 080
.....	TAB1 090
.....	TAB1 100
.....	TAB1 110
.....	TAB1 120
.....	TAB1 130
.....	TAB1 140
.....	TAB1 150
.....	TAB1 160
.....	TAB1 170
.....	TAB1 180
.....	TAB1 190
.....	TAB1 200
.....	TAB1 210
.....	TAB1 220
.....	TAB1 230
.....	TAB1 240
.....	TAB1 250
.....	TAB1 260
.....	TAB1 270
.....	TAB1 280
.....	TAB1 290
.....	TAB1 300
.....	TAB1 310
.....	TAB1 320
.....	TAB1 330
.....	TAB1 340
.....	TAB1 350
.....	TAB1 360
.....	TAB1 370
.....	TAB1 380
.....	TAB1 390
.....	TAB1 400
.....	TAB1 410
.....	TAB1 420
.....	TAB1 430
.....	TAB1 440
.....	TAB1 450
.....	TAB1 460
.....	TAB1 470
.....	TAB1 480
.....	TAB1 490
.....	TAB1 500
.....	TAB1 510
.....	TAB1 520
.....	TAB1 530
.....	TAB1 540
.....	TAB1 550
.....	TAB1 560
.....	TAB1 570

Contrails

	C	TAB1 580
	C		TAB1 590
	C	SUBROUTINE TAB1(A,S,NOVAR,UBO,FREQ,PCT,STATS,NO,NV)	TAB1 600
000014		DIMENSION A(1),S(1),UBO(1),FREQ(1),PCT(1),STATS(1)	TAB1 610
000014		DIMENSION WBO(3)	TAB1 620
000014		DO 5 I=1,3	TAB1 630
000015		5 WBO(I)=UBO(I)	TAB1 640
	C		TAB1 650
	C	CALCULATE MIN AND MAX	TAB1 660
	C		TAB1 670
000021		VMIN=1.0E75	TAB1 680
000022		VMAX=-1.0E75	TAB1 690
000023		IJ=NO*(NOVAR-1)	TAB1 700
000027		DO 30 J=1,NO	TAB1 710
000030		IJ=IJ+1	TAB1 720
000032		IF(S(J)) 10,30,10	TAB1 730
000033		10 IF(A(IJ)-VMIN) 15,20,20	TAB1 740
000037		15 VMIN=A(IJ)	TAB1 750
000042		20 IF(A(IJ)-VMAX) 30,30,25	TAB1 760
000046		25 VMAX=A(IJ)	TAB1 770
000051		30 CONTINUE	TAB1 780
000054		STATS(4)=VMIN	TAB1 790
000056		STATS(5)=VMAX	TAB1 800
	C		TAB1 810
	C	DETERMINE LIMITS	TAB1 820
	C		TAB1 830
000057		IF(UBO(1)-UBO(3)) 40,35,40	TAB1 840
000062		35 UBO(1)=VMIN	TAB1 850
000063		UBO(3)=VMAX	TAB1 860
000065		40 INN=UBO(2)	TAB1 870
	C		TAB1 880
	C	CLEAR OUTPUT AREAS	TAB1 890
	C		TAB1 900
000070		DO 45 I=1,INN	TAB1 910
000071		FREQ(I)=0.0	TAB1 920
000072		45 PCT(I)=0.0	TAB1 930
000076		DO 50 I=1,3	TAB1 940
000077		50 STATS(I)=0.0	TAB1 950
	C		TAB1 960
	C	CALCULATE INTERVAL SIZE	TAB1 970
	C		TAB1 980
000103		SINT=ABS((UBO(3)-UBO(1))/(UBO(2)-2.0))	TAB1 990
	C		TAB11000
	C	TEST SUBSET VECTOR	TAB11010
	C		TAB11020
000107		SCNT=0.0	TAB11030
000110		IJ=NO*(NOVAR-1)	TAB11040
000114		DO 75 J=1,NO	TAB11050
000115		IJ=IJ+1	TAB11060
000117		IF(S(J)) 55,75,55	TAB11070
000120		55 SCNT=SCNT+1.0	TAB11080
	C		TAB11090
	C	DEVELOP TOTAL AND FREQUENCIES	TAB11100
	C		TAB11110
000122		STATS(1)=STATS(1)+A(IJ)	TAB11120
000126		STATS(3)=STATS(3)+A(IJ)*A(IJ)	TAB11130
000131		TEMP=UBO(1)-SINT	TAB11140
000132		INTX=INN-1	TAB11150

Contrails

000135	DO 60 I=1,INTX	TAB11160
000136	TEMP=TEMP+SINT	TAB11170
000140	IF (A(IJ)-TEMP) 70,60,60	TAB11180
000144	60 CONTINUE	TAB11190
000147	IF (A(IJ)-TEMP) 75,65,65	TAB11200
000152	65 FREQ(INN)=FREQ(INN)+1.0	TAB11210
000155	GO TO 75	TAB11220
000156	70 FREQ(I)=FREQ(I)+1.0	TAB11230
000161	75 CONTINUE	TAB11240
000164	IF (SCNT)79,105,79	TAB11250
	C	TAB11260
	CALCULATE RELATIVE FREQUENCIES	TAB11270
	C	TAB11280
000165	79 DO 80 I=1,INN	TAB11290
	C	TAB11310
	CALCULATE MEAN AND STANDARD DEVIATION	TAB11320
	C	TAB11330
000167	80 PCT(I)=FREQ(I)*100.0/SCNT	TAB11300
000175	IF (SCNT-1.0) 85,85,90	TAB11340
000177	85 STATS(2)=STATS(1)	TAB11350
000201	STATS(3)=0.0	TAB11360
000202	GO TO 95	TAB11370
000203	90 STATS(2)=STATS(1)/SCNT	TAB11380
000206	STATS(3)=SQRT(ABS((STATS(3)-STATS(1)*STATS(1)/SCNT)/(SCNT-1.0)))	TAB11390
000217	95 DO 100 I=1,3	TAB11400
000224	100 UBO(I)=WBO(I)	TAB11410
000230	105 RETURN	TAB11420
000231	END	TAB11430

Contrails

```

SUBROUTINE ACPR(ICT,NN,PROP,TOP,RLD,Y,NNN,VAA,HAA,NEE,NPP,WAV,AR,XACPR 010
ILA,CR,RM,RS) ACPR 020
C ACPR 030
C ***** ACPR 040
C ACPR 050
C THIS SUBROUTINE IS A MODIFIED FORM OF THE PROGRAM #ANALYSIS OF ACPR 060
C CONTACT PROBLEM FOR A PAIR OF ROUGH SURFACES# AS DESCRIBED IN THE ACPR 070
C FOLLOWING REFERENCE..... ACPR 080
C ACPR 090
C #TOPOGRAPHIC ANALYSIS OF FRICTION BETWEEN A PAIR OF ROUGH ACPR 100
C SURFACES# BY... PRADEEP K. GUPTA ACPR 110
C SC.D THESIS (1970), DEPT. OF MECH. ENGG., M.I.T.,CAMBRIDGE ACPR 120
C MASSACHUSETTS, U.S.A. ACPR 130
C ACPR 140
C ACPR 150
C THE SUBROUTINE, WITH THE HELP OF VARIOUS OTHER ROUTINES, COMPUTES ACPR 160
C NORMAL AND FRICTION FORCES FOR A PAIR OF ROUGH SURFACES IN ACPR 170
C SLIDING CONTACT. A DESCRIPTION OF INPUT AND OUTPUT VARIABLES AND ACPR 180
C THE EXTERNAL SUBROUTINES USED ARE DESCRIBED BELOW.... ACPR 190
C ACPR 200
C EXTERNAL SUBROUTINES USED..... ACPR 210
C NDIS -- A SUBROUTINE WRITTEN FOR CALCULATION OF NORMAL ACPR 220
C FREQUENCY DISTRIBUTION. ACPR 230
C GUPTA -- THE MODEL FOR INTERACTION OF A PAIR OF ACPR 240
C SPHERICAL ASPERITIES. ACPR 250
C RDIS -- THIS SUBROUTINE IS CALLED ONLY WHEN THE INPUT ACPR 260
C PARAMETER, ICT=1. IT ALLOWS FOR A DISTRIBUTION ACPR 270
C OF RADIUS OF CURVATURE AT THE PEAKS. ACPR 280
C ACPR 290
C SUBROUTINES CALLED BY ANY OF THE ABOVE ROUTINES ARE NOT LISTED ACPR 300
C HERE. THE PARTICULAR ROUTINES SHOULD BE REFERED FOR THIS ACPR 310
C INFORMATION. ACPR 320
C ACPR 330
C ACPR 340
C DESCRIPTION OF INPUT AND OUTPUT PARAMETERS..... ACPR 350
C ACPR 360
C INPUT PARAMETERS ----- ACPR 370
C ICT = 0, IF ALL ASPERITIES ASSUME RADII OF CURVATURE EQUAL TO THE ACPR 380
C AVERAGE RADIUS. ACPR 390
C = 1, IF LOG-NORMAL DISTRIBUTION FOR RADII IS TO BE USED. ACPR 400
C NN = PEAK DENSITY (NO. OF PEAKS PER SQ.IN.). ACPR 410
C PROP = PROPERTY VECTOR OF LENGTH 10, SPECIFYING THE FOLLOWING ACPR 420
C PROPERTIES.... ACPR 430
C PROP(1) = YOUNG'S MODULUS OF MATERIAL ONE (LBS PER SQ IN). ACPR 440
C PROP(2) = YOUNG'S MODULUS OF MATERIAL TWO (LBS PER SQ IN). ACPR 450
C PROP(3) = POISSON'S RATIO OF MATERIAL ONE. ACPR 460
C PROP(4) = POISSON'S RATIO OF MATERIAL TWO. ACPR 470
C PROP(5) = HARDNESS OF SOFTER MATERIAL (LBS PER SQ IN) ACPR 480
C PROP(6) = ULTIMATE SHEAR STRESS OF THE WEAKER MATERIAL ACPR 490
C (LBS. PER SQ.IN.). ACPR 500
C PROP(7) = INTERFACIAL SHEAR STRESS / PROP(6). ACPR 510
C PROP(8) = ADHESION STRESS / PROP(6). ACPR 520
C PROP(9) = SUM OF THE SPECIFIC RESISTANCES OF THE TWO ACPR 530
C MATERIALS (MICRO OHM IN). ACPR 540
C PROP(10)= EXPECTED TUNNEL RESISTIVITY FOR THE INTERFACIAL ACPR 550
C FILM (MICRO OHM SQ IN). ACPR 560
C TOP = TOPOGRAPHY VECTOR OF LENGTH 6, SPECIFYING THE FOLLOWING ACPR 570

```

Contrails

```
C          TOPOGRAPHIC PARAMETERS..... ACPR 580
C          TOP(1) = STD. DEV. FOR PEAKS ON SURFACE ONE (MIL IN). ACPR 590
C          TOP(2) = STD. DEV. FOR PEAKS ON SURFACE TWO (MIL IN). ACPR 600
C          TOP(3) = MEAN FOR PEAKS ON SURFACE ONE (MIL IN). ACPR 610
C          TOP(4) = MEAN FOR PEAKS ON SURFACE TWO (MIL IN). ACPR 620
C          TOP(5) = MEAN RADIUS OF CURVATURE AT PEAKS OF SURFACE ONE ACPR 630
C              (MIL IN). ACPR 640
C          TOP(6) = MEAN RADIUS OF CURVATURE AT PEAKS OF SURFACE TWO ACPR 650
C              (MIL IN). ACPR 660
C          RLD = VECTOR OF LENGTH 6, SPECIFYING REDII OF CURVATURE DISTRIBU- ACPR 670
C              TION AT THE PEAKS..... ACPR 680
C          RLD(1) = MEAN OF LOG-NORMAL DIS. OF RADII FOR SURFACE ONE, ACPR 690
C              (LOG(MIL IN)). ACPR 700
C          RLD(2) = STD. DEV. OF LOG-NORMAL DIS OF RADII FOR SURFACE ACPR 710
C              ONE (LOG(MIL IN)). ACPR 720
C          RLD(3) = MEAN OF LOG-NORMAL DIS. OF RADII FOR SURFACE TWO ACPR 730
C              (LOG(MIL IN)). ACPR 740
C          RLD(4) = STD. DEV. OF LOG-NORMAL DIS OF RADII FOR SURFACE ACPR 750
C              TWO (LOG(MIL IN)). ACPR 760
C          RLD(5) = LOWER BOUND ON THE VALUE OF RADIUS OF CURVATURE ACPR 770
C              (MIL IN). ACPR 780
C          RLD(6) = NUMBER SPECIFYING VARIATION ON LOG(RAD OF CUR) IN ACPR 790
C              TERMS OF MULTIPLES OF STD. DEV. OF DISTRIBUTION ACPR 800
C          Y = SEPARATION BETWEEN MEAN PLANES OF INTERACTING SURFACES ACPR 810
C              (MIL IN). ACPR 820
C              ACPR 830
C              ACPR 840
C          OUT PARAMETERS ----- ACPR 850
C              ACPR 860
C          NNN = TOTAL NUMBER OF PEAKS IN CONTACT PER UNIT NOMINAL AREA ACPR 870
C              (1.0/(IN)**2). ACPR 880
C          VAA = TOTAL AVERAGE NORMAL LOAD SUPPORTED BY INTERACTING ASPERITI- ACPR 890
C              ES PER UNIT NOMINAL AREA (LBS PER SQ IN). ACPR 900
C          HAA = TOTAL FRICTION FORCE DUE TO INTERACTING ASPERITIES PER UNIT ACPR 910
C              NOMINAL AREA (LBS PER SQ IN). ACPR 920
C          NEE = TOTAL NUMBER OF ELASTIC JUNCTIONS PER UNIT NOMINAL AREA ACPR 930
C              (1.0/(IN)**2). ACPR 940
C          NPP = TOTAL NUMBER OF PLASTIC JUNCTIONS PER UNIT NOMINAL AREA ACPR 950
C              (1.0/(IN)**2). ACPR 960
C          WAV = AVERAGE MAX. GEOMETRIC INTERFERENCE BETWEEN INTERACTING ACPR 970
C              ASPERITIES (MIL IN). ACPR 980
C          AR = TOTAL AVERAGE REAL AREA OF CONTACT PER UNIT NOMINAL AREA. ACPR 990
C          XLA = AVERAGE JUNCTION LIFE (MIL IN). ACPR1000
C          CR = ESTIMATED ELECTRICAL CONTACT RESISTANCE PER UNIT NOMINAL ACPR1010
C              AREA (MICRO OHM PER SQ IN). ACPR1020
C          RM = MEAN RADIUS OF A MICRO CONTACT (MIL IN). ACPR1030
C          RS = MEAN OF SQUARES OF RADII OF MICRO CONTACTS ((MIL IN)**2). ACPR1040
C              ACPR1050
C              ACPR1060
C          N.B. IN CASE THE SEPARATION BETWEEN MEAN PLANES (INPUT PARAME- ACPR1070
C              TER, Y) IS TOO LARGE FOR CONTACT TO TAKE PLACE, THE INPUT ACPR1080
C              VALUE OF Y AND THE STANDARDIZED NONDIMENSIONAL VALUE OF Y ACPR1090
C              ARE PRINTED WITH THE MESSAGE #NO CONTACT TAKES PLACE# ACPR1100
C              AND FURTHER EXECUTION IS TERMINATED. THIS CONDITION OF ACPR1110
C              NO CONTACT MAY ALSO TAKE PLACE IF THE NUMBER OF ESTIMATED ACPR1120
C              PEAKS OF HEIGHTS LARGER THAN Y IS ZERO. ACPR1130
C              ACPR1140
C              WHEN THE RADII OF CURVATURE IS DISTRIBUTED OVER THE INTER-ACPR1150
```


Contrails

```

C          ACTING PEAKS, THE TOTAL NUMBER OF ACTIVE ASPERITIES MAY      ACPR1160
C          BE SLIGHTLY LESS THAN NNN DUE TO THE TRUNCATION IN THE      ACPR1170
C          RADII OF CURVATURE CAUSED BY SPECIFIED MINIMUM RADIUS.      ACPR1180
C          IN THIS CASE TOTAL NUMBER OF ASPERITIES IS DETERMINED BY    ACPR1190
C          SUM OF NEE AND NPP.                                          ACPR1200
C                                                                      ACPR1210
C                                                                      ACPR1220
C                                                                      ACPR1230
C          PRADEEP K. GUPTA.                                           ACPR1240
C                                                                      ACPR1250
C*****ACPR1260
C                                                                      ACPR1270
C                                                                      ACPR1280
000024      DIMENSION ZP(201),NUM(201),U(201)                          ACPR1290
000024      DIMENSION RLD(6),PROP(10),TOP(6)                          ACPR1295
000024      COMMON/CONT1/JCT                                          ACPR1300
000024      110  FORMAT(/10X,32HSTATISTICAL PARAMETERS**  SIG= ,E12.5,8H  AVP = ,ACPR1302
          1E12.5,8H  RAD = ,E12.5)                                     ACPR1304
000024      114  FORMAT(10X,2F8.3,2X,23HNO CONTACT TAKES PLACE.)     ACPR1310
C                                                                      ACPR1320
C.....IF REPEATED CALL GO TO 3. ....ACPR1330
C                                                                      ACPR1340
000024      IF(JCT.EQ.1) GO TO 3                                       ACPR1350
000026      E1=PROP(1)                                                 ACPR1350
000027      E2=PROP(2)                                                 ACPR1370
000030      TAU1=PROP(3)                                               ACPR1380
000032      TAU2=PROP(4)                                               ACPR1390
000033      H=PROP(5)                                                  ACPR1400
000035      SY=PROP(6)                                                 ACPR1410
000036      T=PROP(7)                                                  ACPR1420
000040      AS=PROP(8)                                                 ACPR1430
000041      RES1=PROP(9)                                               ACPR1440
000043      RES2=PROP(10)                                              ACPR1450
000044      SIG1=TOP(1)                                                ACPR1460
000046      SIG2=TOP(2)                                                ACPR1470
000047      AVP1=TOP(3)                                                ACPR1480
000051      AVP2=TOP(4)                                                ACPR1490
000052      RAD1=TOP(5)                                                ACPR1500
000054      RAD2=TOP(6)                                                ACPR1510
C                                                                      ACPR1520
C.....CALCULATE NECESSARY CONSTANTS. ....ACPR1530
C                                                                      ACPR1540
000055      AVP=AVP1+AVP2                                              ACPR1550
000057      SIG=SQRT(SIG1*SIG1+SIG2*SIG2)                              ACPR1560
000064      FMAT=(E1*E2/H)/((1.00-TAU1*TAU1)*E2+(1.00-TAU2*TAU2)*E1) ACPR1570
000076      EMAT=FMAT*H/SY                                             ACPR1580
000100      RAD=2.*RAD1*RAD2/(RAD1+RAD2)                               ACPR1590
000105      R1=RAD1/RAD                                               ACPR1600
000107      R2=RAD2/RAD                                               ACPR1610
000110      R=(RAD1+RAD2)/RAD                                          ACPR1620
C                                                                      ACPR1630
C.....GENERATE A NORMAL FREQUENCY DISTRIBUTION FOR PEAKS HEIGHTS. ....ACPR1640
C                                                                      ACPR1650
000112      X=5.0000                                                  ACPR1660
000114      CALL NDIS(X,201,U)                                         ACPR1670
000116      ZP(1)=-5.000000                                           ACPR1680
000117      NUM(1)=U(1)*NN+0.50                                       ACPR1690
000127      KP=201                                                     ACPR1700

```

Contrails

```

000130      DO 9 K=2,KP                                ACPR1710
000132      JK=K-1                                    ACPR1720
000133      NUM(K)=U(K)*NN+0.50                       ACPR1730
000140      9 ZP(K)=ZP(JK)+0.05000                   ACPR1740
000146      WRITE(6,110) SIG,AVP,RAD                 ACPR1750
000157      JCT=1                                     ACPR1960
000160      3 CONTINUE                                ACPR1970
C                                                  ACPR1980
C.....DETERMINE D, FOR A GIVEN VALUE OF Y AND START CALCULATIONS. .... ACPR1990
C                                                  ACPR2000
000160      DZ=(Y-AVP)/SIG                            ACPR2010
000166      NNN=0                                     ACPR2020
000167      VAA=0.                                    ACPR2030
000170      HAA=0.                                    ACPR2040
000171      AR=0.                                     ACPR2050
000172      XLA=0.                                    ACPR2060
000173      CR=0.                                     ACPR2070
000174      RRS=0.                                    ACPR2080
000175      RRSS=0.                                   ACPR2090
000176      NEE=0                                     ACPR2100
000176      NPP=0                                     ACPR2110
000177      WAV=0.                                    ACPR2120
000201      DO 29 K=1,KP                              ACPR2130
C                                                  ACPR2140
C.....CHECK IF CONTACT TAKES PLACE. .... ACPR2150
C                                                  ACPR2160
000203      IF (ZP(K).LE.DZ) GO TO 29                ACPR2170
000206      IF (NUM(K)) 29,29,4                      ACPR2180
000210      4 NNN=NNN+NUM(K)                          ACPR2190
000213      DD=(ZP(K)-DZ)*SIG+AVP                   ACPR2200
000217      WAV=WAV+DD*NUM(K)                       ACPR2210
000224      IF (ICT.EQ.0) GO TO 2                    ACPR2220
C                                                  ACPR2230
C.....IF ICT=1, CALL #RDIS# FOR DISTRIBUTION OF RADII. .... ACPR2240
C                                                  ACPR2250
000225      NO=NUM(K)                                 ACPR2260
000227      CALL RDIS(NO,RLD,DD,EMAT,FMAT,AS,T,RES1,RES2,VA,HA,A,XL,CC,NE,NP,RACPR2270
1S,RSS)                                             ACPR2280
000251      VAA=VAA+VA                                ACPR2290
000253      HAA=HAA+HA                                ACPR2300
000255      AR=AR+A                                    ACPR2310
000257      CP=CR+CC                                  ACPR2320
000261      XLA=XLA+XL                                ACPR2330
000263      RRS=RRS+RS                                ACPR2340
000266      RRSS=RRSS+RSS                             ACPR2350
000270      NEE=NEE+NE                                ACPR2360
000271      NPP=NPP+NP                                ACPR2370
000273      GO TO 29                                  ACPR2380
000277      2 CONTINUE                                ACPR2390
C                                                  ACPR2400
C.....IF ICT=0, COMPUTE FORCES BY CALLING #GUPTA# FOR MEAN RADII. .... ACPR2410
C                                                  ACPR2420
000277      DD=DD/RAD                                 ACPR2430
000301      WMAX=DD                                   ACPR2440
000302      CALL GUPTA(EMAT,FMAT,AS,R1,R2,WMAX,T,VA,HA,A,RR,XL,NE,NP) ACPR2450
000317      VAA=VAA+VA*NUM(K)                       ACPR2460
000324      HAA=HAA+HA*NUM(K)                       ACPR2470
000330      XLA=XLA+XL*NUM(K)                       ACPR2480

```

Contrails

000334		AR=AR+A*NUM(K)	ACPR2490
000340		NEE=NEE+NE*NUM(K)	ACPR2500
000344		NPP=NPP+NP*NUM(K)	ACPR2510
000350		RR=RR*RAD*(1.0E-03)	ACPR2520
000352		RRS=RRS+RR*NUM(K)	ACPR2530
000356		RRSS=RRSS+RR*RR*NUM(K)	ACPR2540
000361		A=A*RAD*RAD*(1.0E-06)	ACPR2550
000364		RC=RES1/(4.*RR) +RES2/A	ACPR2560
000370		CR=CR+NUM(K)/RC	ACPR2570
000375	29	CONTINUE	ACPR2580
	C		ACPR2590
	CTRANSFORM RESULTS INTO APPROPRIATE UNITS.	ACPR2600
	C		ACPR2610
000403		IF(NNN.EQ.0) GO TO 71	ACPR2620
000405		IF(ICT) 5,5,6	ACPR2630
000406	5	PN=SY*RAD*RAD*(0.10E-05)	ACPR2640
000411		VAA=VAA*PN	ACPR2650
000412		HAA=HAA*PN	ACPR2660
000414		AR=AR*RAD*RAD	ACPR2670
000416		XLA=XLA*RAD/NNN	ACPR2680
000422		GO TO 7	ACPR2690
000422	6	VAA=VAA*SY	ACPR2700
000424		HAA=HAA*SY	ACPR2710
000425		XLA=XLA/NNN	ACPR2720
000430	7	F=HAA/VAA	ACPR2730
000432		WAV=WAV/NNN	ACPR2740
000435		AR=AR*(0.10E-05)	ACPR2750
000437		CR=1.0/CR	ACPR2760
000441		RM=RRS/NNN	ACPR2770
000443		RMS=RRSS/NNN	ACPR2780
000446		RM=RM*(1.0E+03)	ACPR2790
000450		RS=RMS*(1.0E+06)	ACPR2800
000452		GO TO 99	ACPR2810
000453	71	WRITE(6,114) Y,DZ	ACPR2820
000463		STOP	ACPR2830
000465	99	CONTINUE	ACPR2840
000465		RETURN	ACPR2850
000466		END	ACPR2860

```

SUBROUTINE RDIS(NN,RLD,DD,EMAT,FMAT,AS,T,RES1,RES2,VA,HA,A,XL,C,NERDIS 010
1,NP,RS,RSS) ..... RDIS 020
C ..... RDIS 030
C ..... RDIS 040
C ***** RDIS 050
C ..... RDIS 060
C SUBROUTINE RDIS ..... RDIS 070
C ..... RDIS 080
C THIS SUBROUTINE COMPUTES THE CONTACT FORCES ETC., AS DONE IN ..... RDIS 090
C ROUTINE #ACPR#,FOR A GIVEN NUMBER OF JUNCTIONS WITH ..... RDIS 100
C A CONSTANT GEOMETRIC INTERACTION WHEN THE RADII OF CURVATURE ARE ..... RDIS 110
C DISTRIBUTED ACCORDING TO A KNOWN DISTRIBUTION FUNCTION. ..... RDIS 120
C ..... RDIS 130
C ..... RDIS 140
C ----- RDIS 150
C EXTERNAL SUBROUTINES CALLED ..... RDIS 160
C ..... RDIS 170
C GUPTA -- THE SUBROUTINE FOR JUNCTION MODEL. ..... RDIS 180
C ..... RDIS 190
C DESCRIPTION OF PARAMETERS ..... RDIS 200
C ..... RDIS 210
C NN -- NUMBER OF INTERACTIONS. ..... RDIS 220
C RLD -- INPUT VECTOR OF LENGTH 6, SAME AS IN #ACPR#. ..... RDIS 230
C DD -- MAXIMUM GEOMETRIC INTERACTION (MIL IN). ..... RDIS 240
C ..... RDIS 250
C ALL OTHER PARAMETERS ARE SAME AS THOSE DESCRIBED IN #GUPTA# ..... RDIS 260
C ..... RDIS 270
C ..... RDIS 280
C N.B. -- A (5 BY 5) JOINT FREQUENCY MATRIX OF TWO RADII IS ..... RDIS 290
C GENERATED. IF THE SIZE OF THIS MATRIX IS TO BE CHANGED ..... RDIS 300
C STATEMENT 400, 410 AND THE DIMENSION STATEMENT 390 ..... RDIS 310
C SHOULD BE MODIFIED ACCORDINGLY. ..... RDIS 320
C ..... RDIS 330
C ..... RDIS 340
C ..... RDIS 350
C PRADEEP K. GUPTA. ..... RDIS 360
C ..... RDIS 370
C ***** RDIS 380
C ..... RDIS 390
000025 DIMENSION RL(5,5),RLD(6),R1(5),R2(5) ..... RDIS 392
000025 COMMON/CONT2/JCT ..... RDIS 395
100 FORMAT(10X,35HVARIATION OF RADII OF CURVATURE** ,6(1X,E12.5)) ..... RDIS 400
000025 L=5 ..... RDIS 410
000026 M=5 ..... RDIS 420
000027 VVA=0. .... RDIS 430
000030 HHA=0. .... RDIS 440
000031 XLA=0. .... RDIS 450
000032 CR=0. .... RDIS 460
000033 AR=0. .... RDIS 470
000034 NNE=0 ..... RDIS 480
000035 NNP=0 ..... RDIS 490
000036 RS=0. .... RDIS 500
000037 RSS=0. .... RDIS 505
000040 IF(JCT.EQ.1) GO TO 2 ..... RDIS 510
000042 R1MAX= EXP((RLD(1)+RLD(2)*RLD(6))/0.43429) ..... RDIS 520
000054 R2MAX= EXP((RLD(3)+RLD(4)*RLD(6))/0.43429) ..... RDIS 530
000066 RE1=(R1MAX-RLD(5))/L ..... RDIS 540
000072 RE2=(R2MAX-RLD(5))/M

```

Contrails

000076		R1(1)=RLD(5)+RE1/2.	RDIS 550
000102		R2(1)=RLD(5)+RE2/2.	RDIS 560
000105		DO 49 I=2,L	RDIS 570
000106	49	R1(I)=R1(I-1)+RE1	RDIS 580
000113		DO 19 I=2,M	RDIS 590
000114	19	R2(I)=R2(I-1)+RE2	RDIS 600
000121		SUM=0.	RDIS 610
000122		DO 29 I=1,L	RDIS 620
000123		RL1=(ALOG10(R1(I)-RE1/2.))-RLD(1))/RLD(2)	RDIS 630
000137		CALL NDTR(RL1,P1,D)	RDIS 640
000141		RL1=(ALOG10(R1(I)+RE1/2.))-RLD(1))/RLD(2)	RDIS 650
000161		CALL NDTR(RL1,P2,D)	RDIS 660
000163		PR1=P2-P1	RDIS 670
000165		DO 29 J=1,M	RDIS 680
000172		RL2=(ALOG10(R2(J)-RE2/2.))-RLD(3))/RLD(4)	RDIS 690
000206		CALL NDTR(RL2,P1,D)	RDIS 700
000211		RL2=(ALOG10(R2(J)+RE2/2.))-RLD(3))/RLD(4)	RDIS 710
000231		CALL NDTR(RL2,P2,D)	RDIS 720
000234		PR2=P2-P1	RDIS 730
000236		RL(I,J)=PR1*PR2	RDIS 740
000242		SUM=SUM+RL(I,J)	RDIS 750
000245	29	CONTINUE	RDIS 760
000256		DO 39 I=1,L	RDIS 770
000257		DO 39 J=1,M	RDIS 780
000260		RL(I,J)=RL(I,J)/SUM	RDIS 790
000264	39	CONTINUE	RDIS 800
000271		WRITE(6,100) (RLD(I),I=1,6)	RDIS 801
000305		JCT=1	RDIS 802
000306	2	CONTINUE	RDIS 804
000306		DO 9 I=1,L	RDIS 810
000313		DO 9 J=1,M	RDIS 820
000314		N=NN*RL(I,J)+0.5	RDIS 830
000322		IF(N) 9,9,1	RDIS 840
000324	1	RAD1=R1(I)	RDIS 850
000326		RAD2=R2(J)	RDIS 860
000330		RAD=2.*RAD1*RAD2/(RAD1+RAD2)	RDIS 870
000335		RR1=RAD1/RAD	RDIS 880
000336		RR2=RAD2/RAD	RDIS 890
000337		WMAX=OD/RAD	RDIS 900
000340		CALL SUPTA(EMAT,FMAT,AS,RR1,RR2,WMAX,T,VA,HA,A,RR,XL,NE,NP)	RDIS 910
000360		PN=RAD*RAD*(0.10E-05)	RDIS 920
000362		VVA=VVA+VA*PN*N	RDIS 930
000367		HHA=HHA+HA*PN*N	RDIS 940
000372		AR=AR+A*RR*RR*N	RDIS 950
000376		XLA=XLA+XL*RR*RR*N	RDIS 960
000402		NNE=NNE+NE*N	RDIS 970
000405		NNP=NNP+NP*N	RDIS 980
000410		PR=RR*RR*(1.0E-03)	RDIS 990
000413		RS=RS+RR*N	RDIS1000
000416		RSS=RSS+RR*RR*N	RDIS1010
000421		A=A*RR*RR*(1.0E-06)	RDIS1020
000425		RC=RES1/(4.*RR) +RES2/A	RDIS1030
000432		CR=CR+N/RC	RDIS1040
000435	9	CONTINUE	RDIS1050
000446		VA=VVA	RDIS1060
000447		HA=HHA	RDIS1070
000451		A=AR	RDIS1080
000453		XL=XLA	RDIS1090

Contrails

000455
000457
000461
000463
000464

C=CR
NE=NNE
NP=NNP
RETURN
END

RDIS1100
RDIS1110
RDIS1120
RDIS1130
RDIS1140

Contrails

```

SUBROUTINE NDTR(X,P,D)
C
C .....
C
C SUBROUTINE NDTR
C
C PURPOSE
C COMPUTES Y = P(X) = PROBABILITY THAT THE RANDOM VARIABLE U,
C DISTRIBUTED NORMALLY(0,1), IS LESS THAN OR EQUAL TO X.
C F(X), THE ORDINATE OF THE NORMAL DENSITY AT X, IS ALSO
C COMPUTED.
C
C USAGE
C CALL NDTR(X,P,D)
C
C DESCRIPTION OF PARAMETERS
C X--INPUT SCALAR FOR WHICH P(X) IS COMPUTED.
C P--OUTPUT PROBABILITY.
C D--OUTPUT DENSITY.
C
C REMARKS
C MAXIMUM ERROR IS 0.0000007.
C
C SUBROUTINES AND SUBPROGRAMS REQUIRED
C NONE
C
C METHOD
C BASED ON APPROXIMATIONS IN C. HASTINGS, APPROXIMATIONS FOR
C DIGITAL COMPUTERS, PRINCETON UNIV. PRESS, PRINCETON, N.J.,
C 1955. SEE EQUATION 26.2.17, HANDBOOK OF MATHEMATICAL
C FUNCTIONS, ABRAMOWITZ AND STEGUN, DOVER PUBLICATIONS, INC.,
C NEW YORK.
C .....
C
000006 AX=ABS(X)
000007 T=1.0/(1.0+.2316419*AX)
000012 D=0.3989423*EXP(-X*X/2.0)
000021 P = 1.0 - D*T*(((1.330274*T - 1.821256)*T + 1.781478)*T -
1 0.3565638)*T + 0.3193815)
000034 IF(X)1,2,2
000036 1 P=1.0-P
000040 2 RETURN
000041 END
```

NDTR 010
NDTR 020
NDTR 030
NDTR 040
NDTR 050
NDTR 060
NDTR 070
NDTR 080
NDTR 090
NDTR 100
NDTR 110
NDTR 120
NDTR 130
NDTR 140
NDTR 150
NDTR 160
NDTR 170
NDTR 180
NDTR 190
NDTR 200
NDTR 210
NDTR 220
NDTR 230
NDTR 240
NDTR 250
NDTR 260
NDTR 270
NDTR 280
NDTR 290
NDTR 300
NDTR 310
NDTR 320
NDTR 330
NDTR 340
NDTR 350
NDTR 360
NDTR 370
NDTR 380
NDTR 390
NDTR 400
NDTR 410
NDTR 420
NDTR 430
NDTR 440
NDTR 450

Contrails

```

SUBROUTINE GUPTA(EMAT,FMAT,AS,R1,R2,WMAX,T,VA,HA,AA,RR,XL,NE,NP)  GUPT 010
C                                                                 GUPT 020
C*****M*****GUPT 030
C                                                                 GUPT 040
C  SUBROUTINE GUPTA                                             GUPT 050
C                                                                 GUPT 060
C      THIS SUBROUTINE COMPUTES THE FRICTION FORCE, NORMAL FORCE  GUPT 070
C AND AREA OF CONTACT FOR TWO SPHERICAL ASPERITIES SUBJECTED TO GUPT 080
C SLIDING INTERACTION.                                         GUPT 090
C                                                                 GUPT 100
C  EXTERNAL SUBROUTINE USED...                                  GUPT 110
C      ELJUN  -- A ROUTINE FOR ELASTIC JUNCTION MODEL.          GUPT 120
C      PSJUN  -- A ROUTINE FOR STRONG PLASTIC JUNCTION MODEL.   GUPT 130
C      PWJUN  -- A ROUTINE FOR WEAK PLASTIC JUNCTION MODEL.     GUPT 140
C      SUBROUTINE CALLED BY ANY OF THE ABOVE ROUTINES ARE NOT  GUPT 150
C LISTED ABOVE. REFER TO THE PARTICULAR SUBROUTINE FOR        GUPT 160
C THIS INFORMATION.                                           GUPT 170
C                                                                 GUPT 180
C  DESCRIPTION OF PARAMETERS.....                              GUPT 190
C      EMAT - MATERIAL CONSTANT (SEE STATEMENT I ACPR 158).     GUPT 200
C      FMAT - MATERIAL CONSTANT (SEE STATEMENT I ACPR 157).     GUPT 210
C      AS  - NON DIMENSIONAL ADHESION STRESS.                   GUPT 220
C      R1  - NONDIMENSIONAL RADIUS OF HARDER ASPERITY.          GUPT 230
C      R2  - NONDIMENSIONAL RADIUS OF SOFTER ASPERITY.          GUPT 240
C      WMAX - MAXIMUM GEOMETRIC INTERFERENCE (NONDIMENSIONAL). GUPT 250
C      T   - STRESS RATIO, INTERFACIAL SHEAR/MAX.SHEAR         GUPT 260
C      VA  - OUTPUT NONDIMENSIONAL NORMAL FORCE.                 GUPT 270
C      HA  - OUTPUT NONDIMENSIONAL FRICTION FORCE.              GUPT 280
C      AA  - OUTPUT NONDIMENSIONAL AVERAGE CONTACT AREA.       GUPT 290
C      RR  - OUTPUT NONDIMENSIONAL AVERAGE RADIUS OF CONTACT.  GUPT 300
C      XL  - OUTPUT NONDIMENSIONAL CONTACT LENGTH.              GUPT 310
C      NE  - OUTPUT INTERGER =1, IF CONTACT IS ELASTIC.         GUPT 320
C      NP  - OUTPUT INTERGER =1, IF CONTACT IS PLASTIC.         GUPT 330
C                                                                 GUPT 340
C                                                                 GUPT 350
C                                                                 GUPT 360
C                                                                 GUPT 370
C                                                                 GUPT 380
C*****M*****GUPT 390
C                                                                 GUPT 400
000021  DIMENSION X(21),V(21),H(21),Z(21),A(21)                GUPT 410
000021  NE=0                                                       GUPT 420
000021  NP=0                                                       GUPT 430
C                                                                 GUPT 440
C.....CALCULATION OF NECESSARY CONSTANTS. ....GUPT 450
C                                                                 GUPT 460
000022  WP=0.5/(FMAT*FMAT)                                         GUPT 470
000024  R=(R1+R2)                                                   GUPT 480
000026  D=R-WMAX                                                    GUPT 490
000027  XMAX= SQRT(R*R-D*D)                                         GUPT 500
C                                                                 GUPT 510
C.....GENERATION OF X-ARRAY. ....GUPT 520
C                                                                 GUPT 530
000034  X(1)=-XMAX                                                  GUPT 540
000036  XE=XMAX/10.                                                 GUPT 550
000040  DO 9 J=2,20                                                 GUPT 560
000045  9  X(J)=X(J-1)+XE                                           GUPT 570

```


Contrails

```

000051      X(21)=XMAX                      GUPT 580
000052      X(11)=0.00                      GUPT 590
C
C.....CHECK IF CONTACT IS ELASTIC OR PLASTIC. ....GUPT 600
C.....GUPT 610
C.....GUPT 620
000053      IF(WMAX.GT.WP) GO TO 2          GUPT 630
C.....GUPT 640
C.....ELASTIC JUNCTION SOLUTION. ....GUPT 650
C.....GUPT 660
000057      NE=1                            GUPT 670
000060      DO 69 J=1,21                    GUPT 680
000062      IF(J.EQ.1 .OR. J.EQ.21) GO TO 6 GUPT 690
000071      IF(J.EQ.11) GO TO 4             GUPT 700
000073      W=R- SQRT(D*D+X(J)*X(J))        GUPT 710
000102      GO TO 5                          GUPT 720
000106      4  W=WMAX                        GUPT 730
000107      GO TO 5                          GUPT 740
000110      6  W=0.00                        GUPT 750
000111      PP=0.                            GUPT 760
000111      SS=0.                            GUPT 770
000112      V(J)=0.                          GUPT 780
000114      H(J)=0.                          GUPT 790
000115      A(J)=0.                          GUPT 800
000116      GO TO 69                         GUPT 810
000117      5  CONTINUE                      GUPT 820
000117      CALL ELJUN(EMAT,W,T,P,S,AR)      GUPT 830
000123      PP=P/AR                           GUPT 840
000125      SS=S/AR                           GUPT 850
000126      V(J)=(P*D + S*X(J))/ SQRT(D*D+X(J)*X(J)) GUPT 860
000143      H(J)=(-P*X(J) + S*D)/ SQRT(D*D+X(J)*X(J)) GUPT 870
000157      A(J)=AR                           GUPT 880
000160      69  CONTINUE                      GUPT 890
C.....GUPT 900
C.....COMPUTE AVERAGES. ....GUPT 910
C.....GUPT 920
000166      XL=2.*XMAX                       GUPT 930
000170      CALL DQSF(XE,V,Z,21)              GUPT 940
000173      VA=Z(21)                          GUPT 950
000175      CALL DQSF(XE,H,Z,21)              GUPT 960
000200      HA=Z(21)                          GUPT 970
000202      CALL DQSF(XE,A,Z,21)              GUPT 980
000205      AA=Z(21)                          GUPT 990
000207      DO 19 J=1,21                      GUPT1000
000214      19  A(J)= SQRT(A(J)/3.14159)      GUPT1010
000227      CALL DQSF(XE,A,Z,21)              GUPT1020
000232      RR=Z(21)                          GUPT1030
000234      GO TO 98                          GUPT1040
C.....GUPT1050
C.....PLASTIC JUNCTION SOLUTION. ....GUPT1060
C.....GUPT1070
C.....GUPT1080
000240      2  NP=1                           GUPT1080
000241      KW=0                              GUPT1090
000242      KS=0                              GUPT1100
000243      WT= SQRT(WMAX)                    GUPT1110
000250      WAC=ASIN(WT/R2)                   GUPT1120
000257      WGAMMA=0.50*ACOS(T)              GUPT1130
000262      WALPHA=WAC                        GUPT1140
000264      PT= SIN(2.*WGAMMA)*2.5708+2.*WGAMMA-2.*WALPHA GUPT1150

```

Contrails

```

000276      DO 89 J=1,21                                GUPT1160
000302      IF (J.EQ.1 .OR. J.EQ.21) GO TO 8            GUPT1170
000312      IF (J.EQ.11) GO TO 10                       GUPT1180
000314      W=R- SQRT(D*D+X(J)*X(J))                   GUPT1190
000323      WTHETA= ATAN( ABS(D/X(J)))                   GUPT1200
000331      GO TO 12                                       GUPT1210
000335      8  W=0.00                                       GUPT1220
000336      WTHETA= ATAN( ABS(D/X(J)))                   GUPT1230
000344      GO TO 12                                       GUPT1240
000350      10 WTHETA=1.570795                             GUPT1250
000351      W=WMAX                                       GUPT1260
000353      12 WDELTA=1.570795-WTHETA                   GUPT1270
000355      WA= SQRT(W)                                   GUPT1280
000357      ALPHA=ASIN(WA/R2)                             GUPT1290
C.....
C.....CHECK IF JUNCTION IS STRONG OR WEAK. .... GUPT1310
C
000372      IF ( COS(2.*WDELTA)-T) 14,14,15             GUPT1320
C
C.....WEAK JUNCTION SOLUTION. .... GUPT1340
C.....
C.....
000404      15  SS=T                                       GUPT1360
000406      CALL PWJUN(J,X(J),W,W,T,PT,WAC,ALPHA,T,AS,PP,AR,KW) GUPT1370
000424      A(J)=AR                                       GUPT1380
000426      S=SS*A(J)                                     GUPT1390
000430      P=PP*A(J)                                     GUPT1400
000432      IF (KW) 16,16,17                             GUPT1410
000440      16  V(J)=(P* COS(WDELTA)-S* SIN(WDELTA))    GUPT1420
000451      H(J)=(P* SIN(WDELTA)+S* COS(WDELTA))    GUPT1430
000462      GO TO 88                                     GUPT1440
000466      17  V(J)=P                                       GUPT1450
000470      H(J)=S                                       GUPT1460
000472      GO TO 88                                     GUPT1470
C.....
C.....STRONG JUNCTION SOLUTION. .... GUPT1480
C.....
C.....
000472      14  U= SQRT(R2*R2-W)/R2                       GUPT1490
000503      XX=X(J)/R2                                   GUPT1500
000505      CALL PSJUN(J,XX,WDELTA,U,AS,WS,X0,PP,SS,AR,KS) GUPT1510
000520      A(J)=3.14159*(AR*R2)**2/(2.*R1*R2/(R1+R2))**2 GUPT1520
000533      S=SS*A(J)                                     GUPT1530
000535      P=PP*A(J)                                     GUPT1540
000537      IF (KS) 24,24,25                             GUPT1550
000541      24  V(J)=(P* COS(WDELTA)-S* SIN(WDELTA))    GUPT1560
000552      H(J)=(P* SIN(WDELTA)+S* COS(WDELTA))    GUPT1570
000553      GO TO 88                                     GUPT1580
000567      25  V(J)=P                                       GUPT1590
000571      H(J)=S                                       GUPT1600
000573      88  IF (PP) 89,23,89                         GUPT1610
000574      89  CONTINUE                                  GUPT1620
C.....
C.....COMPUTATION OF CONTACT LENGTH XL. .... GUPT1640
C.....
000576      IT=21                                       GUPT1650
000577      IF (KW.EQ.1) GO TO 18                       GUPT1660
000601      IF (KS.EQ.1) GO TO 20                       GUPT1670
000603      XL=2.*XMAX                                   GUPT1680
000604      XLC=0.                                       GUPT1690

```

Contrails

```

000506      GO TO 22                                GUPT1740
000606      18  XLC=2.*WT-XMAX                       GUPT1750
000611      GO TO 21                                GUPT1760
000612      20  XLC=2.*WT-XMAX+XO                   GUPT1770
000616      21  XL=2.*XMAX+XLC                       GUPT1780
000621      GO TO 22                                GUPT1790
000622      23  V(J)=V(J-1)                          GUPT1800
000624      H(J)=H(J-1)                              GUPT1810
000626      A(J)=A(J-1)                              GUPT1820
000630      XL=X(J)*XMAX                             GUPT1830
000632      IT=J                                      GUPT1840
000633      XLC=0.                                   GUPT1850
000637      22  CONTINUE                             GUPT1860
C                                                  GUPT1870
C.....COMPUTE AVERAGES.....GUPT1880
C
000635      CALL DQSF(XE,H,Z,IT)                     GUPT1890
000640      HA=Z(IT)                                 GUPT1900
000643      CALL DQSF(XE,A,Z,IT)                     GUPT1910
000646      AA=Z(IT)                                 GUPT1920
000650      AA=AA+A(21)*XLC/2.                       GUPT1930
000654      DO 29 J=1,IT                             GUPT1940
000661      29  A(J)=SQRT(A(J)/3.14159)              GUPT1950
000674      CALL DQSF(XE,A,Z,IT)                     GUPT1960
000677      RR=Z(IT)                                 GUPT1970
000702      DO 59 J=11,IT                            GUPT1980
000707      IF(V(J).GT.0.) GO TO 59                  GUPT1990
000712      NT=J                                     GUPT2000
000712      GO TO 50                                 GUPT2010
000713      59  CONTINUE                             GUPT2020
000716      50  NT=J-1                               GUPT2030
000720      CALL DQSF(XE,V,Z,NT)                     GUPT2040
000723      VA=Z(NT)                                GUPT2050
000725      NDIM=IT+1-NT                            GUPT2060
000727      V(1)=-V(NT)                             GUPT2070
000731      DO 79 J=2,NDIM                           GUPT2080
000736      KT=NT+J-1                               GUPT2090
000740      79  V(J)=V(KT)                           GUPT2100
000746      CALL DQSF(XE,V,Z,NDIM)                  GUPT2110
000751      VA=VA+Z(NDIM)                           GUPT2120
C                                                  GUPT2130
C.....CORRECTION FOR THE AVERAGES.....GUPT2140
C
000754      VA=VA+V(21)*XLC/2.                       GUPT2150
000757      HA=HA+H(21)*XLC/2.                       GUPT2160
000762      RR=RR+A(21)*XLC/2.                       GUPT2170
000766      98  VA=VA/XL                             GUPT2180
000770      HA=HA/XL                                 GUPT2190
000772      AA=AA/XL                                 GUPT2200
000773      RR=RR/XL                                 GUPT2210
000776      RETURN                                   GUPT2220
000776      END                                     GUPT2230

```


Contrails

```

000044      SUM2=SUM2+SUM2                      DQSF 580
000045      SUM2=AUX2-HT*(Y(4)+SUM2+Y(6))      DQSF 590
000052      Z(1)=0.00                          DQSF 600
000054      AUX=Y(3)+Y(3)                      DQSF 610
000056      AUX=AUX+AUX                        DQSF 620
000057      Z(2)=SUM2-HT*(Y(2)+AUX+Y(4))      DQSF 630
000064      Z(3)=SUM1                          DQSF 640
000066      Z(4)=SUM2                          DQSF 650
000067      IF (NDIM-6)5,5,2                    DQSF 660
          C                                     DQSF 670
          C      INTEGRATION LOOP               DQSF 680
000071      2 DO 4 I=7,NDIM,2                    DQSF 690
000073      SUM1=AUX1                           DQSF 700
000074      SUM2=AUX2                           DQSF 710
000076      AUX1=Y(I-1)+Y(I-1)                  DQSF 720
000100      AUX1=AUX1+AUX1                       DQSF 730
000101      AUX1=SUM1+HT*(Y(I-2)+AUX1+Y(I))     DQSF 740
000107      Z(I-2)=SUM1                          DQSF 750
000111      IF (I-NDIM)3,6,6                     DQSF 760
000113      3 AUX2=Y(I)+Y(I)                       DQSF 770
000115      AUX2=AUX2+AUX2                       DQSF 780
000117      AUX2=SUM2+HT*(Y(I-1)+AUX2+Y(I+1))   DQSF 790
000124      4 Z(I-1)=SUM2                         DQSF 800
000131      5 Z(NDIM-1)=AUX1                      DQSF 810
000133      Z(NDIM)=AUX2                         DQSF 820
000135      RETURN                               DQSF 830
000136      6 Z(NDIM-1)=SUM2                      DQSF 840
000140      Z(NDIM)=AUX1                         DQSF 850
000142      RETURN                               DQSF 860
          C      END OF INTEGRATION LOOP         DQSF 870
          C                                     DQSF 880
000143      7 IF (NDIM-3)12,11,8                 DQSF 890
          C                                     DQSF 900
          C      NDIM IS EQUAL TO 4 OR 5         DQSF 910
000145      8 SUM2=1.125E0*HT*(Y(1)+Y(2)+Y(2)+Y(2)+Y(3)+Y(3)+Y(3)+Y(4)) DQSF 920
000156      SUM1=Y(2)+Y(2)                       DQSF 930
000160      SUM1=SUM1+SUM1                       DQSF 940
000161      SUM1=HT*(Y(1)+SUM1+Y(3))            DQSF 950
000165      Z(1)=0.00                            DQSF 960
000167      AUX1=Y(3)+Y(3)                       DQSF 970
000171      AUX1=AUX1+AUX1                       DQSF 980
000172      Z(2)=SUM2-HT*(Y(2)+AUX1+Y(4))      DQSF 990
000177      IF (NDIM-5)10,9,9                    DQSF 1000
000202      9 AUX1=Y(4)+Y(4)                     DQSF 1010
000204      AUX1=AUX1+AUX1                       DQSF 1020
000205      Z(5)=SUM1+HT*(Y(3)+AUX1+Y(5))      DQSF 1030
000213      10 Z(3)=SUM1                         DQSF 1040
000215      Z(4)=SUM2                            DQSF 1050
000216      RETURN                               DQSF 1060
          C                                     DQSF 1070
          C      NDIM IS EQUAL TO 3             DQSF 1080
000217      11 SUM1=HT*(1.25E0*Y(1)+Y(2)+Y(2)-.25E0*Y(3)) DQSF 1090
000225      SUM2=Y(2)+Y(2)                       DQSF 1100
000227      SUM2=SUM2+SUM2                       DQSF 1110
000230      Z(3)=HT*(Y(1)+SUM2+Y(3))           DQSF 1120
000235      Z(1)=0.00                            DQSF 1130
000237      Z(2)=SUM1                            DQSF 1140
000241      12 RETURN                             DQSF 1150

000242      End                                 DQSF 1160

```


Contrails

```

SUBROUTINE PWJUN(J,X,W,WT,PT,WAC,ALPHA,T,AS,PP,A,KW)
C
C*****
C
C SUBROUTINE PWJUN
C
C THIS SUBROUTINE PROVIDES A SOLUTION OF WEAK JUNCTION ACCORDING
C TO GREEN-S SLIP LINE FIELD. THE EQUIVALENT JUNCTION ANGLE IN
C THIS CASE IS COMPUTED BY GEOMETRY.
C
C THE NOMENCLATURE OF INPUT AND OUTPUT PARAMETERS IS SAME AS
C THAT DESCRIBED IN #GUPTA#.
C
C-----
C PRADDEEP K. GUPTA.
C*****
C
000017      WGAMMA=0.50*ACOS(T)
000022      IF(KW) 11,11,3
000030 11     KW=0
000031      IF(J-11) 2,2,1
000033 1     IF(PT-AS) 4,4,3
000036 3     WALPHA=WAC
000037      PP= SIN(2.*WGAMMA)+2.5708+2.*WGAMMA-2.*WALPHA
000050      WL=WT-X/2.
000057      IF(WL) 5,5,6
000061 6     A=(WT*WT*ACOS((WT-WL)/WT)-(WT-WL)*SQRT(2.*WT*WL-WL*WL))*2.
000107      KW=1
000111      GO TO 10
000111 5     A=0.
000112      GO TO 10
000113 2     WALPHA=ALPHA
000114      PP= SIN(2.*WGAMMA)+2.5708+2.*WGAMMA-2.*WALPHA
000125      A= SQRT(W)
000140      GO TO 10
000141 4     WALPHA=ALPHA
000141      A= SQRT(W)
000147      PP= SIN(2.*WGAMMA)+2.5708+2.*WGAMMA-2.*WALPHA
000150      IF(PP-AS) 7,7,8
000157 8     PP=0.
000170      GO TO 10
000171 7     PP=-PP
000173 10     CONTINUE
000173      RETURN
000174      END
PWJU 010
PWJU 020
PWJU 030
PWJU 040
PWJU 050
PWJU 060
PWJU 070
PWJU 080
PWJU 090
PWJU 100
PWJU 110
PWJU 120
PWJU 130
PWJU 140
PWJU 150
PWJU 160
PWJU 170
PWJU 180
PWJU 190
PWJU 200
PWJU 210
PWJU 220
PWJU 230
PWJU 240
PWJU 250
PWJU 260
PWJU 270
PWJU 280
PWJU 290
PWJU 300
PWJU 310
PWJU 320
PWJU 330
PWJU 340
PWJU 350
PWJU 360
PWJU 370
PWJU 380
PWJU 390
PWJU 400
PWJU 410
PWJU 420
PWJU 430
PWJU 440
PWJU 450
PWJU 460

```


Contrails

```

SUBROUTINE PSJUN(J,X,WDELTA,U,AS,WT,X0,PP,SS,A,KS) PSJU 010
C PSJU 020
C***** PSJU 030
C PSJU 040
C SUBROUTINE PSJUN PSJU 050
C PSJU 060
C THIS SUBROUTINE SOLVES THE JUNCTION DEFORMATION PROBLEM PSJU 070
C ACCORDING TO THE GREEN-S SLIP LINE FIELD SOLUTION FOR A STRONG PSJU 080
C PLASTIC JUNCTION. THE EQUIVALENT JUNCTION ANGLE IS COMPUTED BY PSJU 090
C SATISFYING THE INCOMPRESSIBILITY REQUIREMENT BY CALLING #ANGLE#. PSJU 100
C PSJU 110
C THE NOMENCLATURE OF THE INPUT AND OUTPUT PARAMETERS IS SAME AS PSJU 120
C DESCRIBED IN #GUPTA#. PSJU 130
C PSJU 140
C PSJU 150
C PRADEEP K. GUPTA. PSJU 160
C PSJU 170
C***** PSJU 180
C PSJU 190
000016 IF(KS) 12,12,11 PSJU 200
000020 12 KS=0 PSJU 210
000021 IF(J.EQ.1 .OR. J.EQ.21) GO TO 13 PSJU 220
000030 IF(U-1.00) 16,13,13 PSJU 230
000036 16 CONTINUE PSJU 240
000036 CALL ANGLE(U,WALPHA,AR) PSJU 250
000041 GO TO 14 PSJU 260
000045 13 WALPHA=0. PSJU 270
000046 AR=0. PSJU 280
000047 14 IF(0.78539+WDELTA-WALPHA) 5,5,6 PSJU 290
000053 6 WGAMMA=WDELTA PSJU 300
000054 SS= COS(2.*WGAMMA) PSJU 310
000057 PP= SIN(2.*WGAMMA)+2.5708+2.*WGAMMA-2.*WALPHA PSJU 320
000071 IF(J-11) 2,2,1 PSJU 330
000100 1 IF(PP-AS) 4,4,3 PSJU 340
000103 3 PP=0. PSJU 350
000104 GO TO 2 PSJU 360
000105 4 PP=-PP PSJU 370
000107 2 A=AR PSJU 380
000111 GO TO 15 PSJU 390
000112 5 X0=X PSJU 400
000113 KS=1 PSJU 410
000114 WT=1.41421*AR* SIN(WALPHA) PSJU 420
000125 11 WL=WT-(X-X0)/2. PSJU 430
000131 IF(WL) 7,7,8 PSJU 440
000133 8 A=(WT*WT*ACOS((WT-WL)/WT)-(WT-WL)*SQRT(2.*WT*WL-WL*WL))*2. PSJU 450
000161 GO TO 10 PSJU 460
000162 7 A=0. PSJU 470
000163 10 PP=1.0 PSJU 480
000164 SS=1.0 PSJU 490
000166 15 CONTINUE PSJU 500
000166 RETURN PSJU 510
000167 END PSJU 520

```

Contrails

```

SUBROUTINE ANGLE(U,ALPHA,A)                                ANGL 010
C                                                         ANGL 020
C*****ANGL 030
C                                                         ANGL 040
C SUBROUTINE ANGLE                                       ANGL 050
C                                                         ANGL 060
C     THIS SUBROUTINE COMPUTES THE JUNCTION ANGLE ALPHA WHICH ANGL 070
C     MAY BE USED IN THE GREEN-S SLIP LINE FIELD SOLUTION FOR STRONG ANGL 080
C     JUNCTION. THE ANGLE IS COMPUTED FROM THE CRITERION OF INCOMP- ANGL 090
C     RESSIBILITY OF THE MATERIAL DURING PLASTIC DEFORMATION. ANGL 100
C                                                         ANGL 110
C     FOR COMPUTATION OF ALPHA ROUTINE #ASUB# IS USED WHICH IS ANGL 120
C     A MODIFIED FORM OF THE SSP ROUTINE #ORTNI#. NEWTON-S ITERATION ANGL 130
C     METHOD IS USED FOR THE CALCULATION. ANGL 140
C-----ANGL 150
C     THE PARAMETERS OF ANGLE ARE DESCRIBED AS FOLLOWS..... ANGL 160
C     U     - A GEOMETRICAL INPUT PARAMETER,SEE DEFINITION ANGL 170
C           IN APPENDIX II, FIG.(A2-1). ANGL 180
C     ALPHA - OUTPUT VALUE OF THE JUNCTION ANGLE. ANGL 190
C     A     - RADIUS OF CONTACT SPOT MEASURED IN THE UNITS ANGL 200
C           OF THE RADIUS OF CONTACTING SPHERE. ANGL 210
C     EXTERNAL ROUTINE CALLED# #ASUB# - NEWTON-S ITERATION METHOD. ANGL 220
C                                                         ANGL 230
C     N.B. IN CASE THE COMPUTATION OF ALPHA AND A IS NOT POSSIBLE DUE ANGL 240
C     TO ERROR CODES NOTED BY SUBROUTINE ASUB, AN ERROR MESSAGE ANGL 250
C     IS PRINTED OUT AND THE EXECUTION IS TERMINATED. ANGL 260
C                                                         ANGL 270
C                                                         ANGL 280
C                                                         ANGL 290
C*****ANGL 300
C                                                         ANGL 310
C                                                         ANGL 320
C     EXTERNAL FCT                                       ANGL 330
000005 100  FORMAT(/,10X,58H)CALCULATION OF ALPHA NOT POSSIBLE DUE TO ERROR COD ANGL 340
000006 1E IER = ,12,2X,4HU = ,E12.5) ANGL 350
000007 EPS=0.50E-02 ANGL 360
000008 IEND=50 ANGL 370
000009 AP=2.00 ANGL 380
000010 K=0 ANGL 390
000011 3 XST=AP*ACOS(U) ANGL 400
000012 CALL ASUB(X,F,DEF,FCT,XST,EPS,IEND,IER,U) ANGL 410
000013 IF(IER.EQ.1) GO TO 1 ANGL 420
000014 IF(IER.EQ.2) GO TO 1 ANGL 430
000015 IF(X.GT.1.5707963) GO TO 2 ANGL 440
000016 IF(X.LT.0.00) GO TO 2 ANGL 450
000017 ALPHA=X ANGL 460
000018 A=(1.0-U* COS(ALPHA))/ SIN(ALPHA) ANGL 470
000019 GO TO 9 ANGL 480
000020 1 WRITE(6,100) IER,U ANGL 490
000021 STOP ANGL 500
000022 2 AP=AP+1.0 ANGL 510
000023 K=K+1 ANGL 520
000024 IF(K-4)3,4,4 ANGL 530
000025 4 IER=K ANGL 540
000026 GO TO 1 ANGL 550
000027 9 CONTINUE ANGL 560
000028 RETURN ANGL 570
000029 END ANGL 580

```

Contrails

```

SUBROUTINE ASUB(X,F,DERF,FCT,XST,EPS,IEND,IER,U) ASUB 010
C ASUB 020
C ..... ASUB 030
C ASUB 040
C SUBROUTINE ASUB ASUB 050
C ASUB 060
C THIS IS A MODIFIED FORM OF THE SSP ROUTINE DRINI. ASUB 070
C A PARAMETER #U# IS INCLUDED AND THIS IS PASSED TO ASUB 080
C THE EXTERNAL ROUTINE #FCT#. ASUB 090
C ASUB 100
C ASUB 110
C ASUB 120
C PURPOSE ASUB 130
C TO SOLVE GENERAL NONLINEAR EQUATIONS OF THE FORM F(X)=0 ASUB 140
C BY MEANS OF NEWTON-S ITERATION METHOD. ASUB 150
C ASUB 160
C USAGE ASUB 170
C CALL ASUB (X,F,DERF,FCT,XST,EPS,IEND,IER) ASUB 180
C PARAMETER FCT REQUIRES AN EXTERNAL STATEMENT. ASUB 190
C ASUB 200
C DESCRIPTION OF PARAMETERS ASUB 210
C X - DOUBLE PRECISION RESULTANT ROOT OF EQUATION F(X)=0. ASUB 220
C F - DOUBLE PRECISION RESULTANT FUNCTION VALUE AT ASUB 230
C ROOT X. ASUB 240
C DERF - DOUBLE PRECISION RESULTANT VALUE OF DERIVATIVE ASUB 250
C AT ROOT X. ASUB 260
C FCT - NAME OF THE EXTERNAL SUBROUTINE USED. IT COMPUTES ASUB 270
C TO GIVEN ARGUMENT X FUNCTION VALUE F AND DERIVATIVE ASUB 280
C DERF. ITS PARAMETER LIST MUST BE X,F,DERF, WHERE ASUB 290
C ALL PARAMETERS ARE DOUBLE PRECISION. ASUB 300
C XST - DOUBLE PRECISION INPUT VALUE WHICH SPECIFIES THE ASUB 310
C INITIAL GUESS OF THE ROOT X. ASUB 320
C EPS - SINGLE PRECISION INPUT VALUE WHICH SPECIFIES THE ASUB 330
C UPPER BOUND OF THE ERROR OF RESULT X. ASUB 340
C IEND - MAXIMUM NUMRER OF ITERATION STEPS SPECIFIED. ASUB 350
C IER - RESULTANT ERROR PARAMETER CODED AS FOLLOWS ASUB 360
C IER=0 - NO ERROR, ASUB 370
C IER=1 - NO CONVERGENCE AFTER IEND ITERATION STEPS. ASUB 380
C IER=2 - AT ANY ITERATION STEP DERIVATIVE DERF WAS ASUB 390
C EQUAL TO ZERO. ASUB 400
C U - ANY INPUT PARAMETER WHICH IS TO BE PASSED TO THE ASUB 410
C EXTERNAL SUBROUTINE FCT. ASUB 420
C ASUB 430
C REMARKS ASUB 440
C THE PROCEDURE IS BYPASSED AND GIVES THE ERROR MESSAGE IER=2 ASUB 450
C IF AT ANY ITERATION STEP DERIVATIVE OF F(X) IS EQUAL TO 0. ASUB 460
C POSSIBLY THE PROCEDURE WOULD BE SUCCESSFUL IF IT IS STARTED ASUB 470
C ONCE MORE WITH ANOTHER INITIAL GUESS XST. ASUB 480
C ASUB 490
C SUBROUTINES AND FUNCTION SUBPROGRAMS REQUIRED ASUB 500
C THE EXTERNAL SUBROUTINE FCT(X,F,DERF) MUST BE FURNISHED ASUB 510
C BY THE USER. ASUB 520
C ASUB 530
C METHOD ASUB 540
C SOLUTION OF EQUATION F(X)=0 IS DONE BY MEANS OF NEWTON-S ASUB 550
C ITERATION METHOD, WHICH STARTS AT THE INITIAL GUESS XST OF ASUB 560
C A ROOT X. CONVERGENCE IS QUADRATIC IF THE DERIVATIVE OF ASUB 570

```

Contrails

	C F(X) AT ROOT X IS NOT EQUAL TO ZERO. ONE ITERATION STEP	ASUB 580
	C REQUIRES ONE EVALUATION OF F(X) AND ONE EVALUATION OF THE	ASUB 590
	C DERIVATIVE OF F(X). FOR TEST ON SATISFACTORY ACCURACY SEE	ASUB 600
	C FORMULAE (2) OF MATHEMATICAL DESCRIPTION.	ASUB 610
	C FOR REFERENCE, SEE R. ZURMUEHL, PRAKTISCHE MATHEMATIK FUER	ASUB 620
	C INGENIEURE UND PHYSIKER, SPRINGER, BERLIN/GOETTINGEN/	ASUB 630
	C HEIDELBERG, 1963, PP.12-17.	ASUB 640
	C	ASUB 650
	C	ASUB 660
	C	ASUB 670
	C	ASUB 680
	C	ASUB 690
	C	ASUB 700
	C PREPARE ITERATION	ASUB 710
000014	IER=0	ASUB 720
000014	X=XST	ASUB 730
000016	TOL=X	ASUB 740
000017	CALL FCT(TOL,U,F,DERF)	ASUB 750
000033	TOLF=100.*EPS	ASUB 760
	C	ASUB 770
	C	ASUB 780
	C START ITERATION LOOP	ASUB 790
000034	DO 6 I=1,IEND	ASUB 800
000036	IF(F)1,7,1	ASUB 810
	C	ASUB 820
	C EQUATION IS NOT SATISFIED BY X	ASUB 830
000037	1 IF(DERF)2,8,2	ASUB 840
	C	ASUB 850
	C ITERATION IS POSSIBLE	ASUB 860
000040	2 DX=F/DERF	ASUB 870
000041	X=X-0X	ASUB 880
000043	TOL=X	ASUB 890
000044	CALL FCT(TOL,U,F,DERF)	ASUB 900
	C	ASUB 910
	C TEST ON SATISFACTORY ACCURACY	ASUB 920
000060	TOL=EPS	ASUB 930
000060	A=ABS(X)	ASUB 940
000062	IF(A-1.00)4,4,3	ASUB 950
000070	3 TOL=TOL*A	ASUB 960
000072	4 IF(ABS(DX)-TOL)5,5,6	ASUB 970
000076	5 IF(ABS(F)-TOLF)7,7,6	ASUB 980
000101	6 CONTINUE	ASUB 990
	C END OF ITERATION LOOP	ASUB1000
	C	ASUB1010
	C	ASUB1020
	C NO CONVERGENCE AFTER IEND ITERATION STEPS. ERROR RETURN.	ASUB1030
000104	IER=1	ASUB1040
000105	7 RETURN	ASUB1050
	C	ASUB1060
	C ERROR RETURN IN CASE OF ZERO DIVISOR	ASUB1070
000106	8 IER=2	ASUB1080
000110	RETURN	ASUB1090
000110	END	ASUB1100

STATISTICAL ANALYSIS OF ROUGH SURFACE PROFILE -- 21 ***

1 52 1.00000 1.00000 06.0121 417 200000 3.000000

SEQUENCE NUMBERS OF DATA CARDS READ IN ---

R2.1	1	R2.1	2	R2.1	3	R2.1	4	R2.1	5	R2.1	6	R2.1	7	R2.1	8	R2.1	9	R2.1	10	R2.1	11	R2.1	12
R2.1	13	R2.1	14	R2.1	15	R2.1	16	R2.1	17	R2.1	18	R2.1	19	R2.1	20	R2.1	21	R2.1	22	R2.1	23	R2.1	24
R2.1	25	R2.1	26	R2.1	27	R2.1	28	R2.1	29	R2.1	30	R2.1	31	R2.1	32	R2.1	33	R2.1	34	R2.1	35	R2.1	36
R2.1	37	R2.1	38	R2.1	39	R2.1	40	R2.1	41	R2.1	42	R2.1	43	R2.1	44	R2.1	45	R2.1	46	R2.1	47	R2.1	48
R2.1	49	R2.1	50	R2.1	51	R2.1	52	R2.1	53	R2.1	54	R2.1	55	R2.1	56	R2.1	57	R2.1	58	R2.1	59	R2.1	60
R2.1	61	R2.1	62	R2.1	63	R2.1	64	R2.1	65	R2.1	66	R2.1	67	R2.1	68	R2.1	69	R2.1	70	R2.1	71	R2.1	72
R2.1	73	R2.1	74	R2.1	75	R2.1	76	R2.1	77	R2.1	78	R2.1	79	R2.1	80	R2.1	81	R2.1	82	R2.1	83	R2.1	84
R2.1	85	R2.1	86	R2.1	87	R2.1	88	R2.1	89	R2.1	90	R2.1	91	R2.1	92	R2.1	93	R2.1	94	R2.1	95	R2.1	96
R2.1	97	R2.1	98	R2.1	99	R2.1	100	R2.1	101	R2.1	102	R2.1	103	R2.1	104	R2.1	105	R2.1	106	R2.1	107	R2.1	108
R2.1	109	R2.1	110	R2.1	111	R2.1	112	R2.1	113	R2.1	114	R2.1	115	R2.1	116	R2.1	117	R2.1	118	R2.1	119	R2.1	120
R2.1	121	R2.1	122	R2.1	123	R2.1	124	R2.1	125	R2.1	126	R2.1	127	R2.1	128	R2.1	129	R2.1	130	R2.1	131	R2.1	132
R2.1	133	R2.1	134	R2.1	135	R2.1	136	R2.1	137	R2.1	138	R2.1	139	R2.1	140	R2.1	141	R2.1	142	R2.1	143	R2.1	144
R2.1	145	R2.1	146	R2.1	147	R2.1	148	R2.1	149	R2.1	150	R2.1	151	R2.1	152	R2.1	153	R2.1	154	R2.1	155	R2.1	156
R2.1	157	R2.1	158	R2.1	159	R2.1	160	R2.1	161	R2.1	162	R2.1	163	R2.1	164	R2.1	165	R2.1	166	R2.1	167	R2.1	168
R2.1	169	R2.1	170	R2.1	171	R2.1	172	R2.1	173	R2.1	174	R2.1	175	R2.1	176	R2.1	177	R2.1	178	R2.1	179	R2.1	180
R2.1	181	R2.1	182	R2.1	183	R2.1	184	R2.1	185	R2.1	186	R2.1	187	R2.1	188	R2.1	189	R2.1	190	R2.1	191	R2.1	192
R2.1	193	R2.1	194	R2.1	195	R2.1	196	R2.1	197	R2.1	198	R2.1	199	R2.1	200	R2.1	201	R2.1	202	R2.1	203	R2.1	204
R2.1	205	R2.1	206	R2.1	207	R2.1	208	R2.1	209	R2.1	210	R2.1	211	R2.1	212	R2.1	213	R2.1	214	R2.1	215	R2.1	216
R2.1	217	R2.1	218	R2.1	219	R2.1	220	R2.1	221	R2.1	222	R2.1	223	R2.1	224	R2.1	225	R2.1	226	R2.1	227	R2.1	228
R2.1	229	R2.1	230	R2.1	231	R2.1	232	R2.1	233	R2.1	234	R2.1	235	R2.1	236	R2.1	237	R2.1	238	R2.1	239	R2.1	240
R2.1	241	R2.1	242	R2.1	243	R2.1	244	R2.1	245	R2.1	246	R2.1	247	R2.1	248	R2.1	249	R2.1	250	R2.1	251	R2.1	252
R2.1	253	R2.1	254	R2.1	255	R2.1	256	R2.1	257	R2.1	258	R2.1	259	R2.1	260	R2.1	261	R2.1	262	R2.1	263	R2.1	264
R2.1	265	R2.1	266	R2.1	267	R2.1	268	R2.1	269	R2.1	270	R2.1	271	R2.1	272	R2.1	273	R2.1	274	R2.1	275	R2.1	276
R2.1	277	R2.1	278	R2.1	279	R2.1	280	R2.1	281	R2.1	282	R2.1	283	R2.1	284	R2.1	285	R2.1	286	R2.1	287	R2.1	288
R2.1	289	R2.1	290	R2.1	291	R2.1	292	R2.1	293	R2.1	294	R2.1	295	R2.1	296	R2.1	297	R2.1	298	R2.1	299	R2.1	300
R2.1	301	R2.1	302	R2.1	303	R2.1	304	R2.1	305	R2.1	306	R2.1	307	R2.1	308	R2.1	309	R2.1	310	R2.1	311	R2.1	312
R2.1	313	R2.1	314	R2.1	315	R2.1	316	R2.1	317	R2.1	318	R2.1	319	R2.1	320	R2.1	321	R2.1	322	R2.1	323	R2.1	324
R2.1	325	R2.1	326	R2.1	327	R2.1	328	R2.1	329	R2.1	330	R2.1	331	R2.1	332	R2.1	333	R2.1	334	R2.1	335	R2.1	336
R2.1	337	R2.1	338	R2.1	339	R2.1	340	R2.1	341	R2.1	342	R2.1	343	R2.1	344	R2.1	345	R2.1	346	R2.1	347	R2.1	348
R2.1	349	R2.1	350	R2.1	351	R2.1	352	R2.1	353	R2.1	354	R2.1	355	R2.1	356	R2.1	357	R2.1	358	R2.1	359	R2.1	360
R2.1	361	R2.1	362	R2.1	363	R2.1	364	R2.1	365	R2.1	366	R2.1	367	R2.1	368	R2.1	369	R2.1	370	R2.1	371	R2.1	372
R2.1	373	R2.1	374	R2.1	375	R2.1	376	R2.1	377	R2.1	378	R2.1	379	R2.1	380	R2.1	381	R2.1	382	R2.1	383	R2.1	384
R2.1	385	R2.1	386	R2.1	387	R2.1	388	R2.1	389	R2.1	390	R2.1	391	R2.1	392	R2.1	393	R2.1	394	R2.1	395	R2.1	396
R2.1	397	R2.1	398	R2.1	399	R2.1	400	R2.1	401	R2.1	402	R2.1	403	R2.1	404	R2.1	405	R2.1	406	R2.1	407	R2.1	408
R2.1	409	R2.1	410	R2.1	411	R2.1	412	R2.1	413	R2.1	414	R2.1	415	R2.1	416	R2.1	417	R2.1	418	R2.1	419	R2.1	420

Contrails

STATISTICAL ANALYSIS FOR ALL HEIGHTS. VMAG = .000400 HMAG = .036889

HISTOGRAM AND CUMULATIVE DISTRIBUTION. INTERVAL SIZE = 6.600E-03 MIL IN
 HISTOGRAM AND CUMULATIVE DISTRIBUTION. INTERVAL SIZE = 6.600E-03 MIL IN

INT	MIL IN	FREQ	REL	CUM	ORIGIN = 0.	INT	MIL IN	FREQ	REL	COM
1	0.	0	0.000	0.000	0.	27	1.716E-01	1	.013	.787
2	6.600E-03	24	.320	.320	0.	28	1.782E-01	3	.040	.827
3	1.320E-02	21	.280	.600	0.	29	1.848E-01	4	.053	.880
4	1.980E-02	2	.027	.627	0.	30	1.914E-01	21	.280	1.160
5	2.640E-02	0	0.000	.627	0.	31	1.980E-01	50	.667	1.827
6	3.300E-02	0	0.000	.627	0.	32	2.046E-01	208	2.773	4.600
7	3.960E-02	0	0.000	.627	0.	33	2.112E-01	391	5.213	9.813
8	4.620E-02	0	0.000	.627	0.	34	2.178E-01	516	8.880	16.693
9	5.280E-02	0	0.000	.627	0.	35	2.244E-01	621	8.280	24.973
10	5.940E-02	4	.053	.680	0.	36	2.310E-01	1212	16.160	41.133
11	6.600E-02	0	0.000	.680	0.	37	2.376E-01	1410	18.800	59.933
12	7.260E-02	0	0.000	.680	0.	38	2.442E-01	1314	17.520	77.453
13	7.920E-02	0	0.000	.680	0.	39	2.508E-01	762	10.160	87.613
14	8.580E-02	0	0.000	.680	0.	40	2.574E-01	465	6.200	93.813
15	9.240E-02	0	0.000	.680	0.	41	2.640E-01	199	2.653	96.467
16	9.900E-02	1	.013	.693	0.	42	2.706E-01	96	1.280	97.747
17	1.056E-01	0	0.000	.693	0.	43	2.772E-01	48	.640	98.387
18	1.122E-01	1	.013	.707	0.	44	2.838E-01	38	.507	98.893
19	1.188E-01	1	.013	.720	0.	45	2.904E-01	36	.480	99.373
20	1.254E-01	0	0.000	.720	0.	46	2.970E-01	24	.320	99.693
21	1.320E-01	0	0.000	.720	0.	47	3.036E-01	12	.160	99.853
22	1.386E-01	1	.013	.733	0.	48	3.102E-01	5	.067	99.920
23	1.452E-01	1	.013	.747	0.	49	3.168E-01	3	.040	99.960
24	1.518E-01	0	0.000	.747	0.	50	3.234E-01	1	.013	99.973
25	1.584E-01	0	0.000	.747	0.	51	3.300E-01	1	.013	99.987
26	1.650E-01	2	.027	.773	0.	52	3.366E-01	1	.013	100.000

FIRST INTERVAL IS UNDER FLOW BOX AND LAST INTERVAL IS OVER FLOW BOX.

TOTAL NO. OF POINTS = 7500 TOI = 1.74194E+03 AVE = 2.32266E-01 SIG = 2.50927E-02 MIN = 0. MIL INS. MAX = 3.30000E-01 MIL INS.

STATISTICAL ANALYSIS FOR PEAKS OF INTEREST. V066 = .000400 RMAX = .058884

HISTOGRAM OF COMPARATIVE DISTRIBUTION. ORIGIN = 1.944E-01 MIL IN INTERVAL SIZE = 2.432E-03 MIL IN

INT	MIL IN	FREQ	REL	COM	INT	MIL IN	FREQ	REL	COM
1	1.944E-01	0	0.000	0.000	27	2.576E-01	19	3.293	89.601
2	1.968E-01	1	.173	.173	28	2.601E-01	8	1.386	90.988
3	1.993E-01	2	0.900	.173	29	2.625E-01	13	2.253	93.241
4	2.017E-01	3	.520	.693	30	2.649E-01	11	1.906	95.147
5	2.041E-01	6	1.940	1.733	31	2.674E-01	6	1.040	96.187
6	2.065E-01	5	.567	2.690	32	2.698E-01	3	.520	96.707
7	2.090E-01	16	2.773	5.373	33	2.722E-01	2	.347	97.054
8	2.114E-01	6	1.940	6.412	34	2.747E-01	2	.347	97.400
9	2.138E-01	20	3.466	9.879	35	2.771E-01	2	.347	97.747
10	2.163E-01	8	1.386	11.265	36	2.795E-01	1	.173	97.920
11	2.187E-01	8	1.386	12.652	37	2.820E-01	1	.173	98.094
12	2.212E-01	14	2.426	15.078	38	2.844E-01	0	0.000	98.094
13	2.236E-01	16	2.773	17.851	39	2.868E-01	0	0.000	98.094
14	2.260E-01	17	2.946	20.797	40	2.892E-01	3	.520	98.614
15	2.284E-01	23	3.900	24.783	41	2.917E-01	2	.347	98.960
16	2.309E-01	27	4.579	29.463	42	2.941E-01	0	0.000	98.960
17	2.333E-01	33	5.719	35.182	43	2.965E-01	2	.347	99.307
18	2.357E-01	34	5.893	41.075	44	2.990E-01	1	.173	99.480
19	2.381E-01	43	6.797	47.872	45	3.014E-01	0	0.000	99.480
20	2.405E-01	39	6.759	54.755	46	3.038E-01	1	.173	99.653
21	2.430E-01	36	6.759	61.525	47	3.063E-01	0	0.000	99.653
22	2.454E-01	35	6.956	67.591	48	3.087E-01	0	0.000	99.653
23	2.478E-01	37	6.412	74.003	49	3.111E-01	1	.173	99.827
24	2.503E-01	27	4.679	78.683	50	3.136E-01	0	0.000	99.827
25	2.527E-01	22	3.513	82.496	51	3.160E-01	0	0.000	99.827
26	2.552E-01	22	3.513	86.308	52	3.184E-01	1	.173	100.000

Centra

FIRST INTERVAL IS UNDER FLOW BOX AND LAST INTERVAL IS OVER FLOW BOX.

TOTAL NO. OF POINTS = 577 TOT = 1.37720E+02 AVE = 2.38684E-01 SIG = 1.73555E-02 MIN = 1.94400E-01 MAX = 3.16000E-01
MIL INS. MIL INS. MIL INS. MIL INS.

Control

STATISTICAL ANALYSIS FOR RADIUS OF CURVATURE. VMAG = .000+00 HMAG = .038889

HISTOGRAM AND CUMULATIVE DISTRIBUTION. ORIGIN = 2.000E-01 MIL IN INTERVAL SIZE = 1.560E-01 MIL IN

INT	MIL IN	FREQ	REL	COM	INT	MIL IN	FREQ	REL	COM
1	2.000E-01	36	6.239	6.239	27	4.256E+00	0	0.000	95.494
2	3.560E-01	73	12.652	14.891	24	4.412E+00	0	0.000	95.494
3	5.120E-01	62	10.745	29.635	29	4.568E+00	0	0.000	95.494
4	6.680E-01	69	11.958	41.594	30	4.724E+00	0	0.000	95.494
5	8.240E-01	44	7.675	49.220	31	4.880E+00	0	0.000	95.494
6	9.800E-01	55	11.265	60.485	32	5.036E+00	0	0.000	95.494
7	1.136E+00	2	.347	60.832	33	5.192E+00	12	2.080	97.574
8	1.292E+00	57	9.579	70.711	34	5.348E+00	0	0.000	97.574
9	1.448E+00	4	.693	71.404	35	5.504E+00	0	0.000	97.574
10	1.604E+00	4	.693	72.097	36	5.660E+00	0	0.000	97.574
11	1.760E+00	0	0.000	72.097	37	5.816E+00	0	0.000	97.574
12	1.916E+00	63	10.919	83.016	38	5.972E+00	0	0.000	97.574
13	2.072E+00	0	0.000	83.016	39	6.128E+00	0	0.000	97.574
14	2.228E+00	5	.867	83.842	40	6.284E+00	0	0.000	97.574
15	2.384E+00	0	0.000	83.842	41	6.440E+00	0	0.000	97.574
16	2.540E+00	13	2.253	86.135	42	6.596E+00	0	0.000	97.574
17	2.696E+00	0	0.000	86.135	43	6.752E+00	0	0.000	97.574
18	2.852E+00	0	0.000	86.135	44	6.908E+00	0	0.000	97.574
19	3.008E+00	0	0.000	86.135	45	7.064E+00	0	0.000	97.574
20	3.164E+00	8	1.386	87.522	46	7.220E+00	0	0.000	97.574
21	3.320E+00	0	0.000	87.522	47	7.376E+00	0	0.000	97.574
22	3.476E+00	0	0.000	87.522	48	7.532E+00	0	0.000	97.574
23	3.632E+00	0	0.000	87.522	49	7.688E+00	8	1.386	98.960
24	3.788E+00	46	7.972	95.494	50	7.844E+00	0	0.000	98.960
25	3.944E+00	0	0.000	95.494	51	8.000E+00	0	0.000	98.960
26	4.100E+00	0	0.000	95.494	52	8.156E+00	6	1.040	100.000

FIRST INTERVAL IS UNDER FLOW BOX AND LAST INTERVAL IS OVER FLOW BOX.

TOTAL NO. OF POINTS = 577 TOT = 8.43030E+02 AVF = 1.46106E+00 SIG = 1.95396E+00 MIN = 5.35533E-03 MAX = 1.51235E+01
MIL INS. MIL INS. MIL INS.

DISTRIBUTION OF NO. OF CYS. FOR UPPER 25 PERCENT PEAKS.

HISTOGRAM AND CUMULATIVE DISTRIBUTION. ORIGIN = 2.000E-01 MIL IN INTERVAL SIZE = 1.560E-01 MIL IN

INT.	MIL IN	FREQ	HFL	COM	INT	MIL IN	FREQ	REL	COM
1	2.000E-01	22	15.278	14.278	27	4.256E+00	0	0.000	97.917
2	3.560E-01	32	22.222	37.500	28	4.412E+00	0	0.000	97.917
3	5.120E-01	21	14.583	52.083	29	4.568E+00	0	0.000	97.917
4	6.680E-01	24	16.667	68.750	30	4.724E+00	0	0.000	97.917
5	8.240E-01	7	4.861	73.611	31	4.880E+00	0	0.000	97.917
6	9.800E-01	6	4.167	77.778	32	5.036E+00	0	0.000	97.917
7	1.136E+00	1	.694	78.472	33	5.192E+00	0	0.000	97.917
8	1.292E+00	9	6.250	84.722	34	5.348E+00	0	0.000	97.917
9	1.448E+00	1	.694	85.417	35	5.504E+00	0	0.000	97.917
10	1.604E+00	0	0.000	85.417	36	5.660E+00	0	0.000	97.917
11	1.760E+00	0	0.000	85.417	37	5.816E+00	0	0.000	97.917
12	1.916E+00	9	6.250	91.667	38	5.972E+00	0	0.000	97.917
13	2.072E+00	9	0.000	91.667	39	6.128E+00	0	0.000	97.917
14	2.228E+00	2	1.369	93.056	40	6.284E+00	0	0.000	97.917
15	2.384E+00	0	0.000	93.056	41	6.440E+00	0	0.000	97.917
16	2.540E+00	1	.694	93.750	42	6.596E+00	0	0.000	97.917
17	2.696E+00	0	0.000	93.750	43	6.752E+00	0	0.000	97.917
18	2.852E+00	0	0.000	93.750	44	6.908E+00	0	0.000	97.917
19	3.008E+00	0	0.000	93.750	45	7.064E+00	0	0.000	97.917
20	3.164E+00	1	.694	94.444	46	7.220E+00	0	0.000	97.917
21	3.320E+00	0	0.000	94.444	47	7.376E+00	0	0.000	97.917
22	3.476E+00	0	0.000	94.444	48	7.532E+00	0	0.000	97.917
23	3.632E+00	0	0.000	94.444	49	7.688E+00	1	.694	98.611
24	3.788E+00	5	3.472	97.917	50	7.844E+00	0	0.000	98.611
25	3.944E+00	0	0.000	97.917	51	8.000E+00	0	0.000	98.611
26	4.100E+00	0	0.000	97.917	52	8.156E+00	2	1.389	100.000

Controls

FIRST INTERVAL IS UNDER FLOW BOX AND LAST INTERVAL IS OVER FLOW BOX.

TOTAL NO. OF POINTS = 144 TGT = 1.41942E+02 AVE = 9.85707E-01 SIG = 1.95151E+00 MIN = 5.35533E-03 MAX = 1.51235E+01
MIL INS. MIL INS. MIL INS. MIL INS.

DISTRIBUTION OF LOG(RADIUS OF CURVATURE) AT PEAKS.

(N.B. ALL UNITS STATED AS MIL IN AVE, IN FACI, LOG(MIL IN) IN THE FOLLOWING DISTRIBUTIONS.)

INT	MIL IN	FREQ	REL	COM	INT	MIL IN	FREQ	REL	COM
1	-6.990E-01	36	6.239	6.239	27	1.341E-01	0	0.000	70.711
2	-6.569E-01	5	.667	7.105	28	1.661E-01	4	.693	71.404
3	-6.349E-01	7	1.213	8.319	29	1.942E-01	4	.693	72.097
4	-6.228E-01	6	1.040	9.359	30	2.302E-01	0	0.000	72.097
5	-5.704E-01	9	1.500	10.919	31	2.623E-01	0	0.000	72.097
6	-5.384E-01	12	2.000	12.998	32	2.943E-01	63	10.919	83.016
7	-5.067E-01	8	1.356	14.385	33	3.263E-01	0	0.000	83.016
8	-4.747E-01	13	2.253	16.638	34	3.584E-01	5	.867	83.882
9	-4.426E-01	13	2.253	18.891	35	3.904E-01	0	0.000	83.882
10	-4.106E-01	26	4.506	23.397	36	4.225E-01	13	2.253	86.135
11	-3.785E-01	9	0.000	23.397	37	4.545E-01	0	0.000	86.135
12	-3.465E-01	17	2.946	26.343	38	4.866E-01	8	1.386	87.522
13	-3.145E-01	19	3.293	29.636	39	5.186E-01	0	0.000	87.522
14	-2.824E-01	0	0.000	29.636	40	5.506E-01	0	0.000	87.522
15	-2.504E-01	30	5.149	34.835	41	5.827E-01	46	7.972	95.494
16	-2.184E-01	0	0.000	34.835	42	6.147E-01	0	0.000	95.494
17	-1.863E-01	39	6.759	41.594	43	6.468E-01	0	0.000	95.494
18	-1.543E-01	0	0.000	41.594	44	6.788E-01	0	0.000	95.494
19	-1.222E-01	0	0.000	41.594	45	7.108E-01	12	2.080	97.574
20	-9.019E-02	44	7.026	48.220	46	7.429E-01	0	0.000	97.574
21	-5.815E-02	0	0.000	48.220	47	7.749E-01	0	0.000	97.574
22	-2.610E-02	0	0.000	48.220	48	8.070E-01	0	0.000	97.574
23	5.935E-03	65	11.436	60.659	49	8.390E-01	0	0.000	97.574
24	3.744E-02	1	.173	60.832	50	8.710E-01	0	0.000	97.574
25	7.002E-02	0	0.000	60.832	51	9.031E-01	8	1.386	98.960
26	1.021E-01	57	9.479	70.711	52	9.351E-01	6	1.040	100.000

FIRST INTERVAL IS UNDER FLOW BOX AND LAST INTERVAL IS OVER FLOW BOX.

TOTAL NO. OF POINTS = 577 TOT = -5.03965E+01 AVE = -8.73423E-02 SIG = 5.14217E-01 MIN = -2.27121E+00 MAX = 1.17965E+00
MIL INS. MIL INS. MIL INS. MIL INS.

Control

HISTOGRAM AND CUMULATIVE DISTRIBUTION. ORIGIN = -6.990E-01 MIL IN INTERVAL SIZE = 3.204E-02 MIL IN
 (ALL VALUES STATED AS MIL IN AREA IN FACT. LOG(MIL IN) IN THE FOLLOWING DISTRIBUTIONS.)

HISTOGRAM AND CUMULATIVE DISTRIBUTION. ORIGIN = -6.990E-01 MIL IN INTERVAL SIZE = 3.204E-02 MIL IN

INT	MIL IN	FREQ	REL	COM	INT	MIL IN	FREQ	REL	COM
1	-6.990E-01	22	15.278	15.278	27	1.341E-01	0	0.000	84.722
2	-6.669E-01	4	2.778	18.056	28	1.661E-01	1	.694	85.417
3	-6.349E-01	5	3.472	21.528	29	1.982E-01	0	0.000	85.417
4	-6.024E-01	0	0.000	21.528	30	2.302E-01	0	0.000	85.417
5	-5.704E-01	5	3.472	25.000	31	2.623E-01	0	0.000	85.417
6	-5.384E-01	5	3.472	28.472	32	2.943E-01	9	6.250	91.667
7	-5.057E-01	2	1.389	29.861	33	3.263E-01	0	0.000	91.667
8	-4.747E-01	7	5.661	34.722	34	3.584E-01	2	1.389	93.056
9	-4.426E-01	4	2.778	37.500	35	3.904E-01	0	0.000	93.056
10	-4.106E-01	8	5.556	43.056	36	4.225E-01	1	.694	93.750
11	-3.786E-01	0	0.000	43.056	37	4.545E-01	0	0.000	93.750
12	-3.465E-01	7	4.861	47.917	38	4.866E-01	1	.694	94.444
13	-3.145E-01	0	0.000	47.917	39	5.186E-01	0	0.000	94.444
14	-2.824E-01	0	0.000	47.917	40	5.506E-01	0	0.000	94.444
15	-2.504E-01	11	7.639	59.722	41	5.827E-01	5	3.472	97.917
16	-2.184E-01	0	0.000	59.722	42	6.147E-01	0	0.000	97.917
17	-1.863E-01	13	9.028	68.750	43	6.468E-01	0	0.000	97.917
18	-1.543E-01	0	0.000	68.750	44	6.788E-01	0	0.000	97.917
19	-1.222E-01	0	0.000	68.750	45	7.108E-01	0	0.000	97.917
20	-9.019E-02	7	4.861	73.611	46	7.429E-01	0	0.000	97.917
21	-8.458E-02	0	0.000	73.611	47	7.749E-01	0	0.000	97.917
22	-8.101E-02	0	0.000	73.611	48	8.070E-01	0	0.000	97.917
23	-7.744E-02	7	4.861	78.472	49	8.390E-01	0	0.000	97.917
24	-7.387E-02	0	0.000	78.472	50	8.710E-01	0	0.000	97.917
25	-7.027E-02	0	0.000	78.472	51	9.031E-01	1	.694	98.611
26	-6.667E-02	9	6.250	84.722	52	9.351E-01	2	1.389	100.000

FIRST INTERVAL IS UNDER FLOW BOX AND LAST INTERVAL IS OVER FLOW BOX.

TOTAL NO. OF POINTS = 144 TOT = -4.90964E+01 AVE = -3.40947E-01 SIG = 5.61595E-01 MIN = -2.27121E+00 MAX = 1.17965E+00
 MIL INS. MIL INS. MIL INS. MIL INS.

Contracts

*** SUMMARY OF RESULTS. RUN 21 ***

CORRELATION COEFFICIENTS BETWEEN PEAK HEIGHTS AND RADII = -.183 PEAK DENSITY = 3913614 PER SQ IN

ALL HEIGHTS ----- CLA = 1.41343E-02 MIL IN RMS = 2.50927E-02 MIL IN

PEAK HEIGHTS ----- MFAN = 6.41762E-03 MIL IN STD.DEV. = 1.73555E-02 MIL IN

RAD. OF CUR... LOG-NORMAL DISTRIBUTION----- MFAN = -8.73423E-02 STD.DEV. = 5.14217E-01

MODE = 2.01279E-01 MIL IN

MEDIAN = 8.13990E-01 MIL IN

MFAN = 1.64849E+00 MIL IN

MODE = -3.40947E-01

MEDIAN = 8.56697E-02 MIL IN

MFAN = 4.47812E-01 MIL IN

MEAN = 1.05235E+00 MIL IN

STD.DEV. = 5.61595E-01

**** RESULTS OF ASPERITY INTERACTION ****

DESCRIPTION OF INPUT VARIABLES

MATERIAL PROPERTIES ---

YOUNG'S MODULUS FOR MATERIALS 1,2 (LBS PER SQ IN) = 2.9000E+07 2.9000E+07
 POISSON'S RATIO FOR MATERIALS 1,2 = 2.5000E-01 2.5000E-01
 HARDNESS OF SOFTER MATERIAL (LBS PER SQ IN) = 1.1800E+06
 ULTIMATE SHEAR STRESS OF WEAKER MATERIAL (LBS PER SQ IN) = 2.0000E+05
 INTERFACIAL SHEAR STRESS RATIO = 1.0000E+00
 ADHESION STRESS RATIO = 2.0000E+00
 SUM OF SPECIFIC RESISTANCES OF MATERIALS 1,2 (MICRO OHM SQ IN) = 1.5750E+01
 EXPECTED TUNNEL RESISTIVITY (MICRO OHM SQ IN) = 8.6000E-02

TOPOGRAPHIC PARAMETERS ---

PEAK DENSITY = 3913614 PER SQ IN. (MIL IN) = 1.0524E+00 1.0524E+00
 MEAN RADIUS AT PEAKS SURFACE 1,2 (MIL IN) = 6.41762E-03 6.41762E-03
 PEAK HEIGHT DISTRIBUTIONS SURFACE 1,2 (MIL IN) = 1.73555E-02 1.73555E-02
 MEAN (MIL IN) = 3.40947E-01 -3.40947E-01
 STD.DEV. (MIL IN) = 5.61595E-01 5.61595E-01
 LOG(RADIUS) DISTRIBUTIONS SURFACE 1,2 (MIL IN) = 2.00000E-01
 MEAN (LOG(MIL IN)) = -3.40947E-01 -3.40947E-01
 STD.DEV. (LOG(MIL IN)) = 5.61595E-01 5.61595E-01
 MINIMUM SPECIFIED RADIUS (MIL IN) = 2.00000E-01

UPPER LIMIT ON RADIUS GIVEN BY 3.00 TIMES STD.DEV.

EHD CONTACT SPECIFICATIONS ---

HERTZIAN CONTACT SIZE ALONG AND PER. TO ROLLING (MIL IN) = 1.0000E+03 1.0000E+03
 FILM PROTRUSION WIDTH AND DEPTH (MIL IN) = 0. 0.
 NOMINAL FILM THICKNESS (MIL IN) = 5.0000E+02 5.0000E+02
 (MIL IN) = 7.3633E-02

STATISTICAL PARAMETERS** S16= 2.45443E-02 AVP = 1.28352E-02 RAD = 1.05235E+00
 VARIATION OF RADI OF CURVATURE** -3.40947E-01 5.61595E-01 -3.40947E-01 5.61595E-01 2.00000E-01 3.00000E+00

SUMMARY OF COMPUTED RESULTS

MICRO CONTACT DESCRIPTIONS ---

TOTAL NUMBER OF JUNCTIONS = 26068 ELASTIC = 31 PLASTIC = 26005
MEAN AND STD.DEV. OF JUNCTION RADIUS DISTRIBUTION (MIL IN) = 2.6491E-01 4.9858E-02
AVERAGE GEOMETRIC INTERFERENCE AND JUNCTION LIFE (MIL IN) = 2.0772E-02 5.1140E-01

CONTACT FORCES DUE TO ASPERITY INTERACTIONS ---

AVERAGE NORMAL AND FRICTION FORCES (LBS) = 2.4307E+03 1.3740E+03
ESTIMATED FRICTION COEFFICIENT = 5.6529E-01
TOTAL REAL AREA OF CONTACT (SQ IN) = 6.4478E-03
RATIO OF REAL TO APPARENT CONTACT AREA = 6.4478E-03

ESTIMATED ELECTRICAL CONTACT RESISTANCE (MICRO OHM) = 1.3928E+01

N.R. LOG-NORMAL DISTRIBUTION OF RADII OF CURVATURE AT THE PEAKS WAS CONSIDERED.

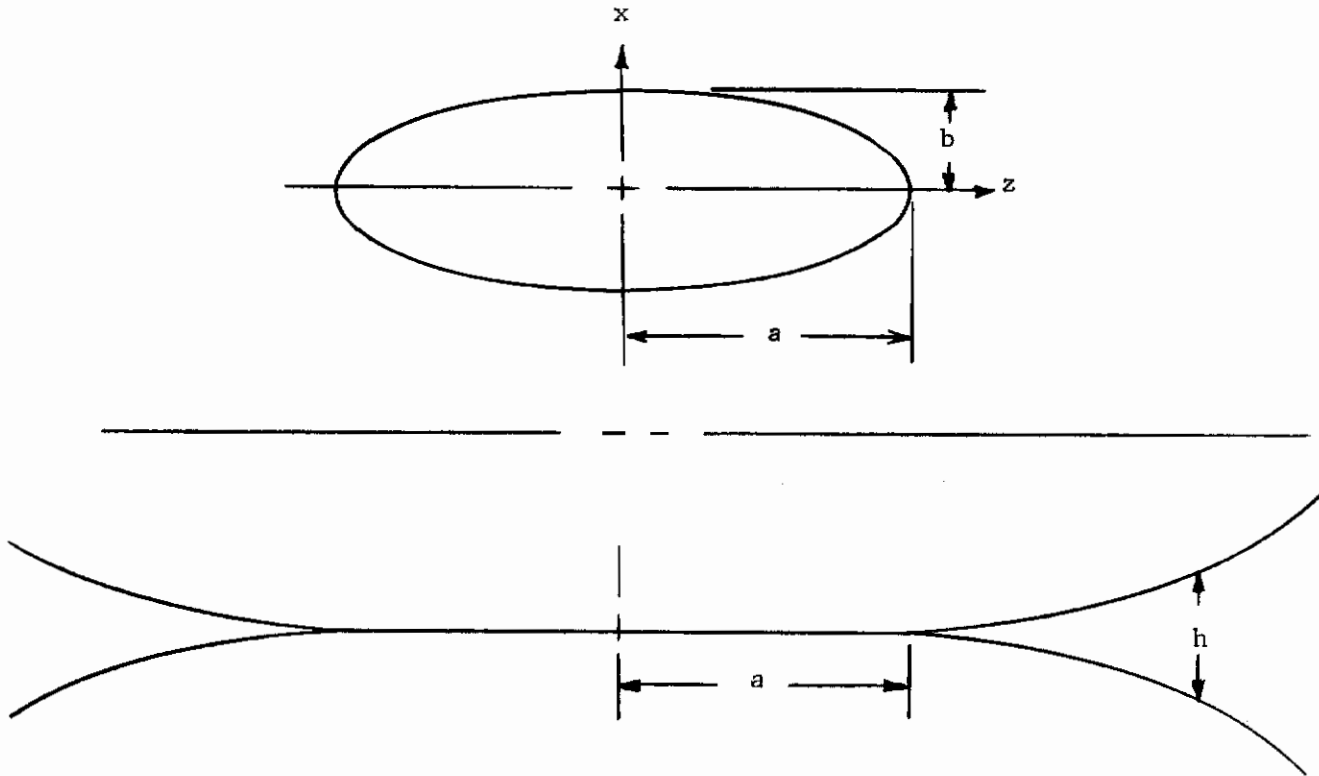
Conrails

Contrails

APPENDIX IV

EQUATIONS FOR DETERMINATION OF THE SEPARATION PROFILE FOR ELLIPTICAL HERTZ CONTACT

A plan and elevation view of an elliptical Hertz contact is shown below.



The exterior Hertz profile h is expressed as function of the coordinate x and y in terms of the elastic module and Poisson's ratio of contacting bodies 1 and 2 (denoted by E_1 , E_2 , ν_1 , and ν_2 respectively), the applied load W and the contact ellipse dimensions a and b in terms of the dimensionless quantities ϕ , ξ , and η are given below:

$$\phi = \frac{2E'a}{3W} h, \quad \xi = \frac{x}{b}, \quad \eta = \frac{y}{a}, \quad \beta = \frac{b}{a}$$

where

$$\frac{1}{E'} = \frac{(1 - \nu_1^2)}{\pi E_1} + \frac{(1 - \nu_2^2)}{\pi E_2}$$

Contrails

The dimensionless separation $\bar{\Phi}(\xi, \eta)$ is determined for Hertz contact theory which may be put in the form

$$\bar{\Phi}(\xi, \eta) = J_2 \xi^2 + J_3 \eta^2 - J_1$$

where

$$J_1 = \int_0^{\bar{u}} \frac{d\zeta}{(1 + \zeta^2)^{1/2} (1 + \bar{\beta}^2 \zeta^2)^{1/2}}, \quad J_2 = \int_0^{\bar{u}} \frac{d\zeta}{(1 + \zeta^2)^{3/2} (1 + \bar{\beta}^2 \zeta^2)^{1/2}}$$

$$J_3 = \int_0^{\bar{u}} \frac{d\zeta}{(1 + \zeta^2)^{1/2} (1 + \bar{\beta}^2 \zeta^2)^{3/2}} \quad \text{and}$$

\bar{u} is determined from the relationship

$$\frac{\xi^2}{1 + \bar{u}^2} + \frac{\eta^2}{1 + \bar{\beta}^2 \bar{u}^2} = 1$$

The integrals J_1 , J_2 and J_3 may be expressed in terms of the elliptic integrals $F(\emptyset, k)$ and $E(\emptyset, k)$ as follows:

$$J_1 = F(\emptyset, k), \quad J_2 = \frac{1}{(1 - \bar{\beta}^2)} (E(\emptyset, k) - \bar{\beta}^2 F(\emptyset, k))$$

and

$$J_3 = \frac{1}{(1 - \bar{\beta}^2)} [F(\emptyset, k) - E(\emptyset, k)] + \frac{\bar{u}}{(1 + \bar{\beta}^2 \bar{u}^2)^{1/2} (1 + \bar{u}^2)^{1/2}}$$

where

$$k = \sqrt{1 - \bar{\beta}^2} \quad \text{and} \quad \emptyset = \tan^{-1} \bar{u}$$

Contrails

and $F(\vartheta, k)$ and $E(\vartheta, k)$ denote the incomplete elliptic integrals of the first and second kind defined as

$$F(\vartheta, k) = \int_0^{\vartheta} \frac{d\theta}{\sqrt{1 - k^2 \sin^2 \theta}} \quad \text{and} \quad E(\vartheta, k) = \int_0^{\vartheta} \sqrt{1 - k^2 \sin^2 \theta} \, d\theta$$

Contrails

REFERENCES

1. Kannel, J.W., Bell, J.C., and Allen, C.M., A Study of the Influence of Lubricant on High-Speed Rolling-Contact Bearing Performance, Technical Report ASD-TR-61-643, Part III, Wright-Patterson Air Force, 1963.
2. McGrew, J.M., Gu, A., Cheng, H.S., Murray, S.F., Elastohydrodynamic Lubrication - Preliminary Design Manual, Technical Report AFAPL-TR-70-27, Wright-Patterson Air Force Base, 1970.
3. Leach, Eugene F., A Direct System for Measuring Torque with the Geared Roller Test Machine, Communication from Caterpillar Tractor Co., May 1969.
4. Crook, A.W., "LUBRICATION OF ROLLERS, IV", Phil. Trans. R. Society, Series A, 1963.
5. Gupta, P.K., Hamilton, G.M., and Hirst, W., "A Three-Disc Machine for Examining Elastohydrodynamic Oil Films," The Chartered Mechanical Engineer, May 1970.
6. Jefferis, J.A., and Johnson, K.L., "Sliding Friction Between Lubricated Rollers," Proc. Instn. Mech. Engrs., 182 (Pt. 1, No. 14), 1967-68.
7. Tallian, T.E. and McCool, J.I., "The Observation of Individual Asperity Interactions in Lubricated Point Contact," ASLE Trans. 11, 1968.
8. Furey, M.J., "Metallic Contact and Friction Between Sliding Surfaces," ASLE Transactions 4, 1961.
9. McCool, J.I., Waltrich, J.B., First Summary Report on Elemental Contact Occurrences in Rollers and Sliding, SKF Industries Inc., 1966.
10. Cameron, A. and Gohar, R., "Theoretical and Experimental Studies of the Oil Film in Lubricated Point Contact," Proc. R. Soc., Series A, 1966.
11. Cameron, A. and Gohar, R., "The Mapping of Elastohydrodynamic Contacts," Preprint 66-LC-21, ASLE/ASME Lubric. Conf., Minneapolis, 1966.
12. Foord, C.A., Wedeven, L.D., Westlake, F.J., and Cameron, A., "Optical Elastohydrodynamics," Vol. 184, Part 1, Proceedings of the Mech. Eng., 1969-1970.
13. Holden, J., "Multibeam Interferometry; Intensity Distribution in the Reflected System," Vol. 62, Part 7, Proceedings of the Physical Society, July 1949.
14. Johnson, K.L., and Cameron, R., "Shear Behavior of Elastohydrodynamic Oil Films at High Rolling Contact Pressures", Vol. 182, Proc. Inst. Mech. Eng., 1967-1968.

REFERENCES (Continued)

15. Crook, A.W., "Lubrication of Rollers, III", Vol. 254, Phil. Trans. R. Society, London, Series A, 1961.
16. Wilson, D.R., Effect of Extreme Conditions on the Behavior of Lubricants and Fluids, Technical Report AFML-TR-67-8, Part III, Wright-Patterson Air Force Base, 1969.
17. Dowson, D. and Higginson, G.R., Elastohydrodynamic Lubrication, Pergamon Press, Oxford, 1966.
18. Kannel, J.W. and Walowit, J.A., "Simplified Analysis for Traction Between Rolling-Sliding Elastohydrodynamic Contacts," Vol. 93, Series F, No. 1, ASME, JOLT, 1971.
19. Gupta, P.K., and Cook, N.H., "Statistical Analysis of Mechanical Interactions of Rough Surfaces". To be published.
20. Gupta, P.K., and Cook, N.H., "Junction Deformation Models for Asperities in Sliding Interaction". To be published.
21. Gupta, P.K., "Topographic Analysis of Friction Between a Pair of Rough Surfaces," Sc.D. Thesis, Dept. of Mechanical Engr., M.I.T., Cambridge, Mass., 1970.
22. Holm, R., Electrical Contacts - Theory and Applications, Springer-Verlag, New York, (4th Edition), 1967.
23. Timoshenko, S., and Goodier, J.N., Theory of Elasticity, McGraw Hill Book Co., New York (2nd Edition), 1951.
24. Greenwood, J.A., and Williamson, J.B.P., "Contact of Nominally Flat Surfaces," Proc. Roy. Soc., Series A, 1966.

DOCUMENT CONTROL DATA - R & D

(Security classification of title, body of abstract and indexing annotation must be entered when the overall report is classified)

1. ORIGINATING ACTIVITY (Corporate author) Mechanical Technology Incorporated 968 Albany-Shaker Road Latham, New York 12110		2a. REPORT SECURITY CLASSIFICATION Unclassified	
		2b. GROUP N/A	
3. REPORT TITLE RESEARCH ON ELASTOHYDRODYNAMIC LUBRICATION ON HIGH-SPEED ROLLING-SLIDING CONTACTS			
4. DESCRIPTIVE NOTES (Type of report and inclusive dates) Second Annual Report February 1970 - February 1971			
5. AUTHOR(S) (First name, middle initial, last name) Richard L. Smith Pradeep K. Gupta Jed A. Walowit John M. McGrew			
6. REPORT DATE December 1971	7a. TOTAL NO. OF PAGES 162	7b. NO. OF REFS 24	
8a. CONTRACT OR GRANT NO. F33615-69-C-1305	9a. ORIGINATOR'S REPORT NUMBER(S) None		
b. PROJECT NO. c. d.	9b. OTHER REPORT NO(S) (Any other numbers that may be assigned this report) None		
10. DISTRIBUTION STATEMENT This document is subject to special export controls and each transmittal to foreign governments or foreign nationals may be made only with prior approval of the Air Force, Aero Propulsion Laboratory, Wright-Patterson Air Force Base, Ohio 45433			
11. SUPPLEMENTARY NOTES		12. SPONSORING MILITARY ACTIVITY Air Force Aero Propulsion Laboratory Fuel, Lubrication & Hazards Division Wright-Patterson AFB, Ohio 45433	
13. ABSTRACT A rolling disc apparatus has been designed and built. Traction between two crown discs lubricated with 5P4E polyphenyl ether have been measured as function of slip rate over a range of Hertz pressure (80,000-140,000 psi), rolling speeds (900-1820 ips), and temperatures (175 F - 215 F). Comparisons are made between measured tractions, Battelle data, and various analytical predictions. The MTI data agree qualitatively with Battelle measurements except that MTI data are found to be relatively insensitive to temperature whereas Battelle reports considerable temperature sensitivity. A semi-empirical mathematical model has been put forth to represent traction measurements. A computer program for analyzing asperity interactions under partial elasto-hydrodynamic conditions has been written and a listing is contained in this report.			

Contract

14 KEY WORDS	LINK A		LINK B		LINK C	
	ROLE	WT	ROLE	WT	ROLE	WT
Elastohydrodynamic Lubrication Traction Film Thickness Rolling Disc Machine Asperity Interactions Polyphenyl Ether Partial Elastohydrodynamics Optical Viscosity Electrical Resistance Elliptical Contact						